SLAC-428
CONF-9211287
UC-414
(M)

STUDIES OF TOP QUARKS AT COLLIDING-BEAM FACILITIES

November 6-7, 1992
University of Wisconsin
Madison, Wisconsin

Volume 2
Proceedings of the 1992 Workshops
on High-Energy Physics with Colliding Beams

Jeanne Rogers, Editor

Prepared for the Department of Energy under contract number DE-AC03-76SF00515. Printed in the United States of America. Available from the National Technical Information Service, U.S. Department of Commerce, 5285 Port Royal Road, Springfield, Virginia 22161.

High Energy Physics with Colliding Beams Conference

Top Quark

University of Wisconsin
Madison, WI

(November 6-7, 1992)

Chairperson: R. Prepost

Program Committee: V. Barger, D. Burke, G. Kane, B. Klima, L. Pandrom, R. Prepost

Sponsors: American Physical Society
Department of Energy
FNAL
University of Wisconsin

High Energy Physics with Colliding Beams

Studies of Top Quarks at Colliding-Beam Facilities

University of Wisconsin - Madison, November 6 & 7, 1992

Friday, November 6

Introduction

9:45	Opening Remarks	M. Ebel
10:00	The Top Questions	G. Kane
10:45	SM Limits on Top	J. Pilcher
11:25	Search for the Top at Fermilab	G.P. Yeh
12:10	*Lunch*	

Top Studies

1:30	Long Range Top Physics at Fermilab	S. Protopoescu
2:15	Top Production and Decay at Colliders	P. Sinervo
3:40	*Break*	
4:00	Interplay between Top Decay and Fragmentation	T. Sjostrand
4:40	Top at Threshold in e^+e^- Collisions - Theory	J. Kuhn
5:20	Probing the Top-Quark Mass-generating Mechanism	S. Willenbrock

Saturday, November 7

Top Studies

9:00	Top at Threshold in e^+e^- Collisions - Experiment	K. Fujii
9:40	Top in the Continuum at e^+e^- Colliders	D. Burke
10:20	*Break*	

Top Phenomenology

10:30	Top Decays to Charged Higgs Bosons	R.J. N Phillips
11:15	Top Decays and Supersymmetry	H. Baer
11:55	Top and Rare Decays	J. Hewett
12:35	*Lunch*	

Top Phenomenology/Theory

2:00	Top and CP Violations	D. Chang
2:40	Ferminon Masses and Mixings	M. Berger

Summary

3:55	Top Physics at Hadron Colliders	R. Hollebeek
4:45	Top Physics at e^+e^- Colliders	M. Peskin
5:30	Working Group Report	G. Kane - Coordinator

1992 Top Quark Participant Listing

Name	Institution
Ahn, Seung-chan	Fermilab
Baer, Howard	Florida State University
Balamurali, V.	University of Notre Dame
Barger, Vernon	University of Wisconsin
Baur, Ulrich	Florida State University
Behrens, Bruce	University of Wisconsin
Bellinger, Jim	University of Wisconsin
Berger, Michael	University of Wisconsin
Bhat, Pushpa	Fermilab
Bhatnagar, Vipin	Fermilab/Panjab University
Biswas, Nripen	University of Notre Dame
Bowser-Chao, David	University of Texas at Austin
Burke, David L.	SLAC
Chang, Darwin	Northwestern University
Cheung, Kingman	Northwestern University
Chopra, Sailesh	Fermilab/Panjab University
Cobau, William	Fermilab/University of Maryland
Cochran, Jim	Fermilab
Crossley, Dennis	University of Wisconsin
Dasu, Sridhara	University of Wisconsin
Doncheski, Mike	University of Wisconsin
Ducati, Beatriz	University of Wisconsin
Ebel, Marvin	University of Wisconsin
Eboli, Oscar	University of Sao Paulo
Fisk, Gene	Fermilab
Fujii, Keisuke	KEK
Goldstein, Gary	Tufts University
Gonzalez-Garcia, Concha	University of Wisconsin
Halzen, Francis	University of Wisconsin
Han, Tao	Fermilab
Heintz, Ulrich	Fermilab/Columbia University
Hernandez, Oscar	McGill University
Hewett, JoAnne	Argonne National Laboratory
Hollebeek, Robert	University of Pennsylvania
Im, Carl	University of Michigan
Iordanidis, Konstantinos	University of Wisconsin
Kalyniak, Pat	Carleton University

1992 Top Quark Participant Listing

Name	Institution
Kane, Gordon	University of Michigan
Kayser, Boris	National Science Foundation
Kehoe, Robert	University of Notre Dame
Klima, Boaz	Fermilab
Kühn, J.H.	Universität Karlsruhe
Lamoureux, Jodi	University of Wisconsin
Long, Bill	University of Wisconsin
Loveless, Richard	University of Wisconsin
Matsui, Takayuki	KEK
Migneron, Roger	University of Western Ontario
Mitchell, Gregory	University of Wisconsin
Narain, Meenakshi	Fermilab
Nelson, Charles A.	SUNY at Binghamton
Nojiri, Mihoko	University of Wisconsin
Ohmann, Paul	University of Wisconsin
Olsson, Martin	University of Wisconsin
Peskin, Michael	SLAC
Peterson, K.A.	Carleton University
Phillips, Ivan	Northwestern University
Phillips, Roger	Rutherford Appleton Laboratory
Pilcher, James	University of Chicago
Pondrom, Lee	University of Wisconsin
Prepost, Richard	University of Wisconsin
Prosper, Harrison	Fermilab
Protopopescu, Serban	Brookhaven National Laboratory
Reeder, Don	University of Wisconsin
Riesselmann, Kurt	University of Wisconsin
Rizzo, Tom	Argonne National Laboratory
Robinett, R. W.	Penn State University
Serbo, Victor	University of Wisconsin
Sheaff, Marleigh	University of Wisconsin
Sinervo, Pekka K.	University of Toronto
Sjostrand, Torbjorn	CERN
Snyder, Scott	Fermilab
Stange, Alan	Brookhaven National Laboratory
Stelzer, Tim	University of Wisconsin
Stong, Mary Louise	University of Wisconsin

1992 Top Quark Participant Listing

Name	Institution
Szalapski, Rob	University of Wisconsin
Thompson, Joey	SUNY at Stony Brook
Vazquez, Ricardo	University of Wisconsin
Willenbrock, Scott	Brookhaven National Laboratory
Wright, Brian	University of Wisconsin
Xu, Hao-Wei	Fermilab
Yeh, Gong Ping	Fermilab
Yehudai, Eran	Fermilab
Yuan, C. P.	Michigan State University
Zeppenfeld, Dieter	University of Wisconsin
Zhang, Liqun	University of Wisconsin

THE TOP QUESTIONS

Gordon Kane
Randall Physics Lab
University of Michigan

ABSTRACT

This talk is intended to survey the main topics that will be covered at this workshop, emphasizing some of the issues and goals. I try to provide an overview of the physics opportunities once the top quark is detected. Most topics have already been studied to some extent in the literature and will be covered in detail in other talks; I also spend a few minutes on some very recent work about the possibility of detecting CP violation at colliders.

TOP QUESTIONS

- OVERVIEW
- MEASURE M_t
  - -- HOW WELL DO WE NEED TO KNOW IT?
- WINDOW FOR NEW DECAYS?
- V_{tb}, V_{cb}
- Γ_{top}, $BR(t \to Wb)$, $\vec{P}_t$, $f_i^{L,R}$
- DETECT TGR AT COLLIDERS?

- WORKING GROUP
  - — GOALS
  - -- PROCEDURES

G. KANE, FERMILAB, Nov 92

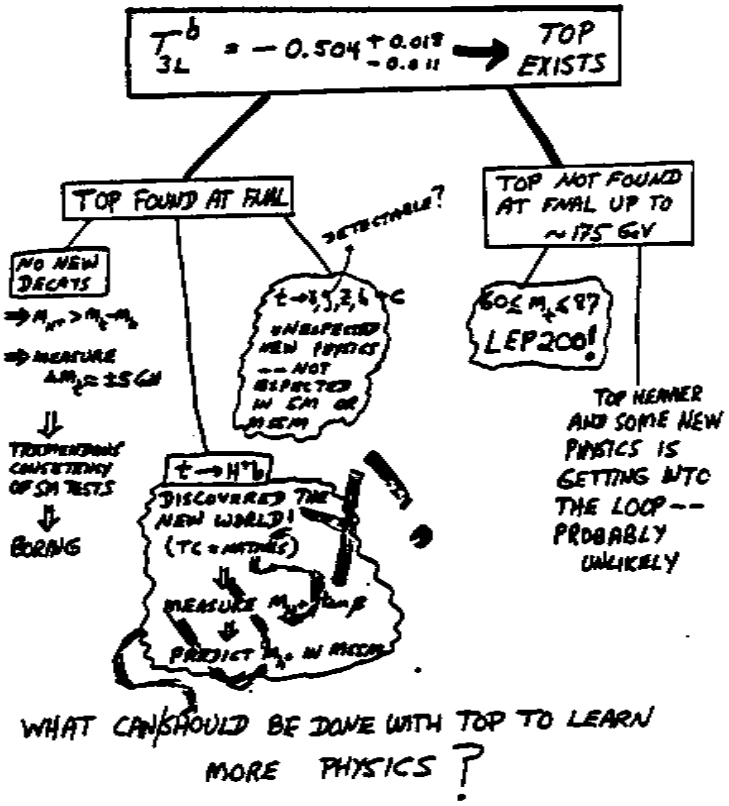

WHAT CAN/SHOULD BE DONE WITH TOP TO LEARN MORE PHYSICS?

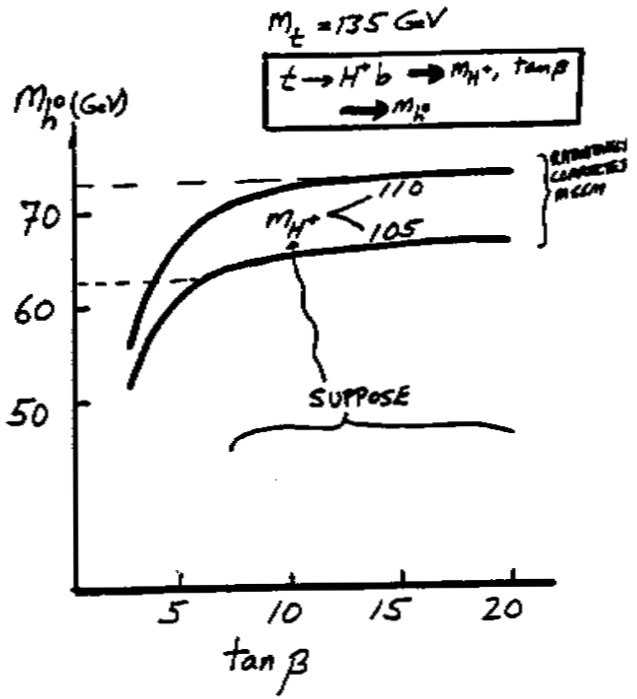

MEASURE m_t

UNSOLVED PROBLEM

- HOW WELL CAN/SHOULD IT BE MEASURED?
- AT WHAT LEVEL CAN WE LEARN NEW PHYSICS?
  - — h^0 EXISTS?
  - — "MEASURE" m_{h^0}?
  - — NEW LEVEL OF PRECISION TESTS?
- PROBLEMS WITH MEASURING m_t
  - — REQUIRES NEW KNOWLEDGE OR ASSUMPTIONS ABOUT α_s IF σ OR THRESHOLD PHYSICS USED — e.g. $\delta\alpha_s/\alpha_s = 1\% \Rightarrow \delta m_t \sim 0.1$ GeV
    [TODAY $\delta\alpha_s/\alpha_s \simeq 12\%$?] YAMAMOTO, SHIMAMOTO 90
  - — IF MEASURE α_s AT $\mu = M_Z$ AND NEED α_s AT $2m_t$, REQUIRE HIGHER ORDER CALCULATIONS TO RETAIN ACCURACY →
  - — IS DEFINITION OF m_t SAME FOR MEASUREMENT AS FOR RADIATIVE CORRECTION USE? — SMALL CORRECTIONS $\sim (\alpha_s/\pi)^2 \simeq 0.2$ GeV?

NOTE:

$$\alpha_1^{-1}(m_t) - \alpha_1^{-1}(m_Z) \approx \underbrace{(\;)}_{\mathcal{O}(1)} \underbrace{\ln \frac{m_t}{m_Z}}_{\approx 0.4} + \cdots$$

$\alpha_3^{-1} \sim 8$

$\alpha_2^{-1} \sim 30$

NEED MORE

- TODAY Δm_W IS LIMITING FACTOR FOR INTERPRETING PRECISION DATA
- $\Delta\rho \sim m_t^2$

$$\Rightarrow \quad m_W^2 - \frac{\alpha_2(m_Z)}{\alpha_1(m_Z)+\alpha_2(m_Z)} m_Z^2 = \frac{3\alpha_2(m_Z)}{16\pi} m_t^2$$

$$\Rightarrow \quad \delta m_W \approx \frac{3\alpha_2}{16\pi} \frac{m_t}{m_W} \delta m_t \approx \frac{\delta m_t}{300}$$

- $\delta m_W = 100$ MeV

$$\Rightarrow \quad \delta m_t = 30 \text{ GeV} = \pm 15 \text{ GeV}$$

GOOD MATCH AT FNAL

AFTER M_W MEASURED BETTER?

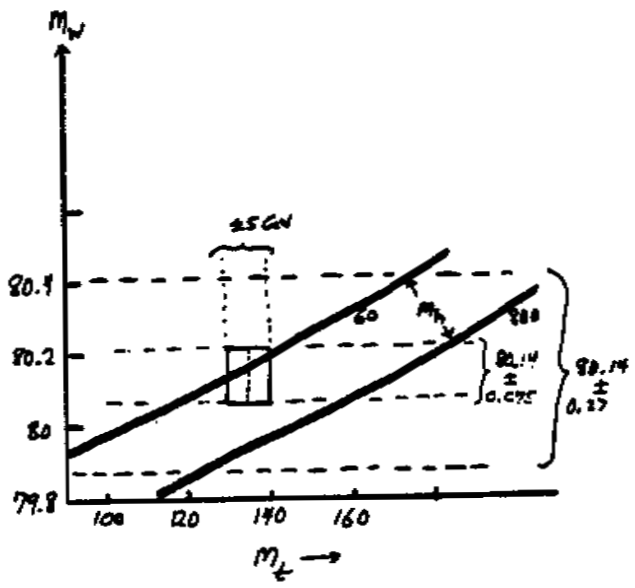

NO SIGNIFICANT GAIN BY MEASURING M_t MORE ACCURATELY

WHAT ABOUT A_{LR}? $(A_{LR} = P_\tau)$

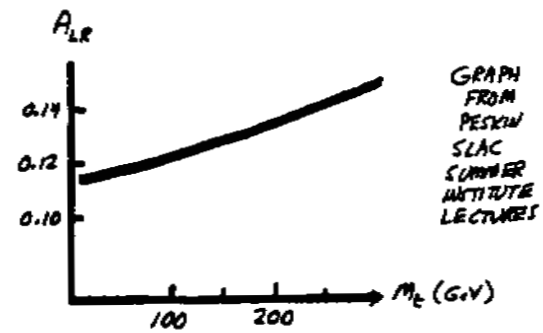

$\Delta A_{LR}/\Delta M_t \simeq 0.04/150 \simeq 0.0003\ \text{GeV}^{-1}$

$\Delta M_t = \pm 5 \Rightarrow \Delta A_{LR} \simeq \pm 0.0015$

$\sim \pm 1\%$ OF A_{LR}

$\Rightarrow$ NEED $\Delta M_t < \pm 5$ WHEN A_{LR} MEASURED TO $\sim 1\%$

CAN WE LEARN ABOUT HIGGS BOSONS FROM PRECISE MEASUREMENTS + 1-LOOP THEORY?
(GLOBAL FIT)

1991 DATA INCLUDED

del Aguila
Martinez
Quiros

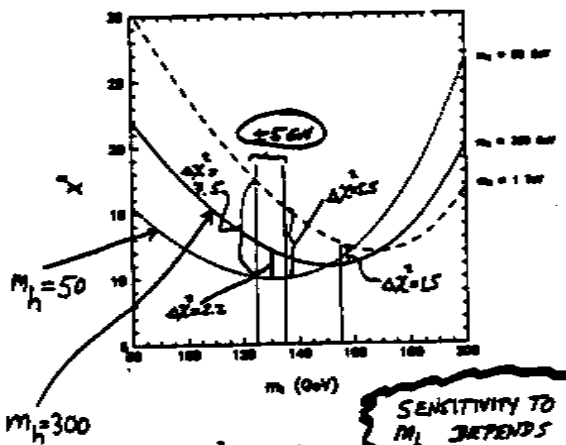

$\Delta\chi^2$	CL
2.7	90%
4	95%
6.7	99%

SENSITIVITY TO m_h DEPENDS ON m_t STRONGLY

UPPER LIMIT ERROR ON m_t VERY IMPORTANT

CAN WE LEARN ABOUT HIGGS BOSONS FROM PRECISE MEASUREMENTS + 1-LOOP THEORY?

BLONDEL
RENARD
VERZEGNASSI

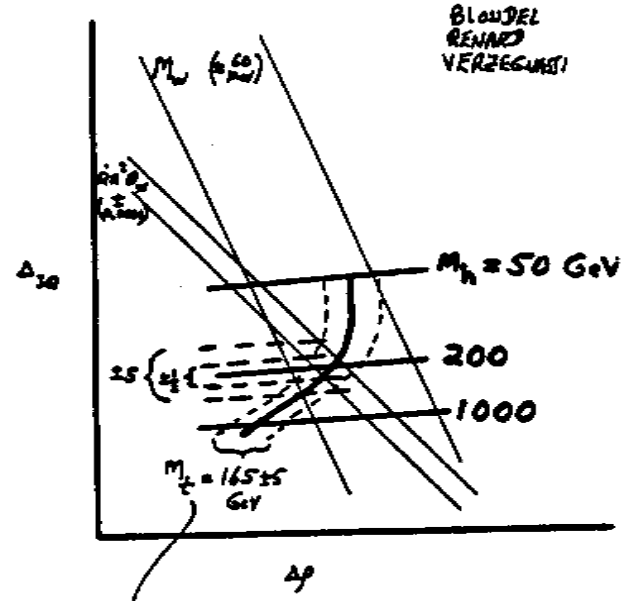

THE "DIFFICULT" REGION

HEAVY TOP ⇒ WINDOW FOR NEW DECAYS?

SEARCH AT FNAL $\sim 10^4\ \bar{t}t$

SSC/LHC $\sim 10^8\ \bar{t}t$

NLC $\sim 10^4\ \bar{t}t$

$t \to H^+ b$

$\to \tilde{t}\tilde{\chi}$

$\to c + \gamma, g, Z, h$ — DETECTABLE?

V_{ts}, V_{td}, TOP IN LOOPS

- MEASURE V_{ts} DIRECTLY?

BR $\sim |V_{bc}|^2 \sim 0.0025$

SSC/LHC?

NLC?✗

- MEASURE V_{td} DIRECTLY? TOO SMALL

V_{bu}

(PDT: 3 FAMILIES, UNITARITY → $|V_{td}| = 3.18 \times 10^{-3}$, $|V_{ts}| = 30.64 \times 10^{-3}$)

PREDICTIONS FOR LOOP PROCESSES -- INDIRECT MEASUREMENT OF V_{ts}, V_{td}

• $K^+ \to \pi^+ \nu \bar{\nu}$ $\qquad BR \sim |V_{ts} V_{td} + \text{CHARM}|^2$

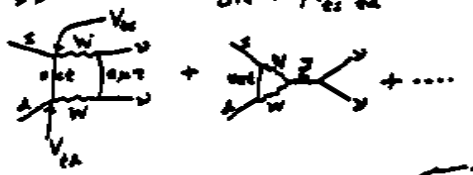

• $\epsilon'/\epsilon \sim |V_{td} V_{ts}| + \cdots$

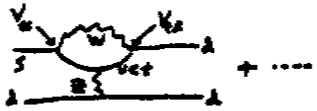

ALL DEPEND ON m_{top} STRONGLY

• $B^0 - \bar{B}^0$ MIXING

$x_d \sim |V_{td}|^2 m_t^2 f_B^2$ $\qquad x_s \sim |V_{ts}|^2 m_t^2 f_B^2$

$x_d / x_s \sim |V_{td}/V_{ts}|^2$

CONSISTENCY AMONG MEASUREMENTS ANOTHER IMPORTANT CONSTRAINT ON NEW PHYSICS -- MAYBE NEED ALL TO GET GOOD ERRORS

ADDITIONAL, RELATED

• TOP PROPERTIES -- SM TESTS

-- MEASURE $\Gamma_{top} \approx 600$ MeV $\quad \left[\frac{m_t}{125}\right]^3$

FINAL BEST?

-- MEASURE $BR(t \to W_{long}\, b)$

$$\cdot \frac{m_t^2/m_W^2}{2 + m_t^2/m_W^2} \{1 + \text{POLARIZATION EFFECT}\}$$

KLY

-- MEASURE $\vec{P}_{top}$ -- TRANSVERSE, LONGITUDINAL

-- NEW, GOOD SM TESTS SINCE TOP SPIN IS ONLY OBSERVABLE QUARK SPIN (IF ANY) -- HADRONIZATION PREVENTS OTHERS -- CAN USE $\vec{P}_{top}$ AS TOOL FOR NEW TESTS OF BTSM)

-- MEASURE $\bar{t}bW$ COUPLINGS

$$\frac{g_2}{\sqrt{2}} \left\{ W_\mu^- \bar{b} \gamma^\mu (f_1^L P_L + f_1^R P_R) t + \frac{\partial_\nu W_\mu^-}{m_W} \bar{b} \sigma^{\mu\nu} (f_2^L P_L + f_2^R P_R) t \right\}$$

(W on shell, $m_b = 0$)

	f_1^L	f_1^R	f_2^L	f_2^R
SM	1	0	0	0
ONE-LOOP QCD	$1 + \frac{\alpha_s}{\pi}$	0	0	$\frac{\alpha_s}{3\pi} \frac{m_t}{m_W} \ln \frac{1}{m_W^2}$
ONE-LOOP EW	$1 + (\cdot) \frac{\alpha_s}{\pi} \frac{m_t^2}{m_W^2}$	0	0	0
TC (SUPPORTED, CONSTRAINED, SCALING)	$1 + (\cdot)^{m_t/\text{TeV}}$			
OTHER NEW PHYSICS	?	?	?	?

WAS IT A SURPRISE THAT m_t IS LARGE?

- PENDLETON + ROSS, FIXED POINT ARGUMENT

  $m_t \sim 135$ GeV

  1981

- m_t LARGE ($\gtrsim m_W$) DRIVES EW SYMMETRY BREAKING IN SUPERSYMMETRY

  1982

  DERMEK, RAY; ALVAREZ-GAUMÉ, POLCHINSKI, WISE; DIMOPOULOS ETAL.

- VELTMAN, ELIMINATE QUADRATIC DIVERGENCE IN m_h AT ONE LOOP $\sim$ 1991

$$\longrightarrow m_t^2 > \left(\frac{3}{4} + \frac{\tan^2\theta_W}{4}\right) m_W^2 \qquad \text{FOR } m_h \to 0$$

$$m_t \gtrsim 0.42\, m_W$$

DETECT $\tilde{G}R$ AT COLLIDERS?

CARL IM
GK

IF IT IS VERY LARGE

- MOTIVATION
  - --GENERATE BARYON ASYMMETRY AT WEAK PHASE TRANSITION?
    - $\Rightarrow$ LARGE $\tilde{G}R$ NEEDED AT WEAK SCALE
    - $\Rightarrow$ TEST THIS EXPERIMENTALLY??
  - --NO TESTS -- COULD HAVE HALF OF ALL EVENTS AT FNAL FROM $\tilde{G}R$ SOURCE AND NOT KNOW IT

- WE (GK + CARL IM) ARGUE THAT EFFECTS SMALLER THAN $\sim \frac{1}{2}\%$ ARE PROBABLY UNDETECTABLE AT COLLIDERS
  - --CLEAR STATISTICALLY AT FNAL, NLC
  - --SSC/LHC $\longrightarrow \sim 10^8\, \tilde{t}\tilde{t},\ 10^9\, W, \ldots$
  - --TWO KINDS OF REASONS:
    - DETECTORS NOT CP-INVARIANT
    - IRREDUCIBLE SM BACKGROUNDS

    +

    STATISTICS TOO LIMITED TO DEAL WITH THESE PROBLEMS BY CUTS, MEASUREMENTS, ETC

DETECTOR EFFECTS

(J. AMIDEI)

— ELECTRIC FIELD ASYM $\sim 10^{-3}$ (?)

— NON-UNIFORM MAGNETIC FIELD $\sim 10^{-3}$ (?)

— CRACKS, ETC $\sim 10^{-3}$ (?)

- MAYBE SOME OR ALL BETTER THAN 10^{-3} — BUT
- TO BELIEVE AN EFFECT WOULD HAVE TO SHOW THIS EXPERIMENTALLY
- HOW? PROBABLY STUDY $W^{\pm}$
- SDC, GEM DETECT $\sim 10^{7}$ $W \to \ell\nu$
- SO STATISTICAL ERROR $\gtrsim \frac{1}{2} 10^{-3}$ ON ANY MEASUREMENT
- SEVERAL INDEPENDENT EFFECTS
  $\Rightarrow$ EXPERIMENTAL SYSTEMATIC ERRORS $\gtrsim$ FEW $\times 10^{-3}$
- BUT TO CLAIM A NEW EFFECT NEED MANY σ
- SO EFFECT PROBABLY MUST BE LARGER THAN $\sim \frac{1}{2}\%$

IRREDUCIBLE SM BACKGROUNDS

① — CAN MIMIC SOME EFFECTS BY FSI

e.g. 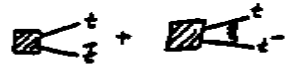

$\Rightarrow$ "CR-VIOLATING" TOP TRANSVERSE POLARIZATION $\sim$ 1-2%

- CAN CALCULATE + CORRECT BUT LEFT WITH UNCERTAIN EFFECT $\sim$ FEW $\times 10^{-3}$
- TOP WIDTH, W WIDTH, ETC $\sim 10^{-3}$ (?)

② — IN pp COLLISIONS INITIAL STATE NOT CP EIGENSTATE, SO HAVE TO CORRECT FOR STRUCTURE FUNCTION EFFECTS, SEVERAL PROCESSES CONTRIBUTING, ETC $\Rightarrow 10^{-3}$ EFFECTS

③ — BACKGROUNDS — NO INTERESTING SAMPLE CLEAN
— GET EW + QCD BACKGROUNDS THAT MIMIC SIGNALS
— IN PRINCIPLE BACKGROUND NOT CR BUT FSI IN BKG MIMIC CR SOMETIMES

e.g. $t\bar{t}$ HAS Wjj BACKGROUND

$\sim \frac{m_t}{m_W} f(\sin^2\theta_W)$ $\sim$ FEW %

④ — ALL EFFECTS THAT DEPEND ON TOP SPIN CAN BE INDUCED BY HADRONIZATION (NOTE POLARIZED Λ's)
— PROBABLY SIGNIFICANT FOR SSC IF $M_t \lesssim 160$ GeV, $|y| < 2.5$ (L. ORR) — MAYBE BETTER AT FNAL

TO CLAIM DETECTION OF CR $\sim \frac{1}{2}\%$ MUST SHOW ALL SUCH EFFECTS ABSENT AT LEVEL $\sim 10^{-3}$

IF ONLY EFFECTS $\gtrsim \frac{1}{2}\%$ ARE DETECTABLE,

ANALYSIS SIMPLER:

$|M|^2 =$ 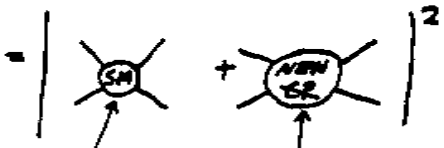

ONLY TREE LEVEL NOT $\lesssim 10^{-3}$

SO THIS MUST INTERFERE WITH SM TREE PROCESS (NONTRIVIAL CONSTRAINT)

→ CAN LIST ALL PROCESSES WITH SM EXTERNAL PARTICLES

e.g. STUDY $\bar{t}tH$ VERTEX

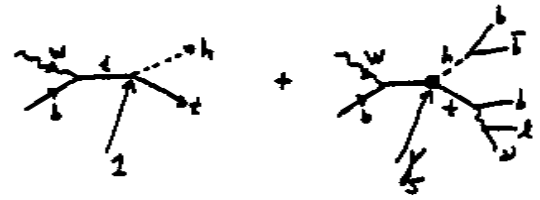

INTERFERENCE TERM IN CROSS SECTION

$$\sim \vec{S}_t \cdot (\vec{\text{beam}} \times \vec{t})$$

TOP DECAY DISTRIBUTION $d\Gamma \sim 1 + P_t \cos\theta_{\hat{S}_t \hat{\ell}^+}$

$$\rightarrow \underbrace{n_{\ell^+\uparrow} - n_{\ell^+\downarrow}}_{\text{WRT } \vec{\text{beam}} \times \vec{t}} \neq 0 \quad \text{IF ER}$$

OBSERVABLE?

- m_t, m_h KNOWN
- TRIGGER ON $\ell^+ + \not{E}_T + \geq 2 b'$s
- REQUIRE $m_{\underset{\text{JETS} \neq b}{bb}} = m_h$, $m_{\ell^+\nu b} = m_t$, NO "HARD"

IF NO EFFECT SEEN ⟹ LIMIT ON $\mathcal{L}_{ER} = \Delta \bar{t} \gamma_5 t h$, MAYBE CONSTRAIN BARYON ASYMMETRY IDEAS

OTHER PROCESSES -- EACH INTERFERES WITH A SM PROCESS WITH SAME EXTERNAL PARTICLES

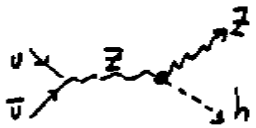

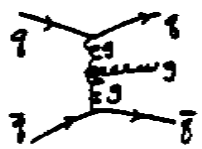

Standard Model Limits on the Top Quark Mass

JAMES PILCHER

University of Chicago
Chicago, IL 60637

ABSTRACT

A review of recent electroweak measurements is presented with special emphasis on those associated with the Z^0. A prediction of the top quark mass is obtained in the context of the minimal standard model. Uncertainty in the Higgs mass is also discussed together with the expected improvement from an accurate direct measurement of the top quark mass.

STANDARD MODEL LIMITS ON TOP QUARK MASS

- will review status of electroweak observables
  - special emphasis on Z^0 physics
- comments on expected evolution
- implications of an accurate direct measurement of M_t
- special thanks to D. Schaile - Univ. of Freiburg

A. Introduction

1. Electroweak Theory

fermions: $\begin{pmatrix}\nu_e\\ e^-\end{pmatrix}\begin{pmatrix}\nu_\mu\\ \mu^-\end{pmatrix}\begin{pmatrix}\nu_\tau\\ \tau^-\end{pmatrix}$ $\begin{pmatrix}u\\ d\end{pmatrix}\begin{pmatrix}c\\ s\end{pmatrix}\begin{pmatrix}t\\ b\end{pmatrix}$

interacting via gauge bosons $\gamma, Z^0, W^\pm$

Born level couplings determined by M_Z, M_W, α

or equivalently M_Z, G_F, α

G_F accurately measured by μ lifetime

reflects M_W

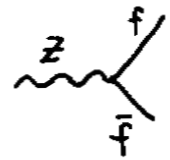

$v = I_3^f - 2Q_f \sin^2\theta_W$

$a = I_3^f$

$\cos\theta_W = \frac{M_W}{M_Z}$

$G_F = \frac{\pi\alpha}{\sqrt{2}} \frac{1}{M_W^2 \sin^2\theta_W}$

- predicts cross sections, decay rates, asymmetries
  - expected accuracy a few percent (most cases)
- measurements now possible with accuracy better than 1%
  - FNAL, LEP, SLAC can produce W's Z's in the lab
  - heroic efforts on parity violation in atoms, ν scattering
- corrections to Born level predictions are measurable

2. Higher Order Corrections

3 classes

QED

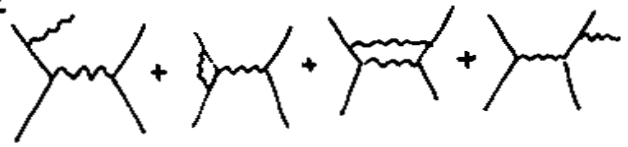

- can be factored from other corrections
- depend on experimental cuts
- computed to full $O(\alpha)$, leading $O(\alpha^2)$, exponentiation of soft photon effects

- not interesting physics but must be corrected for

QCD

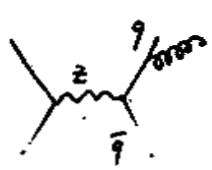

$$\Gamma_{had} = \Gamma_{had}^{0}\left(1 + \underbrace{\frac{\alpha_s}{\pi} + 1.4\left(\frac{\alpha_s}{\pi}\right)^2}_{4\%} + \cdots\right)$$

Γ_{had} measured to 0.4%

- can measure α_s in studies of Z^0 hadronic final states
  - jet ratios, energy-energy correlations, event shapes
  - extract from Z^0 line shape analysis

Electroweak Corrections

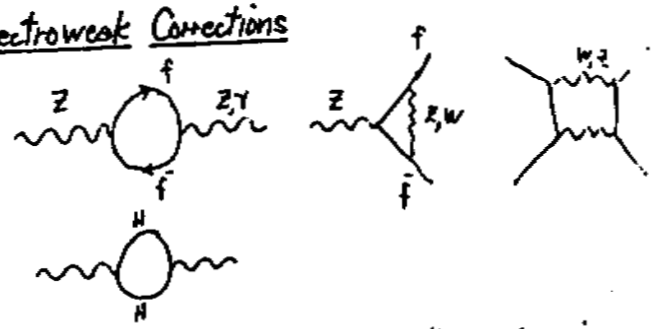

- all calculable in electroweak theory knowing M_Z, G_F, α and M_{top}, M_{Higgs}

- assume t couples like any other u-type quark
  - despite 30 x heavier mass

- assume minimal S.M. Higgs - single Higgs doublet
  - simplest
  - results depend weakly on M_H $\left(\propto \ln\left(\frac{M_H}{M_W}\right)\right)$

- modifications to basic formalism
  Born level relations preserved to good approx^n if

$$\sin^2\theta_W \to \sin^2\bar{\theta}_W$$

$$G_F \to \rho G_F \quad \text{in N.C. processes}$$

$$\rho = \frac{1}{1-\Delta\rho}$$

$$\Delta\rho = a M_t^2 + \cdots$$

- present analysis does not depend on this approximate treatment

- use results of a full calculation
  - all one loop effects
  - dominant 2 loop effects

ZFITTER by Bardin et al. Comp. Phys. Comm. 59, 303 (1990)

$$\left.\begin{matrix} M_Z \\ G_F \\ \alpha \\ M_t \\ M_H \\ \alpha_s \end{matrix}\right\} \longrightarrow \boxed{\text{ZFITTER}} \longrightarrow \begin{matrix}\text{Electroweak} \\ \text{Observables}\end{matrix}$$

B. Electroweak Measurements

1. Z^0 Parameters

primarily LEP results from 1990 + 1991 data
1.7×10^6 Z^0 events (~450k / experiment)
~ 40% of total data now in hand

Lineshape + Cross Sections

measure $\sigma(e^+e^- \to \text{hadrons})$ vs E_{cm}

γZ interference $\lesssim 1\%$

$$\sigma_{ff}(s) = \frac{s}{(s-M_Z^2)^2 + M_Z^2\Gamma_Z^2}\left\{\frac{12\pi\,\Gamma_{ee}\Gamma_{ff}}{M_Z^2} + \frac{I_{\gamma Z}(s-M_Z^2)}{s}\right\}$$

$$+ \frac{4\pi}{3}\,\frac{M_Z^4 Q_f^2 \alpha^2}{s}$$

γ ~1%

$$\approx \frac{12\pi}{M_Z^2}\,\Gamma_{ee}\Gamma_{ff}\left[\frac{s}{(s-M_Z^2)^2 + M_Z^2\Gamma_Z^2}\right]$$

can perform model independent fit for M_Z, Γ_Z, $\sigma_{ff}(s=M_Z^2)$

M_Z

- experimental result reflects absolute energy scale of machine
  - checked with protons on e^- orbit at 20 GeV
    - measure $\Delta\nu_{ep}$
  - resonant depolarization at 93 GeV $\Rightarrow \delta E \sim 1$ MeV
  - flux loop calibration to track time dependent effects

$\Rightarrow \delta M_Z = 6.3$ MeV

- residual non-linearities
  - temperature effects
  - tidal effects
- explore with further depolarization studies
- error dominated by systematic on energy
- averaging procedure

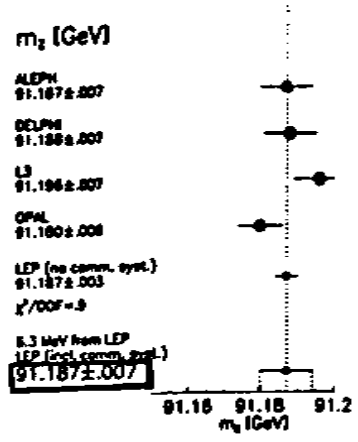

Γ_Z

- based on scan of 7 points
- current statistical error ≈ systematic error
- systematics
  - energy setting error ~ 3 MeV
  - non-linearities in E scale ~ 1.5 MeV

some hope for modest improvement

- Γ_Z vs M_t plot

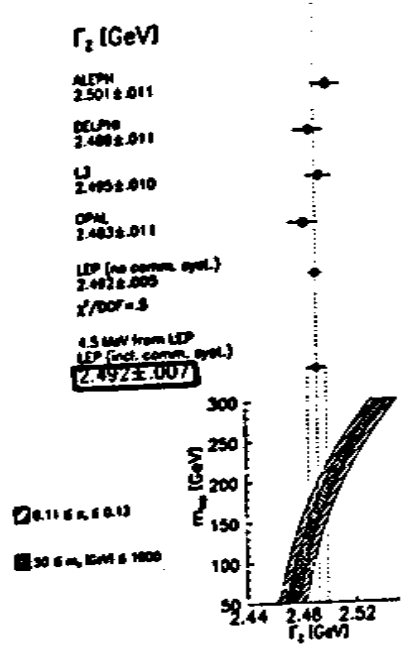

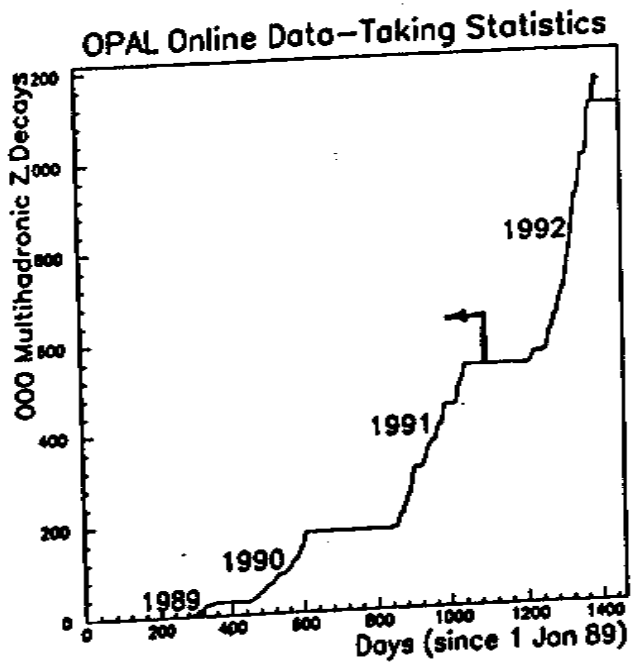

- account for radiative effects by convolution

$$\sigma_{obs}(s) = \int_{s_{min}}^{s} \sigma_{th}(s')\, \varphi(s,s')\, ds'$$

- large effects
  - peak cross section reduced by 30%
- several independent treatments compared
- observed line shape well described
- extract $M_Z, \Gamma_Z, \sigma_{had}^{pole}$ from the fit

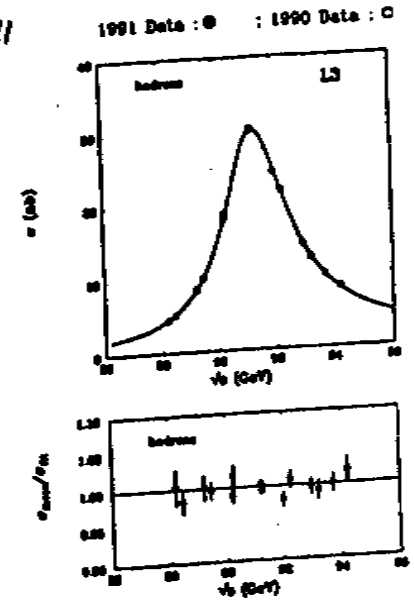

Derived Quantities

$\Gamma_{inv}/\Gamma_{lept}$

- insensitive to M_t, M_H
  - excellent S.M. test

$\Rightarrow N_\nu = 3.04 \pm 0.04$

Γ_{lept}

- independent of α_s
- significant M_t dependence
- requires absolute cross section determination

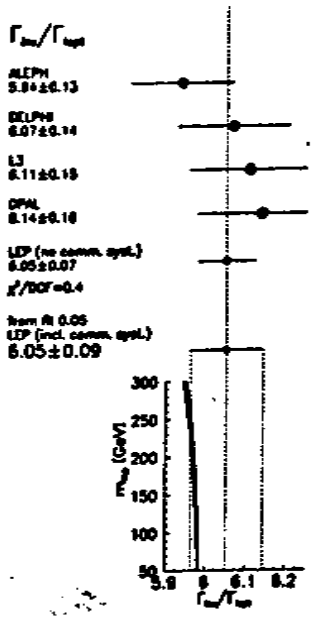

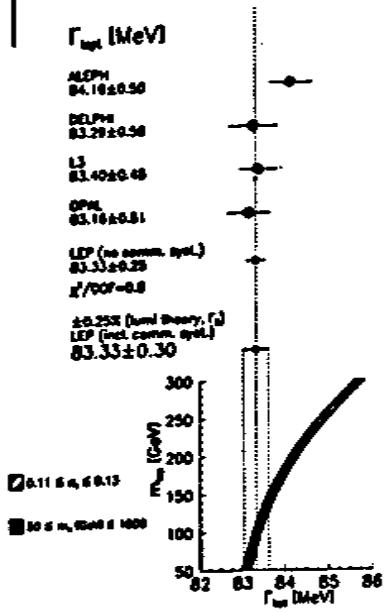

2. Asymmetries

Introduction

- neutral current couplings not L-R symmetric

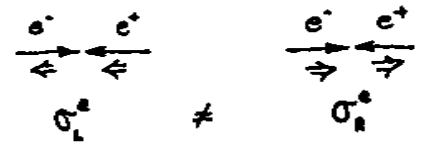

produced with net polarization by unpolarized beams ~14%

fermion pairs from Z^0 decay have net polarization

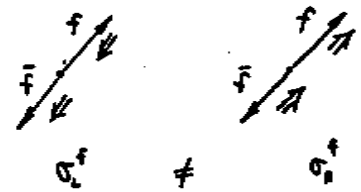

can define asymmetries depending on
- initial state helicity
- final state helicity
- scattering angle

σ_{had}^{pole}

- detector acceptance ~99.5%
- background correction ~0.4%
- needs absolute luminosity
  - from small angle Bhabha scattering
  - exptl. systematic errors ~0.7%
  - Theoretical uncertainty ~0.3%

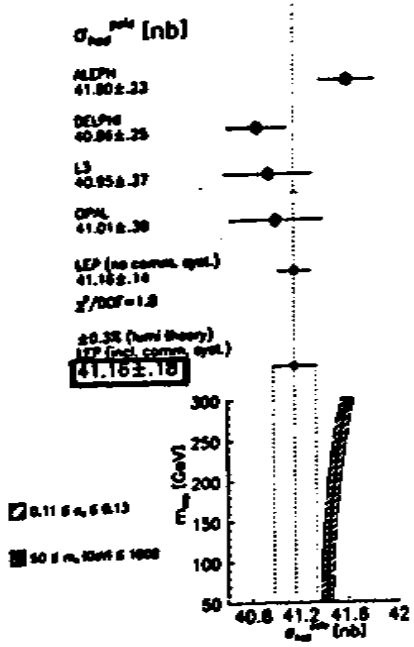

Leptonic Partial Widths

$$R_\ell = \frac{\Gamma_{had}}{\Gamma_{\ell\ell}}$$

- measure for each lepton species
  - good agreement (see later)

$$= \frac{\sigma_{had}}{\sigma_{\ell\ell}}$$

- must correct $\sigma_{e^+e^-}$ for t-channel effects

- can extract individual partial widths using $\sigma_{had}, \Gamma_\ell, R_\ell^{e,\mu,\tau}$

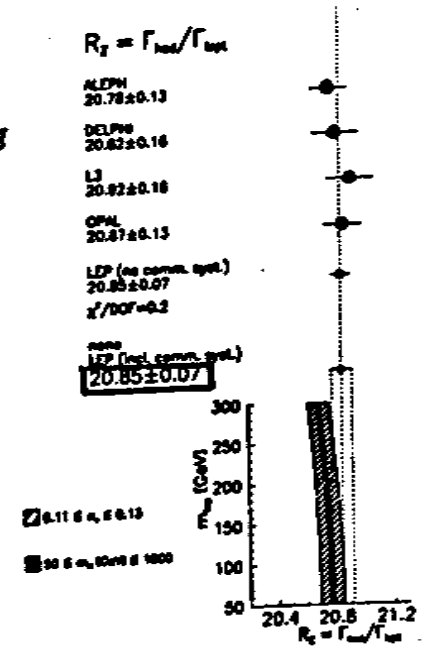

- initial state polarization asymmetry

$$A_{LR} = \frac{\sigma_L^e - \sigma_R^e}{\sigma_L^e + \sigma_R^e}$$

$$= \frac{2 g_A^e g_V^e}{(g_A^e)^2 + (g_V^e)^2} = P_e \qquad |g_A| \sim 10 |g_V|$$

$$\sim 2\left(\frac{g_V^e}{g_A^e}\right) \sim 2(1 - 4\sin^2\theta_W) \sim 14\%$$

- final state polarization asymmetry

$$A_{PL} = \frac{\sigma_R^f - \sigma_L^f}{\sigma_R^f + \sigma_L^f}$$

$$= -\frac{2 g_A^f g_V^f}{(g_A^f)^2 + (g_V^f)^2} = P_f$$

$$\sim -2\left(\frac{g_V^f}{g_A^f}\right)$$ can measure using τ decays

- forward-backward polarization asymmetry
  - polarization of f depends on θ

$$A_{FB}^{Pol} = \frac{A_{PL}(\theta < \frac{\pi}{2}) - A_{PL}(\theta > \frac{\pi}{2})}{A_{PL}(\theta < \frac{\pi}{2}) + A_{PL}(\theta > \frac{\pi}{2})}$$

$$= -\frac{3}{4} P_e$$

$$\sim -\frac{3}{2}\left(\frac{g_V^e}{g_A^e}\right)$$ also measure in τ-decays

forward-backward charge asymmetry (unpol. beam)

$$A_{FB} = \frac{\sigma(\theta < \frac{\pi}{2}) - \sigma(\theta > \frac{\pi}{2})}{\sigma(\theta < \frac{\pi}{2}) + \sigma(\theta > \frac{\pi}{2})}$$

$$= \frac{3}{4} P_e P_f$$

$$\sim 3\left(\frac{g_V^e}{g_A^e}\right)\left(\frac{g_V^f}{g_A^f}\right)$$

$$\sim 3(1 - 4\sin^2\theta_W)^2 \quad \sim 1.5\% \text{ in s.m. for } \ell^+\ell^- \quad \sim 9\% \text{ for } b\bar{b}$$

Measurements

A_{FB}^{pole}

- extract from scan of Z resonance each lepton species separately
- radiative corrections essential

$$A_{FB}^{obs}(s) = \frac{1}{\sigma_f(s)} \int_{s_{min}}^{s} \rho_1(s,s')\, \sigma_{FB}^{0}(s')\, ds'$$

$$\sigma_{FB}^{0} = \sigma_F^{0} - \sigma_B^{0}$$

$A_{FB}^{obs}(M_Z) \sim A_{FB}^{pole} - 0.017$

checked by many groups (ee)
- full $O(\alpha)$; $O(\alpha^2)$ corrections + soft photon resummation
- agreement to $\sim 2\times10^{-4}$ (absolute)

- average A_{FB}^{pole} for all lepton species is shown

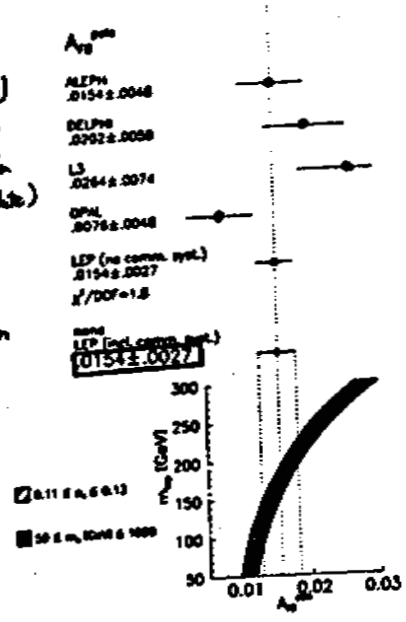

- compare A_{FB}^{pole} and R_Z for e^+e^-, $\mu^+\mu^-$, $\tau^+\tau^-$
  - test of universality of neutral current couplings

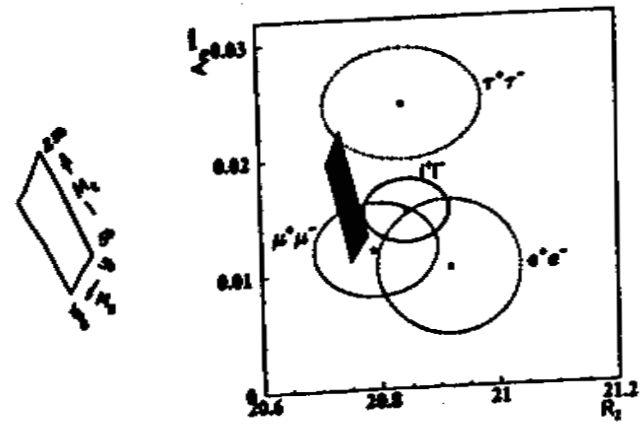

$A_{FB}^{q\bar{q}}$

- measurements done averaging over quark flavor
  - use charge of leading hadrons to discriminate q from $\bar{q}$
  - heavily Monte Carlo dependent

- b-quarks can be tagged via semileptonic decays + kinematic cuts

  use lepton charge to resolve b-jet from $\bar{b}$-jet
  - must correct for mixing

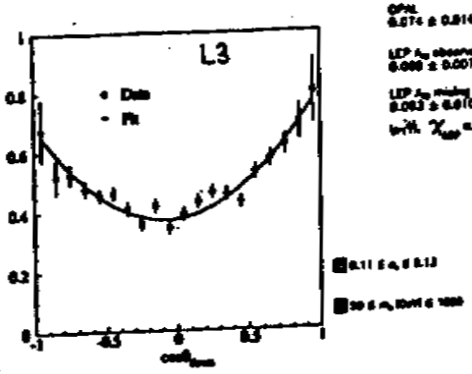

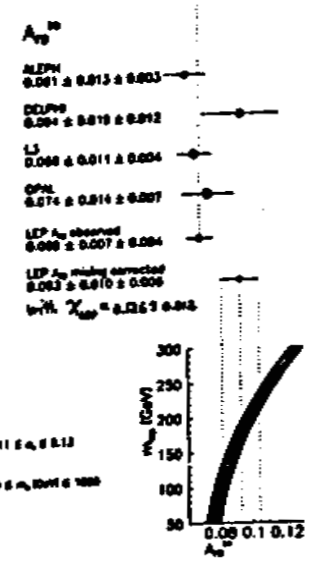

P_τ - τ Polarization

- samples of ~15K τ-pairs per expt.
- modes used

$\tau \to \pi\nu$
$\to e\nu\nu$
$\to \mu\nu\nu$
$\to \rho\nu$
$\to a_1\nu$

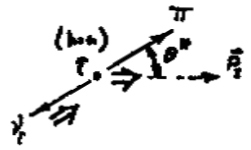

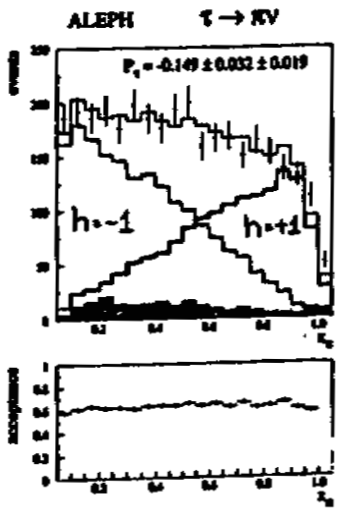

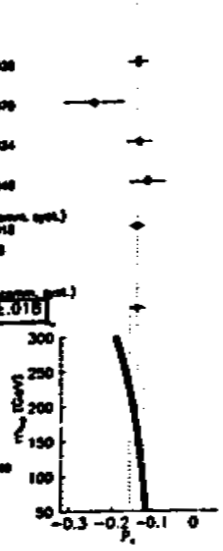

$A_{FB}^{\tau\tau}$ τ F-B polarization asymmetry

- τ polarization depends on polar angle θ because Z^0 is polarized

$P_\tau = 0.120 \pm 0.024 \pm 0.010$ ALEPH (1991+1990)
0.80 ± 0.13 OPAL (1990)

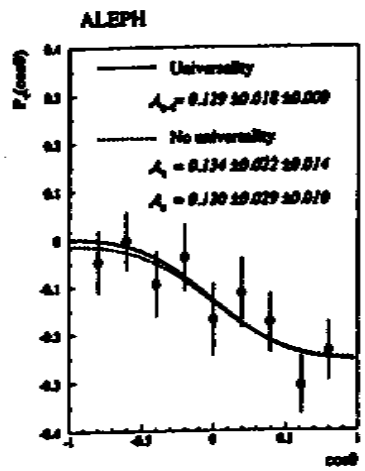

Universality check

- use lepton $A_{FB}^{\ell\ell}$, $\Gamma_{\ell\ell}$, P_τ, P_e to compare g_A and g_V for each lepton species

- conclusion
  - ok to average in SM fit

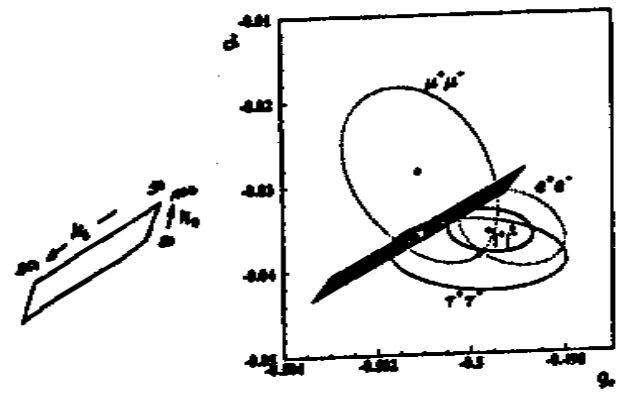

C. Fit of Z^0 Parameters

vary M_t M_H to give best SM fit to data
- allow M_Z to vary within errors
- fit with and without α_s constraint from QCD studies

minimize

$$\chi^2 = \sum_i \frac{\left[x_i^{obs} - x_i^{SM}(M_t, M_H, M_Z, \alpha_s)\right]^2}{\sigma_i^2} + \frac{\left(M_Z^{obs} - M_Z\right)^2}{\sigma_{M_Z}^2} + \frac{\left(\alpha_s^{obs} - \alpha_s\right)^2}{\sigma_{\alpha_s}^2} S_{\alpha_s}$$

- also include correlations

x_i^{SM} from ZFITTER

$\alpha_s^{obs} = 0.120 \pm 0.006$

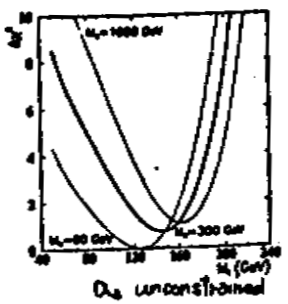

α_s unconstrained

$M_t = 145^{+23}_{-28}{}^{+17}_{-20}$ GeV

$\chi^2/DOF = 3.0/4$

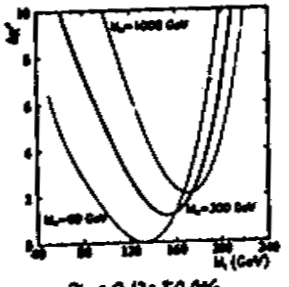

$\alpha_s = 0.120 \pm 0.006$

$M_t = 153^{+21}_{-20}{}^{+18}_{-20}$ GeV

$\chi^2/DOF = 4.1/5$

consistency checks

- compare α_s from unconstrained α_s fit with value measured in analyses of hadronic final states
- once M_t, M_H are fixed M_W is specified
  - compare with CDF + UA2 measurements

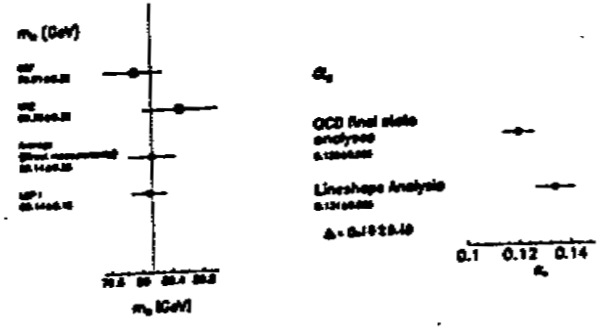

D. Fit with additional S.M. Observables

W mass

CDF $M_W = 79.91 \pm 0.39$ GeV

UA2 $M_W/M_Z = 0.8813 \pm 0.0036 \pm 0.009$

ν scattering (CCFR, CDHS, CHARM)

$\sin^2\theta_W = 0.2283 \pm 0.0052$ (Rolandi - Dallas)

atomic parity violation in Cesium

$$Q_W \sim \rho\left[Z(1-4\sin^2\theta_W) - N\right]$$

$$= -71.04 \pm 1.58 \pm 0.88$$

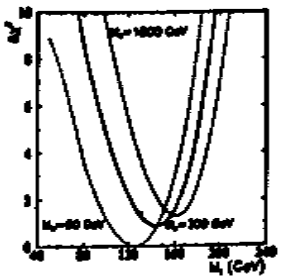

α_s unconstrained

$M_t = 145^{+19}_{-21}{}^{+17}_{-19}$ GeV

$\chi^2/DOF = 4.7/7$

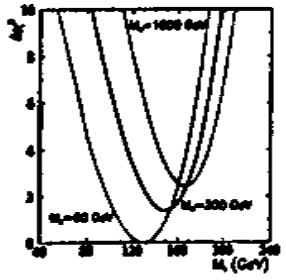

α_s constrained

$M_t = 150^{+18}_{-20}{}^{+17}_{-19}$ GeV

$\chi^2/DOF = 6.6/8$

Consistency checks

- how do results change for different sub-sets of observables?

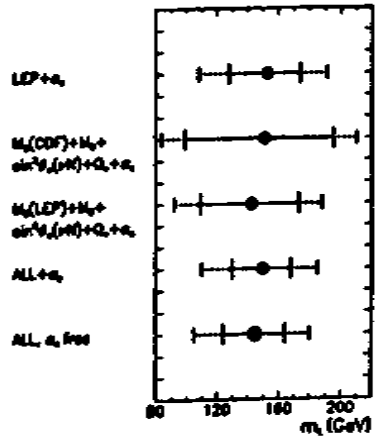

check contribution to χ^2 from each observable

expect ~1/3 of observables outside $\pm 1\sigma$

or.

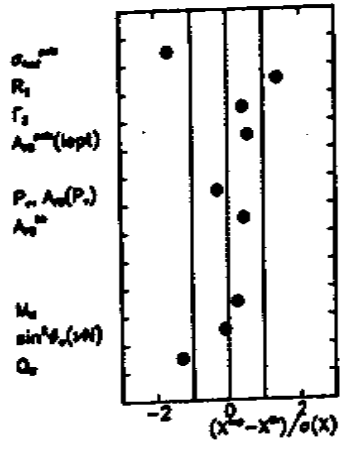

why does χ^2 vary so strongly with M_H

- not true M_H sensitivity
- discussed by D. Schaile, Z Phys. C54, 387 (1992)

fluctuations of data about S.M. values lead to large apparent M_H sensitivity (fluctuations large wrt. variation from M_H)

demonstration using mock data

- consider SM predictions for M_Z = 91.187 GeV, M_t = 126 GeV, M_H = 60 GeV
- look at $\chi^2(M_T, M_H)$ using σ_i of current measurements but SM values for the observations

i.e. no fluctuations in the "data"

- true M_H sensitivity seen

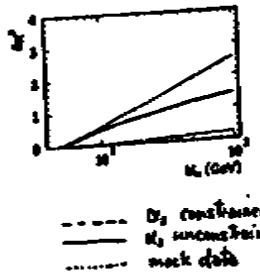

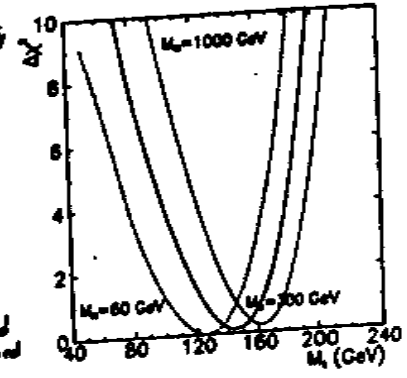

Value of direct M_t measurement on M_H estimate

- assume continued progress on EW observables
  - see D. Schaile, ibid.
- if $M_H = 300$ GeV $\quad \delta M_t = 10$ GeV $\Rightarrow \delta M_H = {}^{+270}_{-150}$ GeV

  $\delta M_t = 5$ GeV $\quad \delta M_H = {}^{+170}_{-110}$

  $\delta M_t = 0.5$ GeV $\quad \delta M_H = {}^{+28}_{-23}$
- could consider in context of other new physics

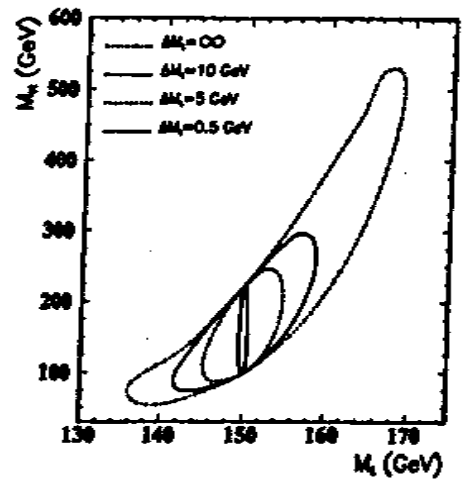

E. Conclusions

1. Best current estimate of Top mass is:

$$M_t = 145 \pm 20 \pm 18 \text{ GeV}$$

variation for $60 < M_H < 1000$ GeV

data are good enough so there is little loss in precision using no α_s constraint

2. Data currently in hand should give error of $\pm 14 \pm 18$ GeV

3. Direct M_t measurement will sharpen sensitivity to new physics.

Input data	M_t (GeV)	χ^2/NDOF
σ, $A_{FB}^{hot,cob}$	$145^{+20}_{-24}{}^{+10}_{-10}$	4.8/3
M_Z(LEP), $\mathcal{P}_{hot}$	$166^{+20}_{-20}{}^{+10}_{-10}$	0/0
M_Z(LEP), A_{FB}^b	$100^{+10}_{-14}{}^{+17}_{-10}$	0/0
LEP only	$\boxed{153^{+21}_{-26}{}^{+10}_{-10}}$	4.9/3
M_Z(LEP), $\sin^2\theta_W(\nu N)$	$138^{+20}_{-20}{}^{+10}_{-17}$	0/0
M_Z(LEP), M_W	$146^{+20}_{-20}{}^{+10}_{-10}$	0/0
M_Z(CDF), M_W, $\sin^2\theta_W(\nu N)$, Q_W	$151^{+20}_{-20}{}^{+10}_{-10}$	2.2/3
M_Z(LEP), M_W, $\sin^2\theta_W(\nu N)$, Q_W	$\boxed{143^{+20}_{-20}{}^{+11}_{-17}}$	2.3/3
LEP + M_W, $\sin^2\theta_W(\nu N)$, Q_W	$\boxed{150^{+20}_{-20}{}^{+17}_{-10}}$	6.5/3

Table 1: Consistency checks for top mass fits to data from LEP, UA2, CDF, CHARM, CDHS and CCFR. The central value and the 1st error refer to $M_H = 300$ GeV, fixed. The 2nd error gives the variation of the central value for Higgs mass values spanning the interval $60 < M_H(\text{GeV}) < 1000$. For all fits the value of α_s has been constrained to $\alpha_s(M_Z^2) = 0.120 \pm 0.006$. Input data: $\sigma = M_Z + \Gamma_Z + R_b + \sigma_{had}^{peak}$, $A_{FB}^{hot,cob}$, $\mathcal{P}_{hot}$, A_{FB}^b from LEP; $\sin^2\theta_W(\nu N)$ from CHARM, CDHS and CCFR; M_Z from CDF; M_W from CDF and UA2; Q_W from atomic parity violation in Cs.

Input data	M_t (GeV)	$\alpha_s(M_Z^2)$	χ^2/NDOF
a) with α_s constraint			
LEP	$153^{+11}_{-16}{}^{+10}_{-10}$		4.9/5
ALL	$150^{+10}_{-16}{}^{+17}_{-10}$		6.6/8
b) without α_s constraint			
LEP	$145^{+10}_{-16}{}^{+17}_{-10}$	$0.124 \pm 0.000 \pm 0.002$	3.0/4
ALL	$145^{+10}_{-16}{}^{+17}_{-10}$	$0.124 \pm 0.000 \pm 0.002$	4.7/7

Table 2: Results of top mass fits to data from LEP, UA2, CDF, CHARM, CDHS, CCFR. The central value and the 1st error refer to M_H = 300 GeV, fixed. The 2nd error gives the variation of the central value for Higgs mass values spanning the interval $60 < M_H(\mathrm{GeV}) < 1000$. For the fits in section a) the value of α_s has been constrained to $\alpha_s(M_Z^2) = 0.120 \pm 0.006$.
Input data:
LEP: $M_Z + \Gamma_Z + R_l + \sigma_{had}^{pole} + A_{FB}^{l,pole} + \mathcal{P}_{tau} + A_{FB}^{b}$
ALL: LEP + $\sin^2\theta_W(\nu N)$ from CHARM, CDHS and CCFR + M_W from CDF and UA2
+ Q_W from atomic parity violation in Cs

	LEP	ALL
M_W [GeV]	$80.14 \pm 0.15 \pm 0.01$	$80.14 \pm 0.13 \pm 0.01$
$\sin^2\theta_W$	$0.2270^{+0.0001}_{-0.0002} \pm 0.0003$	$0.2275^{+0.0001}_{-0.0002} \pm 0.0003$
$\sin^2\theta_W{}^{lept}_{eff}$	$0.2321 \pm 0.0006 \pm 0.0002$	$0.2321 \pm 0.0006 \pm 0.0002$

Table 3: Derived quantities from the fits without α_s constraint above. The central value and the 1st error refer to M_H = 300 GeV, fixed. The 2nd error gives the variation of the central value for Higgs mass values spanning the interval $60 < M_H(\mathrm{GeV}) < 1000$.

Search for the Top at Fermilab

G. P. Yeh
Fermi Lab

ABSTRACT

We present the status of top search at Fermilab. We discuss prospects in the next two years for the discovery of the top quark.

Outline of this talk:

Status of '92 Tevatron, CDF, DO
expecting lots of data in next few months
plots/numbers from '92 data expire immediately

top quark production and detection

DiLepton channel

Lepton + jets channel

Summary and Prospects

$p\bar{p}$ collisions at $\sqrt{s} = 1800$ GeV

$\sigma(total)$	$70\ mb$	$7 \times 10^{-26}\ cm^2$
$\sigma(b\bar{b})$	$30\ \mu b$	$3 \times 10^{-29}\ cm^2$
$\sigma(W)$	$20\ nb$	$2 \times 10^{-32}\ cm^2$
$\sigma(Z)$	$2\ nb$	$2 \times 10^{-33}\ cm^2$
$\sigma(M_t = 150)$	$10\ pb$	$1 \times 10^{-35}\ cm^2$

Goal for next few months

Luminosity $L = 5 \times 10^{30}\ /sec/cm^2$

$\int L dt = 25\ pb^{-1} = 2.5 \times 10^{37}\ /cm^2$

For $t\bar{t}$ detection efficiency $\approx 1\%$,

expect $\approx$ 2.5 DiLepton events if $M_t = 150$

(one event per 10^{12} collisions)

$$N_{\text{events}} = L\,\sigma\,D$$

$\int L\,dt$

L (integrated) luminosity

- 1-2 10^{30} $/cm^2/sec$ in '89 — $4\ pb^{-1}$
- 5 10^{30} $/cm^2/sec$ in '92-'93 — 25
- 1.5 10^{31} $/cm^2/sec$ in '94 — 75
- but need more
  $> 5\ 10^{31}$ $/cm^2/sec$ Main Injector — 1000

σ cross - section

- would be nice to have higher $E_{p,\bar{p}}$
  $\sqrt{s} = 2\,TeV$ in '94 ?

D detection efficiency

- e, μ, γ, $q+g$ jets, ν, τ, $W^{\pm}$, Z^0
  π^+, π^-, π^0, K^+, K^-, K^0, Λ^0 . . .
  Standard Model ingredients and mundane particles
- c, b physics already charming, beautyful
- D_{tt} increases with M_t
- CDF is a versatile Top detector
- upgrades : SVX, η-coverage, dE/dx . . .

Figure 1

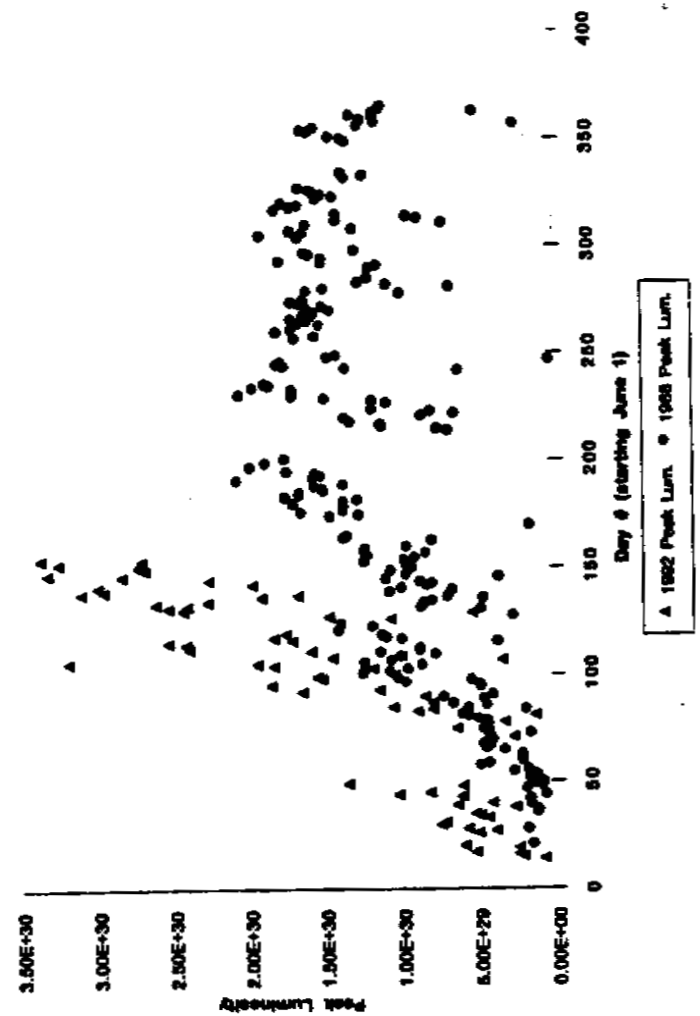

Figure 2

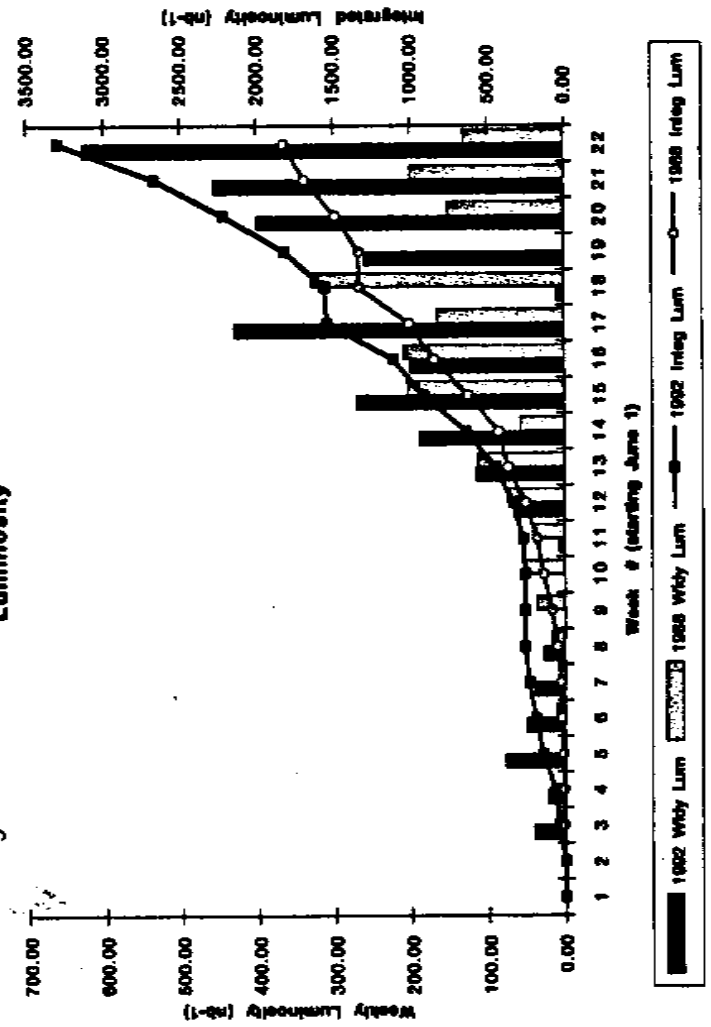

$\int L\,dt \quad (pb^{-1})$

	Goal	delivered	Recorded
'89	1	10	4
'92-'93	25	4	3 CDF
			2 DØ

In the week Nov. 9 – Nov. 15, Tevatron delivered 0.8 pb^{-1} with a peak Luminosity of 4.5×10^{30}

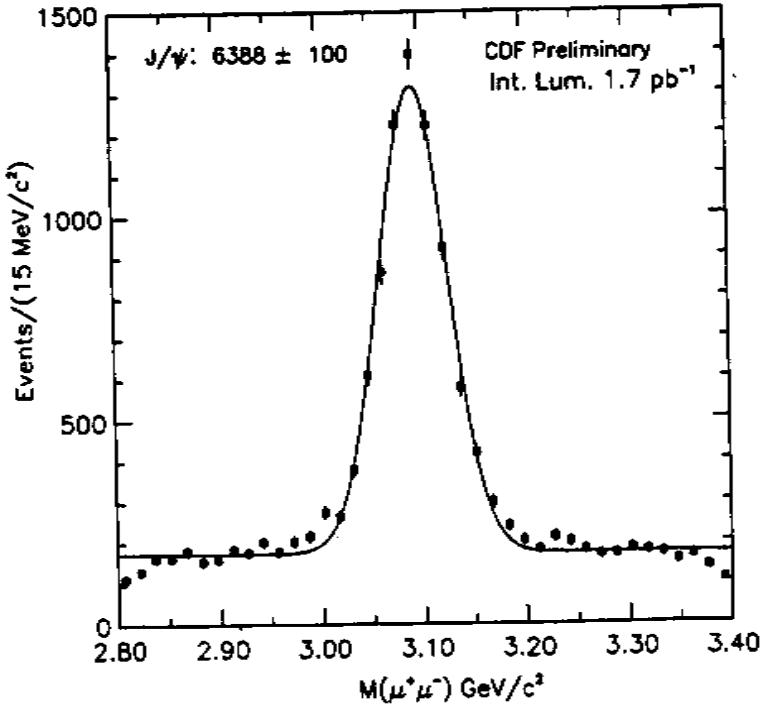

Figure 3: J/ψ sample from low P_T dimuons

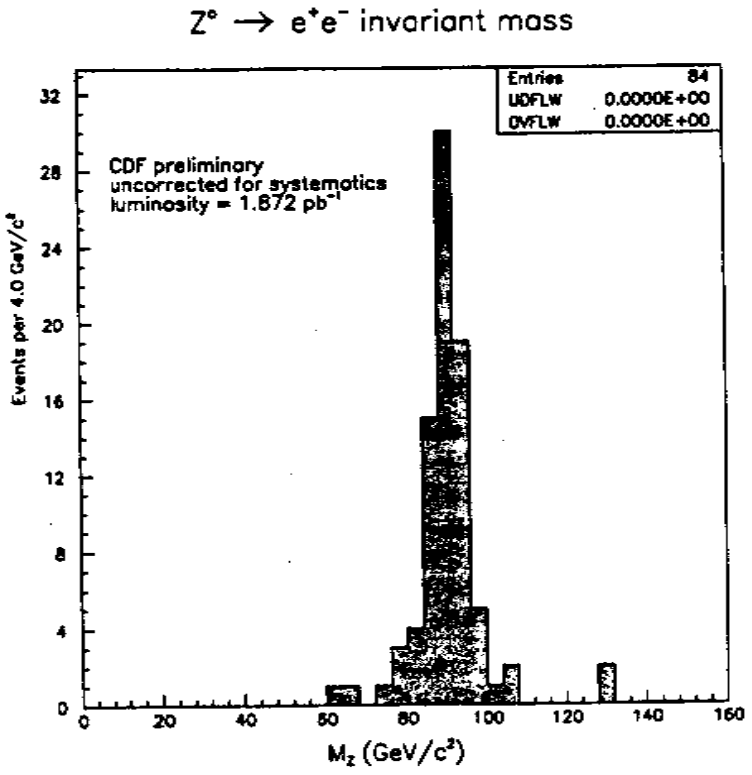

Figure 4: high P_t di-electron sample

Figures 4-8 are useful checks of high P_t lepton identification

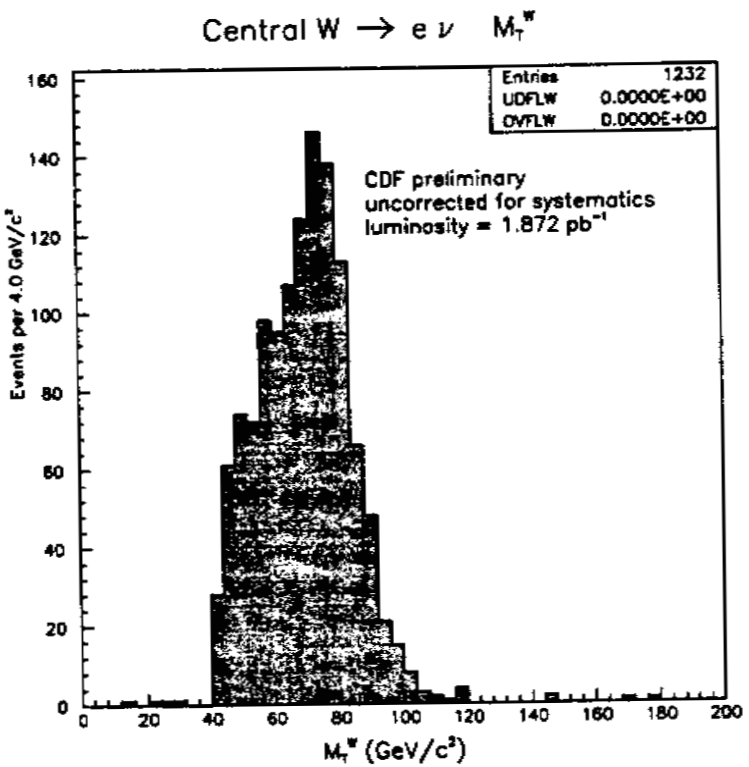

Figure 5: a sample of $W \to e\nu$ with $|\eta_e| < 1$

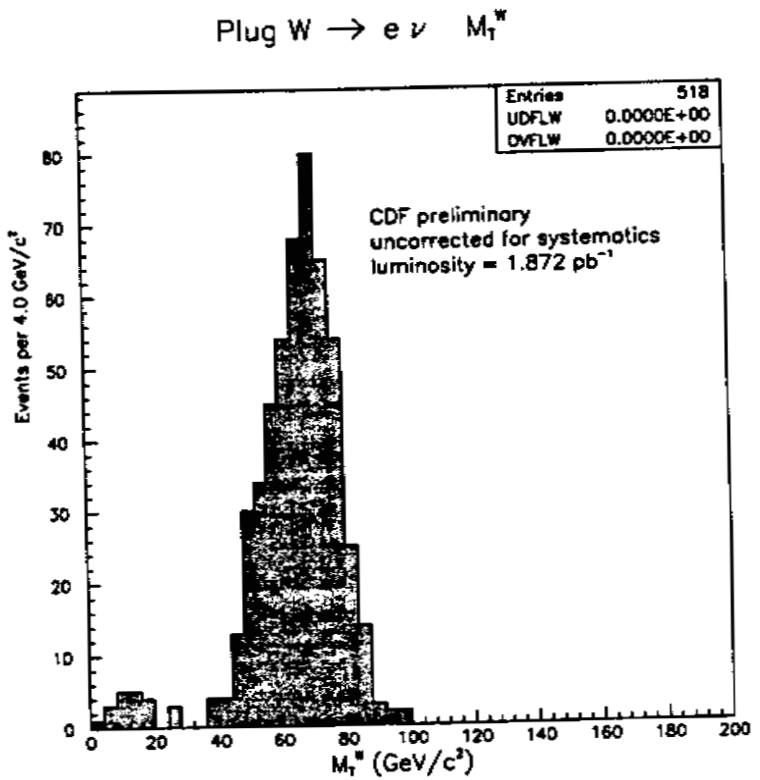

Figure 6: W candidates with $1 < |\eta_e| < 2$

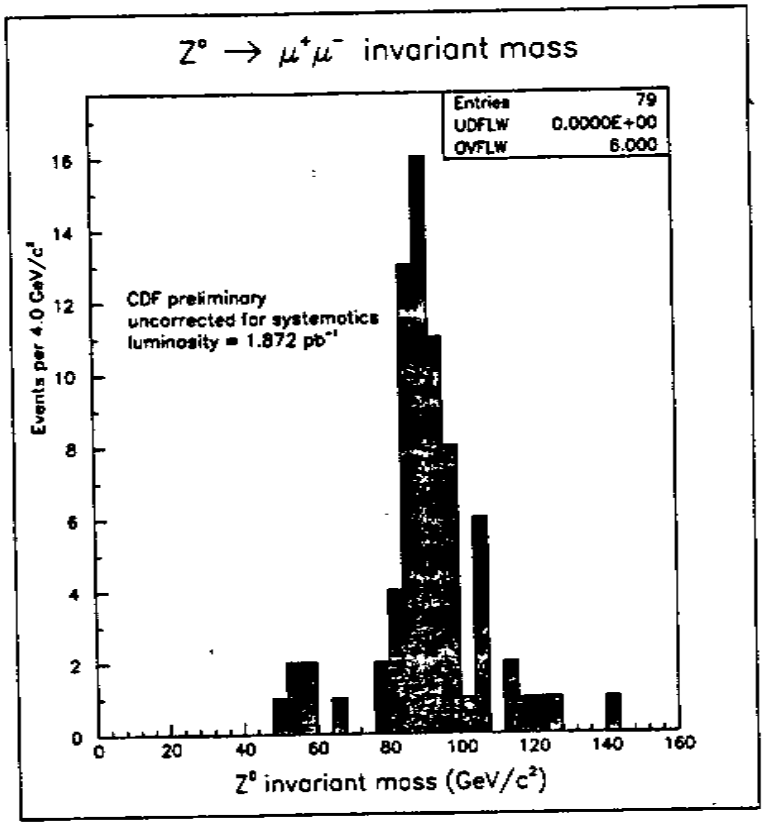

Figure 7: high P_T di-muon sample

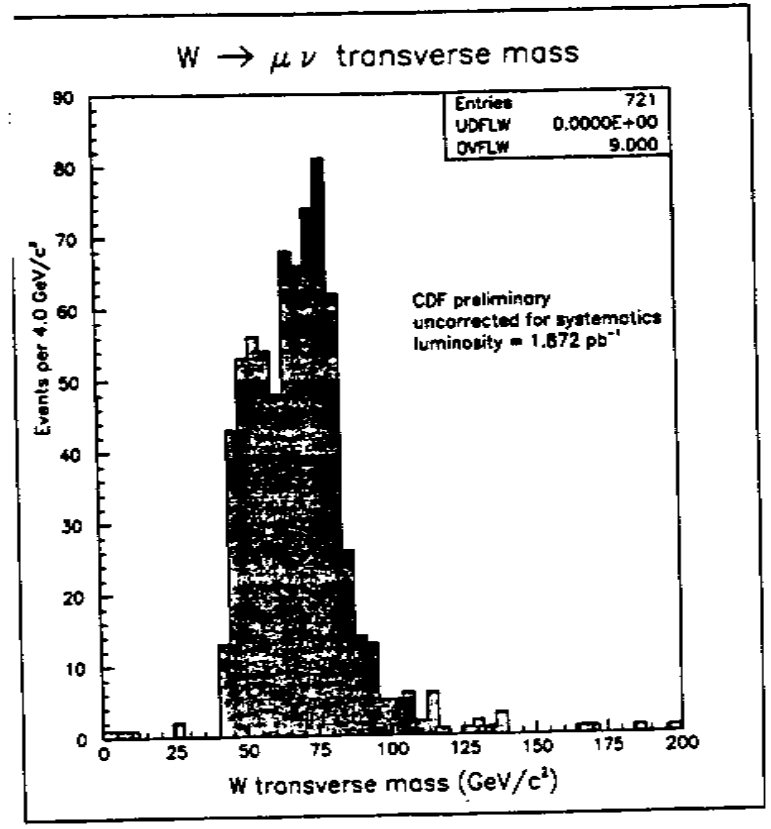

Figure 8: $W \rightarrow \mu\nu$ candidates.

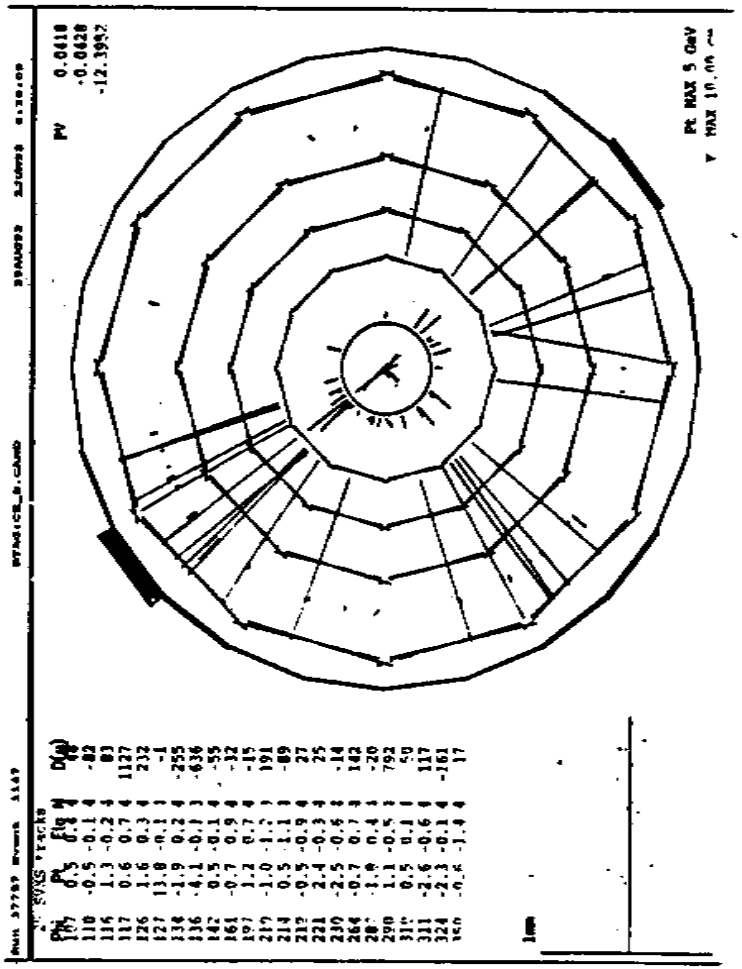

Figure 9: tracks of one event reconstructed from hits in the New Silicon Vertex detector

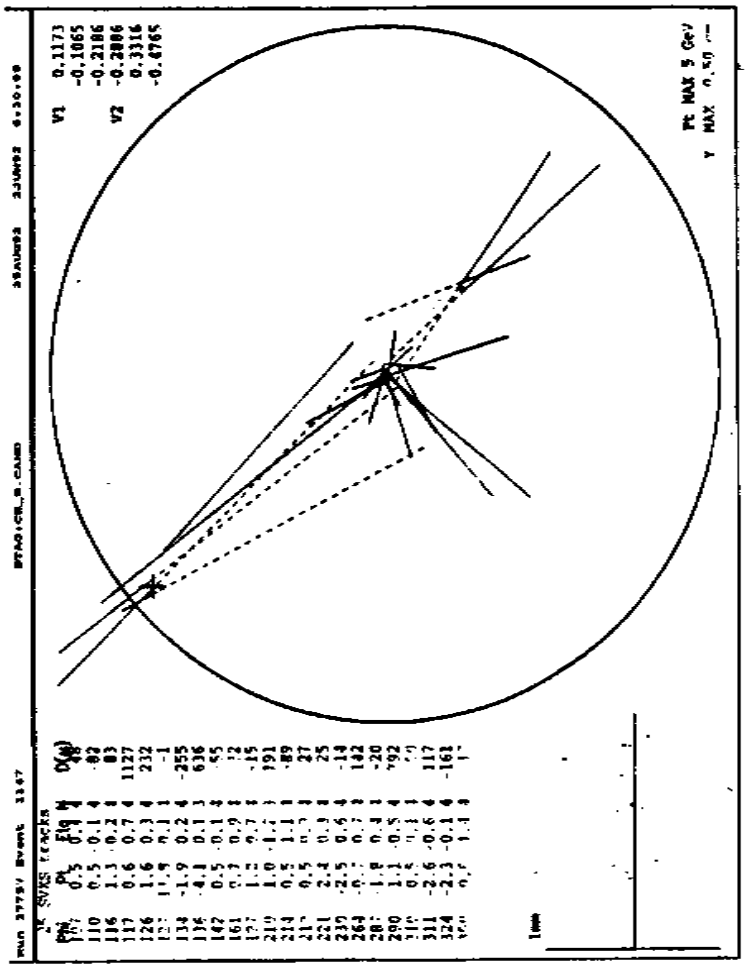

Figure 10: magnified view of the event in Figure 9. Two secondary vertices were found.

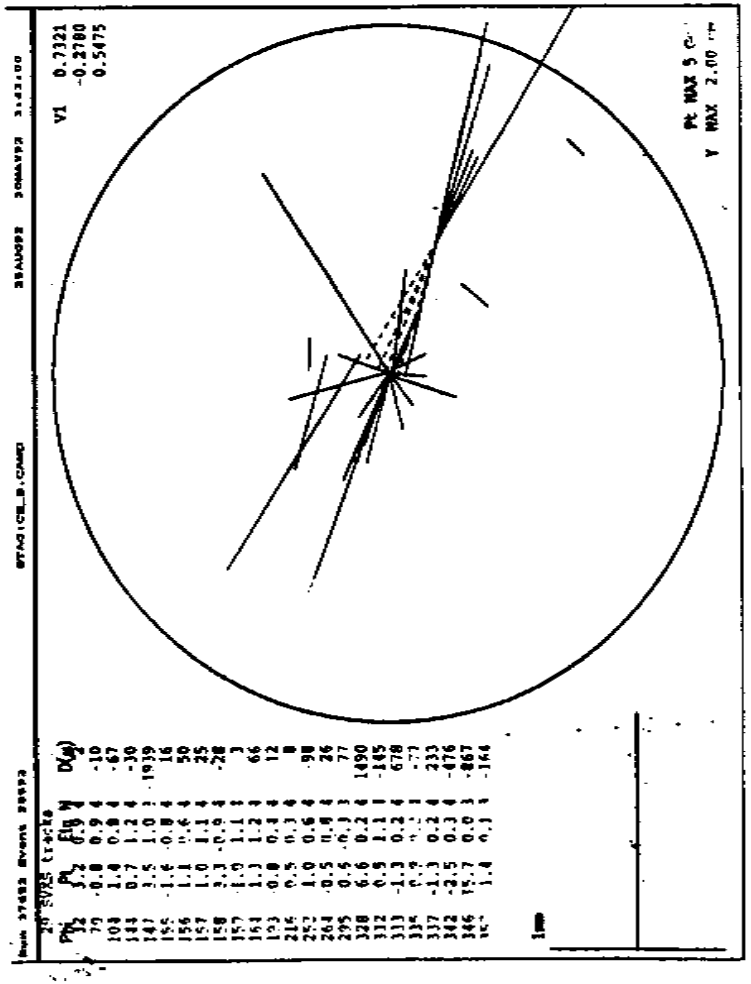

Figure 11: another event showing the secondary vertex was well identified

$p\bar{p} \to t\bar{t}$

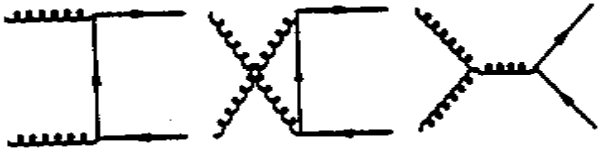

$$\sigma(S) = \sum_{ij} \int dx_1 dx_2 \, \hat{\sigma}_{ij}(x_1 x_2 S, m^2, \mu^2) \, F_i^A(x_1, \mu) F_j^B(x_2, \mu)$$

Calculation should be more reliable for large M_t

R. K. Ellis
FERMILAB-Pub-91/30-T

Top quark production cross section
at Fermilab energies

Mt	1.8 TeV	2.0 TeV	gain
	(pb)		
40	8760.	11000.	
60	1232.	1595.	
80	287.	378.	
100	90.9	120.	
120	35.3	47.0	1.33
140	15.6	21.1	1.35
160	7.65	10.4	1.36
180	3.98	5.52	
200	2.16	3.07	1.42
220	1.20	1.77	
240	0.69	1.04	
260	0.39	0.63	
280	0.23	0.38	
300	0.13	0.23	1.77

A factor of 2 in
σ, Nev, $\int L dt$ or uncertainties
Corresponds to $\Delta M_t \sim 20$ GeV

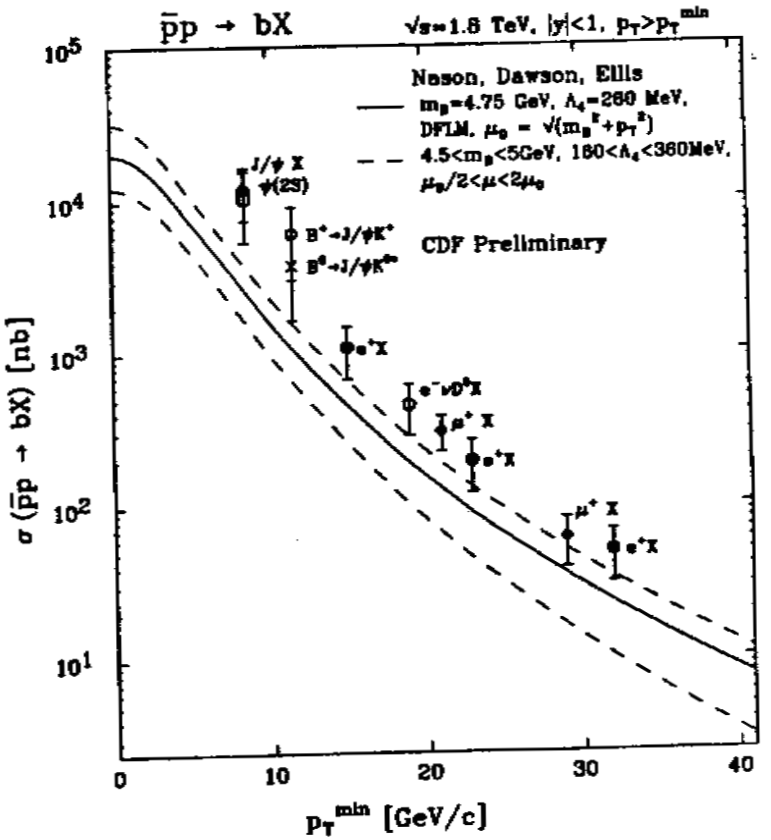

Figure 12
Comparison of measured σ_b with NDE prediction.
Agreement should be much better for σ_t

Top Decays
Searches

$t\bar{t} \rightarrow W b W b$

$t\bar{t} \rightarrow H b H b$

$\hookrightarrow \tau$

Model Independent search

e.g. $\dfrac{\Gamma(W)}{\Gamma(Z)}$

$t\bar{t} \rightarrow W b W b$

each can decay into

$e\nu$, $\mu\nu$, $\tau\nu$

and/or jet(s)

examples:

e	μ	ν	ν	$b\,\not{b}$
e	e	ν	ν	$b\,\not{b}$
μ	μ	ν	ν	$b\,\not{b}$
e	τ	ν	ν	$b\,\not{b}$
μ	τ	ν	ν	$b\,\not{b}$
e		ν	$j_1\ j_2$	$b\,\not{b}$
μ		ν	$j_1\ j_2$	$b\,\not{b}$

Multi jets

Top Strategies

for $t\bar{t} \rightarrow W b W b$

1. Di Lepton
2. Lepton + jets
3. b tagging < SVX / soft leptons
4. Multi jets

M_{top}

Di-lepton Top Search

very clean

small background :

$Z \rightarrow \tau\tau$

$Z \rightarrow b\bar{b}$

WW, WZ

fake e and/or fake μ

DiLepton Analyses with '89 data	Mtop limit		
2 pb-1 0 candidates	60 GeV	Feb. '89	
e mu 1 candidate	72 GeV	May '89	PRL
DiLepton emu + ee + mu mu	84		
DiLepton + L+low_Pt_mu	89	Feb. '90	
DiLepton + L+low_Pt_mu + Plug e	91 GeV	Nov. '91	PRL PRD

Work in progress

Extensive Data and Monte Carlo comparisons

studies on e + tau and mu + tau

Extending dilepton acceptance

Studying b bbar in DiLepton events

studies on Mtop from DiLepton events

From $M_{top} > 91$ GeV PRL

M_{top} (GeV/c^2)	ϵ_{top} (dilepton) (%)	ϵ_{top} ($t \to b \to \mu$) (%)	$\sigma_{t\bar{t}}$ (pb)	N_{events} (in 4.1 pb^{-1})
80	0.68	0.20	291	10.5
90	0.80	0.26	150	6.5
100	0.83	0.29	94	4.3

'92 - '93 Runs:

ADD CMX more μ coverage

$e\tau$ $\mu\tau$

Lepton + track

DØ

2 pb^{-1} each Now $\Rightarrow$ 20 GeV higher

Can also be used for M_{top} from $\sigma_{t\bar{t}}$

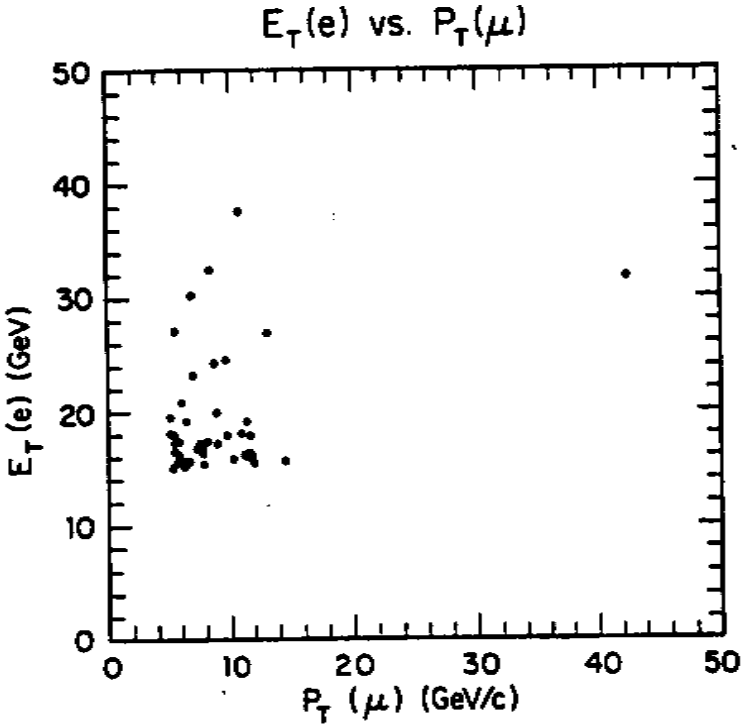

Figure 13: E_T^e vs P_T^μ

One $e\mu$ candidate is well separated from background in the '89 data.

One interesting event from the '92 data is being studied.

'92-'93 and '94 Runs :

new and improved detectors : VTX, CPR, CMUP, CMEX, SVX, improved Plug, dE/dx

heavier top mass region --> higher efficiencies

maximize effciencies : e.g. e (or mu) + tau
low Pt DiLepton

may reach 130 GeV for 25 pb-1 DiLeptons alone
150 GeV combining other analyses

170 GeV for 100 pb-1 DiLeptons alone
200 GeV combining other analyses

lepton + jets Top Search

Large background : $W + jets$

$M_t < M_W$ $\quad M_{Tr}(e\nu)$

$M_t > M_W$ **invariant masses**

b-tagging

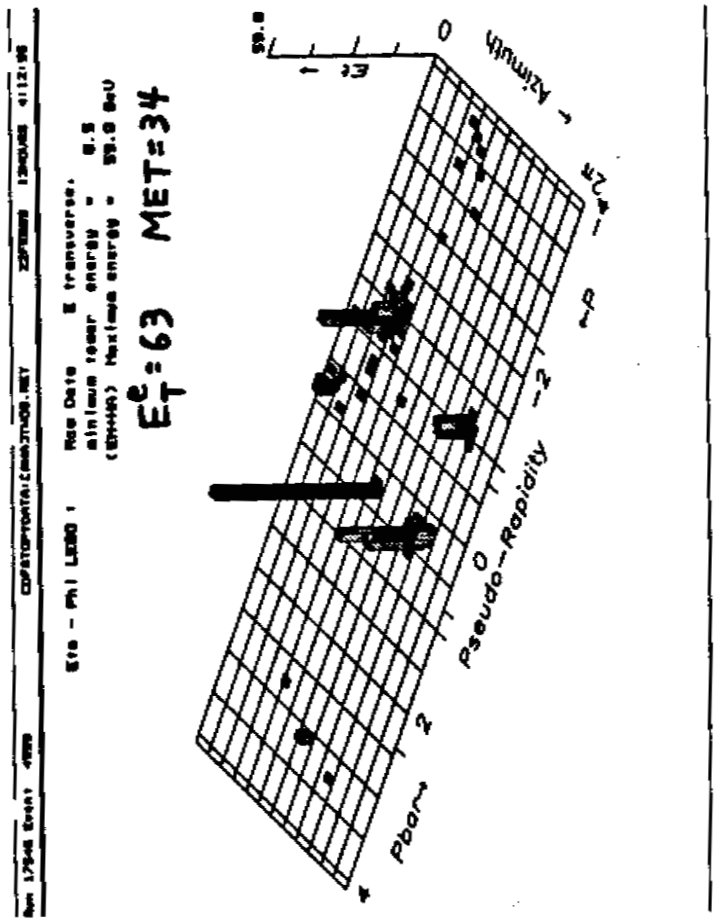

Figure 14: picture of one of the lepton + 4jets events: b tagging with SVX or soft leptons may be necessary to identify $t\bar{t}$ from lepton + jets events.

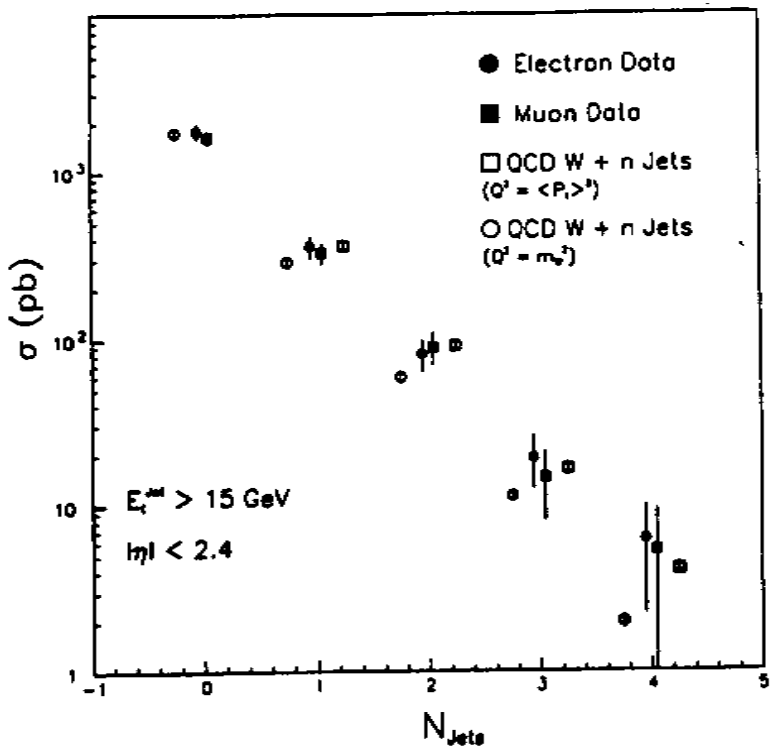

Figure 15 $\sigma(W + njets)$ **as function of jet multiplicity.**

Summary and Prospects

Run 1A in '92-'93, Run 1B in '94:

- expect 6 to 25 times more integrated Luminosity
- Silicon Vertex Detector to identify $b\bar{b}$ in $t\bar{t}$ events
- increased muon acceptance
- higher efficiencies for heavier top quark
- friendly confirmation/competition from D0

CDF Top mass reach :

- 130 to 150 GeV for 25 pb^{-1}
- 170 to 200 GeV for 100 pb^{-1}

Discover the Top quark

measure M_{top} to a few GeV/c^2

very beautiful B physics

WW, WZ, $W\gamma$, $Z\gamma$, . . .

SUSY, H^+, + . . . ?

FUTURE OF TOP PHYSICS

AT THE TEVATRON

Serban Protopopescu
BROOKHAVEN NATIONAL LABORATORY

ABSTRACT

The planned upgrades of the Tevatron and the CDF and DO detectors are described and the possibilities that will open for discovery and study of the top quark.

FUTURE OF TOP PHYSICS AT THE TEVATRON

Serban Protopopescu
Nov. 6, 1992

I. Tevatron Upgrades 1992-1997

II. CDF detector (present and future)

III. DO detector (present and future)

IV. Top physics

a) Discovery limits

b) Measuring the top mass

c) Branching ratios and non-standard decays

TEVATRON UPGRADES

1988-89

Tevatron peak luminosity: $1.6 \cdot 10^{30}$ cm^{-2} sec^{-1}

Total integrated luminosity in CDF: 4.5 pb^{-1}

1992-93

(Ia) Improved separators and $\bar{p}$ source

Present peak luminosity $3.2 \cdot 10^{30}$ cm^{-2} sec^{-1}

Average integrated luminosity/week (DO) in October 1992: 0.25 pb

Peak Luminosity expected to reach $> 5 \cdot 10^{30}$ cm^{-2} sec^{-1}

Total expected integrated luminosity > 20 pb^{-1}

1993-94

(Ib) Linac Upgrade

Expected peak luminosity $1 \cdot 10^{31}$ cm sec

Total expected integrated luminosity 100 pb^{-1}

TEVATRON UPGRADES (cont'd)

1995-96 6 bunches → 36 bunches

Center of mass energy 1.8 TeV → 2.0 TeV

Peak luminosity $1.1 \cdot 10^{31}$ cm^{-2} sec^{-1}

Total integrated luminosity > 100 pb^{-1}

1997-

Main Injector Era

Peak Luminosity $5 \cdot 10^{31}$ cm^{-2} sec^{-1}

Total integrated luminosity 1000 pb^{-1}

CDF DETECTOR

Inner tracking:

5 m. long 1.4 Tesla solenoid

1.4 m. inner radius

Gas drift chamber system

Excellent momentum resolution:

$\frac{\delta p_T}{p_T^2} \sim .001$ $(GeV/c)^{-1}$

High resolution Si Vertex chamber 1.0-3.0 cm radius

Muon detector system:

Central muons momentum measured with inner tracking.

Muon tagging chambers outside calorimeter

coverage $|\eta| < 1.0$

Upgrade Fe wall added to central muon tagging

8λ at 90°
5λ at 45° (to be completed)

Forward muons detected with Fe toroid (1.8 Tesla)

coverage $2.0 < |\eta| < 3.0$

Resolution $\frac{\delta p}{p} \simeq$ 20%-30%

CDF DETECTOR (cont'd)

Calorimetry:

Central Calorimeter

e.m. Pb + scintillator, $\frac{13.5\%}{\sqrt{E}}$

hadronic Fe + scintillator $\frac{70\%}{\sqrt{E}}$ single π, $\frac{95\%}{\sqrt{E}}$ jets

Transition region central to forward 1.1-1.5

Wall Hadronic Calorimeter

Fe + Scintillator

Plug Calorimeter

e.m. Pb + Cu + Gas $28\%/\sqrt{E}$

hadr. Fe + gas $0.1 \cdot E_T + 1.0$ GeV

Upgrade replace gas with scintillator

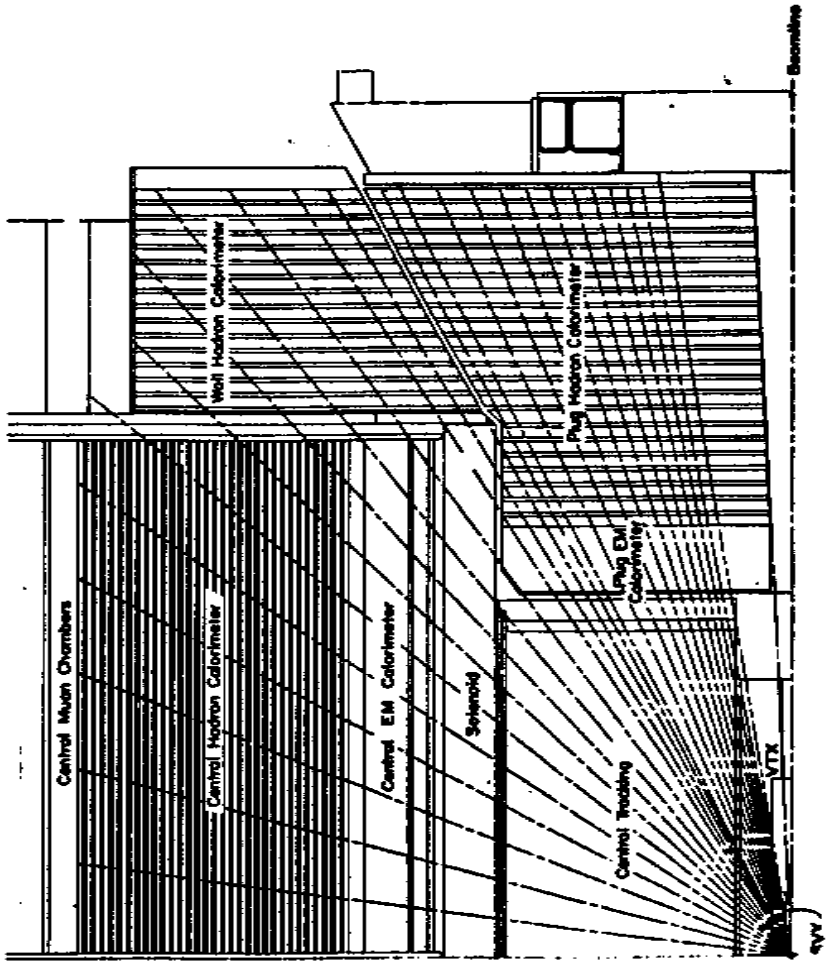

CDF Upgrade

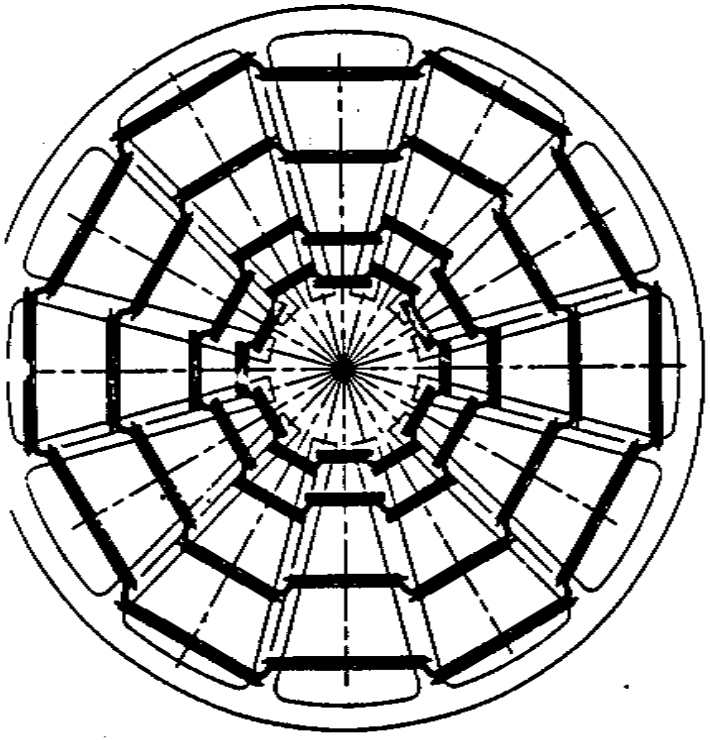

Si Vtx
CDF

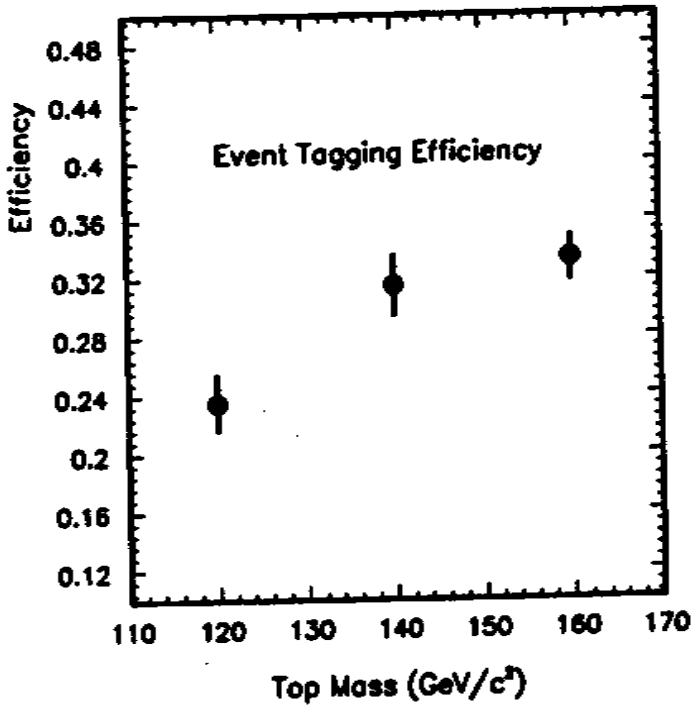
Event Tagging Efficiency
Efficiency
0.48
0.44
0.4
0.36
0.32
0.28
0.24
0.2
0.16
0.12
110
120
130
140
150
160
170
Top Mass (GeV/c²)

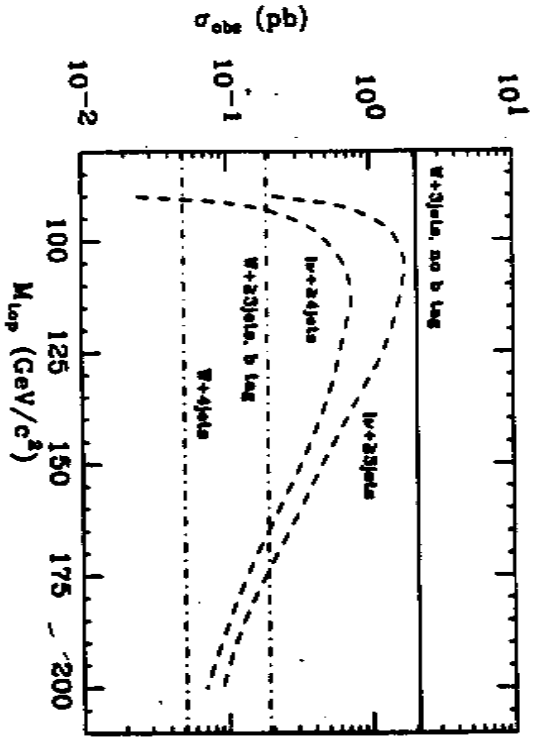

Figure 2: Cross section for $t\bar{t} \to l - \nu - jets$ as a function of top mass: m_t. The cross sections for W + njets is shown without and with a B tag. Jets and leptons were selected with (E_T, η_{max}) values ($\geq$ 15 GeV, 2.0) and ($\geq$ 20 GeV, 1.0) respectively.

DO DETECTOR

Inner tracking:

No Magnetic Field, small volume R=75 cm

Gas drift chamber system inside calorimeter

central, forward resolution 200 μ
vertex resolution 60 μ

TRD (transition radiation detector) $|\eta| < 1.2$

Future

1995-96 Vertex chamber replaced by
Si vtx chamber + Scintillator fiber

1997- Expanded coverage with Si Vtx chamber
All drift chambers replace by Scintillator Fiber
No TRD, replace by pre-shower detector
Superconducting Central Solenoid magnet

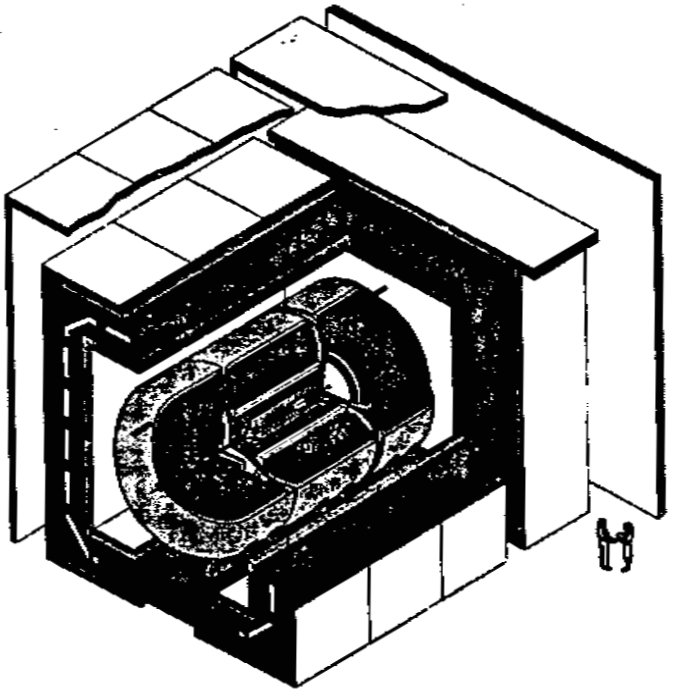

DØ Detector

DO DETECTOR (cont'd)

Calorimeter:

e.m. + hadronic integrated calorimeter

U + liquid Ar

Central catcher Cu + Liquid Ar
End catchers Stainless Steel + Liquid Argon

coverage $-1.0 < \eta < 1.0$ central calorimeter

$1.0 < |\eta| < 1.4$ Inter-Cryostat detectors (ICD)

$1.4 < |\eta| < 3.7$ End cap calorimeters

e.m. resolution 1%-2% + $15\%/\sqrt{E}$

had. resolution 3%-4% + $45\%/\sqrt{E}$ single π

$>70\%/\sqrt{E}$ for jets with Et < 20 GeV

$50\%/\sqrt{E}$ for jets with Et > 100 GeV

No em coverage $1.0 < |\eta| < 1.2$

ICD resolution $100\%/\sqrt{E}$ for jets

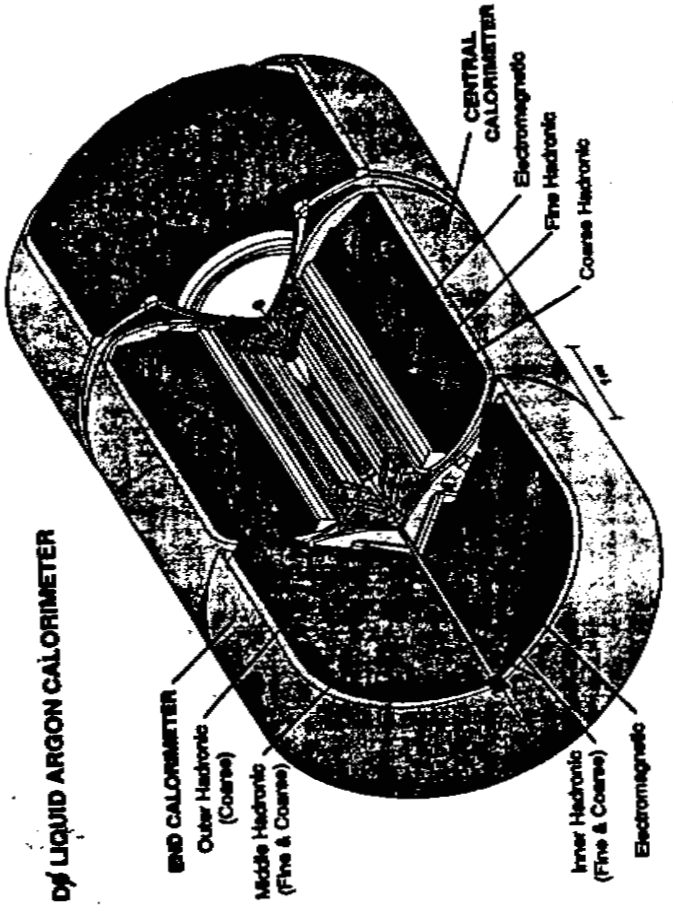

DØ DETECTOR (cont'd)

Muon System:

Gas drift chambers + Fe Toroids

Central toroid coverage

$-1.0 < \eta < 1.0$

End toroids coverage

$1.0 < |\eta| < 2.0$

Small angle toroids coverage

$2.0 < |\eta| < 4.0$

Resolution

$$\frac{\delta p}{p} = \begin{array}{l} 20\% \text{ up to } p\ 100\ \text{GeV} \\ 100\% \text{ at } p\ 500\ \text{GeV} \end{array}$$

CONCLUSIONS

In next 2 years FNAL TeV collider will accumulate 100 pb^{-1}

Goal with main injector is 1000 pb^{-1} by 1998

Discovery Limits:

Luminosity	Claim discovery	90% Upper limit
100 pb^{-1}	150 GeV	>180 GeV
1000 pb^{-1}	220 GeV	>250 GeV

Mass measurements:

For 1000 pb^{-1} error on mass below 180 GeV dominated by systematics, not statistics.
2%-3% systematics will give mass to 5 GeV or better.

Branching ratios:

For 1000 pb^{-1} can set branching ratio limits at 90% CL.

$BR(t \to H_c + c) < 2.5\% BR(H_c \to \tau\nu)$

$BR(t \to Z + c) < 0.3\%$

Top Branching Ratios

Standard Model predicts top with $M_t > M_W$ decays 100% to $W + b$

Test by measuring the ratios of events observed in

di-lepton to lepton + jets channels
and the number of b-jets in top candidate events.

Deviations can occur if top $\to H + b$

H expected to have large BR to $\tau\nu$

$\Rightarrow$ excess of events in
$e + \tau$ and $\mu + \tau$ final states (5% BR)

Assume acceptance 10% and $H_c \to \tau\nu$ 100%
Statistical limit for 120 GeV top and 1000 pb-1

$BR(t \to H_c + c) < 2.5\%$ (95% CL)

Another interesting non-standard decay is

top $\to Z + c$

The BR for t t events with one to $Z \to e^+e^-$ + b and the other to $W \to q\bar{q}$ + b is

$.08 \cdot BR(t \to Z + c)$

For 120 GeV top with 25% acceptance and 1000 pb-1 possible upper limit is

$BR < 0.3\%$ (90% CL)

- Distinction between "Evidence for" and "Discovery of" top
  1. Excess of $e - \mu$ events
  2. Demonstration of $W - b$ decay, couplings
  3. Mass measurement

- Expected event yield for 1 fb^{-1}:

m_{top} (GeV)	e or μ + 4 jets	e - μ
120	1380	240
140	850	98
180	260	24
210	140	12
240	60	5

- Excess of 4 $e - \mu$ events ("evidence for") 245 GeV for 1 fb^{-1} (185 GeV for 200 pb^{-1}).

$m_t = 180$ GeV

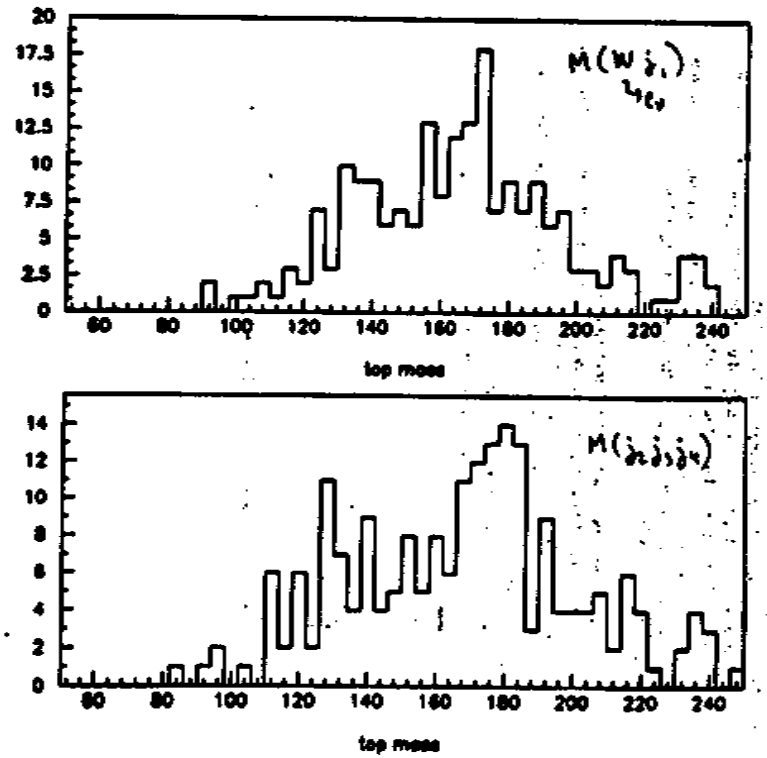

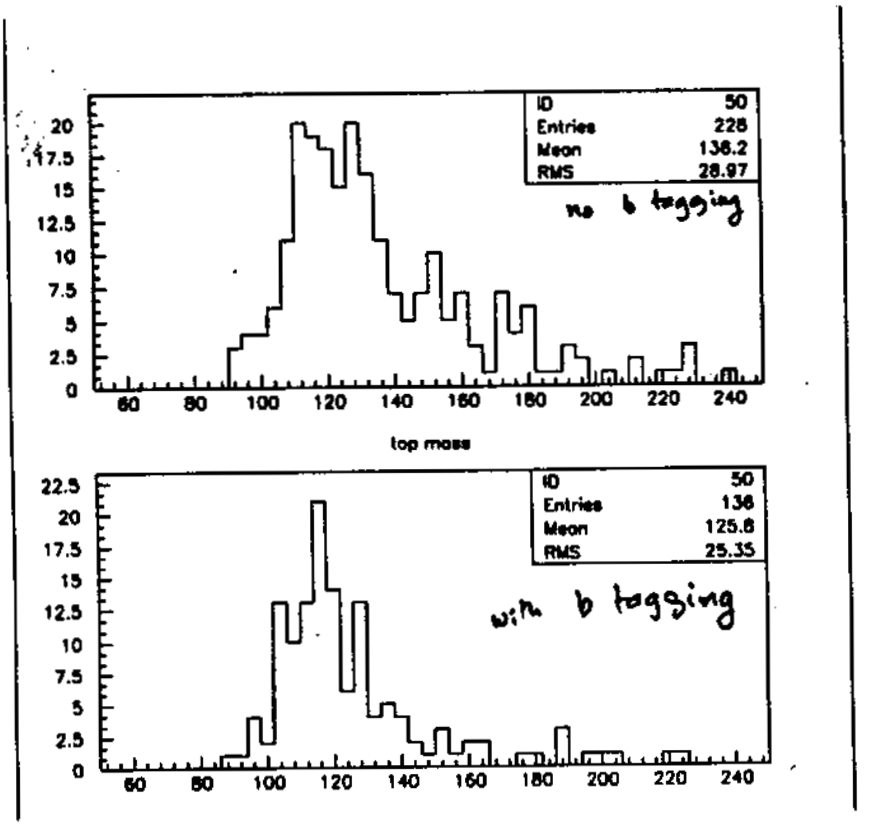
ID 50
Entries 228
Mean 136.2
RMS 28.97
no b tagging
top mass
ID 50
Entries 136
Mean 125.8
RMS 25.35
with b tagging

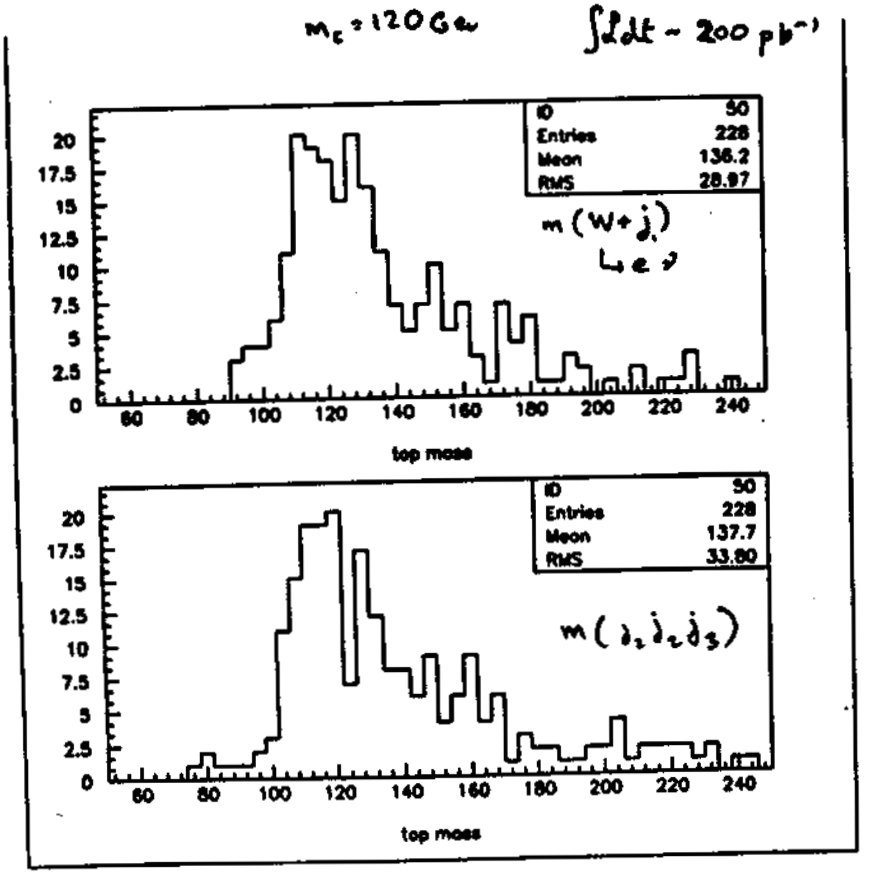
$m_t = 120$ GeV
$\int \mathcal{L} dt \sim 200\ pb^{-1}$
ID 50
Entries 228
Mean 136.2
RMS 28.97
m (W+j)
top mass
ID 50
Entries 228
Mean 137.7
RMS 33.80
$m(j_1 j_2 j_3)$
top mass

top 1 mass = mass (W + b jet)
$\hookrightarrow \ell\nu$

any jet after removing W→jj

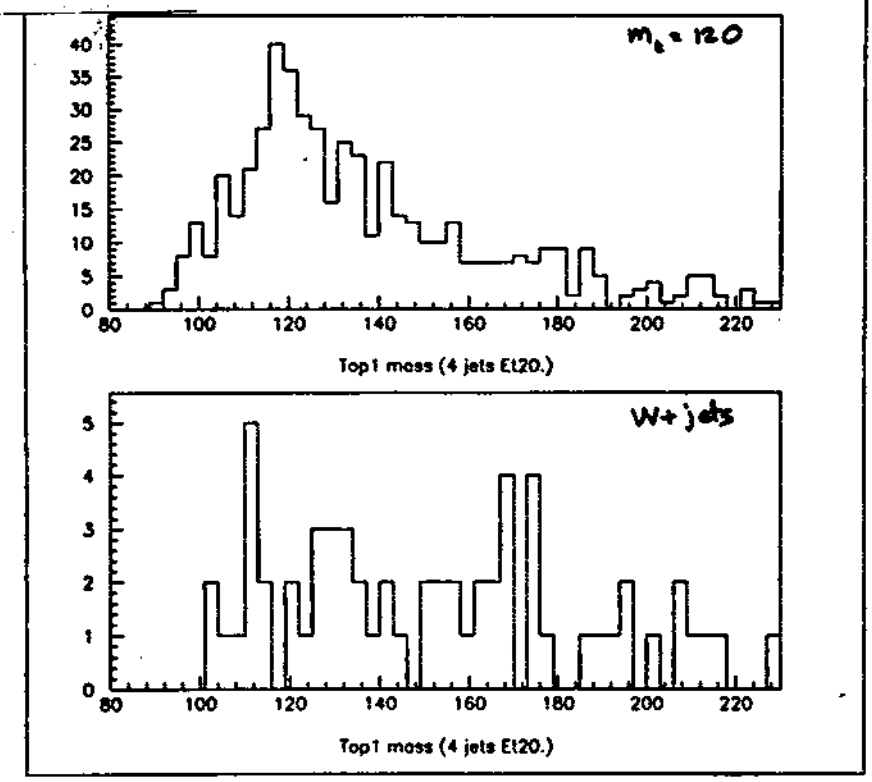

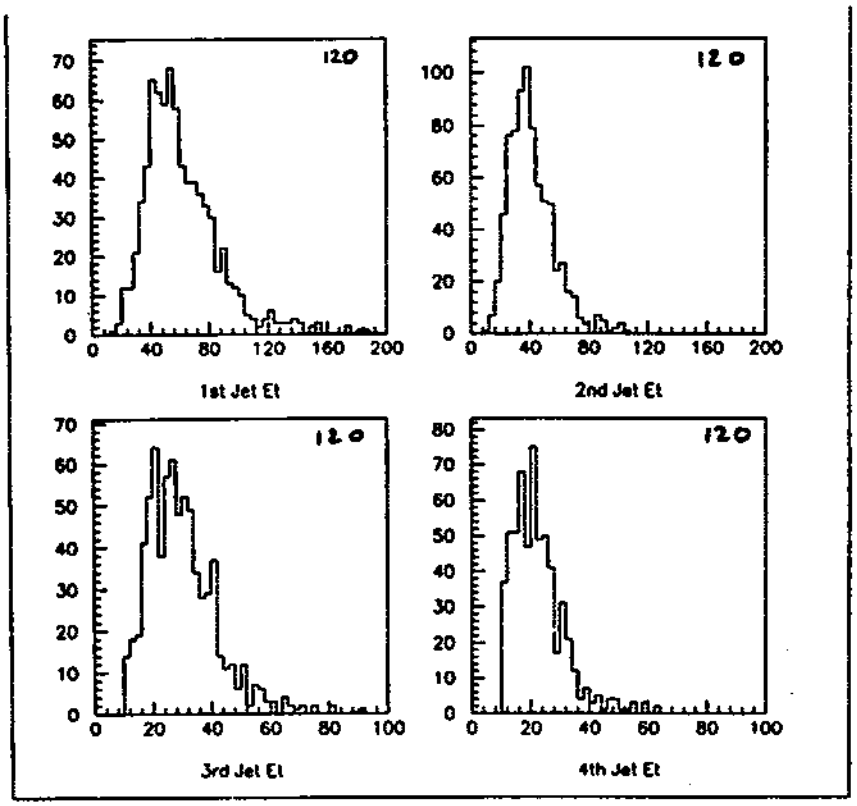

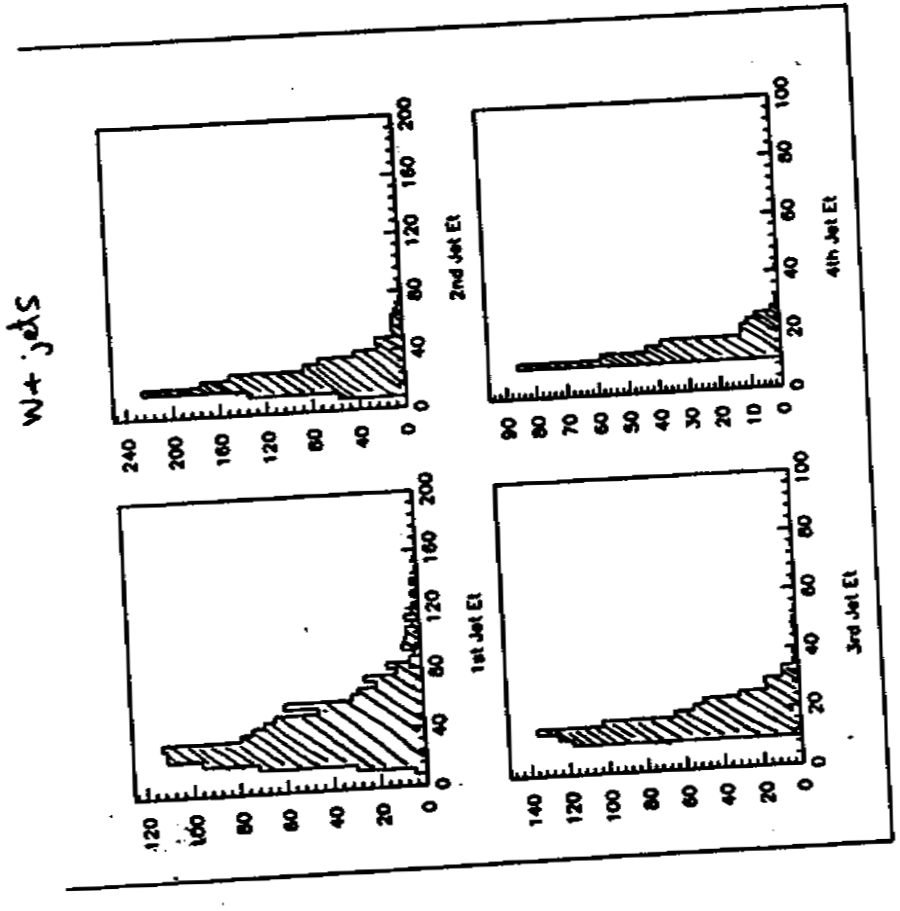

Handles to reduce combinatorial background to W + jet mass spectra:

1) Pick highest the 4 highest Et jets with $\eta < 2.0$. (reduces jets from initial state radiation)

2) For low top masses jet closest to a W has high probability of being b-jet from t-decay

3) Remove from consideration jet-pairs that give mass closest to W-mass

4) Find combination that minimizes mass difference between top 1 and top 2.

5) Tag b-jets. This reduces statistics by 30% and gives correct b only 50% of the time. (if tagged by vertex)
Tagging μ's from b-jets does not help with m_t measurement.

LEPTON + JETS CHANNELS

Event Selection:

lepton Et>15 Gev, Missing Et>15 GeV
3 or more jets, Et>15 GeV

Demonstrate that $t\bar{t}$ production is observed
by showing 2nd W→ jets

Assume Missing Et comes from from W→ l + ν
pz of W can be calculated using W mass constraint
(2 solutions).

W + jet mass spectra should show top mass.

First problem is to get rid of W + jets background

2nd problem is to handle combinatorial background.

mass	100	120	140	180
<no. jets>	3.5	4.2	4.4	4.7
only 4 jets	32%	27%	21%	17%

About 30% of the time W goes to 3 rather than 2 jets.

$m_t = 120$ GeV

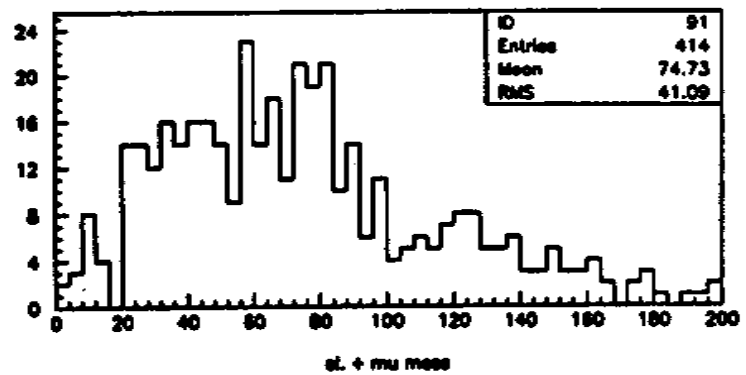

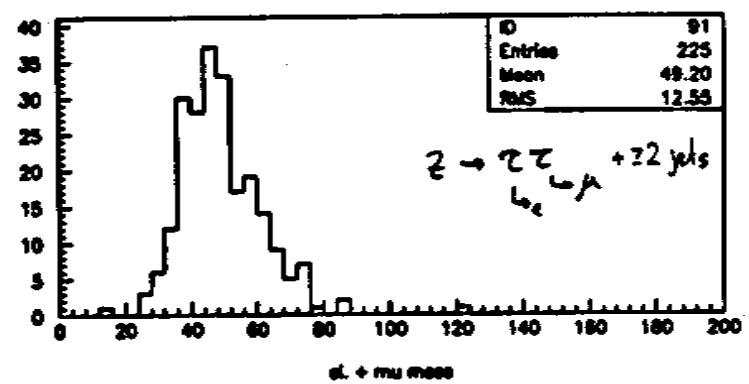

DILEPTON CHANNELS

1) Top mass can be inferred indirectly from cross section:

30% uncertainty leads to

→ m_t uncertainty 10 GeV

2) Dalitz-Goldstein analysis P.R. D45 (1992) 1531

For a given mass use kinematic constraints + knowledge of structure functions to calculate event probability.

For either method background needs to be well understood.

Method 2 needs to take into account initial state radiation (ignored by Dalitz and Goldstein)

mass	100	120	140	180
no. jets	2.3	3.0	3.3	3.5
only 2 jets	30%	25%	23%	20%

Probability of b-quark radiating a gluon increases with top mass.

NUMBER OF EXPECTED EVENTS

For 100 pb^{-1}, E_t >15 GeV (e,μ or jet), $\not{E}_t$ >15 GeV
Acceptance for each lepton 50%

mass (GeV)	cross section (pb)	e,μ (+2 jets)	l+jets(+2)
100	88	50 (30)	570
120	34	20 (16)	300
140	15	10 (9)	160
180	3	2 (2)	40
$Z\to\tau+\tau$	200	30 (7)	
$W\to l+\nu$	4400		150

Theoretical uncertainty on cross section 30%.

Note:
QCD σ for events with 4 jets E_T>20 Gev
116,000 pb

⇒ start with a background
~ 10^7 events

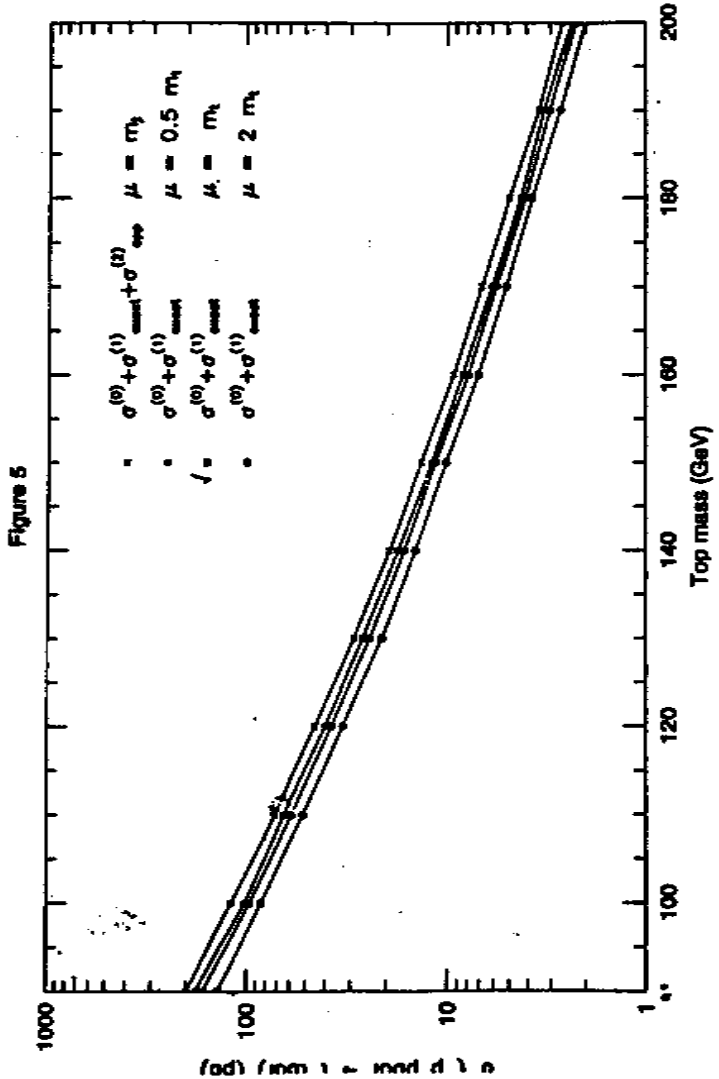

Berends, Giele & Schmidt
FNAL preprint

CROSS SECTION AND BRANCHING RATIOS

The basic processes leading to top production at the Tevatron are well understood and calculable:

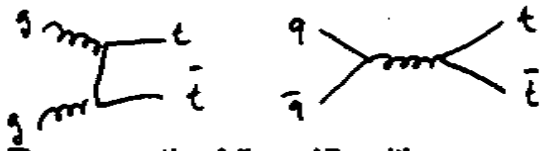

The cross section falls rapidly with mass, roughly a factor of 2 for every 15 GeV above top masses of 100 GeV.

The standard model top expected to decay 100% of the time into W + b (if $M_t > M_W$)

The standard signatures for discovering top involve observing the isolated leptons from the W decays. The branching ratios are easily calculated:

a) electron + muon (one W to electron the other to muon)	2.4%
b) 2 electrons (muons) (both Ws to electrons (muons)	1.2% (x2)
c) electron (muon) +jets (one W to electron (muon) the other to quarks)	14.7% (x2)
d) electron or muon + tau	4.8%

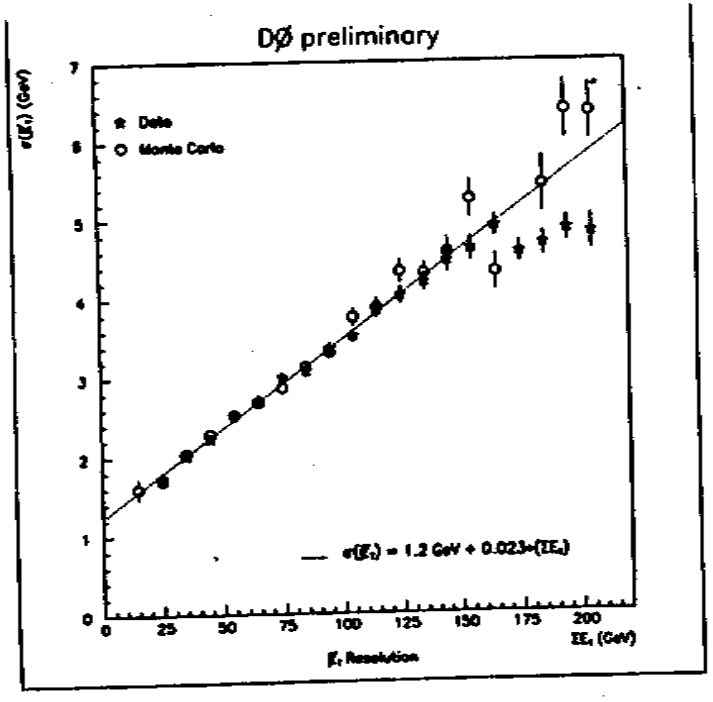
DØ preliminary
Data
Monte Carlo
σ(E_T) = 1.2 GeV + 0.023×(ΣE_T)
σ(E_T) (GeV)
ΣE_T (GeV)
E_T Resolution

$E_T^{jet} > 30$ GeV

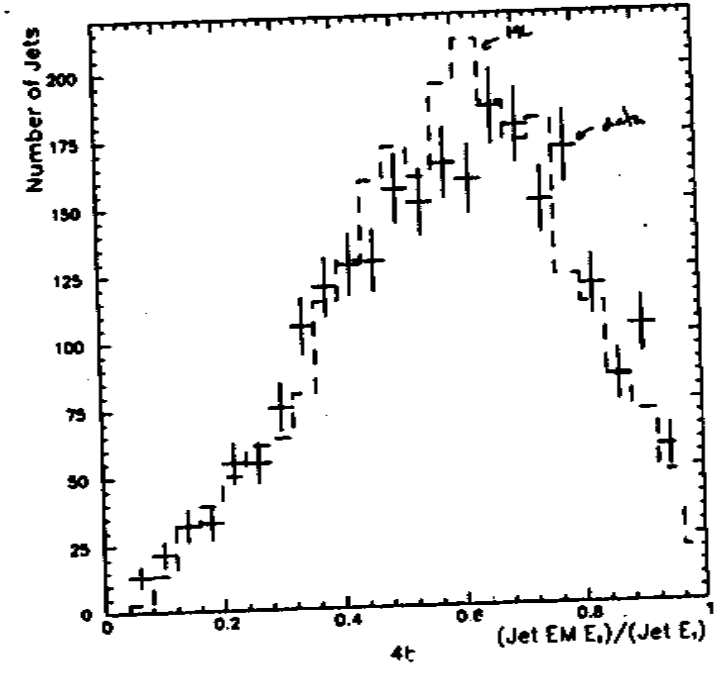
Number of Jets
(Jet EM E_T)/(Jet E_T)
4t

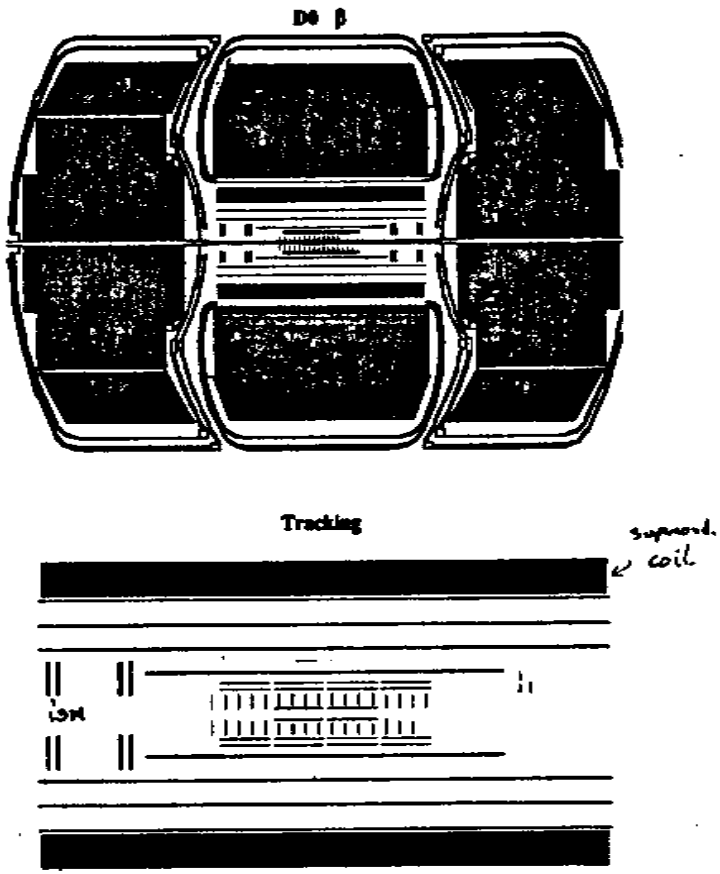

D0 Central Tracking System

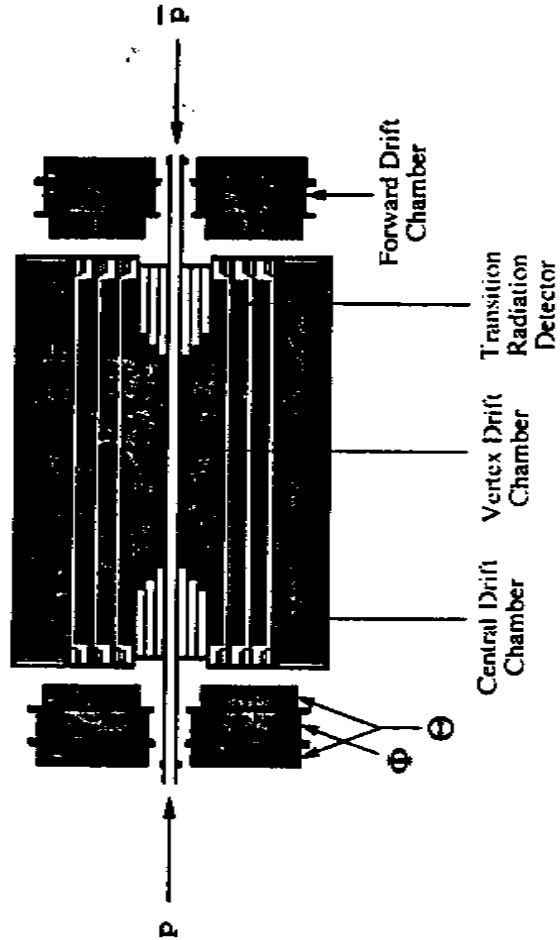

Top Production and Decay at Colliders

C.-P. YUAN

Department of Physics and Astronomy
Michigan State University
East Lansing, MI 48824

ABSTRACT

We discuss the production machanism of the top quark at the hadron colliders: Tevatron, LHC and SSC. We survey the studies on the measurement of the top quark mass, and the decay width $\Gamma(t \to bW^+)$ via the QCD processes $q\bar{q}$, $gg \to t\bar{t}$ at the LHC and the SSC. We show that studying the single top quark production via the W–gluon fusion process can provide unique information on: (*i*) the measurement of the decay width $\Gamma(t \to bW^+)$; (*ii*) probing the symmetry breaking mechanism by measuring the form factor of t-b-W ; (*iii*) testing the Effective–W Approximation prior to supercolliders; (*iv*) testing CP violation by observing different production rates of $\bar{P}P \to tX$ and $\bar{P}P \to \bar{t}X$; (*v*) testing CP violation from the almost hundred percent longitudinally polarized top quark decay; in addition to the measurement of the top quark mass. We show that this process is extremely useful at the Tevatron.

Outline

- Top Quark Production at FNAL, LHC, SSC
  - mechanism
  - polarization of top
- Top Quark Decay
  - m_t
  - Γ_t
- Single Top Production via W-gluon fusion
  - Γ_t
  - Test ~~CP~~
  - Test SM and Probe New Physics

Conclusions

- Top Quark Production at FNAL, LHC and SSC
  - QCD

$gg \to t\bar{t}$ and $q\bar{q} \to t\bar{t}$

$\oplus$

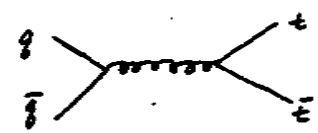

Only involve QCD interactions, which is well tested. Therefore, the production rate is well predicted.

NLO QCD corrections
P. Nason, S. Dawson & R.K. Ellis
W. Beenakker, W.L. Bonthuis, R. Meng, G.A. Schuler & J. Smith
W. Beenakker, H. Kuijf, W.L. van Neerven & J. Smith

2. Electro-Weak - QCD <u>process</u>

(Much more interesting than the usual QCD)

& less known than

$W^+ g \to t \bar{b}$ $\quad$ $(W^- g \to \bar{t} b)$

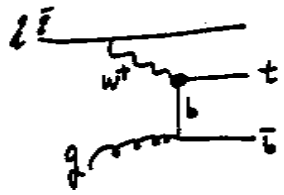

S. Dawson ('85)
S. Willenbrock & D. Reiner ('86)
C-P. Yuan ('90)
J. Collins & C-P. Yuan
F. Anselmo, B. van Eijk, G. Bordes
T. Morris, R. Price, D. Ross, H. Reith
D. Carlson & C-P. Yuan
K. Ellis & S. Parke

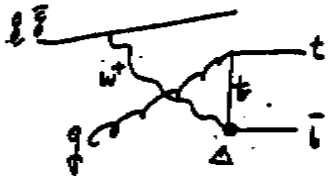

- Sensitive to New Physics
- Measuring Width $\Gamma(t \to bW^+)$
- t is ~100% left-handed polarized
  $\Rightarrow$ Test CP property in t decay

3. Others

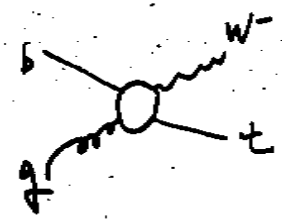

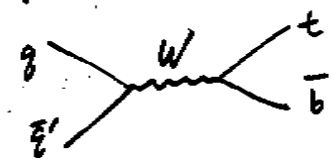

⋮ etc.

For heavy Top Quark Production,

$q\bar{q}, gg \to t\bar{t}$

$Wg \to t\bar{b}$

dominate..

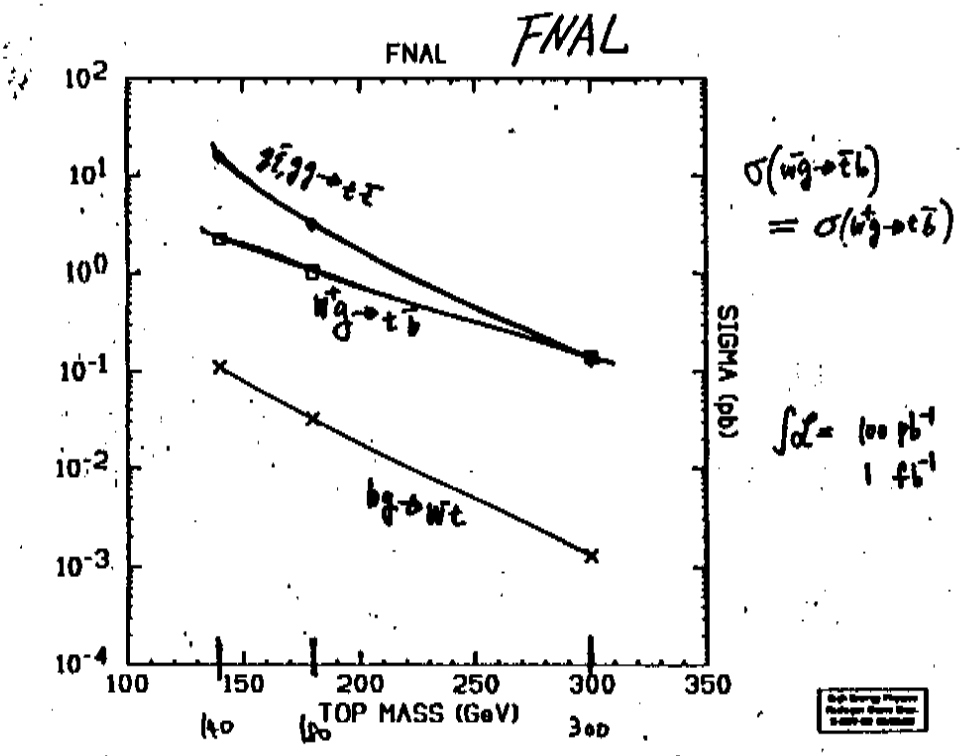
FNAL
FNAL
SIGMA (pb)
TOP MASS (GeV)
$q\bar{q}, gg \to t\bar{t}$
$W^+g \to t\bar{b}$
$bg \to Wt$
$\sigma(W^-g \to \bar{t}b) = \sigma(W^+g \to t\bar{b})$
$\int \mathcal{L} = 100\ pb^{-1}$
$1\ fb^{-1}$

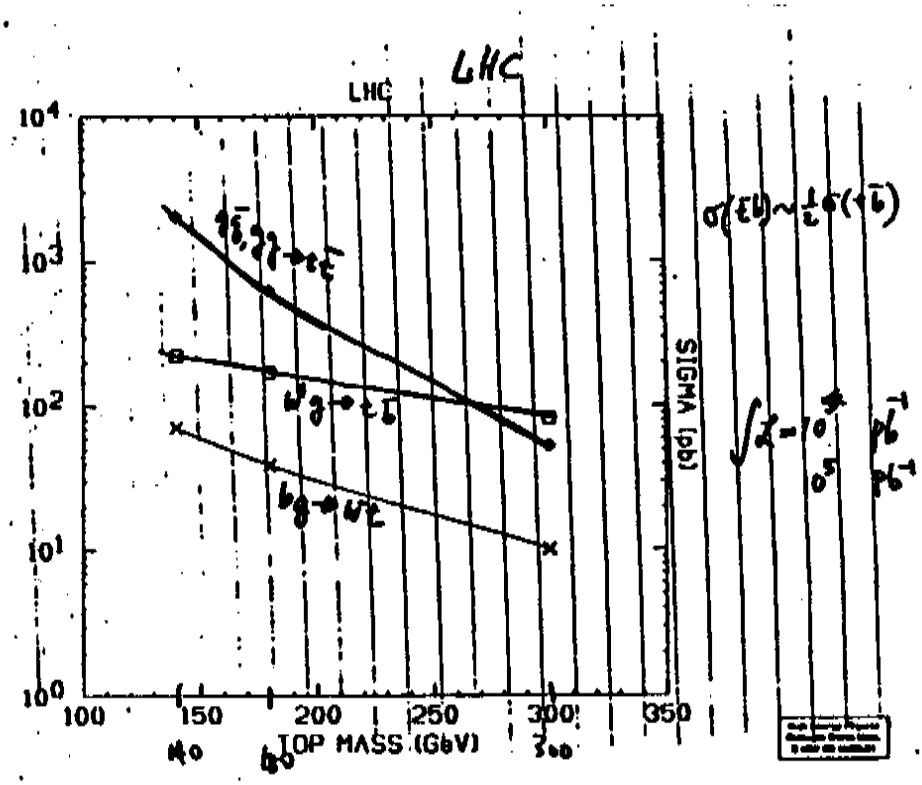
LHC
LHC
SIGMA (pb)
TOP MASS (GeV)
$q\bar{q}, gg \to t\bar{t}$
$W^+g \to t\bar{b}$
$bg \to Wt$
$\sigma(\bar{t}b) \sim \frac{1}{2}\sigma(t\bar{b})$
$\int \mathcal{L} = 10^4\ pb^{-1}$
$10^5\ pb^{-1}$

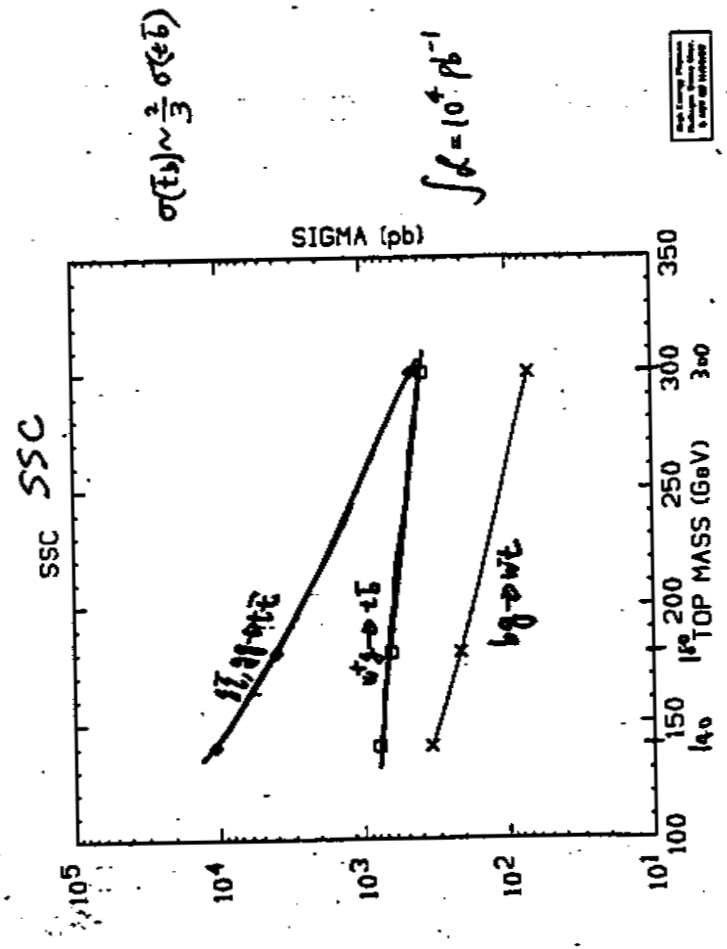

- Polarization of top quark produced from

1) QCD

$$gg,\ q\bar{q} \to t\bar{t}$$

Because the invariance of C (charge conjugation) and P (parity), t can only be polarized perpendicular to the scatter plane

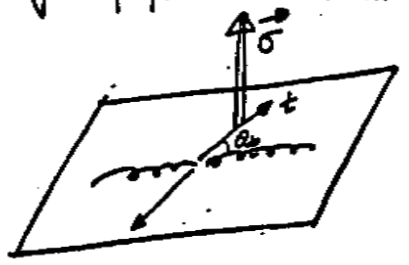

(inclusive single top polarization)

- This transverse polarization only occurs beyond Born level.

$\Rightarrow$ $|\vec{\sigma}|$ is small, less than 2%

W. Bernreuther, G. Guillian
G. Kane, G. Ladinsky & C.-P. Yuan

This transverse polarization can be used to probe large ~~CP~~ effects.

- Longitudinal polarization

It's also possible to probe CP violation asymmetry

$$\frac{\sigma(t_L\bar{t}_L) - \sigma(t_R\bar{t}_R)}{\sigma(t_L\bar{t}_L) + \sigma(t_L\bar{t}_R) + \sigma(t_R\bar{t}_L) + \sigma(t_R\bar{t}_R)}$$

at the 10^{-3} level via the process

$$gg \to t\bar{t}$$

at the SSC.

C. Schmidt & M. Peskin

How about Background?

e.g. $W^+g \to t\bar{b}$, $W^-g \to \bar{t}b$

2) Electro-Weak-QCD

top Quark is ~ 100% left-handed polarized because the charged current is left-handed.

- Top Quark decays via $t \to bW^+$, the polarization of t is self-analyzed.

$\Rightarrow$ Useful for testing CP violation in top decay

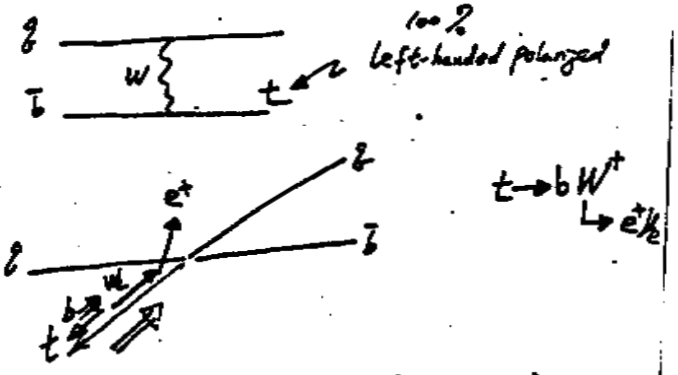

For heavy SM top Quark $(m_t > M_W)$

$$\frac{\text{rate of } (t \to bW_{Long})}{\text{rate of } (t \to bW_{Trans})} \approx \frac{m_t^2}{2M_W^2}$$

- Top Quark Decay

$t \to b W^+$

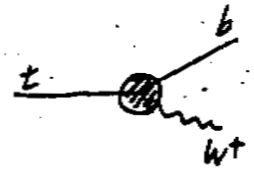

When W^+ couples to massless fermions, e.g. $W^+ \to e^+ \nu_e$, the most general Form factors are

G. Kane
G. Ladinsky
& C.P. Yuan

$$\frac{g}{\sqrt{2}} W_\mu \bar{b} \gamma^\mu \left(f_1^L P_L + f_1^R P_R \right) t$$

$$- \frac{g}{\sqrt{2} M_W} \partial_\nu W_\mu \bar{b} \sigma^{\mu\nu} \left(f_2^L P_L + f_2^R P_R \right) t .$$

- $P_L = \frac{1}{2}(1-\gamma_5)$, $P_R = \frac{1}{2}(1+\gamma_5)$
- In SM, at Born level,

$$f_1^L = 1 \ , \quad f_1^R = f_2^L = f_2^R = 0$$

Radiative Corrections to $t \to b W^+$ in SM

- One loop QCD

M. Jezabek & J. Kühn
C. Li, R. Oakes & T.C. Yuan
J. Liu & Y-P. Yao

$\sim -10\%$ in decay rate

$\sim -1\%$ effect on the fraction f_L of longitudinally polarized W^+ from the decay of an unpolarized t

$$f_L = \frac{N(\lambda_W = 0)}{N(\lambda_W = 0) + N(\lambda_W = +) + N(\lambda_W = -)}$$

No great number

- One loop EW

J. Liu & Y-P. Yao
A. Denner & T. Sack
E. Stelzer, R. Mendel, & R. Meyer
& Aoki
B.A. Irwin, R. Migneron & H. Tsai
C-P. Yuan & T.C. Yuan

$\sim 1\%$ in decay rate (in G_F-scheme).

No $O\left(\frac{g^2 m_t^2}{M_W^2}\right)$ corrections to f_L.

- Using a Monte Carlo program to study the effects of final state QCD radiation on the determination of m_t and W boson polarization for $t\bar{t}$ pairs produced at hadron Colliders.

S. Mrenna & C.-P. Yuan

• How to measure m_t ?
How accurate can m_t be measured ?

LHC Workshop, Aachen, Oct. 1990
SDC Technical Design Report
GEM letter of Intent

(For $m_t \sim 200$ GeV)

1)

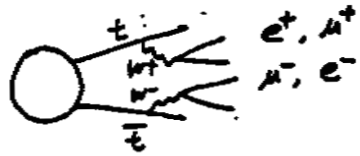

$(\Delta m_t) \sim (10 \sim 15)$ GeV

(Assume SM BR. Error dominated by $\Delta\sigma$)

2)

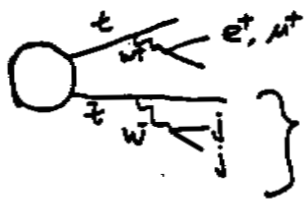

$(\Delta m_{3j}) \sim (5 \sim 10)$ GeV

(nonlinearity & other losses.
energy of jet outside cone.
energy inside cone with underlying event.)

3)

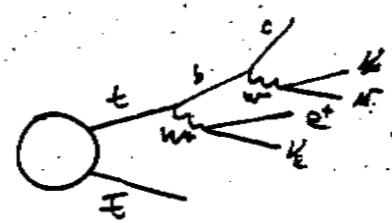

} From the invariant mass of $e^+\mu^-$

SDC concluded

150 ± 0.5 (stat) ± 2.4 (sys) GeV
250 ± 0.8 (stat) ± 3.9 (sys) GeV

$\Rightarrow$ 1.5% accuracy

• Branching Ratio (BR) and Γ_t

1) Comparing

$$\frac{\sigma(\ell + \text{jets})}{\sigma(2\ell + \text{jets})} \quad \text{from } t\bar{t} \text{ events,}$$

LHC Workshop concluded $\delta(BR)_{\text{lepton}} \sim 5\%$

2) SDC studied / concluded ℓ+jets mode from $t\bar{t}$ events,

$\Delta\Gamma_t \sim 9$ GeV for $m_t = 150$ GeV
(Intrinsic width ~ 1 GeV)

But, $W^+ g \to t\bar{b}$ can measure $\Gamma_t(t \to bW^+)$ from its production rate.

$\sigma\Big($ 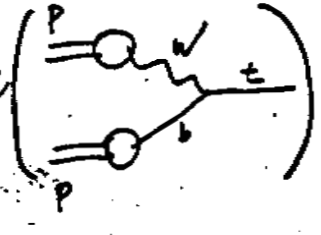 $\Big) \sim \Big|$ 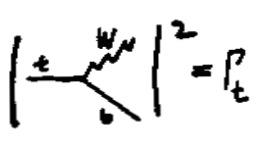 $\Big|^2 = \Gamma_t$

G. Kane, G. Ladinsky, C.-P. Yuan
D. Carlson, C.-P. Yuan

QCD radiative decay of top quark

• At tree level, in SM, SMirma & CPY

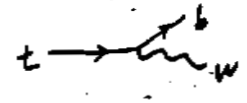

• QCD radiative corrections

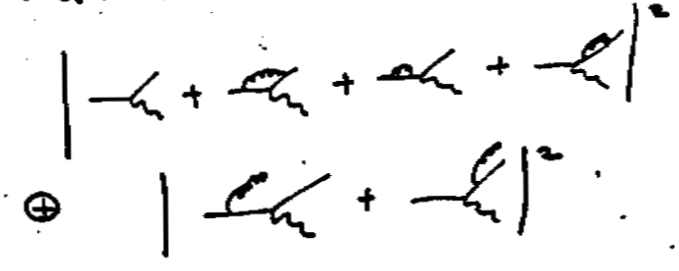

What's the effect on the determination of

• m_t, Γ_t
• W boson polarization
— M_{be}

in $gg, q\bar{q} \to \bar{t}t \to bW^+ \to e^+\nu$, $\bar{b}W^- \to q\bar{q}$

QCD radiative decay of top quark

At SSC $q\bar{q}, gg \to t\bar{t} \to l + j's$

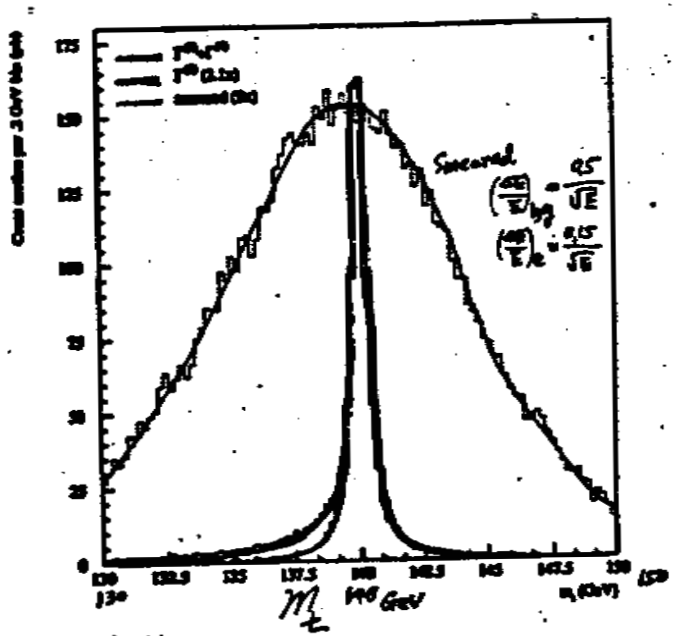

events $(10^4 pb^{-1})$ 8
Br. 4.1×10^{-8}
Br. 4.1×10^{-7}

Γ (Born) width 0.6 GeV
1.0

$Br = 2 \times \left(\frac{2}{9}\right) \times \left(\frac{6}{9}\right) \simeq 0.3$

S. Protopopescu & C.P. Yuan

- Top Quarks Decay $(m_t > M_W)$

– If the $SU(2)$ structure $\begin{pmatrix} t \\ b \end{pmatrix}$ of the standard model holds, then

$$t \to b\, W^+$$

always occurs at tree level in any model.

– For a standard model t, the decay width $t \to b W^+$

$$\Gamma_t \sim 1 \text{ GeV} \left(\frac{m_t}{150}\right)^3$$

lifetime

$$\tau_{decay} = \frac{1}{\Gamma_t} \sim 6.6 \times 10^{-25} \left(\frac{150}{m_t}\right)^3 \text{ sec}$$

$\Rightarrow$ t decays before it feels non-perturbative strong interaction.

$$\left(\frac{1}{\Lambda_{QCD}} \sim \frac{1}{0.2 \text{ GeV}} \sim 3.3 \times 10^{-24} \text{ sec} \right)$$

See T. Sjostrand talk in this Workshop

I. Bigi, V. Poksikian, V. Khoze, J. Kühn

This Process allows FNAL do

"SSC physics"

— Probe Symmetry Breaking

& Generation of Fermion Mass

$\Rightarrow$ Study

① (Longitudinally Polarized W-boson)

$\approx$ Goldstone Boson, spontaneously symmetry breaking)

② Properties of top Quark, eg. Mass, width, and $\not{CP}$

$\Rightarrow$ Need Theories

- Electroweak Chiral lagrangian
- Equivalence Theorem
- QCD "subtraction"
- Effective-W Approximation

[redacted]

Callan-Coleman-Wess-Zumino

$$\frac{G}{H} = \frac{SU(2)_L \times U(1)_Y}{U(1)_{e.m}}$$

R. Feynman & X. Zhang

$U(1)_{e.m}$ invariant interaction

$$W_\mu^+ \bar{t} \gamma^\mu (g_V + g_A \gamma_5) b$$

lift-up the symmetry from H to G.

$$W_\mu^+ \longrightarrow \frac{-i}{2} \mathrm{Tr}\left(\tau_- \Sigma^\dagger (\partial_\mu - i g \frac{\tau}{2} W_\mu^+) \Sigma\right),$$

with

$$\Sigma = e^{\frac{i \tau_a \phi_a}{v_a}}$$

$a = 1, 2, 3$

$v = v_a = v = 246$ GeV

($g_V = g_A$, $g_V = -g_A = 1$ at tree level, in SM)

$\Rightarrow$ $\boxed{\frac{1}{2v} (\partial_\mu \phi) \bar{t} \gamma^\mu (g_V + g_A \gamma_5) b.}$

(New physics likely show up in processes involving ϕ and/or t)

$\Rightarrow$ Study Goldstone boson ϕ & heavy fermion t

$\Rightarrow$ $Wg \to tb$ Process is the useful one to probe both $\phi \approx W_L$ and t

Equivalence Theorem

Ward Identity

$$\left(-\partial W + M_W \phi\right)\left|\begin{matrix}\text{Physical}\\ \text{state}\end{matrix}\right\rangle = 0$$

J. Cornwall, D. Levin, G. Tiktopoulos
C. Vayonakis
R. Lee, C. Quigg & H. Thacker
M. Chanowitz, M. Gaillard
M. Gunion, J. Kogut & H. Haber
Y.-P. Yao & C.-P. Yuan
J. Bagger & C. Schmidt
H. Veltman
N.J. Ho, K.P. Hong, X. Li

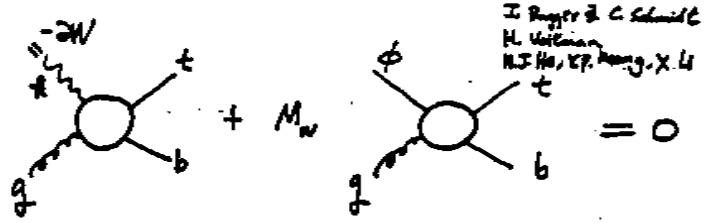

Longitudinal polarization vector of W boson

$$\varepsilon_L(k) = \frac{k}{M_W} + O\left(\frac{M_W}{E_W}\right)$$

If $M_W \ll E_W$, then

$$(\text{Longitudinal } W) \approx (\text{Goldstone Boson } \phi)$$

Since $\left(\phi \to t\,b\right) \sim \frac{m_t}{M_W}$,

$W_L q \to t b$ becomes more important for heavier top quark

QCD "Subtraction"

J. Collins, W.K. Tung
F. Olness, W.K. Tung
D. Dicus, S. Willenbrock
J. Collins & G.P. Ying

(A)

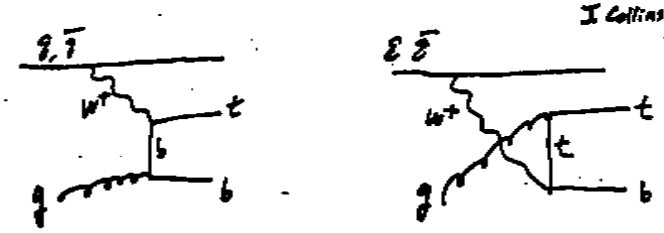

(B)

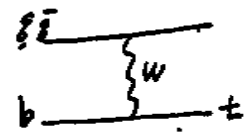

(C)

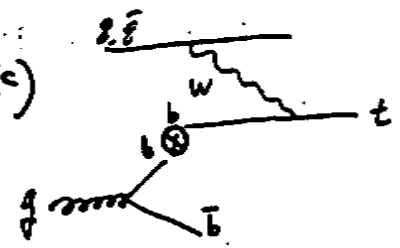

"True Cross Section" = (A) + (B) − (C)

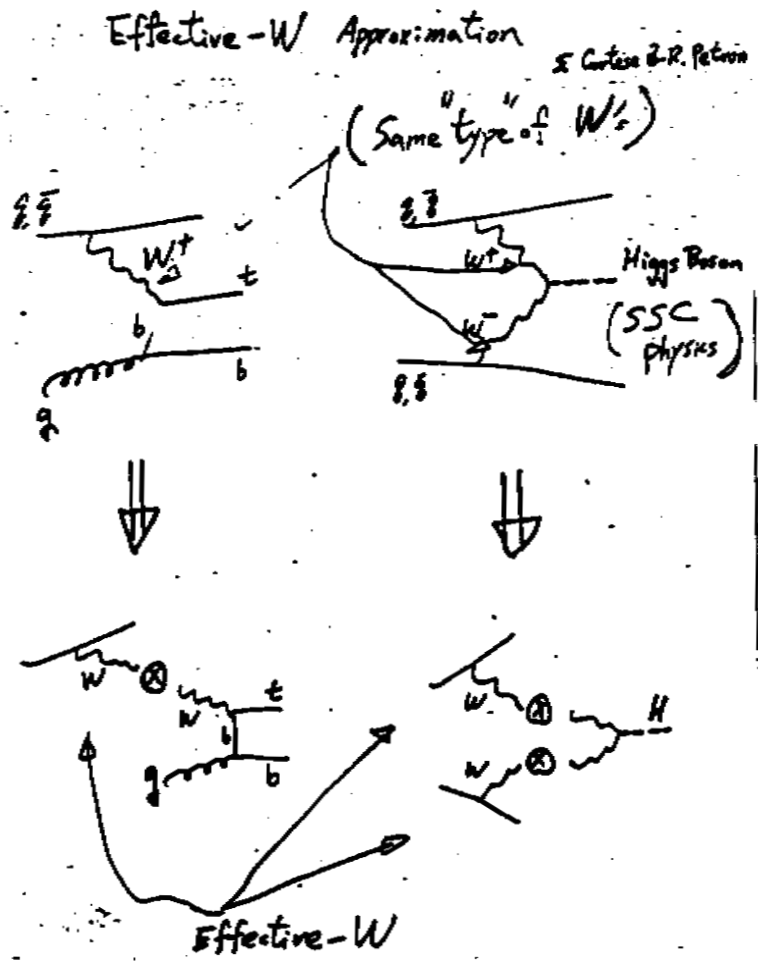
Effective-W Approximation
(Same "type" of W's)
Higgs Boson
(SSC physics)
Effective-W

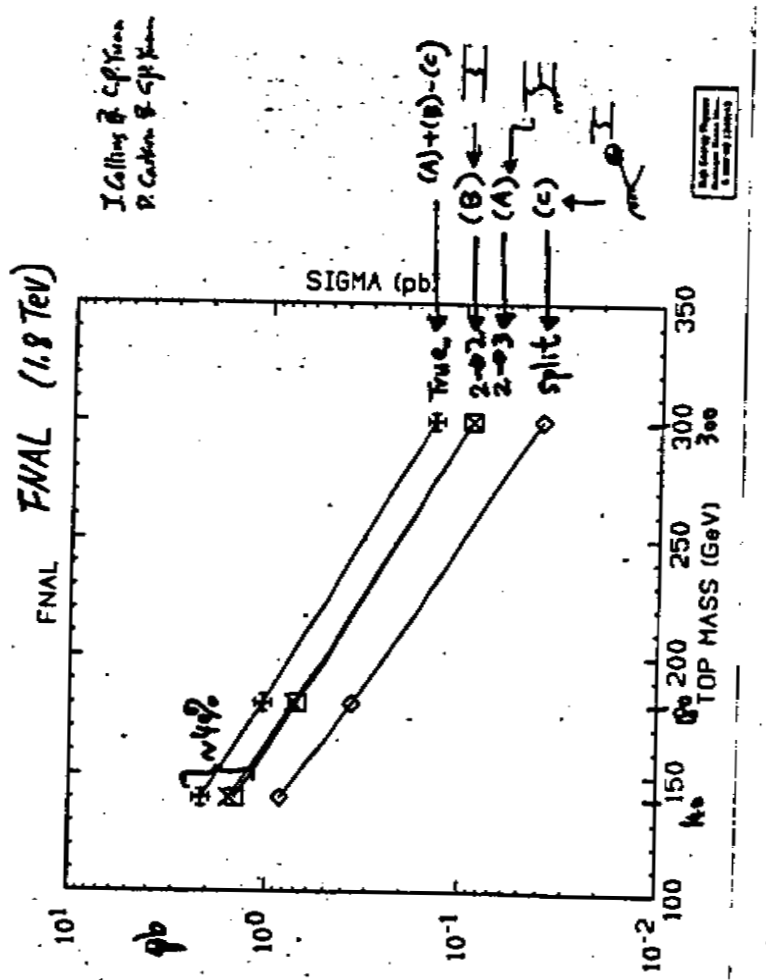
FNAL
FNAL (1.8 TeV)
SIGMA (pb)
TOP MASS (GeV)
(A)+(B)-(C)
(B)
(A)
(C)
True
2→2
2→3
split

- Single Top Quark Production via W-gluon fusion

this process allows the measurement of

$\Gamma_t(t \to bW^+)$

& t-b-W form factors

from its production rate.

S. Mrenna, C.P. Yuan
G. Kane, G. Ladinsky, C.P. Yuan
D. Carlson, C.P. Yuan

Because the produced top quark is polarized, this process can test

$\cancel{CP}$

from its decay.

G. Kane, G. Ladinsky, C.P. Yuan
B. Grzadkowski, J. Gunion

- Using the Wg fusion process

(1) Measuring width of t

This process at SSC can be treated as

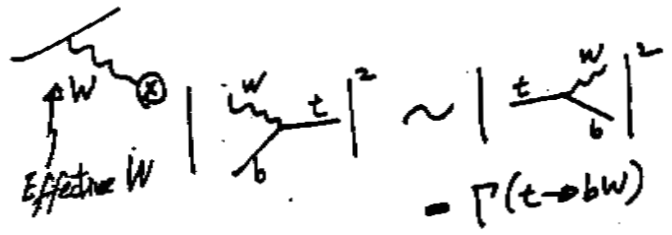

$= \Gamma(t \to bW)$

Therefore, $\Gamma(t \to bW)$ can be measured by counting the production rate of t.

Model Independent width measurement as long as we identify it's a top quark event via this process.

(2) Test CP violation in the decay of t

— If the expectation value of

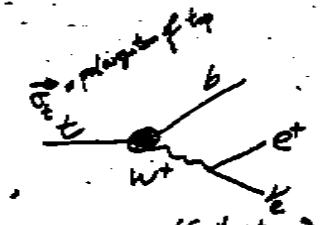

$$\langle \vec{\sigma}_t \cdot \vec{p}_{e^+} \times \vec{p}_b \rangle \neq 0 ,$$

then T-invariance is violated. (Similar to Neutron electric dipole moment)

$\Rightarrow$ CP is violated in t decay

A. Soni & Lindsey, CP½, P. Grządkowski, J. Gunion

— Large CP violation Effects would be relevant to Baryogenesis considered in Cosmology physics.

— Large CP violation Effects exist in some models

Note: $|\vec{\sigma}_t| \lesssim 2\%$ in QCD process
$|\vec{\sigma}_b| \sim 100\%$ in Electroweak-QCD process

• Measuring $|V_{ts}|$?

1) Decay

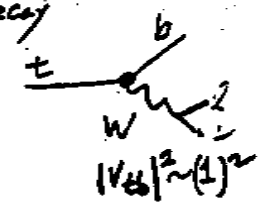

$|V_{tb}|^2 \sim (1)^2$

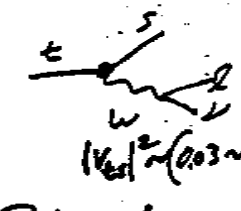

$|V_{ts}|^2 \sim (0.03 \sim 0.06)^2 \sim 10^{-3}$ few

Background ?

2) Production

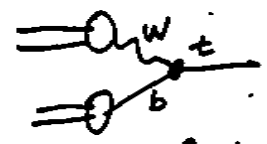

$|V_{tb}|^2 \sim 1$

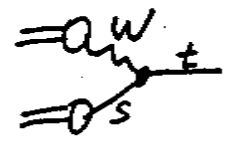

$|V_{ts}|^2 \sim$ few $\cdot 10^{-3}$

— How well do we know (will) parton distribution of b and s ?

— How accurate do we know (will) the production rate of this process ? (Scale dependence ? Hard part matrix element ?)

- Pure leptonic mode

FNAL $\quad m_t = 140$ GeV

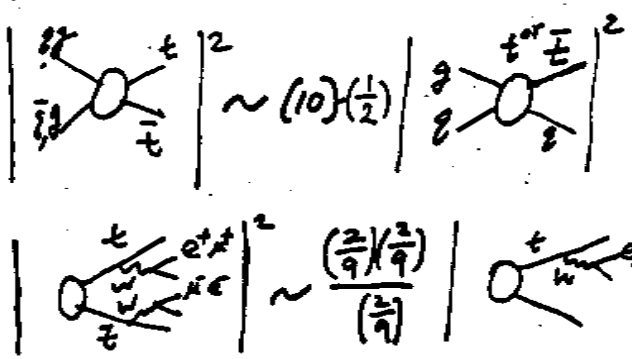

Therefore,

$$\left(\begin{array}{c}\text{Pure leptonic mode}\\ \text{of } t\bar{t}\end{array}\right) \sim (1,1)\cdot\left(\begin{array}{c}\text{Pure leptonic mode}\\ \text{of } t\bar{b}\\ \text{or } \bar{t}b\end{array}\right)$$

How about detection efficiency ?
Backgrounds ?

C-P. Yuan
P. Carlson & C-P. Yuan

With Main Injector
($\int \mathcal{L} = 1\ fb^{-1}$)

Signal ~ a couple of hundreds in SM
Background ~ signal
(W+jets, $t\bar{t}$)
with kinematic cuts included for $W^+ b q(\bar{b})$, $W^+ \to e^+\nu$, $\mu^+\nu$
and $W^- \bar{b} q(b)$, $W^- \to e^-\nu$, $\mu^-\nu$ modes

"New" handle :

— b-tagging (Vertex detector, $|\eta_b| < 2$, $p_T^b > 40$ GeV)

— top quark polarization
(q-b correlation)

neural network can further discriminate background from signal.

At Tevatron

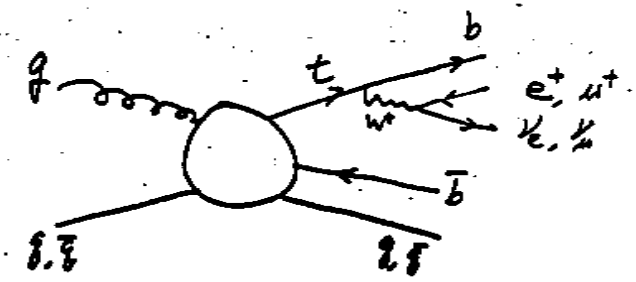

Signature very different from the usual QCD process $gg, q\bar{q} \to t\bar{t}$.

- If the charge of the lepton is identified, then the spectator quark rapidity distribution is asymmetric with $\langle y_q \rangle \sim 1.6$.
- Both b and ℓ^+ have $|y| < 2$.
- t is left-handed polarized in $m_b = 0$ limit.

$\Rightarrow$ Can use the correlation between b and $q, \bar{q}$ to further suppress W+ jets background.

(D. Carlson & C.P. Yuan)

FNAL

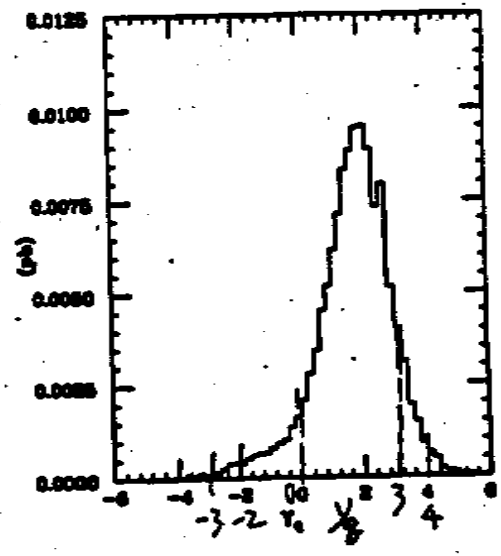

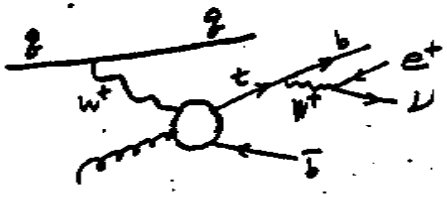

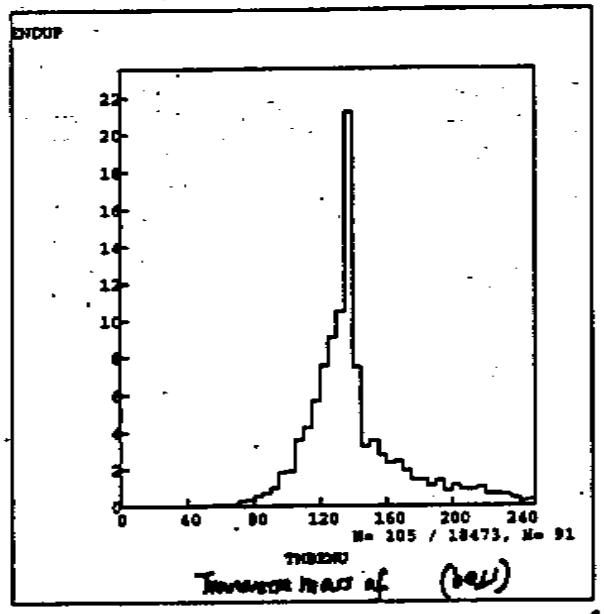

Transverse mass of (bℓν)

FNAL, $\int \mathcal{L} = 1\ fb^{-1}$

$m_t = 140$ GeV

(ℓ + 2 jets) mode

$p_T^{\ell} > 15$, $|y^{\ell}| < 4$

$p_T^{q} > 15$, $|y^{q}| < 2$

$\Delta R > 0.4$, $\not{E}_T > 15$

$\cos\theta_{\ell q} > -0.4$

b-tagging: $p_T^b > 40$, $|y^b| < 2$

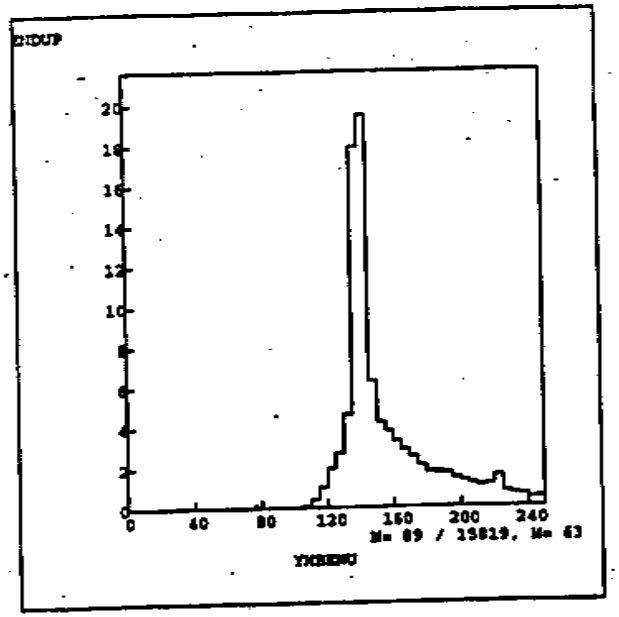

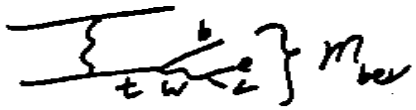

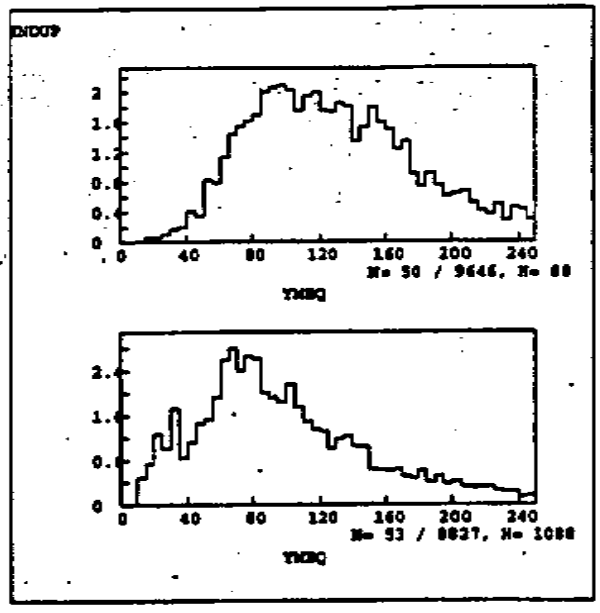
ENDUP
YMBQ
N= 50 / 9646, M= 88
YMBQ
N= 53 / 8827, M= 1088

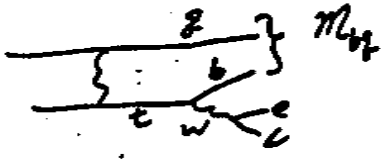
q
m_{bq}
b
t
W
e
ν

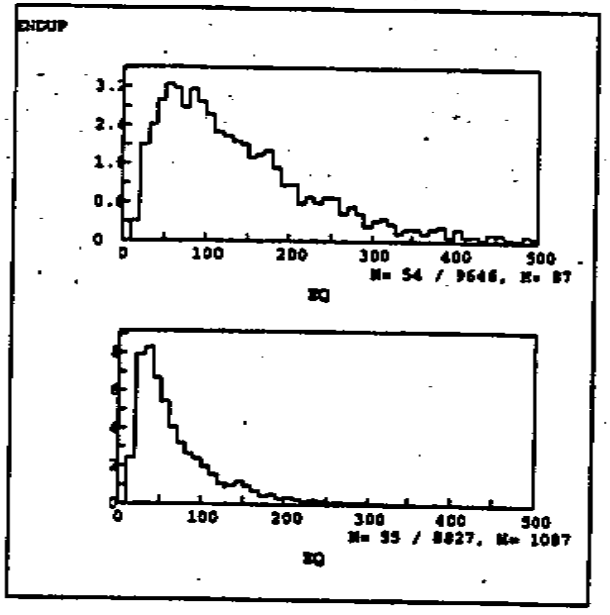
ENDUP
EQ
N= 54 / 9646, M= 87
EQ
N= 55 / 8827, M= 1087

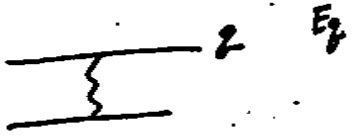
q
E_q

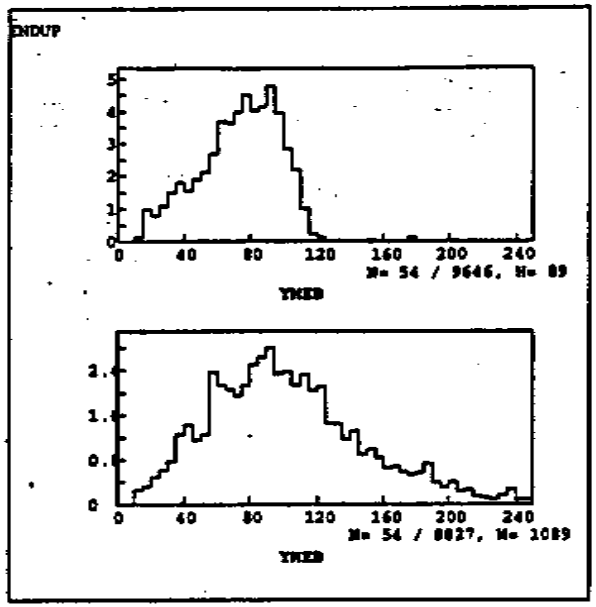
ENDUP
YMEB
N= 54 / 9646, M= 89
YMEB
N= 54 / 8827, M= 1089

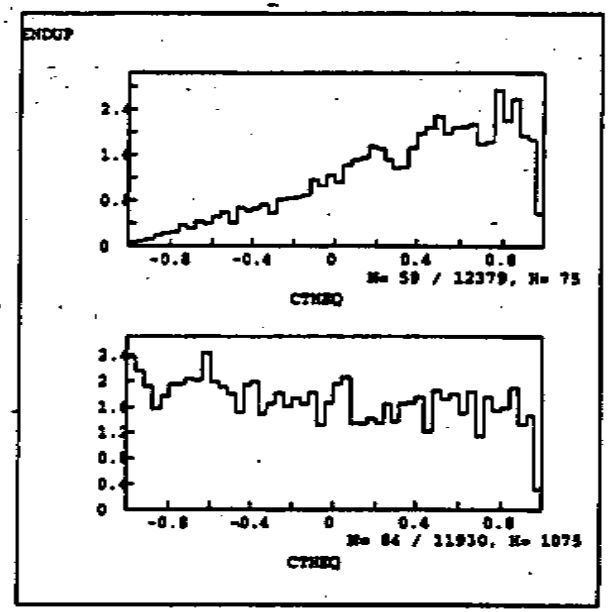
ENDUP
CTHEQ
N= 59 / 12379, M= 75
CTHEQ
N= 84 / 11930, M= 1075

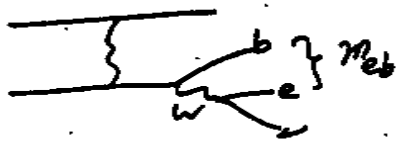
b
e
W
m_{eb}

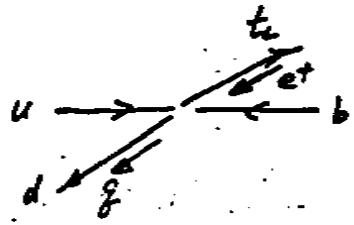
t_u
e^+
u
b
d
g

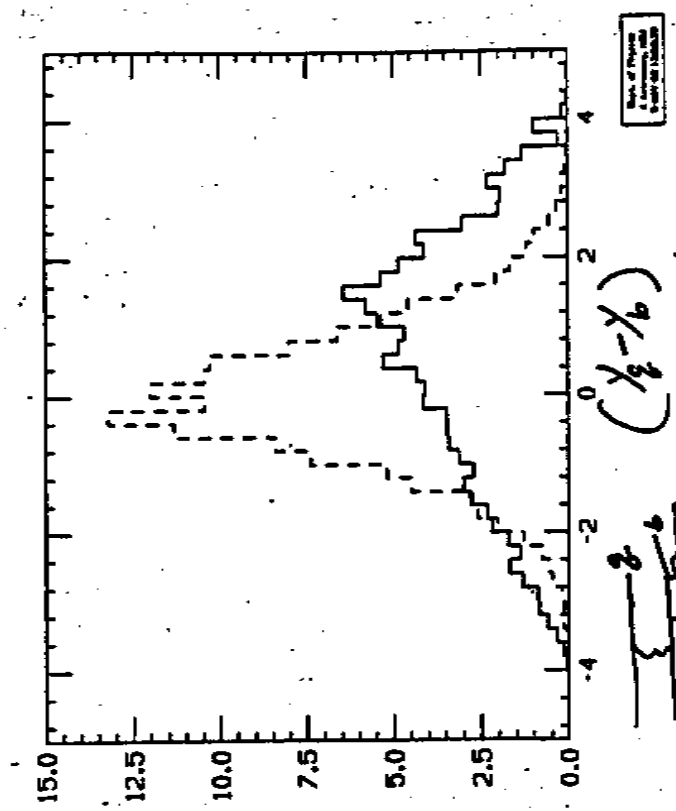
15.0
12.5
10.0
7.5
5.0
2.5
0.0
-4
-2
0
2
4

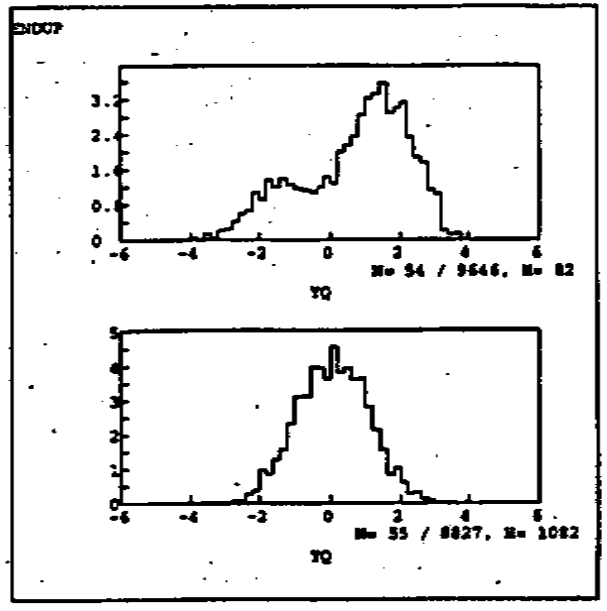
EMOOP
N= 54 / 9646, N= 82
TQ
N= 55 / 8827, N= 1082
TQ

Conclusion

- If t is SM top quark,
  then $m_t \lesssim 200$ GeV
  Find it in 1~4 years at FNAL.
  If not, $\gtrsim 8$ years, at SSC, LHC.

- Once find t
  — Test SM
  (Many predictions get precise)

  — Probe New Physics

- The Electro-Weak-QCD process is Extremely Interesting, and unique in many aspects: Testing CP violation, Measuring width, Probing Symmetry Breaking Mechanism ...

Top at the SSC and LHC

Pekka K. Sinervo
Department of Physics
University of Toronto
Toronto, CANADA
M5S 1A7

November 6, 1992

Abstract

The experimental prospects for top quark studies at the Superconducting Supercollider (SSC) and the Large Hadron Collider (LHC) are reviewed. Estimates are made of the precision by which the top quark mass and branching ratios can be measured at these high energy hadron colliders, and the potential signatures for a charged Higgs boson lighter than the top quark are discussed.

Top at the SSC and LHC

P. Sinervo
University of Toronto

November 6, 1992

I Introduction
II Top Production and Decay
III Detector Requirements
IV Mass Measurement
V Branching Ratios
VI Charged Higgs Complications
VII Associated Production of Top
VIII Conclusions

Introduction

The standard model requires a top quark:

- asymmetry in $e^+e^- \to b\bar{b}$ scattering
- limits on FCNC in b decays
- $B^0 - \bar{B}^0$ mixing
- Electroweak radiative corrections

$M_{top} \sim 130 \pm 35$ GeV/c^2

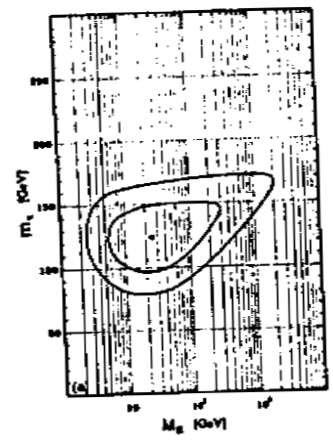

J. Ellis, G.L. Fogli and E. Lisi, PLB 292 (1992)

Studying Top at the SSC/LHC

Strong motivations to study top at SSC and LHC

- CDF/D0 will only have small top samples, e.g.
  - $\sim 100\ e^{\pm}\mu^{\mp}$ events for 500 pb^{-1} and M_{top}= 130 GeV/c^2
  - Measure mass to $\sim$ 5 GeV/c^2
- Intrinsically large $\sigma_{t\bar{t}}$ in pp Collisions
  - Measure mass and branching ratios
  - Measure couplings and other properties
  - Search for new physics
- Significant background to Higgs search
  - $H \to W^+W^-$ vs $t\bar{t} \to W^+ b\, W^- \bar{b}$
  - Intrinsic S/N is $O(10^{-3})$
- Top "tag" may be useful/essential in Higgs search

$$pp \to H\, t\bar{t}, \quad H \to \gamma\gamma$$

Top Production and Decay

$\sigma_{t\bar{t}}$ has been calculated to order α_s^3 by Nason *et al.* (NP B303, 607 (1988)).

...from ECFA 90-133 Vol II

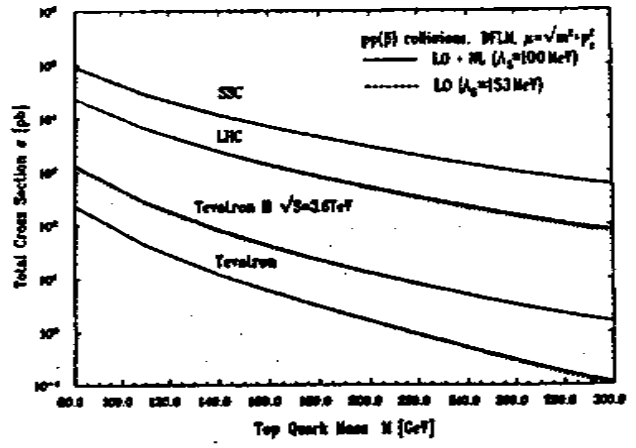

- Uncertainties are order ±30%. (NP B308, 724 (1988))

Rates are enormous by Tevatron standards

SSC	12 nb	1.2×10^7 per year	for M_{top}= 150 GeV/c^2
LHC	2 nb	2.0×10^7 per year	

Various processes contribute to top production

$$g\,g \to t\bar{t}$$
$$q\,q \to t\bar{t}$$
$$W\,g \to t\,\bar{b}$$
$$g\,b \to t\,W$$

...from ECFA 90-133 Vol II

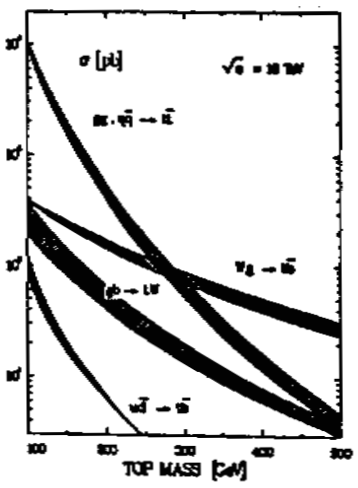

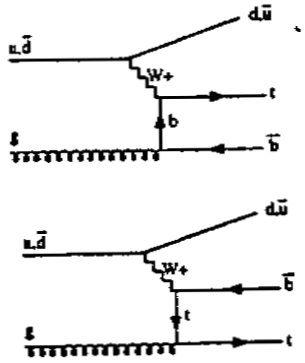

Associated production is also important for Higgs search

$$pp \to H\,t\bar{t}$$

The standard model top decays via charged current:

- *semi-leptonically:*

$$t \to W^+ b, \quad W^+ \to \begin{cases} e^+ \nu_e \\ \mu^+ \nu_\mu \\ \tau^+ \nu_\tau \end{cases} \qquad BR = 1/3$$

- *hadronically:*

$$t \to W^+ b, \quad W^+ \to \begin{cases} c\,\bar{s} \\ u\,\bar{d} \end{cases} \qquad BR = 2/3$$

Other modes are predicted in non-minimal models:

- E.g., if a charged Higgs exists, then also could have

$$t \to H^+ b, \quad H^+ \to \begin{cases} c\,\bar{s} \\ \tau^+ \nu_\tau \end{cases}$$

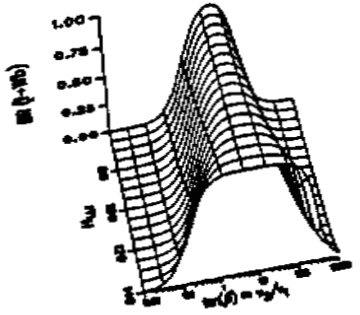

K. Ragan & P. Tipton, private comm.

Top quark typically produced with $< P_T > \sim M_{top}/2$

- decay products are at moderate P_T
- and pseudorapidity $|\eta| \lesssim 2.5$

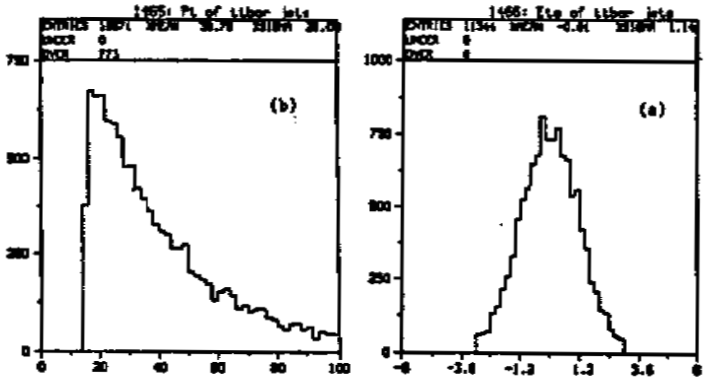

...from SDC-30, P. Sinervo et al.

Decay modes involving leptons are most promising

- Reduces QCD backgrounds
- Provides a signature for charged current decay
- Leptons are isolated and have $P_T \gtrsim 20$ GeV/c

Cf. UA1, UA2 and CDF

Primary backgrounds come from W + Jet production

Detector Requirements

1. Identify isolated, moderate P_T leptons
   - ($\gtrsim 30 - 40$ GeV/c) gives several Hz of leptons
   - requires fine segmentation ($\Delta\eta \times \Delta\phi \sim 0.05 \times 0.05$)
2. Reconstruct complex jet topologies
   - Calorimeter resolution of
   $$\sigma_E \sim 0.7\sqrt{E}$$
   - Hadron calorimeter segmentation of ~ 0.1
3. Measure $\not{E}_T$ reasonably well
4. Tag b hadrons
   - Use non-isolated leptons or displaced vertices
   - Perhaps essential for *lepton + jets* channel
   - Useful for background studies

Lepton Isolation is an important tool to reduce backgrounds

- Energy in cone of radius $R \equiv \sqrt{\Delta\eta^2 + \Delta\phi^2} = 0.3$

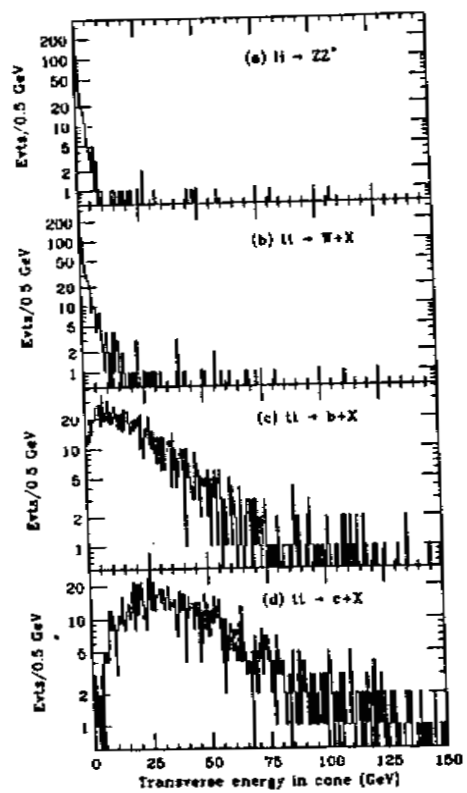

from SDC-92-201 (SDC Technical Design Report)

MC simulation of physics and electronics pileup show that isolation is not seriously compromised

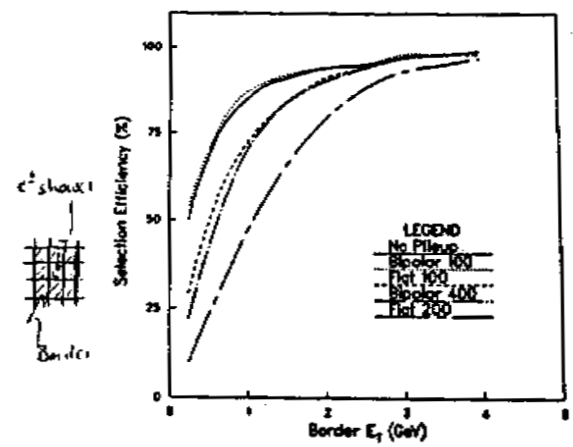

...from SDC-30

- Somewhat more sensitive at LHC
- Can use long shaping times for calorimeter readout

Dilepton Channels

The $e^{\pm}\mu^{\mp}$ channel is the cleanest channel

- Rate is equal to e^+e^- and $\mu^+\mu^-$ combined
- No Drell-Yan backgrounds

At SSC, requiring lepton P_T

- $P_T > 20$ GeV/c
- $|\eta| < 2.5$

yields $\sim 10^6$ events per SSC year (10^{40}cm^{-2})

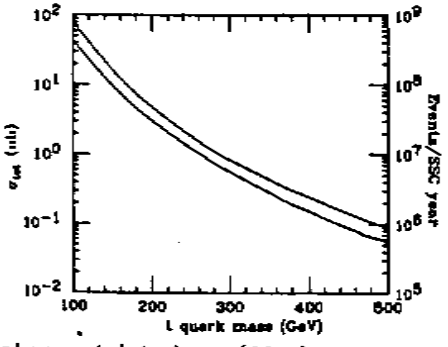

...SDC-92-201

Theoretical uncertainty in $\sigma_{t\bar{t}}(M_{top})$

$\Rightarrow \sigma_{M_{top}} \sim 10 - 15$ GeV/c^2

A similar analysis for LHC illustrates cleanliness

- Require lepton $P_T > 50$ GeV/c
- $\sum E_T < 10$ GeV in cone of $R = 0.4$ for both leptons
- $|\eta| < 1.5$

yields 3×10^5 events in $\int \mathcal{L}\,dt = 10^{41}$ cm^{-2}

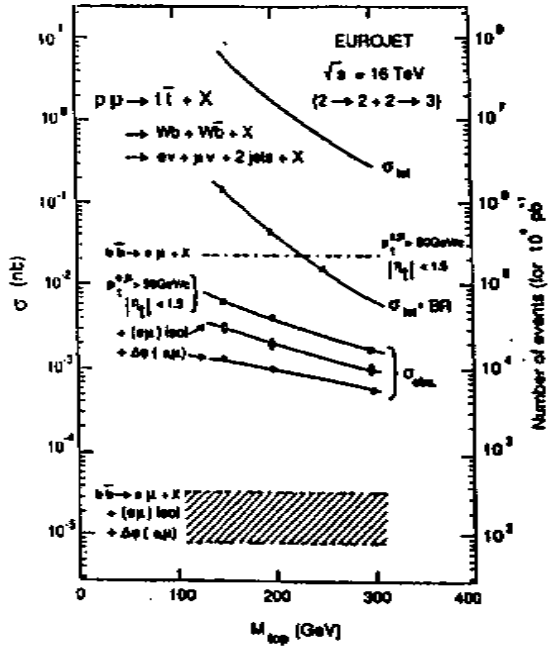

...ECFA-90-133

A more sensitive M_{top} measurement comes from sequential dileptons

$$t \rightarrow W^+ b \rightarrow \mu^- X$$
$$\hookrightarrow e^+ \nu_e$$

Identify $W \rightarrow e^+ \nu_e$ and $b \rightarrow \mu^- X$ using isolation

- Electron $P_T > 20$ GeV/c
- $\sum E_T < 4$ Gev in $R < 0.2$ around electron
- Muon $P_T > 20$ GeV/c
- $\sum E_T > 20$ Gev in $R < 0.4$ around muon
- $P_T(e\mu) > 100$ GeV/c

$\Rightarrow 7 \times 10^4$ events per year

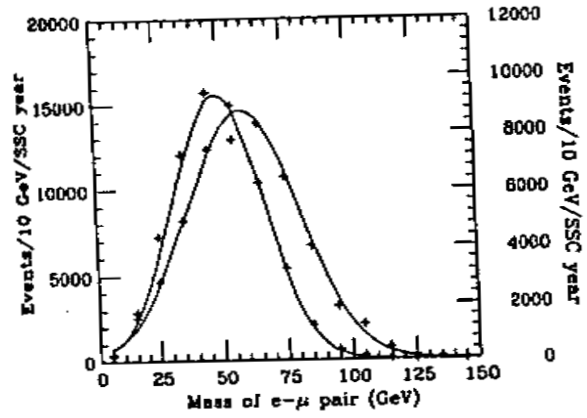

$< M(e\mu) >$ sensitive to M_{top}

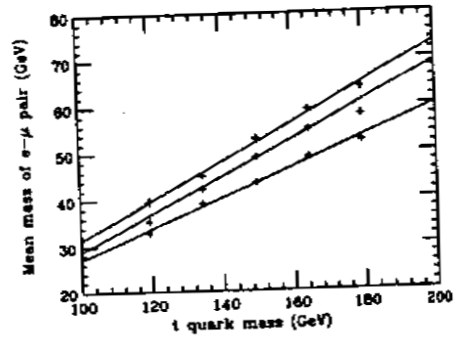

SDC-92-201

Uncertainty in M_{top} dominated by systematic uncertainties

Effect	$\sigma_{M_{top}}$ (GeV/c^2)
b quark fragmentation	1.5
t quark P_T	1.9
Statistics (1 year)	0.5

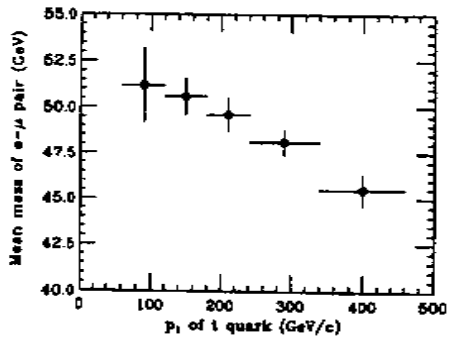

SDC-92-201

⇒ Can expect to measure M_{top} to $\sim 2-3$ GeV/c^2

Lepton + Jets

The *lepton + jets* mode provides inherently more rate

- Can perform full reconstruction
- Can directly measure M_{top} and BR

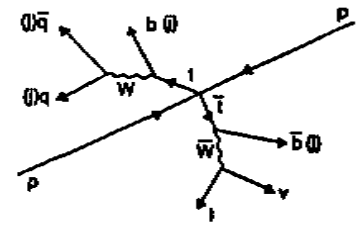

- However, jet combinatorics are a problem

SSC and LHC groups have made extensive studies

- Agree that kinematical selection can reconstruct top
  - Require isolated lepton with $P_T \gtrsim 40$ GeV/c
  - Require 3 jets with high P_T cut
- More efficiently done using b quark tag

SDC approach takes advantage of b quark tagging

- Allows measurement to be done at low luminosity
- Better control of systematics in M_{top} measurement

Selection requires

- Isolated lepton with $P_T > 40$ GeV/c
- ≥ 3 jets ($R = 0.5$ cone used for clustering)
- $P_T > 30$ and $|\eta| < 2.5$ for jets
- One jet to be tagged as b quark ($\epsilon \sim 30\%$)
- $P_T > 200$ GeV/c of 3-jet system

Resulting event rate for 1 SSC year is

	$M_{top} = 150$ GeV	$M_{top} = 250$ GeV
$\sigma(t\bar{t})$	12 nb	1.5nb
$N_{t\bar{t}}$	1.2×10^8	1.5×10^7
Branching ratio	8/27	8/27
Lepton ID, geometric	0.43	0.56
Lepton ID, isolation	0.85	0.85
b jet, geometric	0.51	0.71
b jet tag	0.30	0.30
$N(p_t(3\text{-}jet)) > 200$ GeV/c	158,000	—
$N(p_t(3\text{-}jet)) > 300$ GeV/c	—	39,400

...SDC-92-201

$M(jj)$ distribution for non-b jets shows clear W

- Require $65 < M(jj) < 95$ GeV/c^2

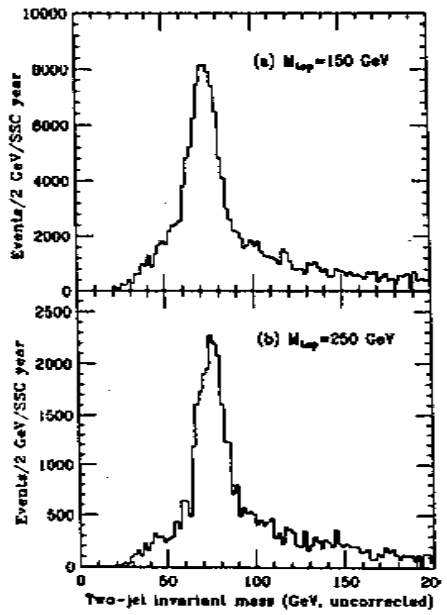

SDC-92-201

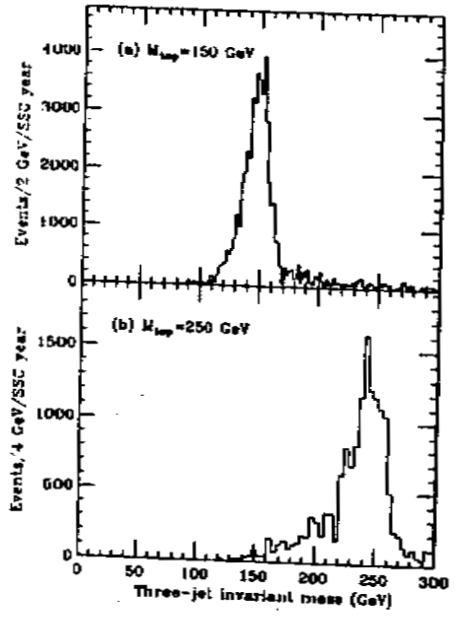

Three jet invariant mass requiring two jets to form a W candidate (selecting peak in previous plot).

Systematics in M_{top} dominated by jet energy scales

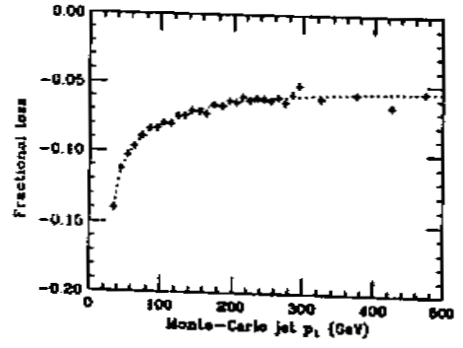

SDC-92-201

- Use MC to correct for clustering effects, etc.
- Can calibrate low-energy jet scale using W signal
- b quark fragmentation

$$\sigma_{M_{top}} \sim 2 - 3\mathrm{GeV/c^2}$$

Top Branching Ratios

Although $e^{\pm}$ and $\mu^{\pm}$ decay modes are most accessible,

$$t \to \tau \nu_\tau b$$

is detectable using single-prong $\tau \to \pi^- X$ decays

Require

- isolated lepton with $P_T > 40$ GeV/c(from W decay)
- one jet with $P_T > 30$ tagged as b hadron
- isolated, charged track with $P_T > 50$ GeV/c

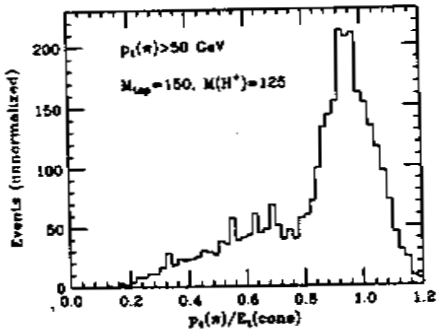

$\Rightarrow$ uncertainty in relative τ rate is $\lesssim 5\%$

Observation of top in

$pp \to e^{\pm}\mu^{\mp}$	$\propto BR(t \to e\,\nu_e\,b) \times BR(t \to \mu\,\nu_\mu\,b)$
$pp \to l^{\pm} l^{\mp}$	$\propto BR(t \to l\,\nu_l\,b)^2$
$pp \to \mu^{\pm} + jets$	$\propto BR(t \to \mu\,\nu_\mu\,b) \times BR(t \to q\,\bar{q}\,b)$
$pp \to e^{\pm} + jets$	$\propto BR(t \to e\,\nu_e\,b) \times BR(t \to q\,\bar{q}\,b)$
$pp \to \tau^{\pm}\tau^{\mp}$	$\propto BR(t \to \tau\,\nu_\tau\,b) \times BR(t \to q\,\bar{q}\,b)$

Allows measurement of relative BR's to $1-5\%$

- Limited by systematic uncertainty in efficiency
- Depends on isolation of lepton and physics models

Charged Higgs

Heavy charged Higgs coupling to top is detectable

- May see it in $BR(t \to \tau X)/BR(t \to e/\mu X)$

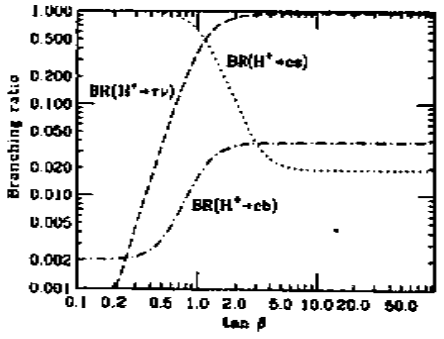

SDC-92-201

Can also reconstruct it's 3-jet final states in

$$pp \to t\bar{t} \to W^+ b\, H^- \bar{b}$$

- Follow same jet reconstruction technique
- Cut on three-jet system to reduce combinatorics
- Require one b quark jet be tagged

Resulting $M(jj)$ distribution for $M_{H^+} = 125$ GeV/c^2 is

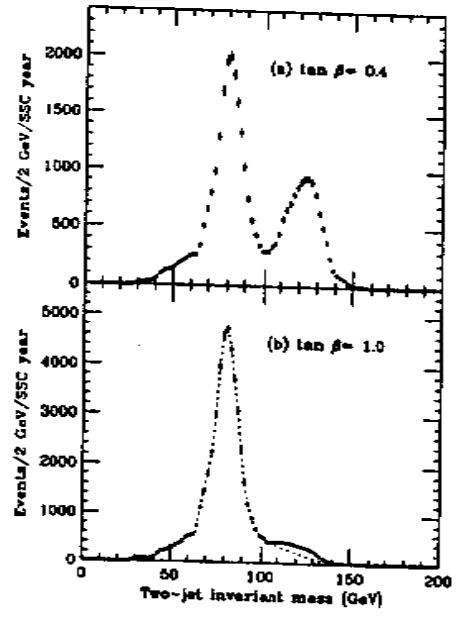

SDC-92-201

H^+ is clearly detectable over a large range of $\tan\beta$.

- Characterize signal as excess over background
- Plot statistical significance vs $\tan\beta$

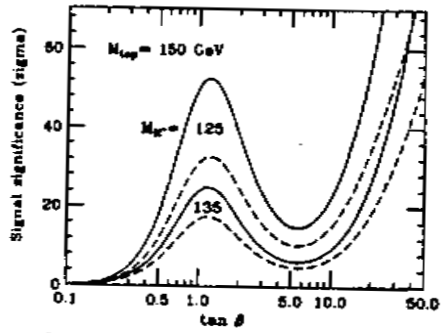

SDC-92-201

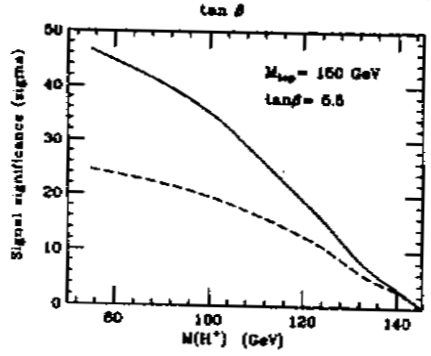

Associated Top Production

$pp \to H\, t\bar{t}$ may be important for a light Higgs search

- The WW channel is closed and $Z\,Z^*$ is rate-limited
- $H \to \gamma\gamma$ is largest potential rate
  - QCD diphoton backgrounds are enormous

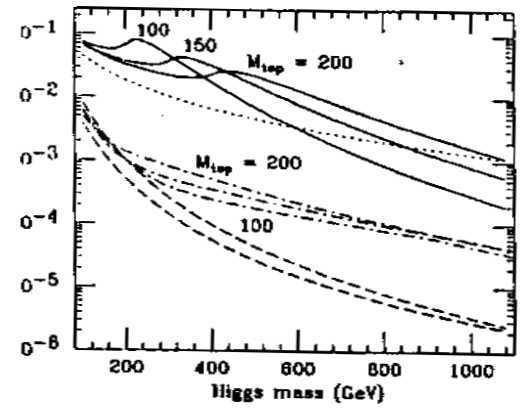

SDC-92-203

Tag $t\bar{t}$ system with isolated, high P_T lepton

- Reduces QCD fake backgrounds to manageable level
- Isolation removes $b\bar{b}\,\gamma\gamma$ background
- No longer need high-precision EM calorimetry

"Reach" in $\gamma\gamma l X$ channel complements $Z Z^*$

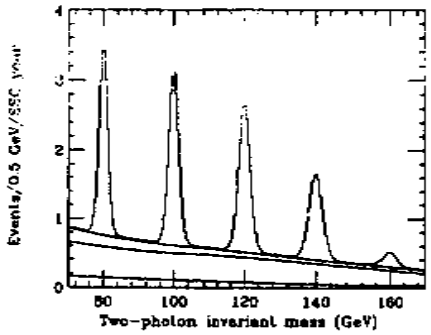

SDC-92-201

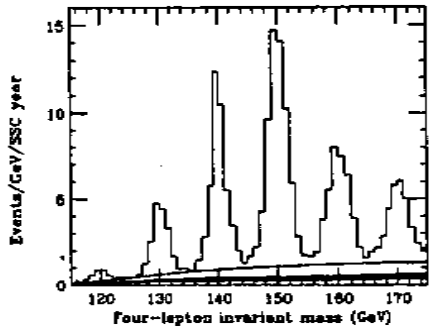

Background to Higgs Search

Extensive studies have looked at implications of "heavy" top to Higgs search

- Forced to abandon "simple" $H \to W^+W^-$ search
- Requires substantially more sophisticated approach
  - WW fusion process and forward jet tagging
  - stringent kinematic cuts

Makes understanding $t\bar{t}$ production and decay kinematics even more important

Conclusions and Summary

SSC and LHC are inherent "top factories"

- Dominate low and intermediate mass scale physics
- Next generation "calibration" signal

Measure M_{top} to $\sim 2-3$ GeV/c^2 in 1 year of operation

- Limited by systematics
- Could eventually reduce uncertainty to $\lesssim 1$ GeV/c^2(?!)

Branching ratios measured to $\lesssim 5\%$ in 1 year

- Test universality of couplings
- Sensitive to charged Higgs

Useful tag for low mass Higgs ($M_H \lesssim 100$ GeV/c^2)

Serious background to $H \rightarrow W^+W^-$

References and Bibliography

The following articles, and the references contained therein, discuss many of the topics relevant to top quark physics at the SSC and LHC.

1. *Compact Muon Solenoid Letter of Intent*, LHCC 92-3 (October 1992).
2. *SDC Technical Design Report*, SDC-92-201 (April 1992).
3. *Discovery limit of the charged Higgs boson via top quark decay at future hadron colliders*, D. P. Roy, Phys. Lett. **B283** (1992), 403.
4. *W boson-top quark background to heavy Higgs boson production*, G. A. Ladinsky and C.-P. Yuan, Phys. Rev. **D43** (1991), 789.
5. *Large Hadron Collider Workshop Proceedings, Vol II*, ed. G. Jarlskog and D.Rein, ECFA 90-133 (December 1990).
6. *The Total Cross Section for the Production of Heavy Quarks in Hadronic Collisions*, P. Nason, S. Dawson and R. K. Ellis, Nucl. Phys. **B303** (1988), 607.

Interplay between Top Decay and Fragmentation

Torbjörn Sjöstrand
Theory Division, CERN
CH-1211 Geneva 23, Switzerland

Abstract

For a range of top quark masses, the top decay time is comparable to its fragmentation time. Under these circumstances, the particle production involving the original t and $\bar{t}$ may have time to start, only to be cut short by the top decays. Additional production involves the b and $\bar{b}$ quarks created in the decays. We show that the topology of the produced particles in e^+e^- annihilation is changed as a function of the top lifetime. As a consequence, it could be possible to use experimental momentum measurements to probe the space-time structure of the top fragmentation and decay processes. By contrast, effects are more smeared out in hadron collisions, and it does not seem these issues will confuse top searches and top mass determinations.

Interplay between Top Decay and Fragmentation

Torbjörn Sjöstrand
CERN/TH

1) Introduction
2) $e^+e^- \to t\bar{t}$; no QCD radiation
3) $e^+e^- \to t\bar{t}$; with QCD radiation
4) $p\bar{p} \to t\bar{t}X$
5) Summary

reference (2+3):
T.S + P. Zerwas, in "e^+e^- collisions at TeV energies", ed. P. Zerwas, DESY 92-123A, p. 162

Top lifetime

If $m_t > m_W + m_b$ then

$$\Gamma_t = \frac{G_F m_t^3}{8\sqrt{2}\pi}\sqrt{(1-r_W-r_b)^2-4r_W r_b}\left\{(1-r_b)^2+(1+r_b)r_W-2r_W^2\right\}$$

where $r_W = \frac{m_W^2}{m_t^2}$ and $r_b = \frac{m_b^2}{m_t^2}$

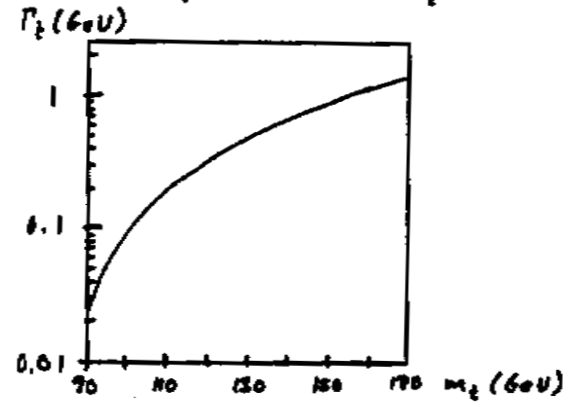

$$\langle \tau \rangle = \frac{\hbar}{\Gamma_t} = \frac{0.2\ \text{GeV}\cdot\text{fm}}{\Gamma_t} \quad (\text{with } c=1)$$

$$\langle t \rangle = \gamma \cdot \langle \tau \rangle$$

$$\langle x \rangle = v \cdot \langle t \rangle = \beta\gamma \frac{\hbar}{\Gamma_t}$$

Top fragmentation

Assume confinement in string picture ⇒ linear confinement with string tension $\kappa = 1$ GeV/fm

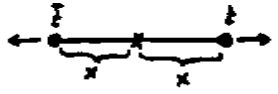

equations of motion:

$$\frac{dp}{dt} = -\kappa \quad \Rightarrow \quad p(t) = p(0) - \kappa t$$

$$\frac{dE}{dt} = -v(t)\cdot\kappa \Rightarrow E(t) = E(0) - \kappa x$$

ΔE = top energy lost to string before top decay ⇒ available for particle prod.

$$\langle \Delta E \rangle = \kappa \cdot \langle x \rangle = \kappa \cdot \beta\gamma \frac{\hbar}{\Gamma_t}$$

e.g. $\sqrt{s} = 500$ GeV, $m_t = 100$ GeV:

$$\langle \Delta E \rangle = 1 \text{ GeV/fm} \cdot 2.3 \cdot \frac{0.2 \text{ GeV}\cdot\text{fm}}{0.1 \text{ GeV}} = 4.6 \text{ GeV}$$

(i.e. $\langle E_{frag_m} \rangle = 2 \cdot \langle \Delta E \rangle \sim 9$ GeV)

For stable top could write fragmentation funct., e.g. Peterson et al.:

$$f(z) \propto \frac{1}{z\left(1 - \frac{1}{z} - \frac{\varepsilon}{1-z}\right)^2}$$

$z_Q \sim 1/m_Q^2 \quad \Rightarrow \quad \varepsilon_t/\varepsilon_b \sim m_b^2/m_t^2$

no QCD radiation ⇒ $\varepsilon_t \sim 10^{-4}$

$\langle \Delta E \rangle \approx (1 - \langle z \rangle)\cdot E_t \approx (1 - 0.96)\cdot E_t$

e.g. $\sqrt{s} = 500$ GeV ⇒ $\langle \Delta E \rangle \approx 10$ GeV

i.e. compare

$\langle \Delta E \rangle$ (top stable) ≈ 10 GeV

$\langle \Delta E \rangle$ (before t decay) ≈ 5 GeV

⇒ some, but not all, particle formation takes place before top decay

first steps construct toy model

1) without QCD radiation
2) with semileptonic decays $t \to b\, \ell^+ \nu_\ell$

String topologies

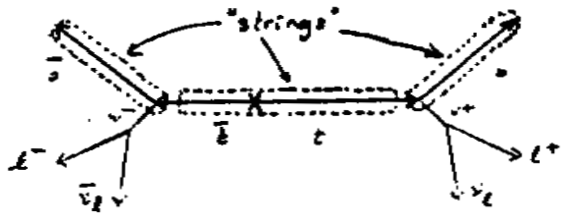

"3 string scenario"
("long-lived" t; may include τ formation)

In limit $m_t \gg 100$ GeV decays occur rapidly:

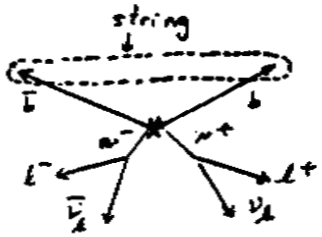

NOTE: string has net upwards motion

"1 string scenario"

Intermediate situation also possible:

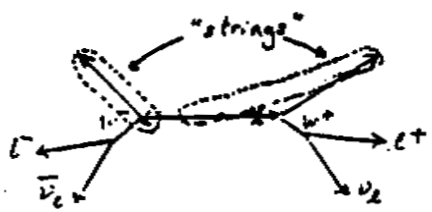

"2 string scenario"

Fragmentation scheme

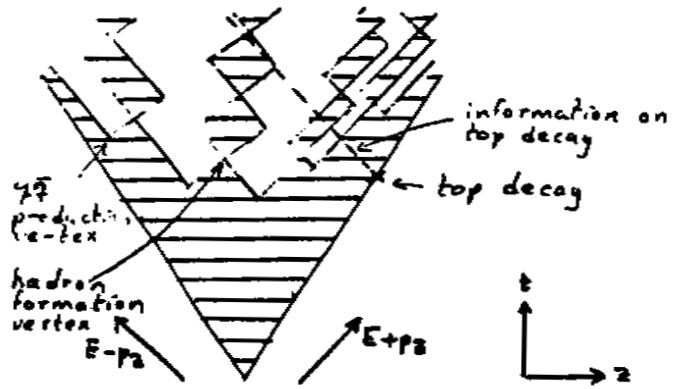

1) form hadrons as if t and $\bar{t}$ stable
2) select τ for t and $\bar{t}$
   ⇒ reconstruct decay vertices
   ⇒ define forward lightcones
3) if hadron formation vertex not in t or $\bar{t}$ decay forward lightcone
   ⇒ "early" particle ⇒ unaffected
4) other particles "late" ⇒ not formed
   ⇒ remove, store energy in effective $\bar{q}$ (q) for t ($\bar{t}$) end at time of decay
5) do $t \to b$ ($\bar{t} \to \bar{b}$) decay
6) string fragmentation $t+\bar{q}$ ($\bar{t}+q$)

e^+e^- events without QCD radiation

study $e^+e^- \to t\bar{t}$ at $\sqrt{s} = 500$ GeV;
no QCD or QED radiation (no γ, no g)

quantity	$m_t = 90$	$m_t = 100$	$m_t = 120$
Γ (GeV)	0.023	0.093	0.73
$\mathcal{R}\langle\bar{t}\rangle$ (GeV)	9.56	2.14	0.61
$\mathcal{R}\langle t\rangle$ (GeV)	23.5	5.55	1.28
$\langle n_{total}\rangle$	6.45	6.15	5.55
$\langle n_{early}\rangle$	3.52	1.81	0.26
$\langle n_{late}$ (not $t,\bar{t}$)$\rangle$	0.92	2.33	3.30
Prob(3 string)	94%	71%	18%

Prob(3 string) = Prob(≥ 1 hadron formed before t <u>and</u> $\bar{t}$ decays)

In following:
compare the 3-string events with equivalent number of 1-string events

currently no 2-string events $\Rightarrow$ not full mix

Rapidity distributions: "early" vs. "late"

$\bar{t} \longleftarrow \quad t \longrightarrow \qquad \longrightarrow z$ axis

primary particles produced in string, excluding top hadrons
"early" = produced before top decays
"late" = produced after top decays $\Rightarrow$ NOT produced

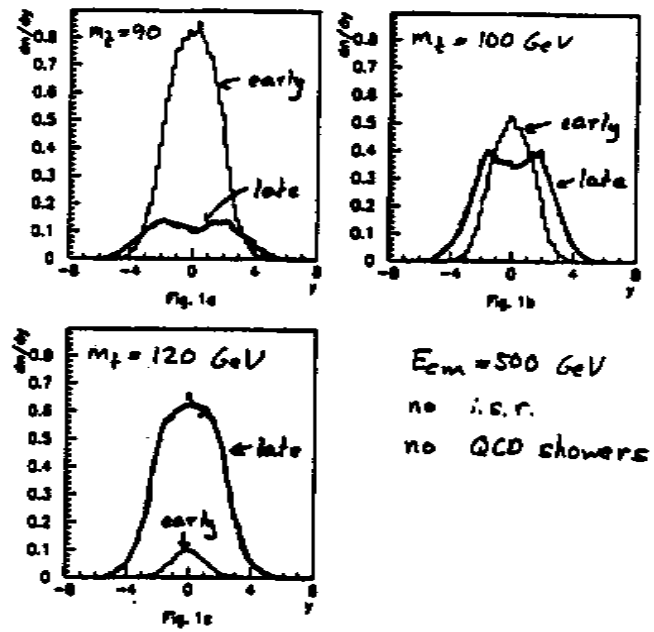

$E_{cm} = 500$ GeV
no i.s.r.
no QCD showers

$\rightarrow m_t = 100$ GeV as crossover

Rapidity distributions: 3-string vs. 1-string

$\bar{t}$ — t → z axis

charged final state particles

most final state particles from B decays

⇒ remove by

1) microvertex information
2) $p_\perp$ cuts
3) y cuts (after jet finding)

↓ decreasing efficiency

all particles

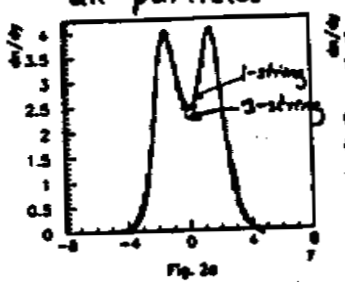

Fig. 2a

B decay products removed

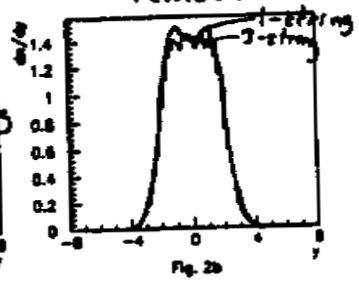

Fig. 2b

E_{cm} = 500 GeV

m_t = 100 GeV

no i.s.r.

no QCD showers

Particle distribution in event plane

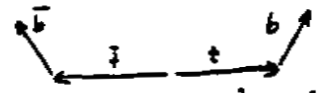

consider planar events with b and $\bar{b}$ on same side

all charged particles m_t = 100 GeV

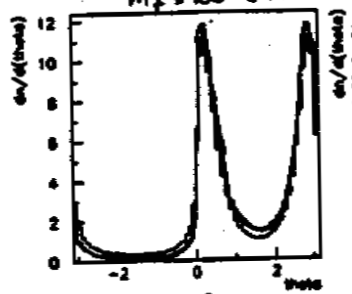

Fig. 3a

B products removed m_t = 100

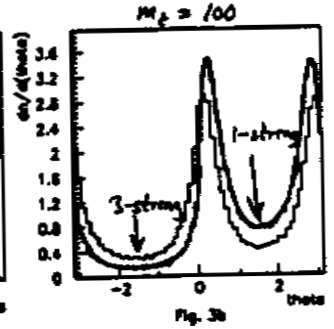

Fig. 3b

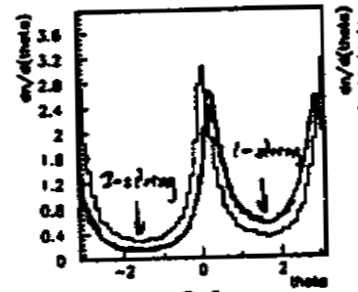

Fig. 3c

B products removed m_t = 90 GeV

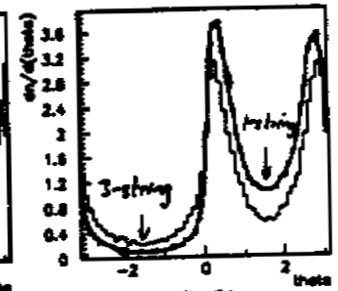

Fig. 3d

B products removed m_t = 120 GeV

E_{cm} = 500 GeV

no i.s.r.

no QCD showers

Particle distribution around event axis

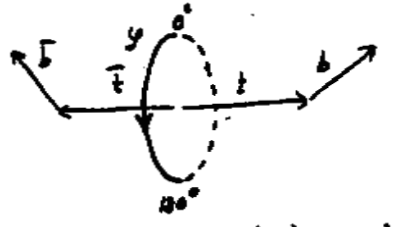

consider charged particles with $|y|<1$
$\Rightarrow$ pick out region of large string effects

all charged particle — B products removed

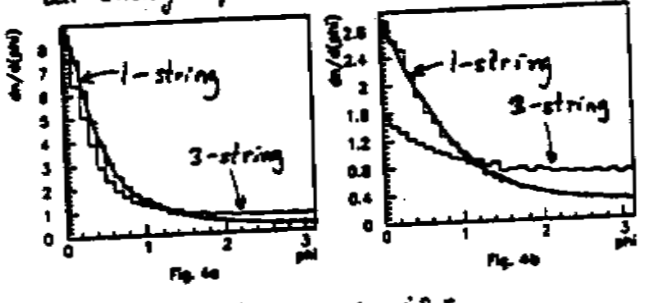

$m_t = 100$ GeV — no i.s.r.
$E_{cm} = 500$ GeV — no QCD showers

admixture measurement
$\Rightarrow$ t lifetime measurement
(but precision lousy)

Gluon emission effects

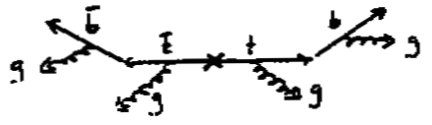

$$|\mathcal{M}|^2 \propto |A(t\to tg)+A(\bar{t}\to\bar{t}g)+A(b\to bg)+A(\bar{b}\to\bar{b}g)|^2$$
$$= \widehat{t\bar{t}} + \widehat{tb} + \widehat{\bar{t}\bar{b}} + \underbrace{\text{interference}}_{\to 0 \text{ when } \Gamma_t \to 0}$$

complete formulae in limit $E_g \to 0$:
G. Jikia, Phys. Lett. B257 (1991) 196
V.A. Khoze, W.J. Stirling, LH Orr,
DTP/92/14 and UCD-92-05

MC prescription : subdivide in two terms

$$|\mathcal{M}|^2 = \underbrace{f_1(p_t, p_{\bar{t}}; p_g)}_{\text{"emission off } t, \bar{t}\text{"}} + \underbrace{f_2(p_t, p_{\bar{t}}, p_b, p_{\bar{b}}; p_g)}_{\text{"emission off } b, \bar{b}\text{"}}$$

alt. 1: $$f_1 = -\frac{m_t^2}{(p_t p_g)^2} - \frac{m_t^2}{(p_{\bar{t}} p_g)^2} + \frac{2 p_t p_{\bar{t}}}{(p_t p_g)(p_{\bar{t}} p_g)}$$

alt. 2: $$f_1 = -\frac{m_t^2}{(p_t p_g)^2 + m_t^2\Gamma_t^2} - \frac{m_t^2}{(p_{\bar{t}} p_g)^2 + m_t^2\Gamma_t^2}$$
$$+ \frac{2(p_t p_{\bar{t}})\left[(p_t p_g)(p_{\bar{t}} p_g) + m_t^2\Gamma_t^2\right]}{\left[(p_t p_g)^2 + m_t^2\Gamma_t^2\right]\left[(p_{\bar{t}} p_g)^2 + m_t^2\Gamma_t^2\right]}$$

Radiation + fragmentation scheme

1) Allow emission off $t, \bar{t}$:
   $1 \le E_g \le 20$ GeV ; up to 4 gluons
   E, p conservation by boost + rescaling

2) Fragment $tg \ldots g\bar{t}$ string
   assuming g ordered in rapidity along string

3) Select τ and do top decays

4) Remove "late" particles ;
   here use simpler picture than before :
   a) assume $q\bar{q}$ production vertices
      at fixed time $\tau_q = \langle \tau_{fragm} \rangle$
   b) include mass $\Rightarrow$ prod. vertex τ_i for hadron i
   c) $x_i = \tau_i \cdot p_i/m$
   d) correct (reduce) for fragm. p_z component

5) Allow emission off $b, \bar{b}$:
   $1 \le E_g \le 10$, $\min(m_{bg}, m_{\bar{b}g}) > 6$ GeV,
   up to 20 gluons, subdivided by side
   E, p conservation in $(t, \bar{t})$ rest frame

6) Fragment $bg \ldots g\bar{q}$ $(\bar{b}g \ldots gq)$ string

Note 1: $\kappa_s = 0.25$, as 1st ord. κ_s at PETRA/PEP
Note 2: $s_t \approx 10^{-4}$ should be reduced to
$s_l \approx 10^{-5}$ when full QCD radiation
(scaling up from b)
Note 3: 1-string : all radiation before fragm.

Rapidity distributions : "early" vs. "late"

$\bar{t} \longleftarrow \quad \longrightarrow t \qquad \longrightarrow z$ axis

primary particles produced in string,
excluding top hadrons
"early" = produced before top decays
"late" = produced after top decays $\Rightarrow$ NOT produced

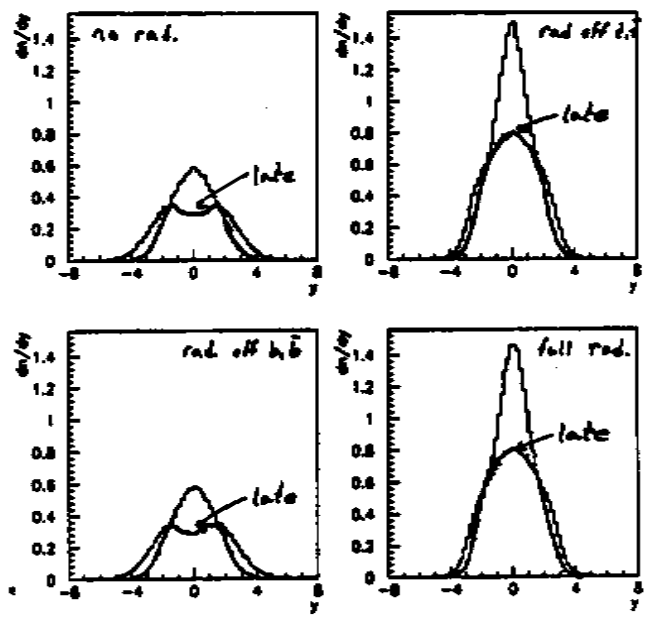

$E_{cm} = 500$ GeV
$m_t = 100$ GeV
no i.s.r.
$\varepsilon_t = 10^{-4}$
QCD radiation subdivision all. 2

Rapidity distributions : 3-string vs. 1-string
charged final state particles

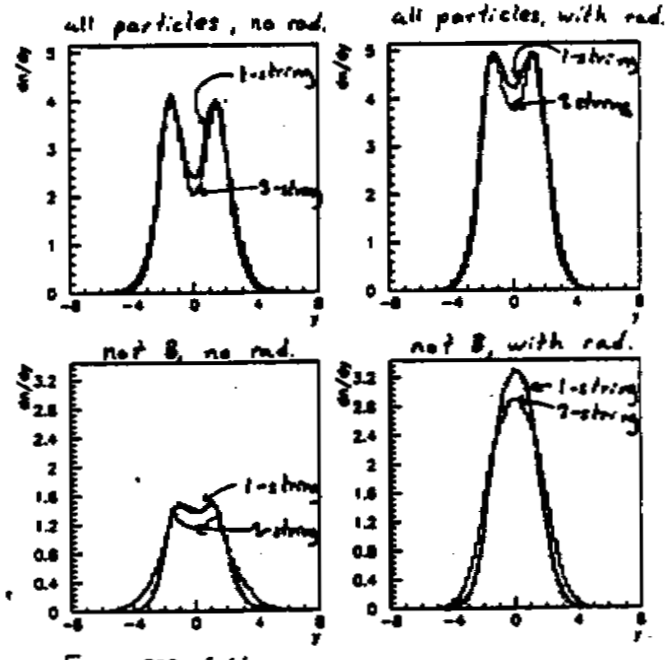

$E_{cm} = 500$ GeV
$m_t = 100$ GeV
no i.s.r.
$\varepsilon_t = 10^{-4}$
QCD radiation subdivision alt. 2

Particle distribution in event plane

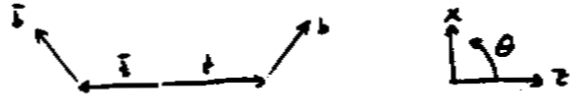

consider planar events with $b, \bar{b}$ on same side
charged final state particles not from $B, \bar{B}$

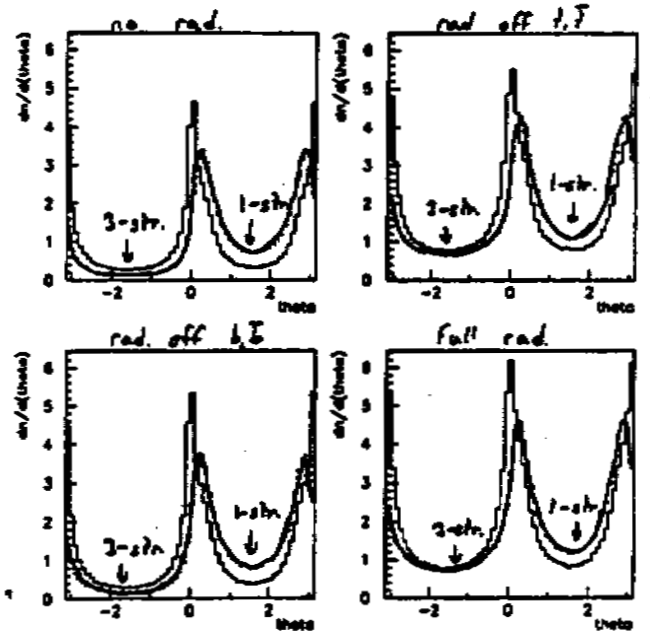

$E_{cm} = 500$ GeV
$m_t = 100$ GeV
no i.s.r.
$\varepsilon_t = 10^{-4}$
QCD radiation subdivision alt. 2

Particle distribution around event axis

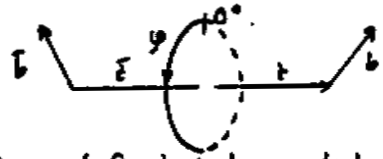

charged final state particles in range $|y|<1$
not from $t, \bar{t}$

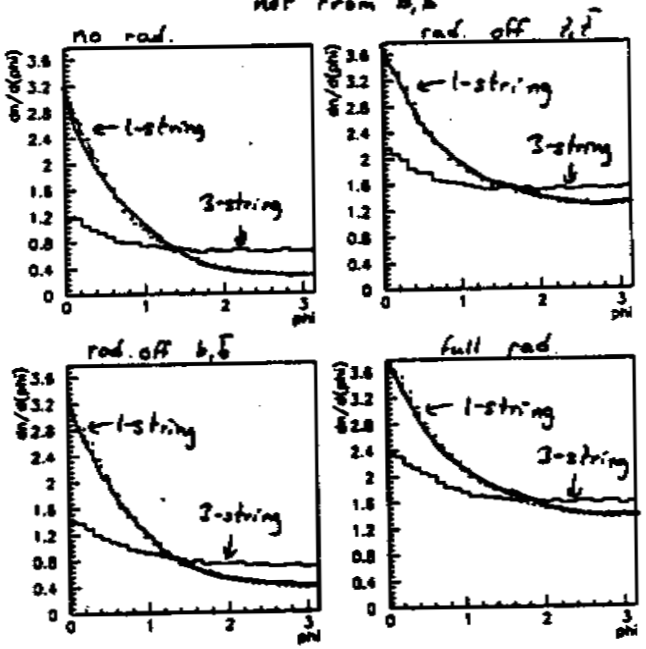

$E_{cm} = 500$ GeV
$m_t = 100$ GeV
no i.s.r.
$\varepsilon_t = 10^{-4}$
QCD rad. alt. 2

P(3-string) = 73% without
= 82% with
QCD rad. off $t, \bar{t}$

Particle distribution around event axis
as before, except $\varepsilon_t = 10^{-5}$

charged final state particles in range $|y|<1$
not from $t, \bar{t}$

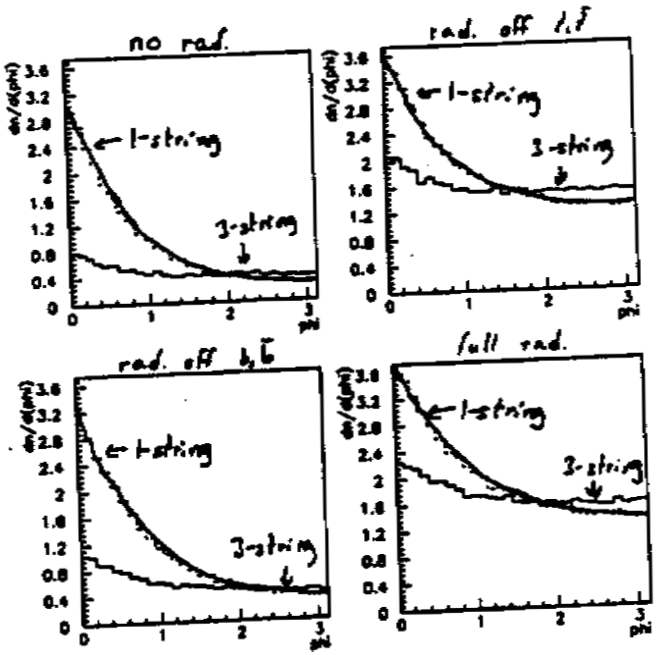

$E_{cm} = 500$ GeV
$m_t = 100$ GeV
no i.s.r.
$\varepsilon_t = 10^{-5}$
QCD rad. alt. 2

P(3-string) = 56% without
= 76% with
QCD rad. off $t, \bar{t}$

Particle distribution around event axis
as before, except QCD radiation alt. 1
charged final state particles in range $|y|<1$
not from $B, \bar{B}$

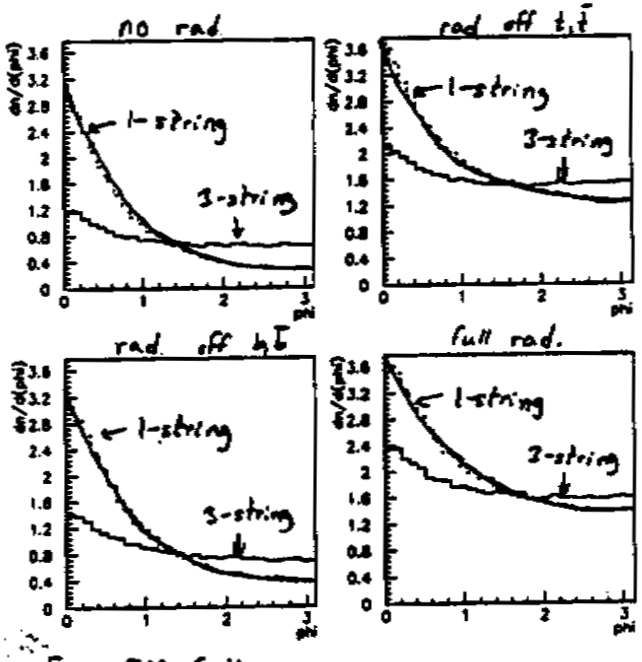

$E_{cm} = 500$ GeV
$m_t = 100$ GeV
no i.s.r.
$\varepsilon_t = 10^{-4}$
QCD radiation alt. 1

$P(3\text{-string}) = 73\%$ without
$= 82\%$ with
QCD rad. off $t,\bar{t}$

Particle distribution around event axis
as before, except $m_t = 120$ GeV
charged final state particles in range $|y|<1$
not from $B, \bar{B}$

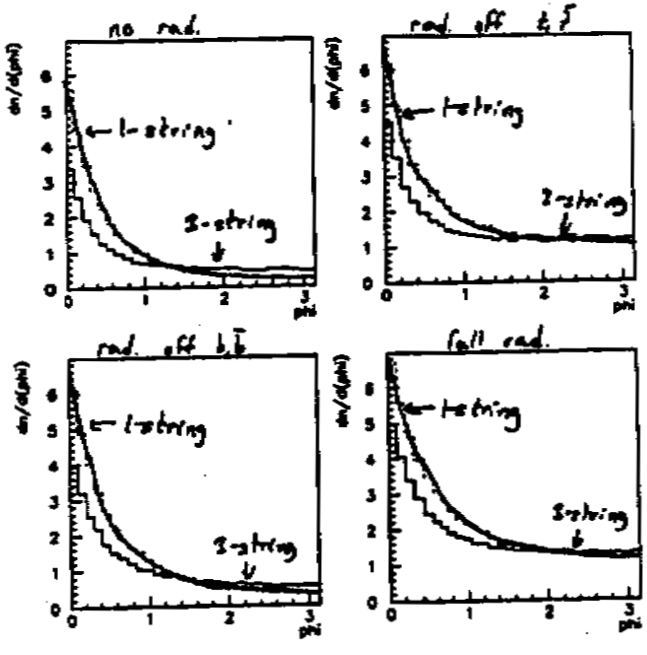

$E_{cm} = 500$ GeV
$m_t = 120$ GeV
no i.s.r.
$\varepsilon_t = 10^{-4}$
QCD rad. alt. 2

$P(3\text{-string}) = 30\%$ without
$= 36\%$ with
QCD rad. off $t,\bar{t}$

Particle distribution around event axis
as before, except E_{cm} = 1000 GeV and m_t = 120 GeV
charged final state particles in range $|y| < 1$
not from $B, \bar{B}$

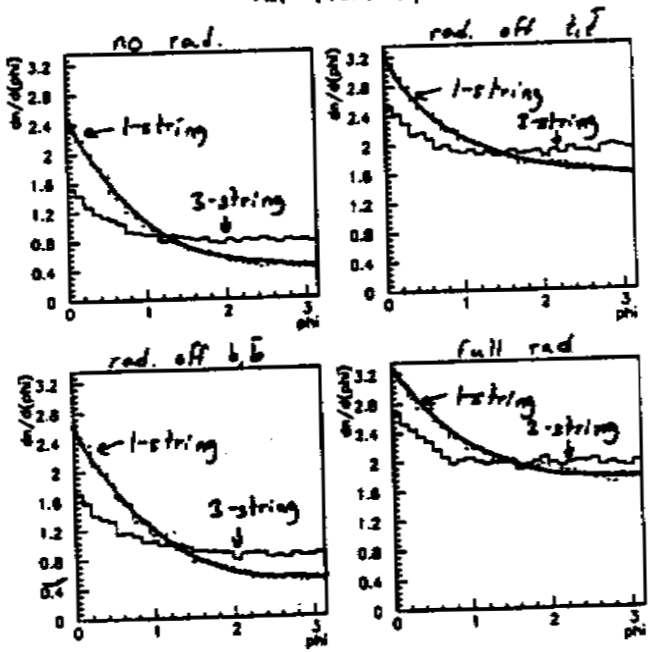

E_{cm} = 1000 GeV
m_t = 120 GeV
no i.s.r.
$\varepsilon = 10^{-4}$
QCD rad. alt. 2

P(3-string) = 59% without
= 61% with
QCD rad. off $t, \bar{t}$

$t\bar{t}$ production in $p\bar{p}$ events

Would top decay timescale affect event topology, e.g. t mass determinations (and hence search strategies) ?

Typical production graph :

⇓

string topology

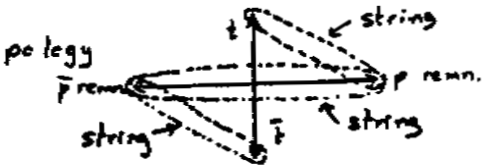

Possible scenarios:

1) t fragments first, then decays

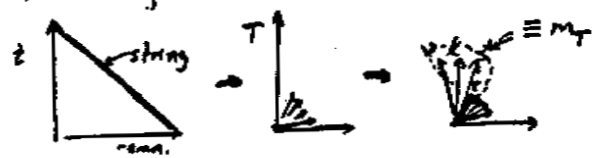

in principle, T mass can be reconstructed

2) t decays first, then b fragments

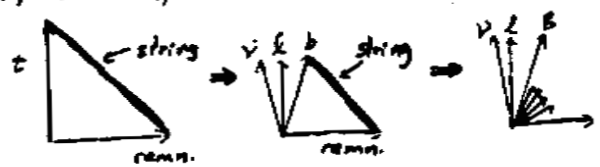

no concept of conserved mass in fragm...

t mass reconstruction

example: $p\bar{p}$ at $\sqrt{s} = 1800$ GeV

cf. t fragmentation before/after t decay

in 3 scenarios

1) no QCD rad., minimal underlying event
2) final state rad. off t & b (parton showers), no initial state rad., minimal underlying event
3) initial and final state rad., maximal und. evt.

Two reconstructions

A) $t \to b \ell \nu_\ell$:

- assume $p_W = p_\ell + p_{\nu_\ell}$ correctly known (!)
- cluster jets with $R < 0.7$ and $E_\perp > 10$ GeV
- look at ≤ 2 highest-$p_\perp$ jets
- combine with "best" p_W $\rightarrow$ "$m_T^{2\nu}$" $= (p_{jet} + p_W)^2$

B) $t \to b j_2 j_2$:

- cluster jets with $R < 0.7$ and $E_\perp > 10$ GeV
- look at all 3-jet combinations $\rightarrow$ "m_T^{2n}" $= (p_{j_1} + p_{j_2} + p_{j_2})^2$
- look at combination with mass closest to m_t

Charged multiplicity distribution

$p\bar{p} \to t\bar{t}X$ at $\sqrt{s} = 1800$ GeV,

$t \to b \ell \nu_\ell$ $(\bar{t} \to \bar{b} \ell \nu_\ell)$, $m_t = 120$ GeV

charged multiplicity of whole event

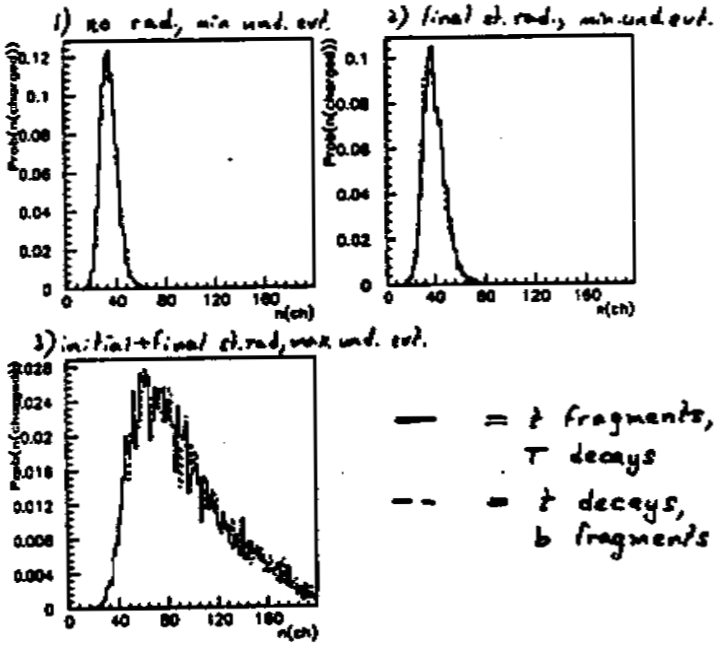

W+jet mass distribution
$p\bar{p} \to t\bar{t}X$ at $\sqrt{s} = 1800$ GeV
$t \to b\ell\nu_\ell$ ($\bar{t} \to \bar{b}\ell\nu_\ell$), $m_t = 120$ GeV
jet finding $R<0.7$ and $E_\perp > 10$ GeV

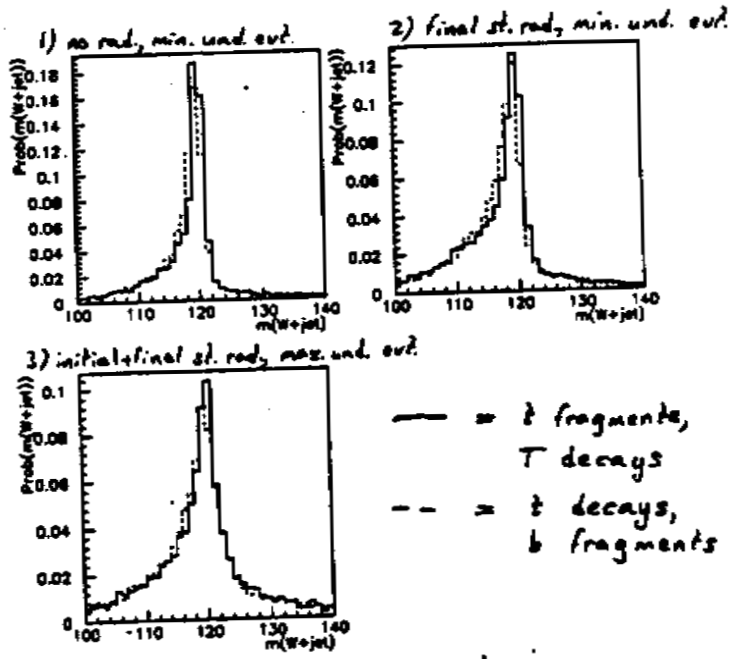

$\langle m_{Wj} \rangle$ (GeV)

	t fragm.	t decays
1	119.1 ± 7.4	117.8 ± 7.3
2	117.0 ± 8.5	116.6 ± 8.1
3	119.1 ± 10.4	119.1 ± 10.2

W+jet mass distribution
$p\bar{p} \to t\bar{t}X$ at $\sqrt{s} = 1800$ GeV
$t \to b\ell\nu_\ell$ ($\bar{t} \to \bar{b}\ell\nu_\ell$), $m_t = 140$ GeV
jet finding $R<0.7$ and $E_\perp > 10$ GeV

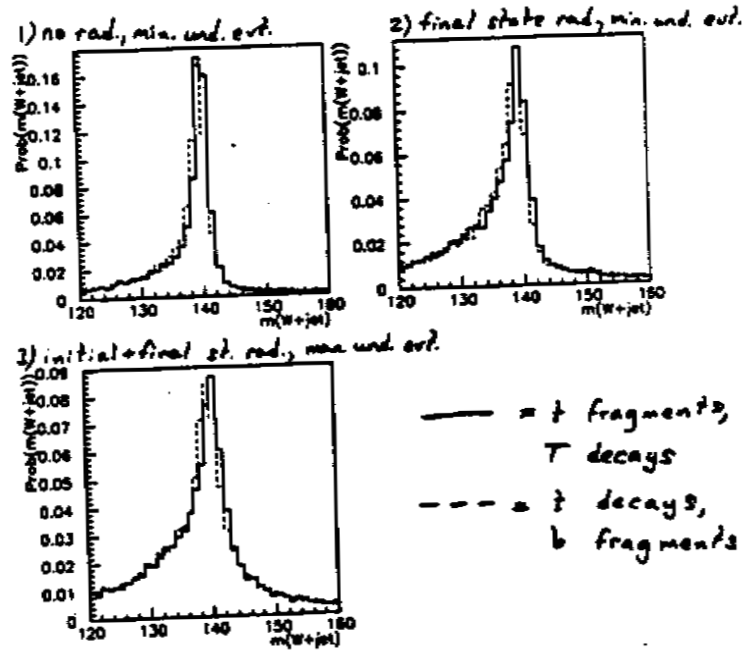

$\langle m_{Wj} \rangle$ (GeV)

	t fragm	t decays
1	136.2 ± 8.7	136.0 ± 8.3
2	134.0 ± 10.4	134.0 ± 10.2
3	135.1 ± 11.2	135.2 ± 11.0

Charged multiplicity distribution

$p\bar{p} \to t\bar{t}X$ at $\sqrt{s} = 1800$ GeV

no constraints on t decay modes

$m_t = 120$ GeV

charged multiplicity of whole event

1) no rad., min. und. evt.

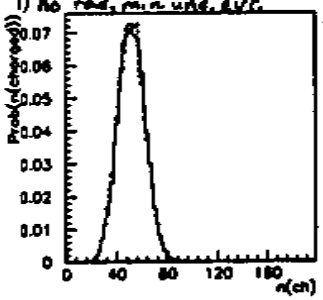

2) final st. rad., min. und. evt.

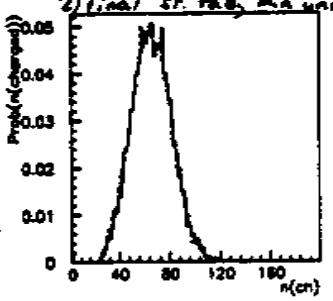

3) initial+final st. rad., max. und. evt.

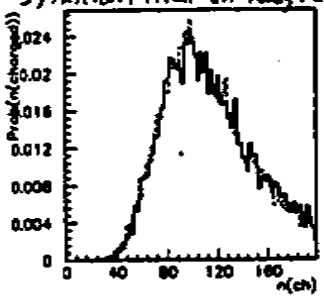

—— = t fragments, τ decays

- - - = t decays, b fragments

jet + jet + jet mass distribution

$p\bar{p} \to t\bar{t}X$ at $\sqrt{s} = 1800$ GeV

$t \to bW$ with $W \to \ell\nu$ and $q\bar{q}$

$m_t = 120$ GeV

jet finding $R < 0.7$ and $E_\perp > 10$ GeV

1) no rad., min. und. evt.

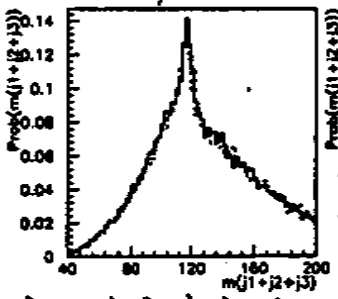

2) final state rad., min. und. evt.

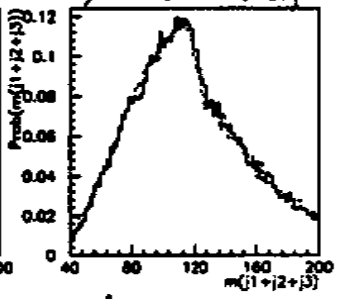

3) initial+final st. rad., max. und. evt.

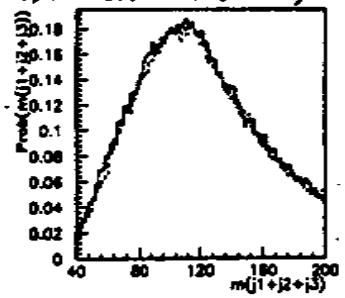

—— = t fragments, τ decays

- - - = t decays, b fragments

	$\langle n_{jet} \rangle$ t fragm.	t decays
1	4.60	4.56
2	4.79	4.77
3	5.63	5.60

Summary

- $m_t = 100 - 120$ GeV
  interesting crossover region
  $t_{fragmentation} \approx t_{decay}$

- in e^+e^- under controlled conditions
  several variables show some dependence,
  a few large dependence on scenario :
  unique way to measure t lifetime?

- QCD emission complicates picture,
  have not yet full understanding ⇒ more work,
  but nothing radically new

- not so important in $p\bar{p}$
  – discovery potential unchanged
  – $\Delta m \lesssim 0.5$ GeV
  same for standard e^+e^- (?)

Top at Threshold in e^+e^- Collisions*

Theory

Johann Kühn
Institut für Theoretische Teilchenphysik
Universität Karlsruhe
D-7500 Karlsruhe 1, Germany

Abstract

I. Theoretical predictions for top quark production in the threshold region are presented. The interplay between the large width of the top quark and the QCD potential and its effect on the total cross section is reviewed. It it shown that the resonance region and the region of open top production can be connected in a smooth manner. The sensitivity of the cross section to m_t and α_s is emphasised. The impact of electroweak radiative corrections and the production cross section is studied. It is shown that the effect of Higgs exchange can be treated in perturbation theory if its mass is above ~50 GeV and the relation between perturbative treatment and the Yukawa potential is presented.

II. The momentum distribution of top quarks is evaluated by solving the Lippman-Schwinger equation in momentum space. The dependence of the Greens function on m_t, Γ_t, and E_{beam} is explored.

III. The dependence of the width of the top quark on bound state effects is discussed. Important ingredients are the reduction of phase space, final state interaction, and time dilation.

IV. Predictions for top production at a "Compton collider" are presented. The influence of resonances, perturbative QCD corrections and of laser and electron beam polarisation is explored.

*Work in part supported by BMFT Project Nr. 055KAP94P1.

$t\bar{t}$ production in the threshold region

J. KÜHN, KARLSRUHE

I) Total cross section
- A) QCD
- B) Electroweak effects

II) Momentum distributions

III) s-dependent Γ_t ?!

IV) $\gamma\gamma \to t\bar{t}$

I) Total cross section/QCD

study of "toponium" or its remnant
- ➡ QCD potential at short distance
- ➡ determination of m_t
- ➡ study of top decays, couplings

short life time of boundstate $(2\Gamma_t)^{-1}$
comparable or less than time of revolution
$\approx$ Bohr radius/velocity $\sim (\alpha_s m_t)^{-1}/\alpha_s$

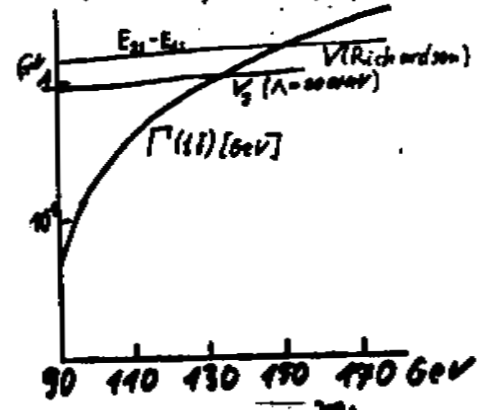

$m_t \approx 100-120$ GeV
well separated 1S resonance!

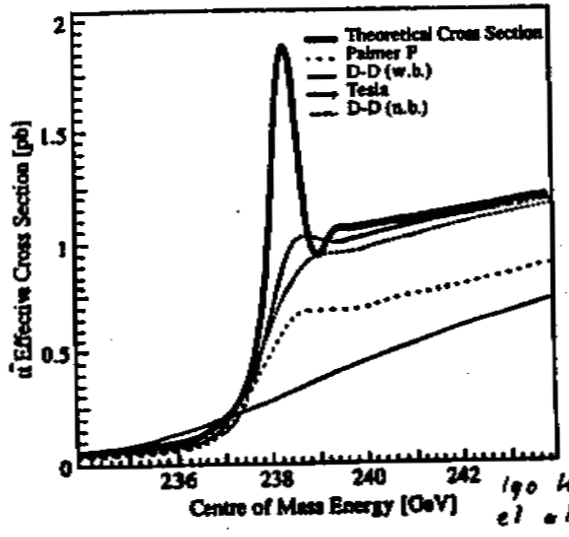

Igo Kemenes et al.

high radial excitations / large m_t

➡ $\sum$ many overlapping resonances

convenient formulation in terms of Greens function (Fadin+Khoze)

$$\sigma(e^+e^- \to t\bar{t}) = \frac{24\pi^2\alpha Q_t^2}{s\, m_t^2} \sum_n |\psi_n(0)|^2 \frac{\Gamma_t}{(E_n-E)^2+\Gamma_t^2}$$

$$= \quad " \quad \sum_n \mathrm{Im}\, \frac{\psi_n(0)\,\psi_n^*(0)}{E_n - E - i\Gamma_t}$$

$$= \quad " \quad \mathrm{Im}\, G(0,0,E+i\Gamma)$$

$$\left(-\frac{\nabla^2}{m_t} + V(\vec{r}) - E - i\Gamma\right) \cdot G(\vec{r};\vec{r}'=0, E+i\Gamma) = \delta(\vec{r})$$

can be solved numerically for QCD potential (Strassler Peskin)

⇒ strong dependence on α_s (short distance part of $V(\vec{r})$)
large distances cut off by Γ_t.

resonance and continuum join smoothly

(Güsken, K, Zerwas)

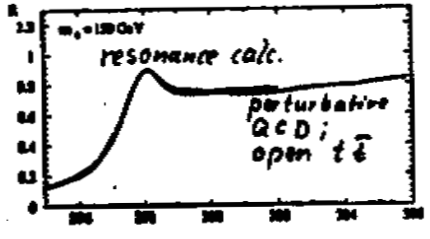

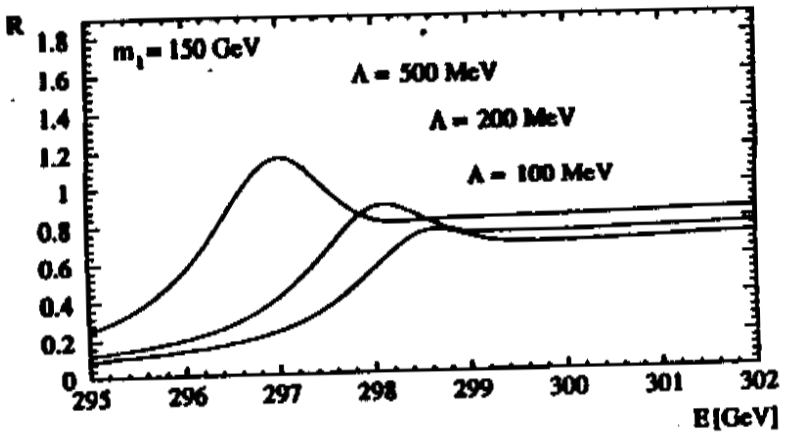
R
m_t = 150 GeV
Λ = 500 MeV
Λ = 200 MeV
Λ = 100 MeV
1.8
1.6
1.4
1.2
1
0.8
0.6
0.4
0.2
0
295
296
297
298
299
300
301
302
E [GeV]

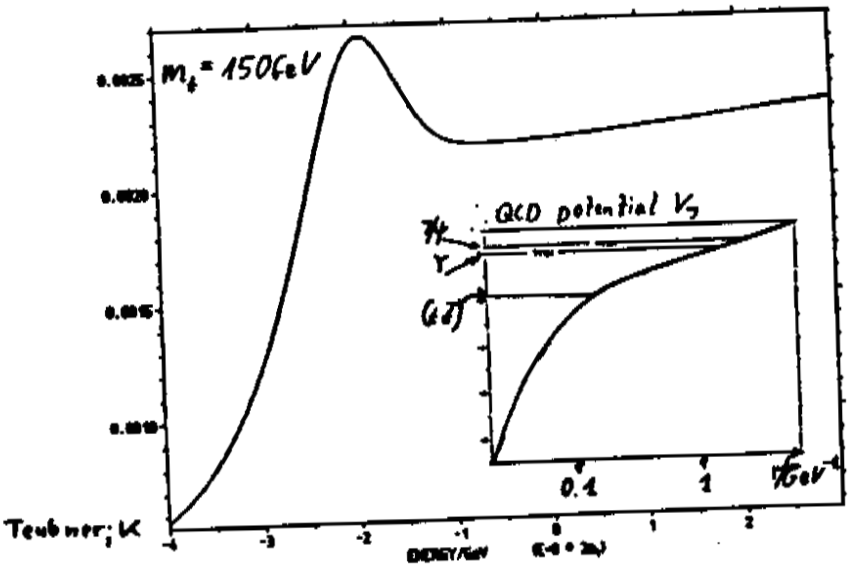
m_t = 150 GeV
QCD potential V_J
ψ_t
Υ
$(t\bar{t})$
0.1
1
$\sqrt{s}$ GeV
Teubner; K

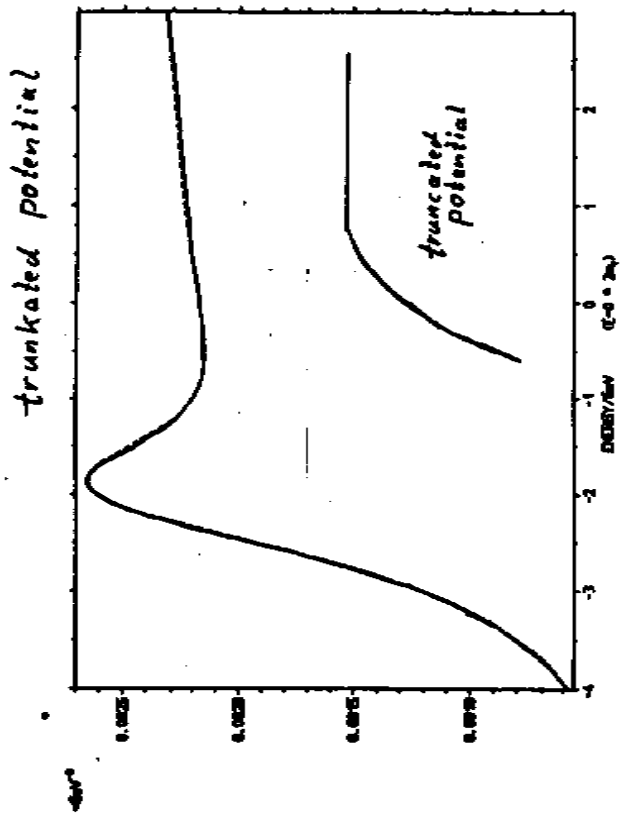

Inclusion of initial state rad. and linac energy spread

➡ peak disappears
sharp rise at threshold remains

➡ location + height of step

➡ determination of m_t and $V(r)$

Example

Igo-Kemmes, ...

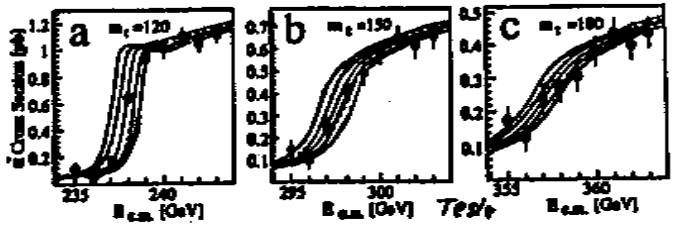

— ± 200 MeV
— ± 400 MeV

10^6 s/point

nominal accuracy .. 0.1 – 0.5 GeV

input α_s, Γ_t.

in addition: height → sensitivity towards potential

I)B) Total cross section weak effects

$\sigma(e^+e^- \to t\bar{t}) = F_{ew} \cdot F_{QCD}$

electro weak interact. (Born + $O(\alpha)$) depends on α, M_W, M_Z, m_H...

QCD resonances, threshold behav.

F_{ew}:

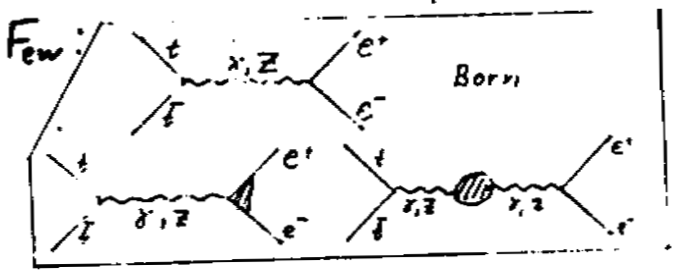

+ corrections attached to top

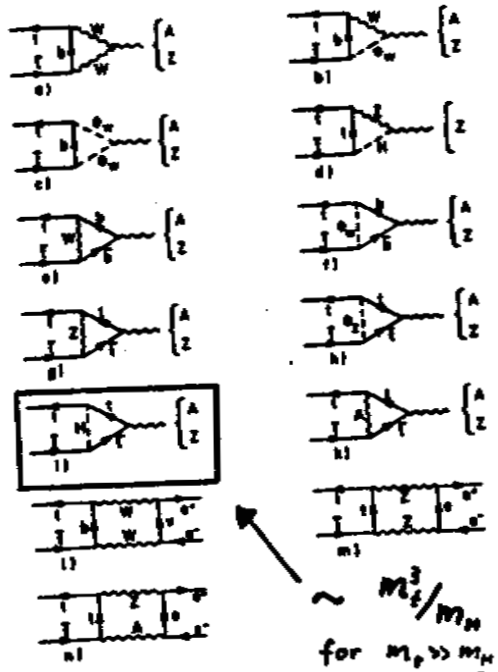

$\sim m_t^3/m_H$ for $m_t \gg m_H$!

Fig. 1: Feynman diagrams relevant for the evaluation of one loop corrections. Permutations have been omitted.

threshold behaviour: Weak corrections – Higgs

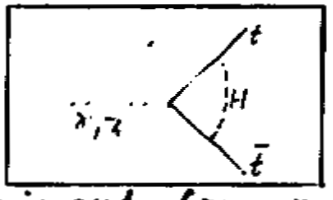

dominant for $m_t \sim 150-200$ GeV and light Higgs.

static Yukawa potential for $m_H \ll m_t$

$$V(r) = \frac{\sqrt{2}\, G_F\, m_t^2}{4\pi} \cdot \frac{e^{-r m_H}}{r}$$

"Coulomb singularity" $\sim \frac{m_t}{m_H}$

$\Rightarrow$ leading correction (enhancem.)

$$\frac{\sqrt{2}\, G_F\, m_t^2}{4\pi} \; \frac{m_t}{m_H}$$

realistic masses:
$\Rightarrow$ all corrections have to be evaluated.

Fig 8a

main results:

1) enhancement for heavy top and light Higgs up to 30%

Fig 9a

2) retardation effects are important
instantaneous Yukawa potential is not adequate.

Fig. 10b

3) asymmetry for long. pol. beams

$$A_{LR} = \frac{\sigma_L(e^+e^- \to t\bar{t}) - \sigma_R(e^+e^- \to t\bar{t})}{+}$$

exhibits little dependence on m_H

Fig. 10c

4) Small m_H $\rightarrow$ large correction at threshold
$\rightarrow$ rapid energy variation
$\sim \frac{1}{m} \frac{m_t^2}{v^2} \frac{1}{\sqrt{m_H^2 + p^2}}$

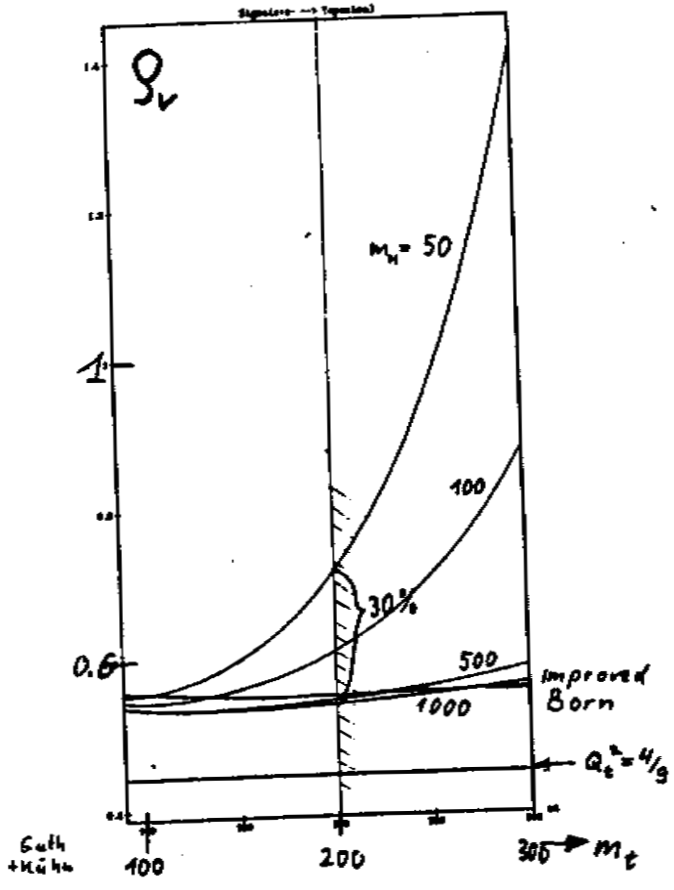
ρ_V
$m_H = 50$
100
30%
500
1000
improved Born
$Q_t^2 = 4/9$
1
0.6
100
200
300
m_t
Guth +Kühn

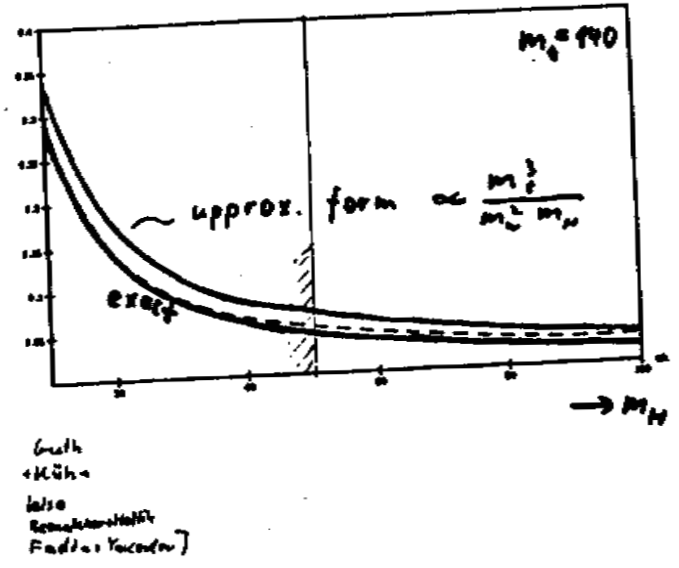
$m_t = 140$
~ approx. form $\propto \frac{m_t^3}{m_W^2 m_\mu}$
exact
$\rightarrow m_H$
Guth
+Kühn

$$A_{RL} = \frac{\sigma_L(e^+e^- \to t\bar{t}) - \sigma_R(e^+e^- \to t\bar{t})}{\sigma_L(e^+e^- \to t\bar{t}) - \sigma_R(e^+e^- \to t\bar{t})}$$

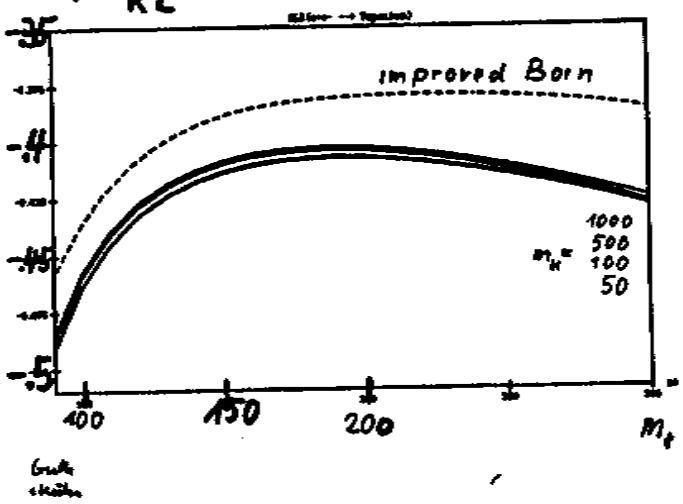

A_{LR} either with long. pol. beams or through analysis of (polarized) top decays!

energy dependence of corrections from Higgs exchange

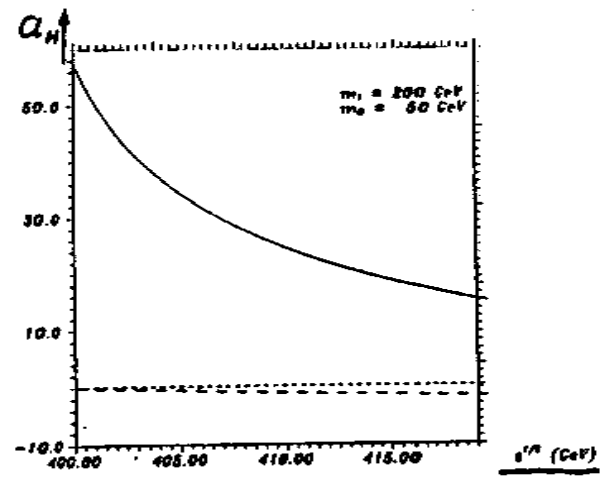

Correction factor to rate

$$\left(1 + \underbrace{\frac{\alpha}{4\pi \sin^2\theta_W}}_{\approx 1/100} a_H\right)^2$$

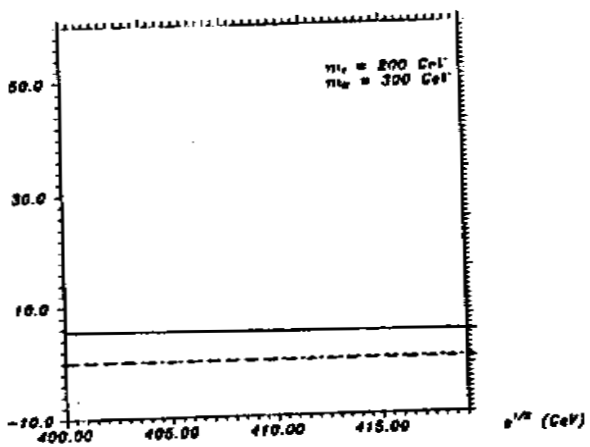

II) momentum distrib. of quarks in toponium

Jezabek, K, Teubner
Sumino, Fujii, Hagiwara

Greens function in momentum space determines top-momentum distribution:

$$\frac{d\sigma}{d^3\vec{p}}(\vec{p},E) = \frac{24\pi^2\alpha^2 Q_t^2}{s}\frac{1}{m_t^2}\Gamma_t |G(\vec{p},E+i\Gamma)|^2$$

coincides for well separated resonances with

$$\left.\frac{dN}{d\vec{p}}\right|_{E=E_n} = |\tilde{\Psi}_n(\vec{p})|^2$$

many overlapping resonances ⇒ Greens fct.

Solve Lippman-Schwinger equation for complex energies and QCD potential

$$G(\vec{p},E+i\Gamma) = G_0(\vec{p},E+i\Gamma) + G_0(\vec{p},E+i\Gamma)\int\frac{d^3q}{(2\pi)^3}\tilde{V}(\vec{p}-\vec{q}) \cdot G(\vec{q},E+i\Gamma)$$

with $G_0 = \frac{1}{E+i\Gamma_t - p^2/m_t}$

➡ smooth behaviour for E at 1S peak
oscillations close to threshold
long tail at large $\vec{p}$: $\frac{dN}{d^3\vec{p}} \sim 1/p^4$

technical comments:

Lippman-Schwinger-Integral-Equation
$\Rightarrow$ $(N \times N)$ system of linear equ.

G in momentum space.
$\Rightarrow$ V in momentum space

$$V_{pert}(Q^2) = -\frac{16\pi}{3}\frac{\alpha_s(Q^2)}{Q^2}\left[1+\left(\frac{31}{3}-\frac{10}{9}n_f\right)\frac{\alpha_s}{4\pi}\right]$$

$$V(p) = \begin{cases} V_{pert}(p^2) & p > 5\,GeV \\ V_{Richardson}(p^2) & p < 5\,GeV \end{cases}$$

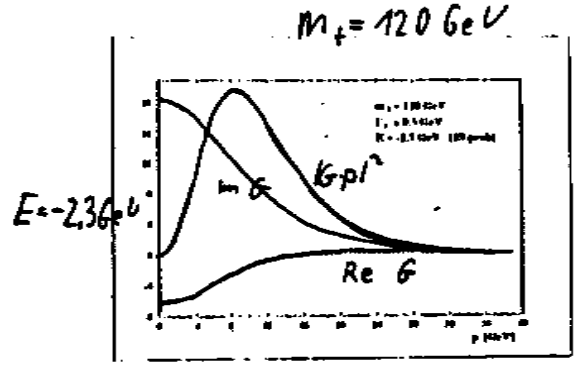

Figure 2: Green function $\mathcal{G}(p, E+i\Gamma_t)$ for $m_t = 120$ GeV and $E = -2.3$ GeV (1S peak) : $Re\mathcal{G}$ $[1/GeV]$ (dashed), $Im\mathcal{G}$ (dotted), and $|p\mathcal{G}(p)|^2 \cdot 0.002$ (solid).

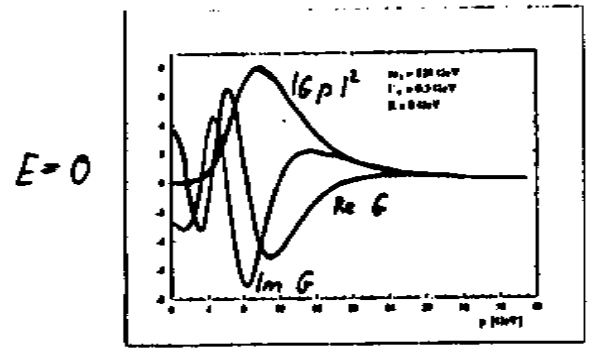

Figure 3: Green function $\mathcal{G}(p, E + i\Gamma_t)$ for $m_t = 120$ GeV and $E = 0$: $Re\mathcal{G}$ $[1/GeV]$ (dashed), $Im\mathcal{G}$ (dotted), and $|p\mathcal{G}(p)|^2 \cdot 0.002$ (solid).

wide momentum spread for
$E < 0$ (1S peak)
"sharp" momentum $|\vec{p}| \approx \sqrt{m_t E}$
for E above threshold;
tail!

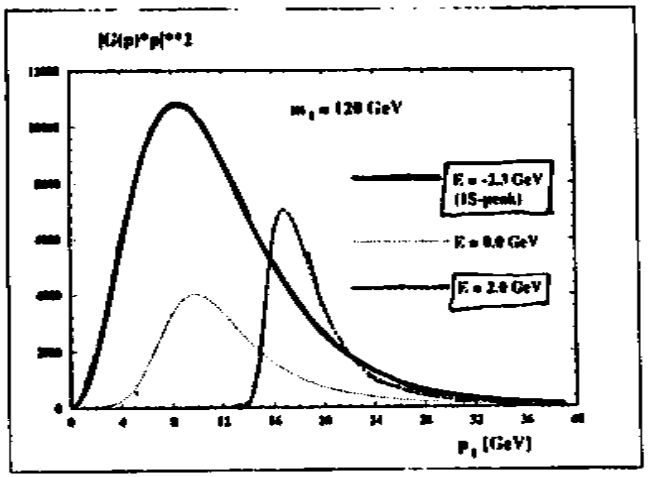

important difference between
narrow and wide resonances!??
$\langle p_t \rangle$ increases drastically!

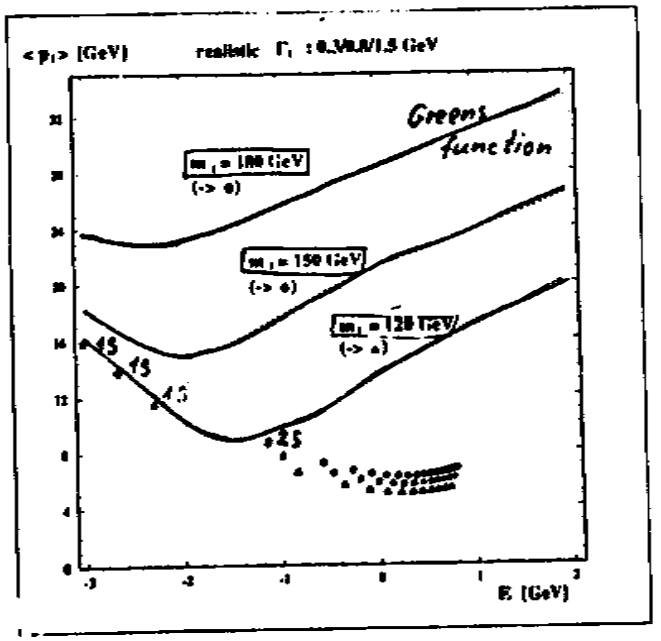

Probing the Top-Quark Mass-Generating Mechanism

S. Willenbrock
Brookhaven National Laboratory

Abstract

In the standard Higgs model, both the weak vector bosons and the fermions obtain mass via the same mechanism. In contrast, I discuss a model in which these masses are associated with different Higgs doublets. I discuss the prospects for detecting the effects of the Higgs scalar associated with top-quark mass generation at the Tevatron, LHC/SSC, and e^+e^- linear colliders.

Probing the top-quark mass-generating mechanism

Measuring the top-quark Yukawa cou

S. Willenbrock

Brookhaven Natl. Lab

Electroweak interaction: $SU(2) \times U(1)$

What generates W, Z masses and fermion masses?

Standard Higgs model:

$$\langle \phi \rangle = \begin{pmatrix} 0 \\ v \end{pmatrix} \rightarrow \begin{array}{l} M_W = \frac{1}{2} g v \\ m_f = y_f v \end{array}$$

Higgs couplings determined:

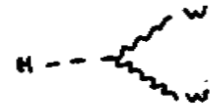

igM_W

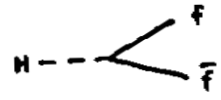

$-i \frac{g}{2} \frac{m_f}{M_W}$

Unitarity bound on scale of fermion mass generation

Recall bound on W_L^3 mass generation:

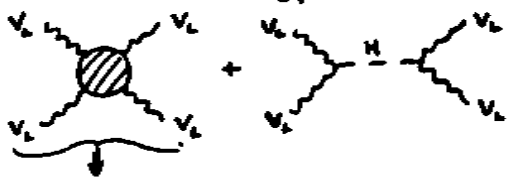

$\sim g^2 \frac{m_H^2}{M_W^2}$

Dicus + Mathur
Lee, Quigg, + Thacker

$a \sim g^2 \frac{s}{M_W^2}$

$|\mathrm{Re}\, a| < \frac{1}{2} \Rightarrow \boxed{s \lesssim (1.2\ \mathrm{TeV})^2}$ Chen + Gaillard

---

Bound on fermion mass generation:

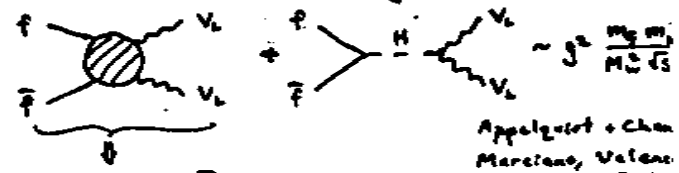

$\sim g^2 \frac{m_f m_f}{M_W^2 \sqrt{s}}$

Appelquist + Chen
Marciano, Valencia + S.W.
M. Berger + Chen.

$a \sim g^2 \frac{m_f \sqrt{s}}{M_W^2}$

$|\mathrm{Re}\, a| < \frac{1}{2} \Rightarrow$

$\sqrt{s} \lesssim 5$ TeV	$m_f = 100$ GeV
2.5 TeV	200 GeV

Top-quark mass-generating mechanism within reach of future colliders!

Standard Higgs model economical: generates both M_V and m_f

However, nature may not have chosen this model

Should search experimentally for separate V and f mass generation

M. Berger + Chen

How?

Our guide: two-Higgs-doublet model

ϕ_1	ϕ_2
W, Z	fermions
$v_1 = v$	$v_2 \ll v_1$

$\tan\beta = \frac{v_2}{v_1} \ll 1$ opposite of SUSY

Haber-Kane-Sterling model I ($\alpha = 0$)

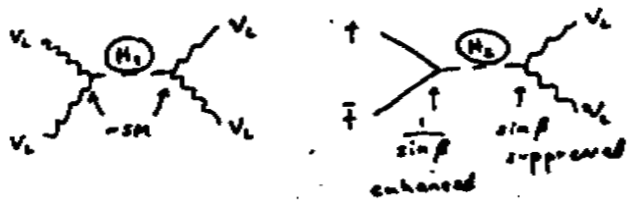

Also:

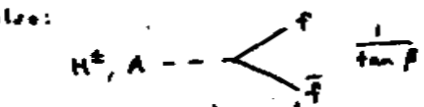

$\frac{1}{\tan\beta}$ enhanced

All Yukawa's enhanced

Constraints on $\tan\beta$: ($m_t = 200$ GeV)

$t\bar{t}H_2$ perturbative, $K\bar{K}$, $B\bar{B}$, $B\bar{B}$ mixing, etc... $\Rightarrow$ $\tan\beta \gtrsim 1/3$

Burgi, Hewett, Phillips

Probing the top-quark Yukawa couplings at colliders

Ex: $m_t = 200$ GeV $\tan\beta = 1/3$

1. Tevatron

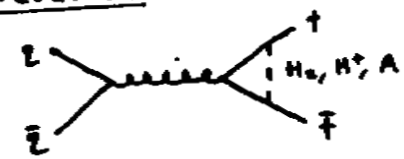

Stange + S.W.

"Pride": Standard model H, W_L, Z_L

$\Delta\sigma \sim g^2 \frac{m_t^2}{M^2}$

m_H (GeV)	$\Delta\sigma$
50	0%
100	+0.8%
1000	-1.0%

Tiny! ?

Reason: cancellation between low and high energy

Two-doublet model ($m_{H^\pm}, m_A \gg m_{H_2}$)

m_{H_2} (GeV)	$\Delta\sigma$
50	+1.4%
100	+2.2%
1000	+0.4%

$= \frac{1}{\sin^2\beta} = 10$

Too small to observe

2. LHC/SSC

Production of H_2, H^+, A (H_1 - like H)

H_2 production:

Gaemers + Hoogeveen
Stange + S.W.

a.)

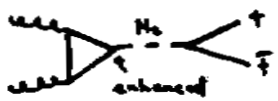

"Background"

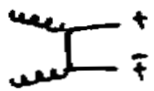

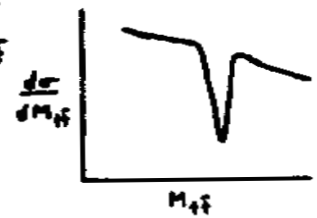

detectable?

b.)

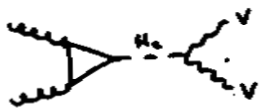

$\sigma \sim \sigma_{SM}$ but $\Gamma \sim \frac{2}{3}\Gamma_{SM}$ Good

c.)

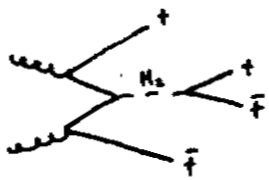

$\sim 10^3/yr \times \frac{1}{\sin^2\beta}$

Beats all bkd - but signature? 3f?

Barger, Mangano, Phillips

LHC/SSC - looks possible

3. $e^+e^- \to t\bar{t}$

H_2 production, but also

Kuang
Teskin + Strassler
Penner, Guth, Kühn

a.) Threshold

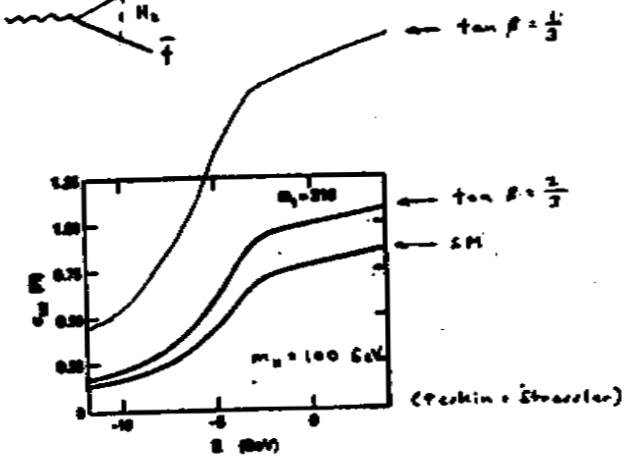

(Teskin + Strassler)

Great for "light" H_2

b.) Continuum

Beenakker, van der Marck, Hollik

m_{H_2}	$\Delta\sigma_{SM}$
50	-9%
100	-6.6%
1000	-6.4%

$\times \frac{1}{\sin^2\beta}$ Great

$\Delta\sigma_{\text{s-subtract}}$ needed

e^+e^- great probe

Summary and conclusion:

- Top-quark mass-generating mechanism within reach of future colliders
- Separate mass-generating mechanisms for V and f
  - ⇒ two-Higgs-doublet model with enhanced Yukawa couplings
- Probes of model:
  1. Tevatron no
  2. LHC/SSC good
  3. e^+e^- very good

Comment: Extended Higgs models proper way to address "anomalous" Higgs couplings

Ex:

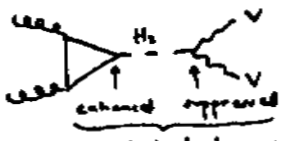

dictated by unitarity
automatic in broken gauge theory

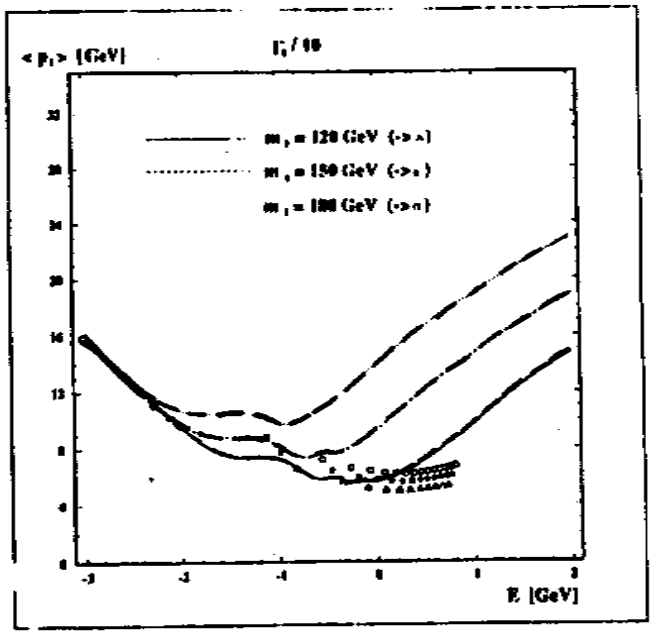

'Fermi motion' ⇒ smearing of momenta of decay products

$t \to b + W$

W not affected by final state interaction

⇒ probe of wave function

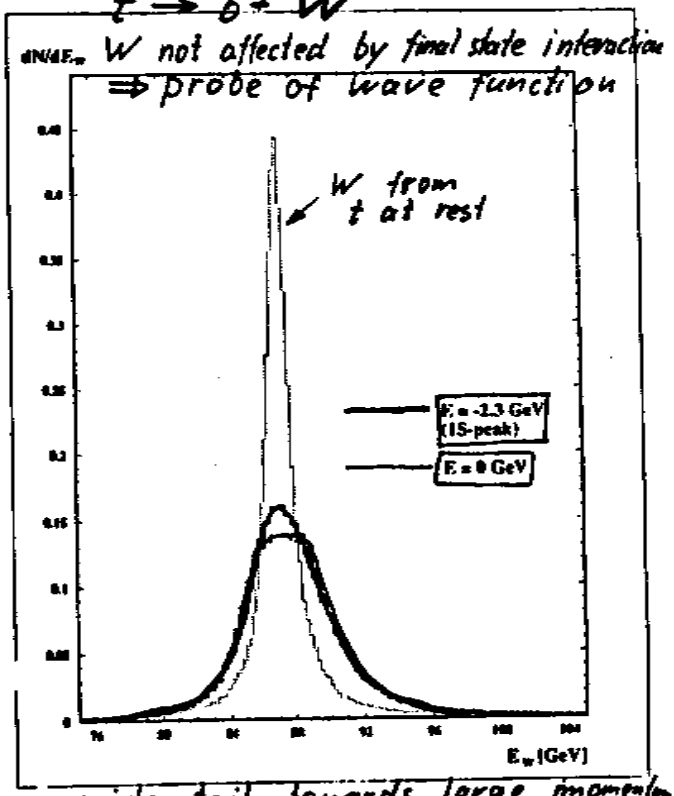

wide tail towards large momenta

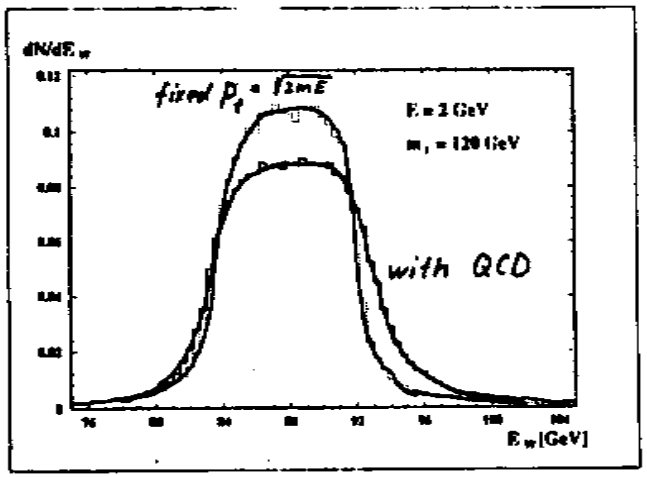

important impact on
t reconstruction

α_s dependence

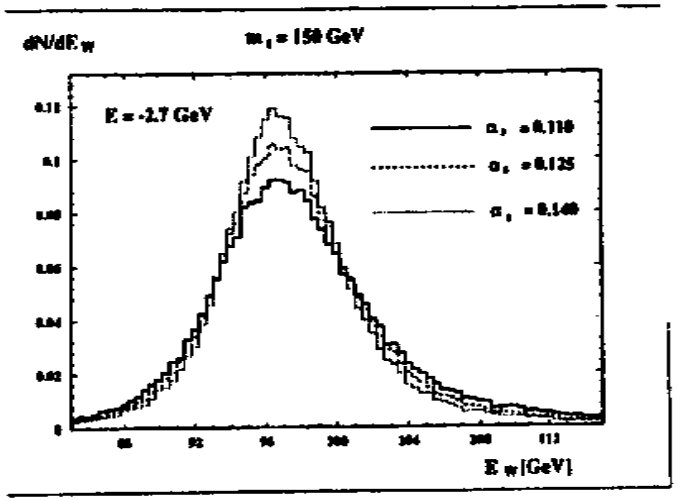

Effects to be included in addition momentum dependent width:

$$\Gamma_1(s) = \theta(s - m_W^2)\frac{G_F \sqrt{s}}{8\pi\sqrt{2}}\left(s - 3\frac{m_W^4}{s} + 2\frac{m_W^6}{s^2}\right)$$

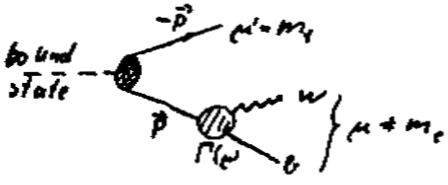

Altarelli et al. 82
Jezabek + K 87
Sumino et al 92

But: a) final state interaction
b) time dilatation
(Huff (1961): decay of bound muon!)
Sumino et al.
→ Jezabek + Teubner:
phase space reduction and wave function enhancement } compensate largely
[“final state interaction”]

what remains: time dilatation + constraint $m(b\bar{b}) \geq 12$ GeV

Impact of $\Gamma(p)$ on $|G(p)|^2 p^2$

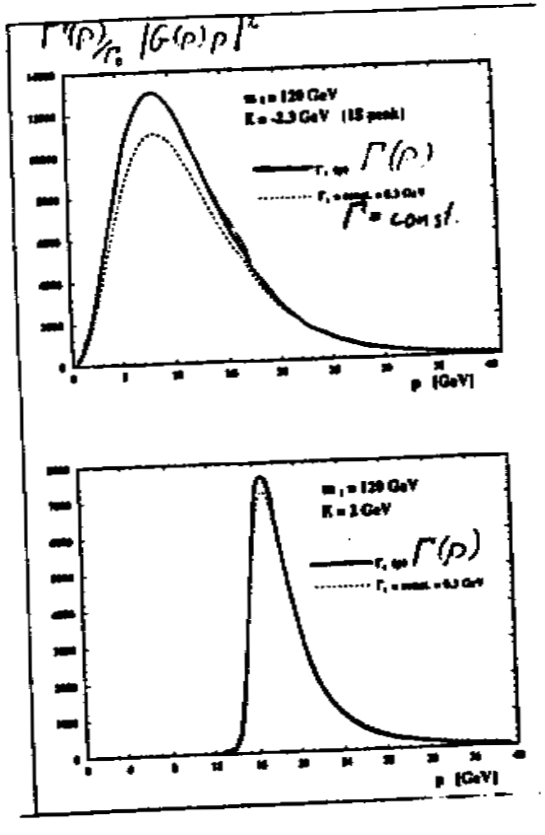

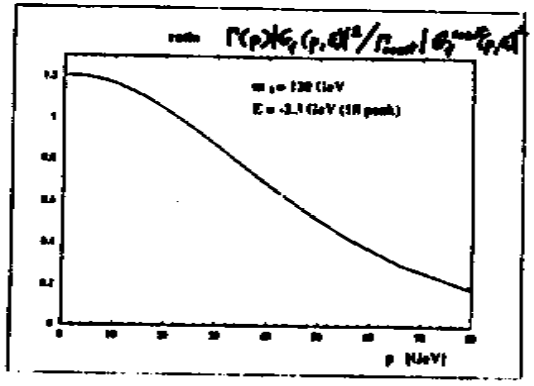

Jezabek
+ Teutner

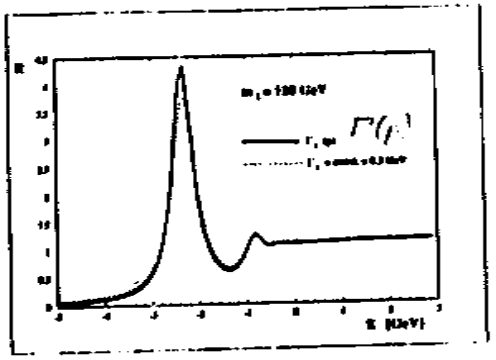

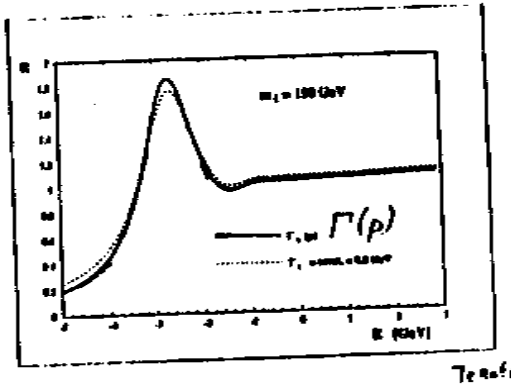

Teryaev
+ Teutner

momentum distribution of W

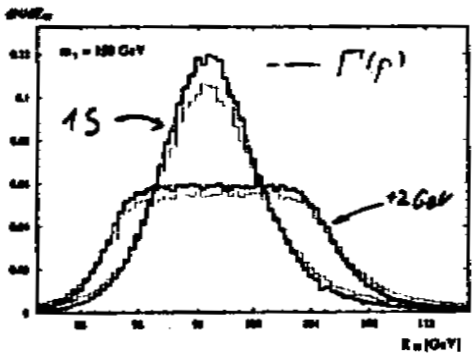

e^+e^- collider / SUMMARY

- m_t with high precision
- laboratory for perturbative QCD
  (potential at short distances)
- large Yukawa coupling

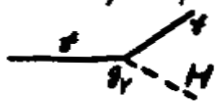

$g_Y = \frac{m_t}{v} = m_t\sqrt{\sqrt{2}G_F} \sim \mathcal{O}(1)$

mechanism of fermion mass generation

- test of V-A ?

- decays beyond the SM
  (often difficult in hadron collid.)
  $t \to b H^+$, SUSY decays
  FCNC

3) $t\bar{t}$ production at "Compton collider"

back scattered laser-light:
e^+e^- collider ⇒ $\gamma\gamma$ collider

for equal helicities of e and laser photon
⇒ energetic, strongly polarized γ

equal helicities of both laser photons
⇒ helicity of $\gamma\gamma$ dominantly 0

➡ enhanced $\sigma(\gamma\gamma \to t\bar{t})$ in threshold region F16

Important changes through QCD corrections! Kramer, Zerwas, Zerwas; K., Mirkes, Steglich

resonance region: $\gamma\gamma \to \eta_t$
and open production $\gamma\gamma \to t\bar{t}$
joined smoothly F17

➡ large enhancement of effective $\sigma(\gamma\gamma \to t\bar{t})$ after folding with $\gamma\gamma$ luminosity F18

effective $\gamma\gamma$ Luminosities

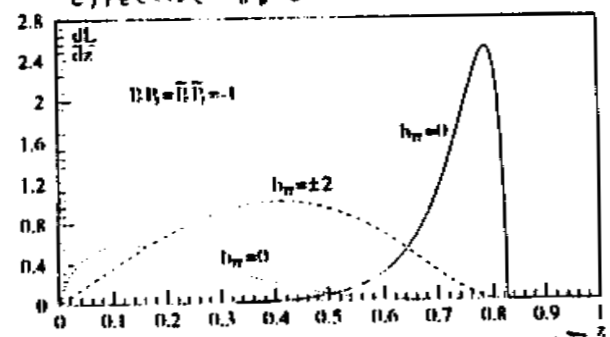

effective cross section $\gamma\gamma \to t\bar{t}$

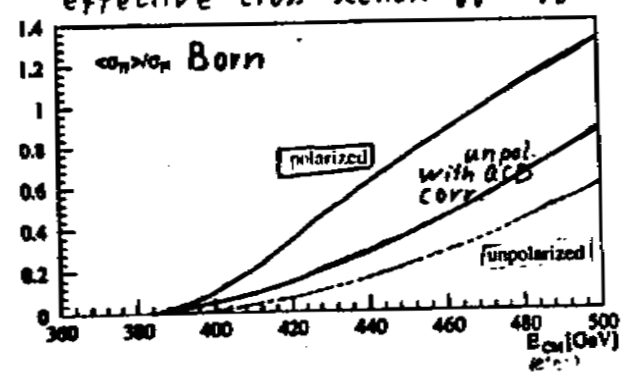

K., Mirkes, Steglich

$$\sigma_{\gamma\gamma\to t\bar{t}(g)} = \frac{\alpha^2 Q^4 N_c}{s}\left[f_{tt}^{(0)} + \frac{4}{3}\frac{\alpha_s}{\pi} f_{tt}^{(1)}\right]$$

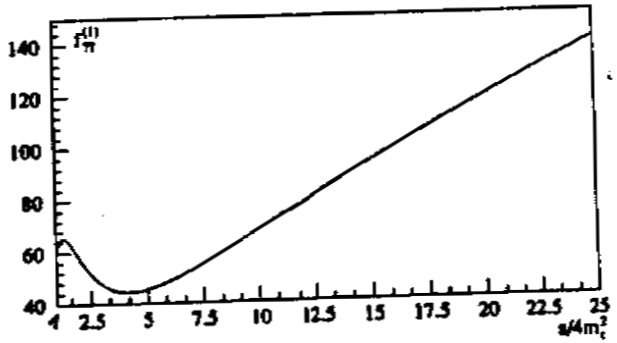

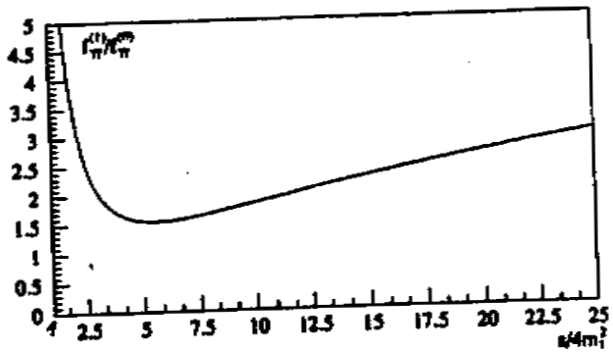

$$f_{tt}^{(0)} = \frac{6-2\beta^2}{\beta}\ln\frac{1+\beta}{1-\beta} - 8 + 4\beta^2$$

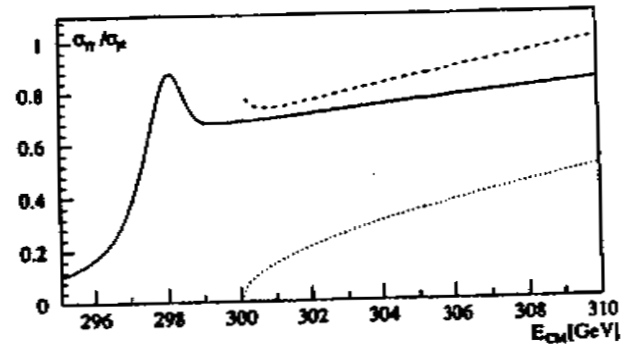

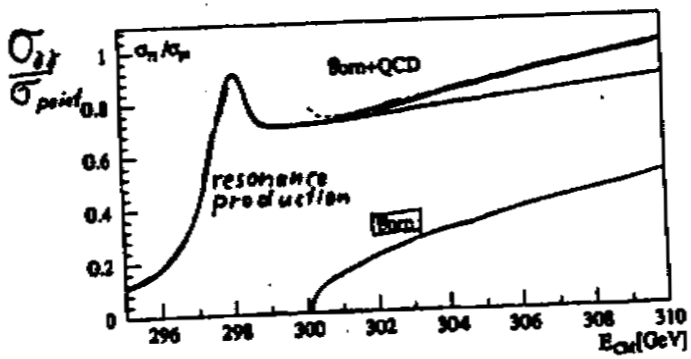

References

Top decay

Born predictions

J.H. Kühn: Acta Phys. Pol. B 12(1981)347; Acta Phys. Austr. Suppl. XXIV(1982)203.
I.I.Y. Bigi, Y. Dokhitser, V. Khose, J.H. Kühn, P. Zerwas: Phys. Lett. B 181(1986)157.

QCD corrections

M. Jezabek and J.H. Kühn: Phys. Lett. B 207(1988)91; Nucl. Phys. B 314(1989)1, 320(1989)20.
A. Czarnecki, M. Jezabek, J.H. Kühn: Nucl. Phys. B 351(1991)70.

Production in e^+e^- collisions

Total cross section

J.H. Kühn and P.M. Zerwas: Phys. Rep. 167(1988)321 and references therein.
V.S. Fadin and V.A. Khose: JETP Lett. 46(1987)525; Sov. J. Nucl. Phys. 48(1988)309.
J.M. Strassler and M.E. Peskin: Phys. Rev. D 43(1991)1500.
W. Kwong: Phys. Rev. D 43(1991)1488.

Electroweak corrections

B. Grzadkowski, P. Krawczyk, J.H. Kühn, R.G. Stuart: Nucl. Phys. B 281(1987)18.
A. Guth and J.H. Kühn: Nucl. Phys. B 368(1992)38, 377(1992)3.

Momentum distributions of top quarks

M. Jezabek, J.H. Kühn, T. Teubner: Karlsruhe preprint TTP92-18.
Y. Sumino et al.: Preprint UT-594.
M. Jezabek and T. Teubner: In preparation.

$\gamma\gamma \to t\bar{t}$, including polarisation and QCD correction

J.H. Kühn, E. Mirkes and J. Steegborn: Karlsruhe preprint TTP92-28.

Recent reviews

Working Group on "Top Quark Physics", experimental aspects, CERN-PPE 92-05, G. Bagliesi et al., conv. P. Igo-Kemenes.
Working Group on "Top Quark Physics", theoretical aspects, TTP92-19, W. Bernreuther et al., conv. J.H. Kühn.

Top at Threshold in e^+e^- Collisions
– Experiments –

Keisuke FUJII

Bitnet: TKSF@JPNKEKTR
National Laboratory for High Energy Physics (KEK)
Tsukuba 305, Japan

ABSTRACT

We describe experimental aspects of top physics at future e^+e^- linear colliders, focusing on the $t\bar{t}$ threshold. Detailed studies of both the total and the differential crossections provide us with opportunities for precision determinations of various parameters of the standard model.

1 Top, Its New Features

As has been shown in the previous talks[1], the top quark is expected in the mass range:

$$m_W < m_Z \lesssim m_t \lesssim 200 \text{ GeV}, \tag{1}$$

which implies the following. i) The top is certainly in a 0.5 TeV linear collider's reach. ii) There is a chance to see the top Yukawa interaction. iii) The top decays directly into bW, which essentially saturates the branching fraction in the standard model and is dominant in most of its extensions. Therefore, the identification of the top quark is easy. iv) The dominance of the $t \to bW$ mode leads to a large top width as shown in Fig.1. For instance, the width is about 1 GeV for $m_t = 150$ GeV and becomes as large as 2.5 GeV for $m_t = 200$ GeV. This large width originates from the $t \to bW_L$ decay (the dashed curve in Fig.1, which grows as m_t^3. In this sense, the heavy top is a longitudinal W factory.

The most important new feature is probably this large top width that makes the top physics at future linear colliders unique. As pointed out by FADIN and KHOZE[2] in their pioneering paper, the large top width acts as an infrared cutoff (the top decays before entering the non-perturbative regeme), which allows us a reliable cross section estimate based on *perturbative* QCD. Therefore, we can perform a clean test of QCD at the $t\bar{t}$ threshold. More importantly, since we can calculate QCD contribution unambiguously, other tiny effects such as the Higgs exchange contribution is extractable. Since the heavy top quark decays before entering the non-perturbative regeme, there will be no t-hadron formation. This means that we can measure the top polarization. This unique feature will be discussed by BURKE in the next talk.

In e^+e^- collisions, we can exploit the following processes to produce top quarks: i) $e^+e^- \to t\bar{t}$, ii) $e^+e^- \to t\bar{t}Z$[3], iii) $e^+e^- \to t\bar{t}H$[4], and iv) $e^+e^- \to \nu\bar{\nu}t\bar{t}$[5]. The tree-level production cross sections for these processes are shown in Fig.2 for $m_t = 100, 150$, and 200 GeV. At low energies, process (i) is dominant (> 5k events are expected for an integrated luminosity of 10 fb^{-1} at $\sqrt{s} = 0.5$ TeV), while at higher energies the remaining processes become of interest (see Fig.3 for physics relevant to each of these processes). Since the top physics at higher energies will be covered by the next talk, we will concentrate on the $t\bar{t}$ threshold.

2 Formulation and Physics Involved

2.1 Threshold Correction

In the threshold region, the t and $\bar{t}$ quarks are slow and stay close to each other for relatively long time, thereby allowing multiple exchange of gluons (and Higgses, if its light). This gives rise to a threshold correction, which can be expressed as the sum of ladder diagrams, to the tree-level amplitude for the $e^+e^- \to t\bar{t}$ process (see Fig.4). The sum of the ladder diagrams corresponds to the $t\bar{t}$ potential which is determined by the QCD coupling(α_s), the Higgs mass(m_H), and the normalized top Yukawa coupling($\beta_H \equiv g_{tH}/g_{tH}(SM)$). The mass and the width of the top quark enter the t and $\bar{t}$ propagators. As stressed earier, the large top width thus cuts off the ladders and, therefore, makes irrelevant the long-range part of the $t\bar{t}$ potential. The threshold correction, denoted by Γ in Fig.4, can thus be reliably calculated and provides us with a powerful tool to extract various physics involved in it. The threshold correction factor is proportional to the Green's function defined by

$$\tilde{G}(\mathbf{p}; E) \equiv \langle \mathbf{p} \,|\, G \,|\, \mathbf{r}' = 0 \rangle, \tag{2}$$

where G satisfies the Schrödinger equation

$$\left(H - E - \frac{i}{2}\Gamma_\theta\right) G = 1. \tag{3}$$

H is the Hamiltonian given by

$$H = \frac{\mathbf{p}^2}{m_t} + V_{sl}(\mathbf{r}), \tag{4}$$

E the energy measured from the threshold ($E = \sqrt{s} - 2m_t$), and Γ_θ is the toponium width.

The dominant correction comes from the S-wave contributions which modify the vector part of the $tt\gamma$ and ttZ vertices. FADIN and KHOZE[2] were the first to calculate the S-wave contributions to the total $t\bar{t}$ cross section, with the help of the optical theorem. STRASSLER and PESKIN[6] then refined their results, by using a realistic QCD potential. SUMINO, FUJII, HAGIWARA, MURAYAMA, and NG[7] extended their method to the calculation of differential cross sections, which necessitates the introduction of a running toponium width to preserve the unitarity relation.

On the other hand, the axial vector coupling, which is absent in the zeroth order approximation, comes from the P-wave contributions and appears as an $O(\beta)$ correction to the differential cross section through the S-P interference, where β is the velocity of the top quark. SUMINO and MURAYAMA[8] calculated this effect and pointed out that it produces an observable forward-backward asymmetry.

2.2 Inclusion of Initial State Radiation

It is well known that the initial state radiation has to be properly taken into account in the vicinity of a resonance state. We inculde this by convoluting the

differential cross section without the initial state radiation ($d\sigma^0_{t\bar{t}}$) with the radiator function introduced in reference[9]:

$$d\sigma_{t\bar{t}} = \left(1 + \frac{2\alpha_0}{\pi}(\frac{\pi^2}{6} - \frac{1}{4})\right) \int_0^1 dz \beta_e \left(z^{\beta_e - 1}(1 + \frac{3}{4\beta_e}) - (1 - \frac{z}{2})\right) d\sigma^0_{t\bar{t}}(\hat{s}) \quad (5)$$

where

$$\begin{aligned} \hat{s} &= s \cdot (1 - z) \\ \beta_e &= \frac{2\alpha_0}{\pi}\left(\log(\frac{s}{m_e^2}) - 1\right). \end{aligned} \quad (6)$$

The fine structure constant α_0 is taken to be 1/137 here, since the relevant energy scale is of low energy. We will examine how this affects the total and differential cross sections later.

3 Theoretical Expectations

In this section, we examine the theoretical expectations derived from the formulation presented above. We assume, in what follows, $m_t = 150$ GeV, which roughly corresponds to the current best estimate from the precision electroweak measurements[1].

3.1 Total Cross Section

In the top mass range of our interest, the width of the resonance is almost saturated by the single quark decay ($\Gamma_\Theta \simeq 2\Gamma_t$), so that the other decay modes involving $t\bar{t}$ annihilations are negligible. The total $t\bar{t}$ cross section in the threshold region thus involves the following parameters:

$$\sigma_{t\bar{t}}(\sqrt{s}, m_t, \Gamma_t, \alpha_s(m_Z), m_H, \beta_H). \quad (7)$$

Figs.5-a) to -d) demonstrates the dependences of the threshold shape on these parameters.

As shown in Fig.5-a) the first S-wave peak position shifts downward, while the peak itself is enhanced, when α_s increases. This is because, when the potential becomes deeper, the binding energy and the wave function at the origin also become larger. We expect, therefore, a positive correlation between m_t and α_s, when the peak position is fixed.

On the other hand, the correlation between m_t and the top width (Γ_t) is small as seen in Fig.5-b). When the width becomes narrower, the peak height increases, while the tail part decreases. Notice that in Fig.5-b), $|V_{tb}|^2$ is defined by

$$|V_{tb}|^2 = \Gamma_t/\Gamma_t(SM : |V_{tb}|^2 = 1), \quad (8)$$

and can be greater than unity when there is some additional decay modes such as $t \to bH^+$ or $t \to \tilde{t}\tilde{X}^0$ or both.

The most interesting is the Higgs effects. Since this effect is given in the first approximation by an attractive Yukawa potential[10]

$$V_H(r) \simeq -\frac{\sqrt{2}G_F}{4\pi}(\beta_H m_t)^2 \frac{e^{-m_H r}}{r}, \quad (9)$$

the Higgs-exchange contribution is expected to be large for smaller m_H and larger β_H. Notice that the range of this potential is controlled by the Higgs mass (m_H) and is short compared to the QCD potential. Therefore, the Yukawa potential does not change the resonance position very much, but makes the wave function at the origin significantly larger, thereby making the cross section larger everywhere in the threshold region. Figs.5-c) and -d) demonstrate this as the dependences on m_H and β_H, respectively.

3.2 Momentum Distribution

The total cross section is proportional to the imaginary part of the coordinate space Green's function at the origin:

$$\sigma_{t\bar{t}} \propto \mathrm{Im}\langle \mathbf{r} = 0 | G | \mathbf{r}' = 0 \rangle, \quad (10)$$

while the differential cross section is proportional to the square of the momentum space Green's function:

$$\frac{d\sigma_{t\bar{t}}}{d|\mathbf{p}|} \propto |\langle \mathbf{p} | G | \mathbf{r}' = 0 \rangle|^2. \quad (11)$$

Therefore, it is expected that the measurement of the momentum distribution of the top quark provides additional information. Unfortunately, the Higgs exchange potential, being of short range, does not change the shape of the distribution siginificantly. On the other hand, the change in the top width or the strong coupling constant induces a measurable effect on the momentum distribution.

Fig.6-a) shows how the momentum distribution changes with α_s at the $t\bar{t}$ threshold ($E = 0$). The peak momentum increases with α_s. This behavior is expected from the virial theorem which predicts that the average top momentum is roughly given by $m_t\alpha_s$. Notice that the correlation between m_t and α_s is opposite here to that of the threshold shape measurement. This suggests the possibility of precision simultaneous determinations of m_t and α_s.

The dependence on the top width is shown in Fig.6-b), where the peak shifts toward the higher momentum side, when the top width gets larger. This is because, when the width grows, the top decays at shorter distance where the $t\bar{t}$ potential is deeper.

3.3 Forward-Backward Asymmetry

So far, we have been concentrating on the S-wave contributions to the Green's function, since the P-wave contributions to the total cross section and the momentum distribution are of $O(\beta^2)$ and, therefore, can be ignored. The P-wave contributions, however, may produce a measurable forward-backward asymmetry through the S-P interference as an $O(\beta)$ correction to the differential cross section.

Fig.7 illustrates the locations of the S- and P-wave resonances. The first S-wave resonance ($1S$) stands alone but the second ($2S$) and higher ($nS : n > 2$) S-wave resonances are accompanied by P-wave resonances. When the $t\bar{t}$ potential is exactly Coulombic, the S- and P-wave resonances are exactly mass-degenerate for $n > 1$. In the case of a realistic QCD potential, the P-wave states, which feel the longer-distance part of the $t\bar{t}$ potential compared to the S-wave states, acquire larger binding energies and have slightly lower masses. In any case, when we sit at the $1S$ peak, the S-P interference must vanish, if the level splitting between the $1S$ and the $2S$ states is much larger than the widths of the resonances. The level splitting is determined by α_s, while the onium widths are controlled by the top width. Therefore, we expect that the measurement of the forward-backward asymmetry of the top quark reconstructed from the bW final state allows us to extract additional information on the top width and the strong coupling constant.

Fig.8-a) shows the forward-backward asymmetry at the $1S$ peak as a function of $E(\equiv \sqrt{s}-2m_t)$ for $\alpha_s(m_Z) = 0.11, 0.12$, and 0.13. As expected, the asymmetry gets larger when α_s decreases, though the difference is rather small.

Fig.8-b) on the other hand, demonstrates the sensitivity to the top width. The asymmetry is enhanced, as the top width grows, since the S-P overlapping becomes more significant.

4 Real Life Experiments

In this section, we consider how to carry out the measurements discussed above in real life experiments. For this purpose, we will first examine how beam energy spread and beamstrahlung modify the ideal distributions presented above. Then, we describe the Monte Carlo event generator, necessary for the subsequent studies. A brief discussion on the event selection follows this. The selected events are then used to simulate the measurements of the total and the differential cross sections in a realistic environment.

4.1 Beam Effects

Fig.9-a) shows an example of effective center-of-mass energy distribution in the presence of beam energy spread and beamstrahlung[11]. The sharp peak at $\sqrt{s_{eff}}/\sqrt{s_0} = 1$ (the δ-function part) corresponds to the no beamstrahlung case, while the long tail downwards is due to beamstrahlung photons. What we observe in real life experiments is the convolution of this effective $\sqrt{s}$ distribution with the ideal distributions in the previous section. Since the effect of the beamstrahlung is expected to be similar to that of the initial state radiation, we will examine how the distributions change in three steps: i) no initial state radiation (ISR) and no beam effects, ii) with the ISR but without the beam effects, and iii) with both of the ISR and the beam effects.

Fig.9-b) shows this for the total cross section. We can see that the ISR reduces the observable cross section significantly, though the $1S$ peak is still visible. The beam effects, the beam energy spread in particular, smear out the $1S$ peak. The main effect of the beamstrahlung is, in this case, a loss of usable luminosity.

Fig.9-c) is for the momentum distribution, where we can see that the peak position is quite stable against the ISR and the beam effects, in spite of the significant change in the lower momentum region.

The forward-backward asymmetry at the $1S$ peak is insensitive to the ISR effect and, therefore, should also be insensitive to the beamstrahlung effect. The beam energy spread is the one that affects the asymmetry at the $1S$ peak siginificantly (see Fig.9-d)).

Since we have learned that the beam energy spread is the major problem with our planned precision measurements, we should also be aware of the effects of the structure inside the δ-function part. In order to see the effects more clearly, we switch off the beamstrahlung here and examine how the threshold shape changes with the beam energy spread for two kinds of spectra, flat-top and double-peak which is more realistic. Fig.10-a) is the blowup of the δ-function part for these two spectra with various beam energy widths and Fig.10-b) is the corresponding threshold shape. We can see that, when the beam energy spread is greater than 0.4 %, the structure inside the δ-function part affects the threshod shape.

The effects of the beam effects can be summarized as follows. i) The beamstrahlung reduces the usable luminosity in the threshold region. In other words, the usable part is essentially restricted to the δ-function part. Therefore, we need to know the height of the δ-function part accurately for precision measurements. ii) The beam energy spread is the major source of the peak smearing. When the energy spread is less than 0.4 %, however, the threshold shape is practically independent of the structure inside the δ-function part. If we cannot achieve such a narrow band beam, we need to measure the spectrum inside the δ-function part with a high energy resolution.

MILLER proposed a method for the differential luminosity measurement[12]. His method consists of two steps. In the first step, we measure undistorted beam energies of electrons and positrons separately. The experience at SLC suggests that the precision obtainable at this stage is 1/2500. In the second step, we look at Bhabha events and measure acollinearity. Using the undistorted beam energy

distributions and the acollinearity angle distribution, we estimate the effective center of mass energy distribution. According to his analysis, a precision better than 1/1000 can be expected.

4.2 Monte Carlo Event Generation

Before moving on to event selection, it is useful to make a few comments on the Monte Carlo event generation. When the top width exceeds a typical hadronization scale, there will be no t-hadron formation[13]. Then the polarization information of parent top quarks is transfered to decay daughters which give rise to angular correlations in the final state particles. In order to take proper account of this effect, we should use the full helicity amplitudes. As for the color neutralization, we assume that the color flux is spanned between b and $\bar{b}$ quarks. Since we are going to reconstruct top quarks by jet invariant mass method, it is also important to consider gluon emissions from b or $\bar{b}$ quarks as well as those from W decay daughters. The point here is the energy scale to be used for the parton showering from b or $\bar{b}$ quarks. We should not, for instance, set $Q_{max} = \sqrt{(p_b + p_g)^2}$, but, instead, should set $Q_{max} = m_t - M_W$, since the gluon emission is controlled by the acceleration the b or $\bar{b}$ quarks receive when their parent t or $\bar{t}$ quarks decay[14]. Consequently, the 4-momentum adjustments after parton showering should be made within the bW systems. The gluon emissions from t or $\bar{t}$ quarks, which are not incuded here could modify the event shape. We assume, however, that there will be no soft-gluons from t or $\bar{t}$ quarks, again because of the large top width acting as an infrared cutoff. Therefore its effect on the event selection efficiency we are going to discuss in the following subsection will be $O(\alpha_s)$. It is also essential to include initial state radiations as well as beam energy spread and beamstrahlung, since they may change the event shape significantly. In order to take all of these effects into account, we have used the HELAS system[15] for helicity amplitude calculations and the BASES-SPRING system[16] for phase-space integrations and event generations.

4.3 Event Selection

The signature of $t\bar{t}$ pair production is two b quarks and two W bosons in the final state. The two W bosons decay into either $q\bar{q}'$ or $l\bar{\nu}$. Therefore the final state configurations are i) two b-jets and four jets from W's(45 %), ii) two b-jets, two jets and one charged lepton(44 %), and iii) two b-jets and two charged leptons(11 %). Case i) is useful for the total cross section and the momentum distribution measurements, while case ii) is the only channel to measure the forward-backward asymmetry in practice. We are not getting into details of the event selections but just mention that the basic cuts used in these analyses can be classified into the following three groups: a) event shape cuts such as those on the number of charged particles, the number of jets, and thrust, b) mass cuts to select W's and t's by jet invariant mass method, and c) requirements of leptons in cases ii) or iii). If available, b-tagging is a powerful tool to reduce the combinatorial back ground in the parton reconstruction by jet-invariant mass method.

In order to measure the threshold shape reliably, we need to select $t\bar{t}$ events with a good S/N ratio. In the case of JLC parameters, the effective cross section at the threshold is about 0.4 pb for m_t = 150 GeV while that of the largest background(W^+W^- productions) is about 14 pb. We need some 10^{-3} suppression. Let us see how this can be achieved, taking case i) as an example. Fig.11-a) shows a typical 6-jet event expected for case i). When we look at this event in the calorimeter, we have Fig.11-b) where we can clearly see six jets. Histogrammed in Figs.12-a) and -b) are the visible energy and the transverse momentum for the intial sample, respectively, where the final sample distributions are also shown as hatched histograms. Fig.13 is the scatter plot of the 2-jet invariant masses corresponding to two W candidates for the final sample where their projections are also shown. The cut on the invariant masses is depicted as a square in the figure. Fig.14 is a similar plot for the 3-jet invariant masses corresponding to the bW candidates at the threshold. The smooth curve indicates the location of the m_t cut. Finally, Fig.15 shows the thrust distributions for the $t\bar{t}$ signals and the W^+W^- background, just before the final thrust cut indicated by an arrow in the same plot. After this final cut, the detection efficiency is 26 % while the signal to background ratio greater than 10. This detection efficiency translates to about 58 % when the $W \to q\bar{q}$ branching ratio of 67 % is taken into account. We can obtain similar efficiencies and signal to background ratios for cases ii) and iii).

4.4 Determination of Various Parameters

4.4.1 Threshold Scan

Using the $t\bar{t}$ sample so obtained, we can determine the parameters that enter the threshold formula. The question is how well we can do this. KOMAMIYA[17] made the first attempt to answer it, assuming no beam energy spread and beamstrahlung. Then FUJII[18] studied the same problem with beam energy spread and beamstrahlung taken into account. MIQUEL[19] compared various machine parameters and FUJII[20] refined the analysis using a new formalism[7] to calculate the threshold cross section.

Fig.16-a) is an example of the energy scan to determine m_t and $\alpha_s(M_Z)$. Each data point corresponds to 1 fb^{-1} and was generated with $|V_{tb}|^2 = 1$, $\alpha_s(m_Z) = 0.12$, and $M_H = \infty$(no Higgs). By fitting these data points to the threshold formula convoluted with the natural beam energy spread and the beamstrahlung spectra, we obtain a contour plot shown in Fig.16-b) The strong correlation between m_t and $\alpha_s(m_Z)$ stems from the fact that the resonance mass decreases as $\alpha_s(m_Z)$ increases. If $\alpha_s(m_Z)$ is known, we have $\Delta m_t \simeq 0.1$ GeV and even if

$\alpha_s(m_Z)$ is totally unconstrained, we can expect $\Delta m_t \simeq 0.2$ GeV.

Fig.17-a) is a similar plot for the determination of $|V_{tb}|^2$. Again we assume 1 fb^{-1} per point. The corresponding contour plot (Fig.17-b)) shows no correlation between m_t and $|V_{tb}|^2$ and indicates $\Delta|V_{tb}|^2 \simeq 0.15 \sim 0.20$.

Figs.18-a) and -b) are examples for the m_H and β_H measurements where the energy points are chosen in the same way as with Figs.16-a) and 17-a). The m_H-β_H^2 contour is given in Fig.18-c). In the case of $\beta_H^2 = 1$(SM) the scan is sensitive to a m_H up to about 120 GeV. It should be noted that the energy points used here are by no means optimized. Prior to the actual energy scan, we will have a fairly good estimate of m_t as will be described in the next talk by BURKE. Based on this knowledge, we should be able to improve the precision of the measurements by optimizing the energy points to maximize the sensitivities to the model parameters discussed above.

4.4.2 Measurement of Momentum Distribution

The momentum distribution of the top quark reflects the shape of the $t\bar{t}$ potential that it probes. Therefore, the momentum distribution provides additional information on m_t, $\alpha_s(m_Z)$, and Γ_t. MATSUI and FUJII studied how well we can measure the momentum distribution. To measure the top momentum, we need to select well reconstructed $t\bar{t}$ events, since missing neutrinos easily distort the observed momentum distribution. For this purpose, we use 6-jet final states and impose very tight selection cuts. To match such tight cuts, the detector must have a good energy resolution to effectively remove events with high momentum neutrinos.

Fig.19-a) is an example of the reconstructed momentum distribution at the $t\bar{t}$ threshold, where the Monte Carlo distribution is compared with the theoretical expectations for $\alpha_s(m_Z) = 0.11$, 0.12, and 0.13. The Monte Carlo data points were generated with $\alpha_s(m_Z) = 0.12$ and $|V_{tb}|^2 = 1$ and plotted with no acceptance correction. The overall detection efficiency is 2 % in this example. We can see that the Monte Carlo distribution is reasonably well reproduced by the theoretical expectation for the corresponding $\alpha_s(m_Z)$ value. The discrepancy in the higher momentum region is due to still remaining missing neutrinos. As stated in Section 3, the correlation between m_t and $\alpha_s(m_Z)$ in this measurement is opposite to that of the threshold scan. Therefore, we can determine both m_t and $\alpha_s(m_Z)$ by simultaneously fitting the threshold shape and the momentum distribution. Here, however, we assume that m_t is known and see how sensitive the momentum peak position is to $\alpha_s(m_Z)$. The dependence of the peak position on $\alpha_s(m_Z)$ is shown in Fig.19-b) where the dotted lines indicate the 1-σ bounds when an integrated luminosity of 100 fb^{-1} is accumulated. The expected statistical error on $\alpha_s(m_Z)$ is 0.001, in this example, if m_t is known and $|V_{tb}|^2 = 1$.

Fig.20-a) compares the same Monte Carlo distribution with the theoretical expectations for three different values of the top width: $|V_{tb}|^2 = 0.8$, 1.0, and 1.2. Again, the Monte Carlo distribution is well reproduced by the theoretical curve for the corresponding $|V_{tb}|^2$ value. Fig.20-b) shows the sensitivity to the top width. In this example, $\Delta|V_{tb}|^2 = 0.08$ is expected for 100 fb^{-1}, when m_t and $\alpha_s(m_Z)$ are known.

4.4.3 Measurement of Forward-Backward Asymmetry

In order to measure the forward-backward asymmetry, we have to know the charge of the reconstructed 3-jet system, which necessitates the use of the 4-jet+lepton final state. Fig.21-a) plots the total cross sections and the forward-backward asymmetries for $\alpha_s(m_Z) = 0.11$, 0.12, and 0.13, as functions of the energy measured from the $t\bar{t}$ threshold, inculding both the intial state radiation and the beam effects. Fig.21-b) shows the asymmetry at the $1S$ peak as a function of $\alpha_s(m_Z)$. The dotted lines in the figure indicate the 1-σ bounds expected for 40 k detected events. Unfortunately, the sensitivity to $\alpha_s(m_Z)$ is poor. This, however, improves for higher m_t values, since a heavier top has a larger width, which enhances the observable asymmetry.

The situation is better for the sensitivity to the top width. Fig.22-a) is a similar plot to Fig.21-a) but with different top widths for a fixed $\alpha_s(m_Z) = 0.12$. The asymmetry at the $1S$ peak is plotted as a function of $|V_{tb}|^2$ in Fig.22-b) If m_t and $\alpha_s(m_Z)$ are known, 40 k detected events allow us to determine the top width with a relative statistical error of 5 %.

5 Summary and Conclusion

The large decay width expected for a heavy top quark gives the $t\bar{t}$ threshold essentialy new features distinct from that of the lighter $q\bar{q}$ threshold. The large width acts as an infrared cutoff and allows reliable estimates of the QCD contributions to the threshold cross sections, which, in turn, make possible the extraction of other tiny effects such as Higgs-exchange contributions. It should be also noted that event selection can be efficiently carried out by reconstructing the $bWbW$ final states through the jet-invariant-mass method.

There are many ways to extract physics involved in the vertex correction at the $t\bar{t}$ threshold. We can measure the threshold shape by energy scan. Given 11 energy points with 1 fb^{-1} each, we can determine the top mass with a statistical error of $\Delta m_t = 0.2$ GeV, even if α_s is totally unconstrained. If m_t is known, on the other hand, we can expect $\Delta\alpha_s(m_Z) = 0.002$. The expected statistical error on the top width is $\Delta\Gamma_t/\Gamma_t = 0.2$, when $\alpha_s(m_Z)$ is known. The sensitivity to the Higgs-exchange effects extends up to $m_H \lesssim 120$ GeV, if the Yukawa coupling is that of the standard model. These results, however, assume a good control of the beam energy spread, $\Delta E_{beam} \lesssim 0.4$ %(FWHM), or a precision differential luminosity measurement.

The momentum spectrum measurement at the $t\bar{t}$ threshold is less dependent on the beam effects. It should be also emphasized that the correlation between m_t and $\alpha_s(m_Z)$ is opposite to that of the threshold scan. This allows precision measurements of m_t and $\alpha_s(m_Z)$ when combined with the threshold scan. The sensitivity of the top momentum measurement to $\alpha_s(m_Z)$ is expected to be $\Delta\alpha_s(m_s) \simeq 0.001$ for 100 fb^{-1}, when m_t is known. Given the same statistics, we expect $\Delta\Gamma_t/\Gamma_t \simeq 0.08$, provided that m_t and $\alpha_s(m_Z)$ are known from other sources. As for the Higgs-exchange effects, no additional information is available from the momentum measurement.

The forward-backward asymmetry at the $1S$ peak gives additional information on the top width. 40 k detected $t\bar{t}$ events in the 4-jet+lepton mode provides us with an opportunity to measure the top width with a statistical error of $\Delta\Gamma_t/\Gamma_t \simeq 0.05$, if m_t and $\alpha_s(m_Z)$ are known. This, however, requires a small beam energy spread or a precise knowledge of the differential luminosity.

In conclusion, the $t\bar{t}$ threshold is rich in interesting physics and gives us a good reason to build a sub-TeV linear collider.

Acknowledgements

The author wishes to thank all the members of the JLC working group for useful discussions and comments. In particular, K. Hagiwara, K. Hikasa, Y. Sumino, and C. Ng, T. Matsui, and H. Murayama deserve special mention. If it were not for their contributions, this work could not be completed. The author is very grateful to Professors D. Burke, J. Kühn, and M. Peskin for valuable discussions. Finally the author would like to express his hearfelt gratitude to the workshop organizers for their efforts to make this workshop so comfortable and so fruitful.

References

[1] J. Pilcher, talk given at this workshop.

[2] V. Fadin and V. Khoze, *Sov. J. Nucl. Phys.* **48** (1988) 309.

[3] K. Hagiwara, H. Murayama, and I. Watanabe, KEK Preprint 90-125 (1990), T. Tauchi, K. Fujii, and A. Miyamoto, KEK Preprint 90-148 (1990).

[4] A. Djouadi, J. Kalinowski, and P. Zerwas, DESY 91-104.

[5] T. Tsukamoto, KEK Preprint 91-17 (1991).

[6] M. Strassler and M. Peskin, *Phys. Rev.* **D43** (1991) 1500.

[7] Y. Sumino, K. Fujii, K. Hagiwara, H. Murayama, and C. Ng, KEK Preprint 91-6 (1992), also to be published in *Phys. Rev.* **D46** No.11(1992).

[8] Y. Sumino and H. Murayama, UT-605 (1992).

[9] See for instance, F. Berends in *Z Physics at LEP-I*, CERN Yellow Report No.89-08, vol.1.

[10] As pointed out by J. Kühn at this workshop, the potential approximation overestimates the Higgs-exchange contribution, since it ignores the retardation effect due to the finite Higgs mass.

[11] K. Yokoya, plenary talk given at *Workshop on Physics and Experiments with Linear Colliders*, Saariselkä, Finland, September 1991.

[12] M. Frary and D. Miller, DESY 92-123A (1992) 379.

[13] J. Kühn, *Acta Physica Austriaca, Suppl.* **XXIV** (1982) 203, I. Bigi, Y. Dokshitzer, V. Khoze, J. Kühn, and P. Zerwas, *Phys. Lett.*, **B181** (1986) 157, T. Sjöstrand, talk given at this workshop.

[14] K. Hagiwara, private communication.

[15] H. Murayama, I. Watanabe, and K. Hagiwara, KEK Preprint 91-11 (1992).

[16] S. Kawabata, *Comp. Phys. Comm.* **41** (1986) 127.

[17] S. Komamiya, SLAC-PUB-5324 (1991).

[18] K. Fujii, KEK Preprint 90-187 (1991).

[19] R. Miquel, talk given at *Workshop on Physics and Experiments with Linear Colliders*, Saariselkä, Finland, September 1991, see also DESY 92-123A.

[20] K. Fujii, KEK Preprint 92-6 (1992).

Figure Captions

Fig. 1 Top quark width as a function of top mass.

Fig. 2 Total cross sections for $t\bar{t}$, $t\bar{t}Z$, $\nu\bar{\nu}t\bar{t}$, and $t\bar{t}H$ productions for three representative top masses: (a) $m_t = 100$ GeV, (b) $m_t = 150$ GeV, and (c) $m_t = 200$ GeV.

Fig. 3 Physics relevant to the processes plotted in Fig.?7.

Fig. 4 The threshold correction to the $t\bar{t}$ pair production process.

Fig. 5 The dependence of the threshold shape on a) $\alpha_s(m_Z)$, b) $|V_{tb}|^2$, c) m_H, and d) β_H (the normalized Yukawa coupling), in the case of $m_t = 150$ GeV.

Fig. 6 The dependence of the top momentum distribution at the $t\bar{t}$ threshold on a) $\alpha_s(m_Z)$, and b) $|V_{tb}|^2$, in the case of $m_t = 150$ GeV.

Fig. 7 A schematic diagram showing the locations of the S- and P-wave resonances.

Fig. 8 The dependence of the forward-backward asymmetry at the $1S$ peak on a) $\alpha_s(m_Z)$, and b) $|V_{tb}|^2$, in the case of $m_t = 150$ GeV.

Fig. 9 (a) The effective center of mass energy distribution in the presence of beam energy spread and beamstrahlung. The effects of the initial state radiation and the beam energy spread and beamstrahlung on (b) the threshold shape, (c) the momentum distribution, and (d) the forward-backward asymmetry.

Fig. 10 (a) The reduced center of mass energy distributions including the effects of initial state radiations and natural beam energy spread but leaving out the effect of beamstrahlung. Distributions for two kinds of spectra, flat-top and double-peaked which is more realistic, are shown for various beam energy spreads. (b) Corresponding threshold shapes.

Fig. 11 (a) A typical 6-jet event from $e^+e^- \to t\bar{t} \to bW^+\bar{b}W^-$ where both W^+ and W^- decay into $q\bar{q}$. (b) The same event in the calorimeter.

Fig. 12 (a) E_{vis} and (b) P_T distrigutions for intial (open histograms) and final (hatched histograms) samples.

Fig. 13 A scatter plot of the invariant masses of the 2-jet systems reconstructed as W boson candidates together with their projection to each axis.

Fig. 14 A similar plot for the invariant masses of the 3-jet systems reconstructed as bW candidates at the $t\bar{t}$ threshold.

Fig. 15 Thrust distributions for the $t\bar{t}$ signal and the W^+W^- background with all but the thrust cut indicated by an arrow.

Fig. 16 (a) An example of energy scan to determine m_t and $\alpha_s(M_Z)$ where each point corresponds to 1 fb^{-1}. (b) The contour resulting from the fit to the data points.

Fig. 17 (a) An example of energy scan to determine m_t and $|V_{tb}|^2$ where each point corresponds to 1 fb^{-1}. (b) The contour resulting from the fit to the data points.

Fig. 18 (a) An example of energy scan to determine M_H and β_H^2 where the effective cross section curves are superimposed for several M_H values. (b) The same plot with the effective cross section curves for several β_H^2 values. (c) The contour resulting from the fit to the data points.

Fig. 19 (a) The reconstructed top momentum distribution at the $t\bar{t}$ threshold, compared with the theoretical expectations for $\alpha_s(m_Z) = 0.11, 0.12$, and 0.13 for $m_t = 150$ GeV. The Monte Carlo events were generated with $\alpha_s(m_Z) = 0.12$ and plotted with no acceptance correction. (b) The momentum peak position as a function of $\alpha_s(m_Z)$. The dotted lines indicate the 1-σ bounds expected for an integrated luminosity of 100 fb^{-1}.

Fig. 20 (a) Similar to Fig.19 but compared with the theoretical distributions for different top widths. (b) The momentum peak position as a function of $|V_{tb}|^2$. The dotted lines indicate the 1-σ bounds expected for an integrated luminosity of 100 fb^{-1}.

Fig. 21 (a) The forward-backward asymmetry and the $t\bar{t}$ cross section for $\alpha_s(m_Z) =$ 0.11, 0.12, and 0.13, as functions of the energy measured from the threshold. (b) The forward-backward asymmetry at the $1S$ peak as a function of $\alpha_s(m_Z)$. The dotted lines indicate the 1-σ bounds expected for 40 k reconstructed $t\bar{t}$ events.

Fig. 22 (a) The forward-backward asymmetry and the $t\bar{t}$ cross section for $|V_{tb}|^2 =$ 0.8, 1.0, and 1.2, as functions of the energy measured from the threshold. (b) The forward-backward asymmetry at the $1S$ peak as a function of $|V_{tb}|^2$. The dotted lines indicate the 1-σ bounds expected for 40 k reconstructed $t\bar{t}$ events.

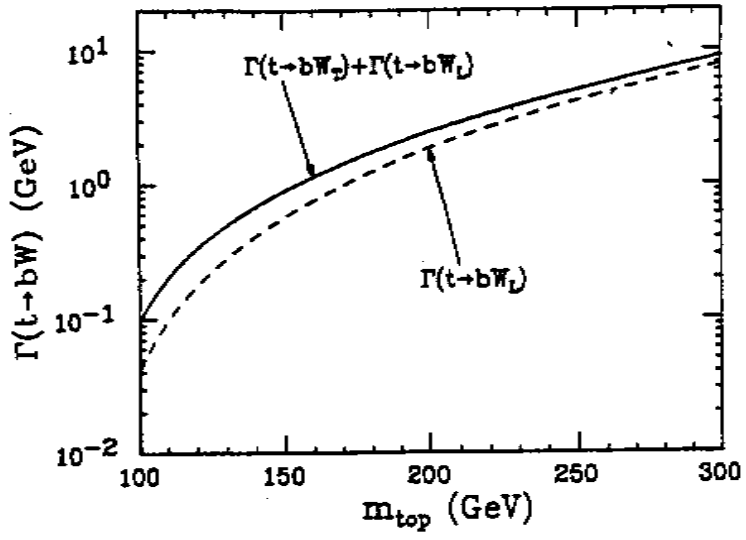
Γ(t→bW_T)+Γ(t→bW_L)
Γ(t→bW_L)
Γ(t→bW) (GeV)
m_top (GeV)

Fig.1

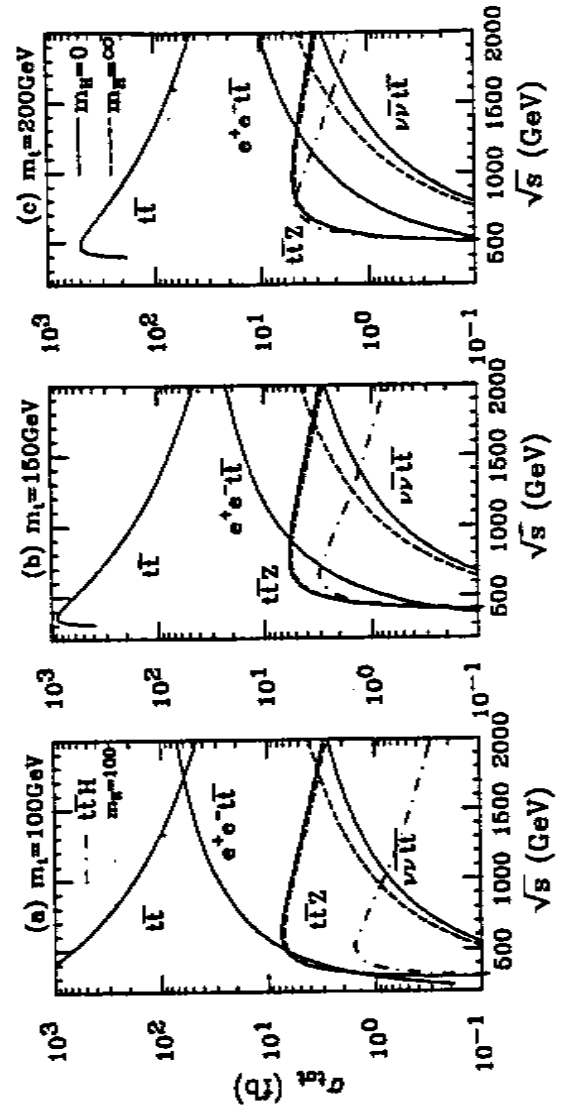
(a) m_t=100GeV
(b) m_t=150GeV
(c) m_t=200GeV
m_H=100
m_H=0
m_H=∞
tt̄
tt̄H
e⁺e⁻→tt̄
tt̄Z
tt̄ν_ℓν̄_ℓ
σ_tot (fb)
√s (GeV)

Fig.2

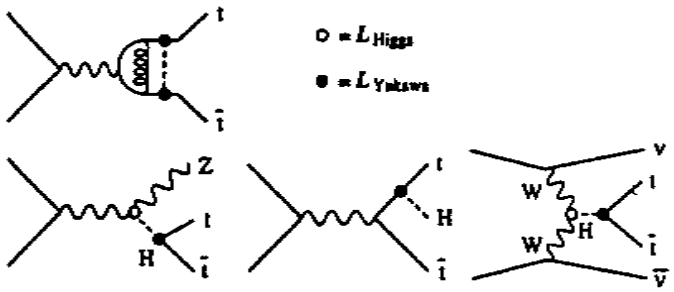

Fig.3

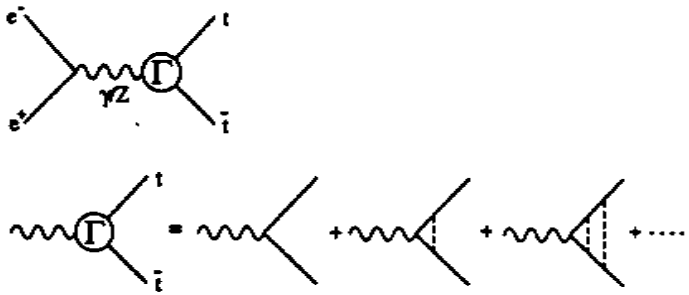

Fig.4

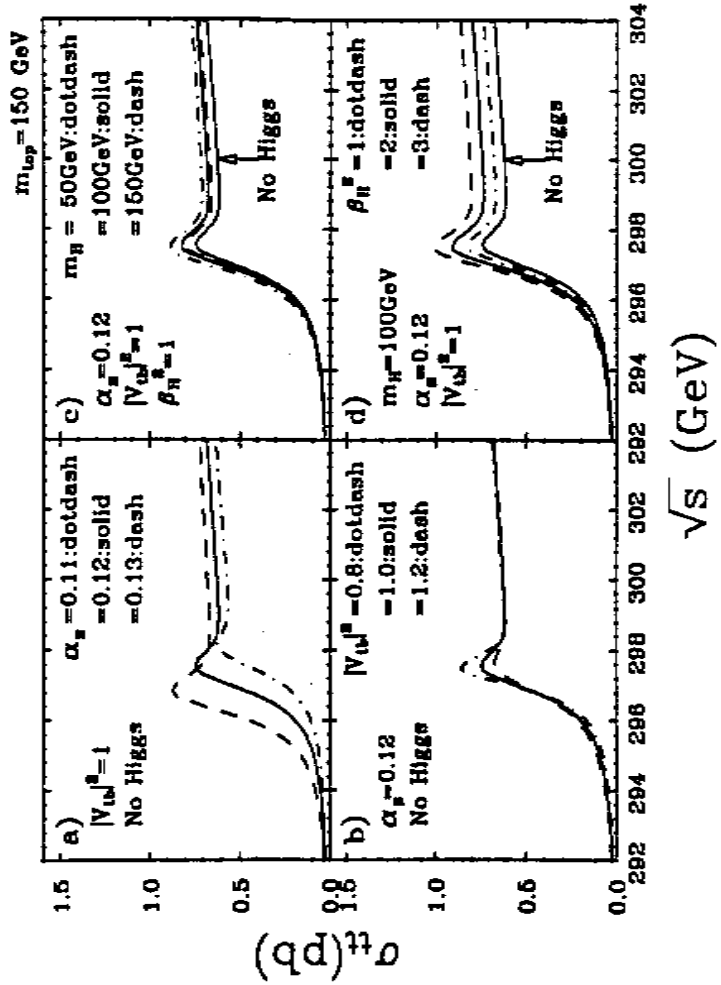

Fig.5

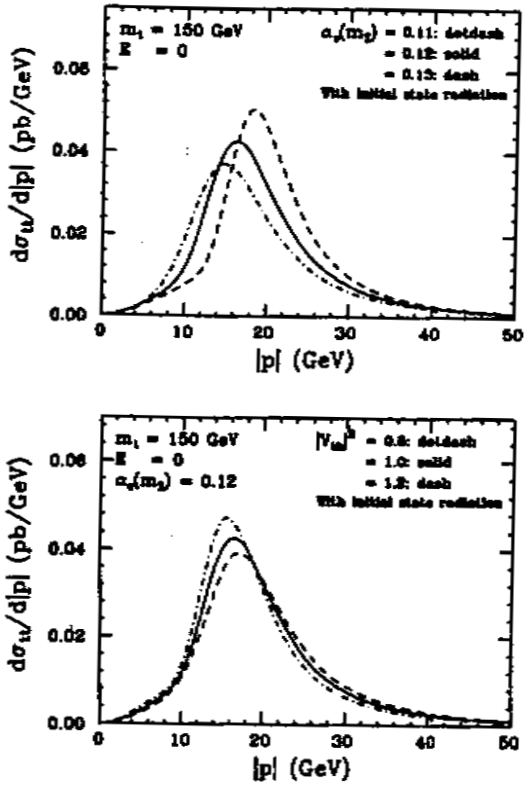

Fig.6

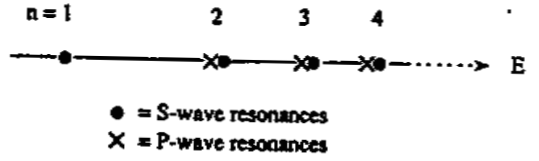

Fig.7

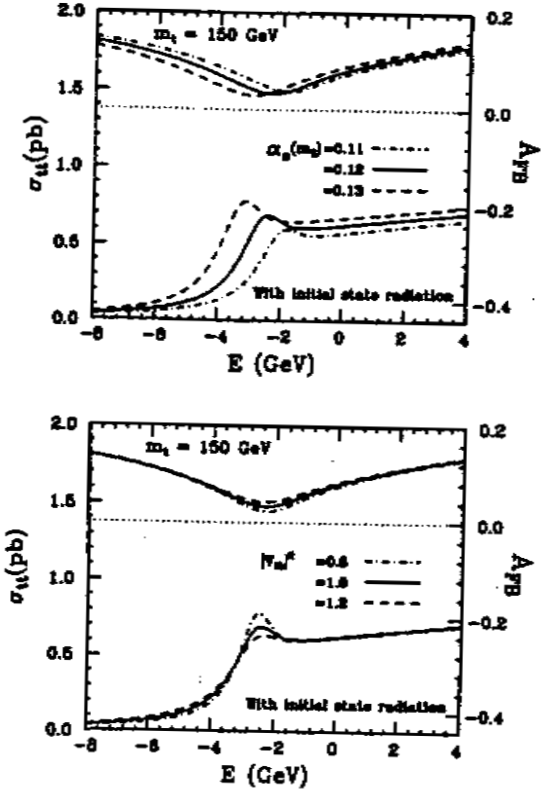

Fig.8

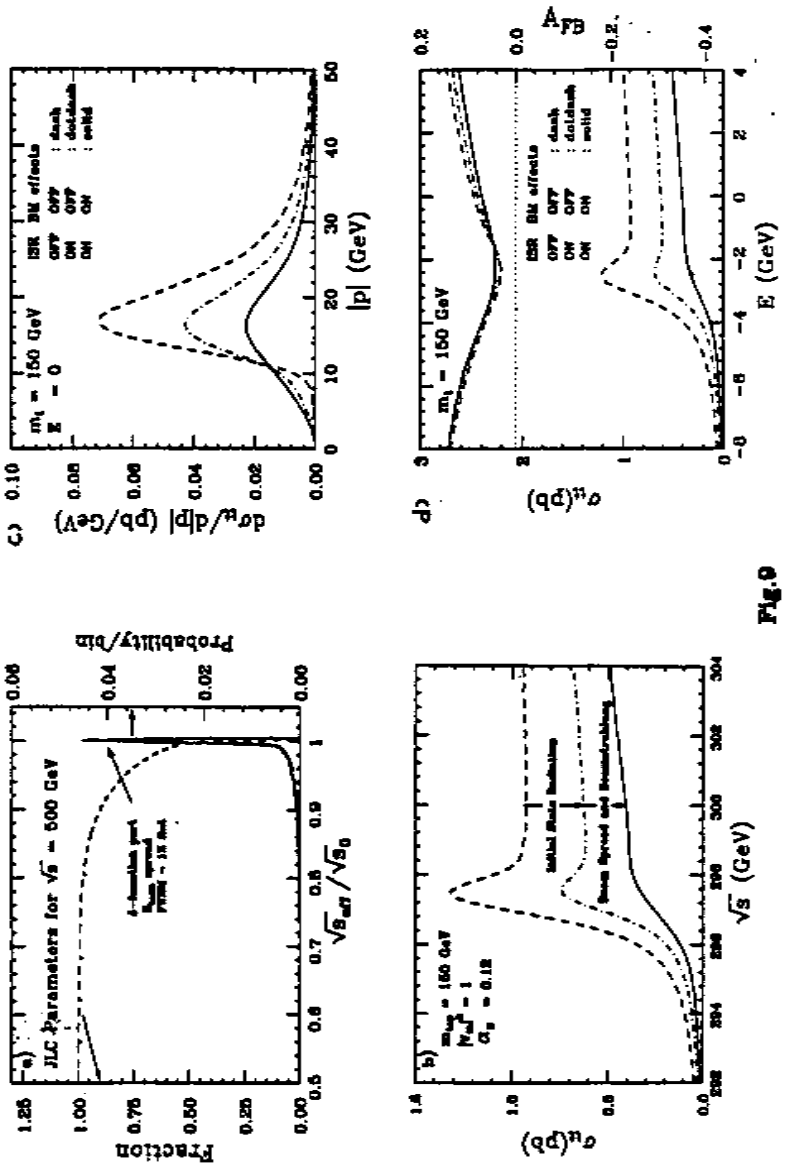
a) JLC Parameters for √s = 500 GeV
Fraction
Probability/bin
√s_eff/√s_0
b)
σ_tt(pb)
√s (GeV)
c)
dσ_tt/d|p| (pb/GeV)
|p| (GeV)
d)
σ_tt(pb)
A_FB
E (GeV)

Fig.9

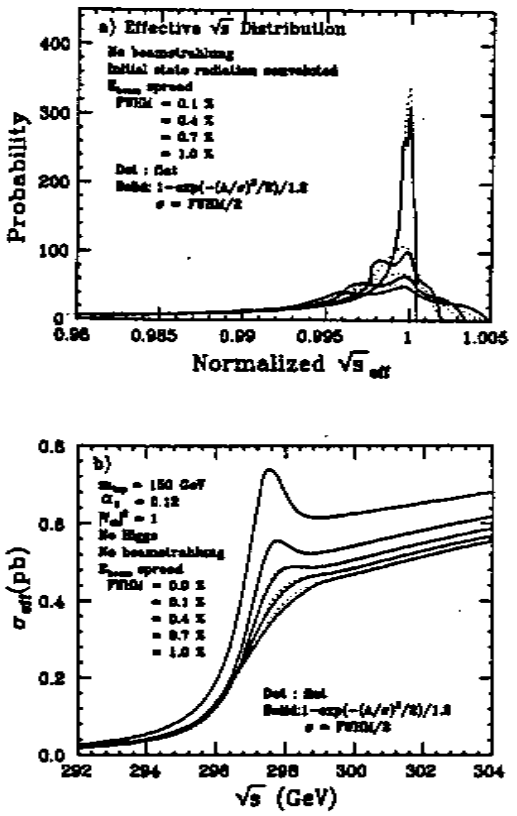
a) Effective √s Distribution
Probability
Normalized √s_eff
b)
σ_eff(pb)
√s (GeV)

Fig.10

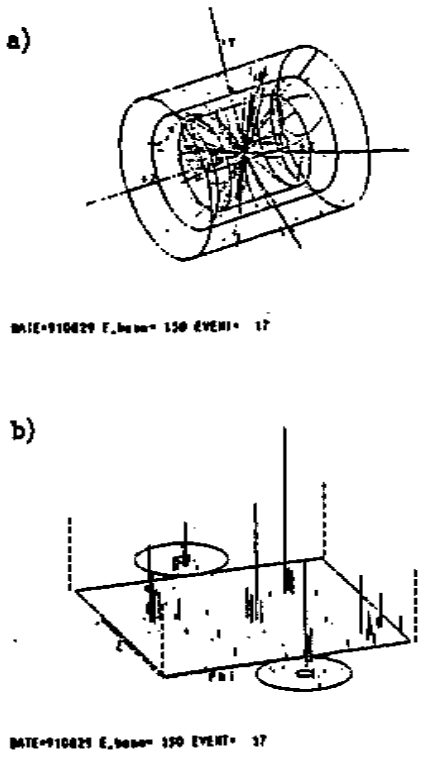

Fig.11

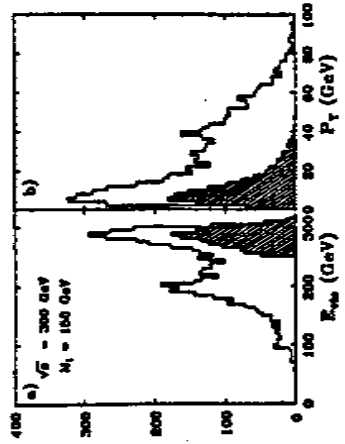

Fig.12

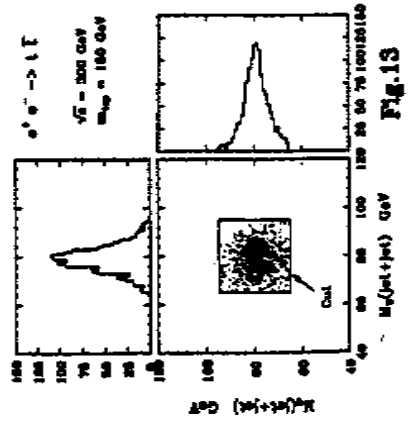

Fig.13

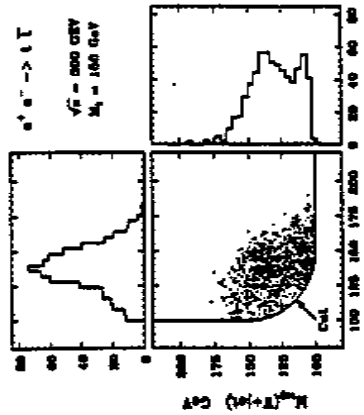

Fig.14

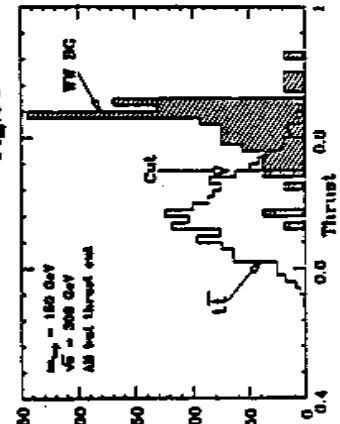

Fig.15

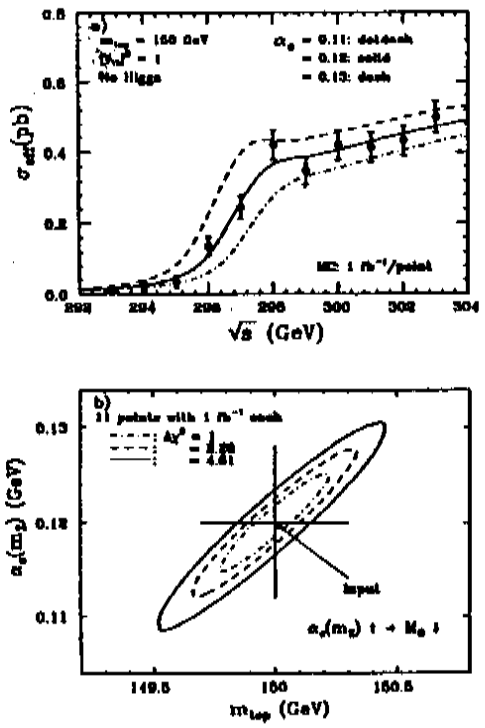

Fig.16

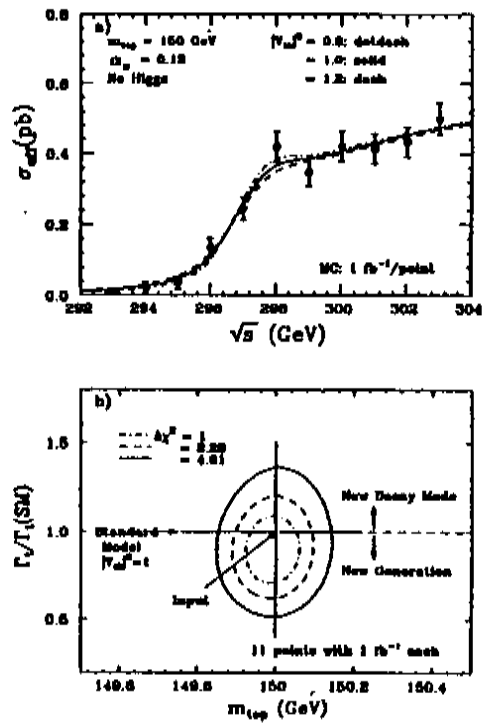

Fig.17

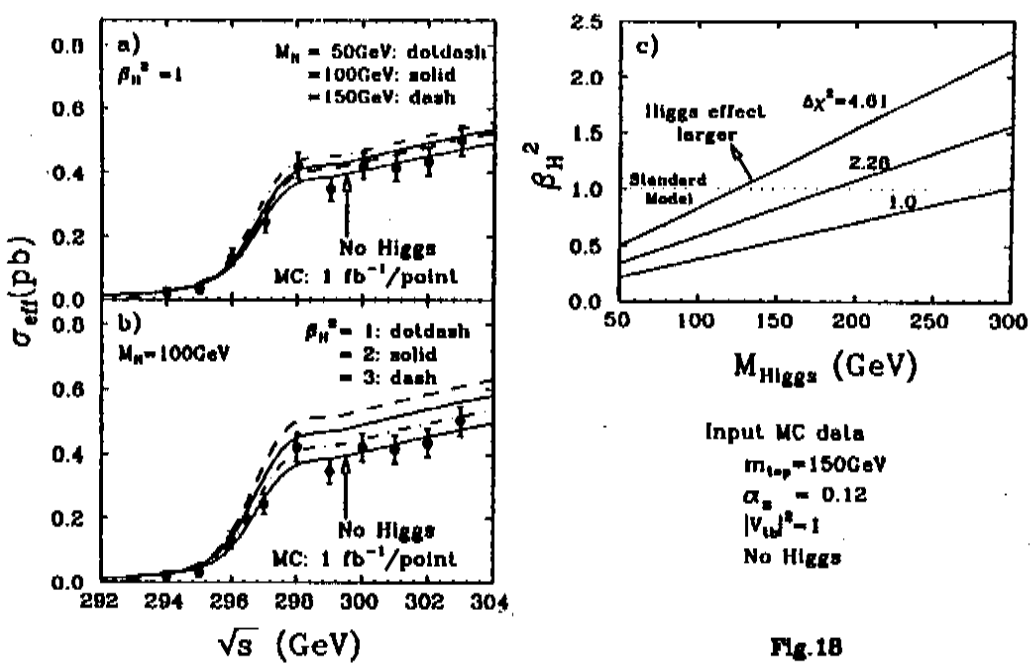

Fig.18

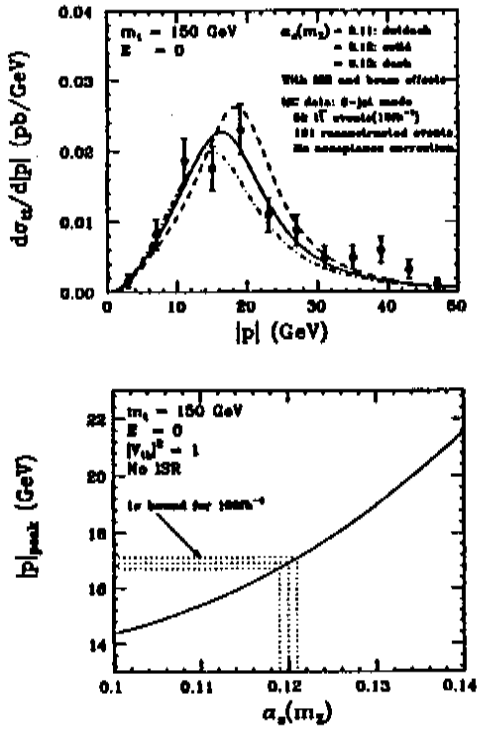

Fig.19

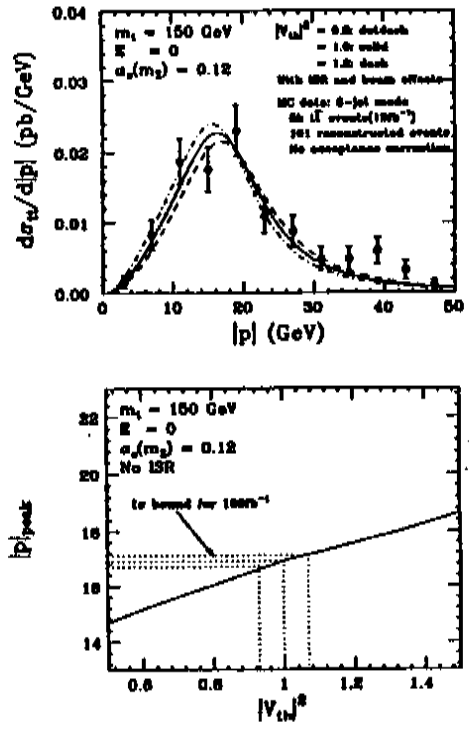

Fig.20

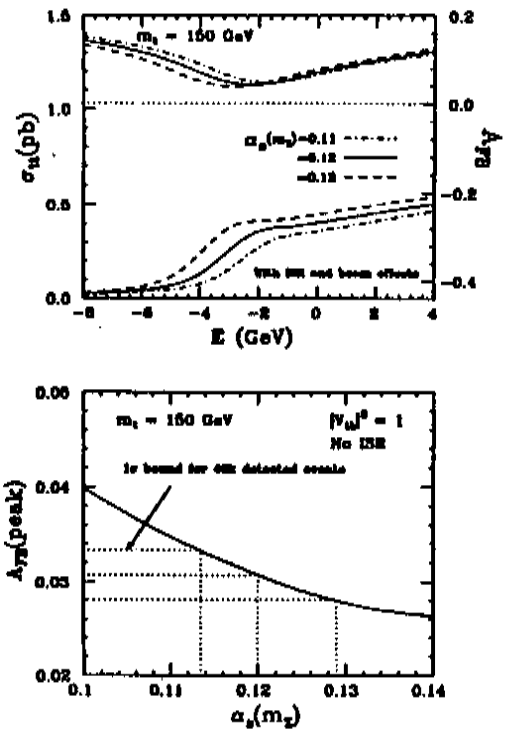

Fig.21

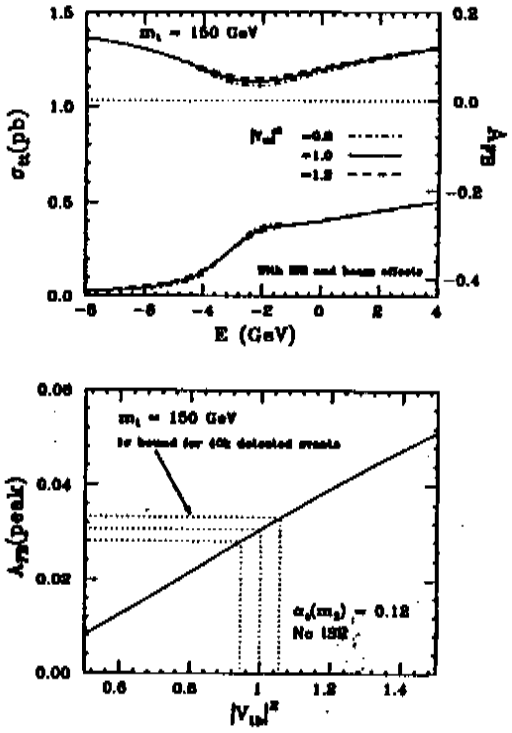

Fig.22

OPEN TOP at LINEAR ELECTRON-POSITRON COLLIDERS

D. L. Burke
Stanford Linear Accelerator Center
Stanford California

Abstract

Experimental studies of top quarks produced in e^+e^- interactions at center of mass energies above pair threshold will yield important information about the couplings of the top to charged and neutral weak currents. Some important aspects of the experimental environment that can be expected at future e^+e^- linear colliders are presented in this talk, and techniques to isolate and analyse top quark production and decay in the continuum are reviewed. Physics topics that are discussed include measurement of the top production cross section and measurement of form factors in the production and semileptonic decay of the top. These measurements make essential use of the unique capability of an electron-positron collider to produce highly polarized top quarks, and yield searches for anamolous couplings of the top quark and possible new currents in top decay. Measurement of the top Yukawa coupling and searches for rare top decays are also discussed.

OPEN TOP at LINEAR ELECTRON-POSITRON COLLIDERS

D. Burke
SLAC

Madison
November 1992

e^+e^- ENERGY FRONTIER

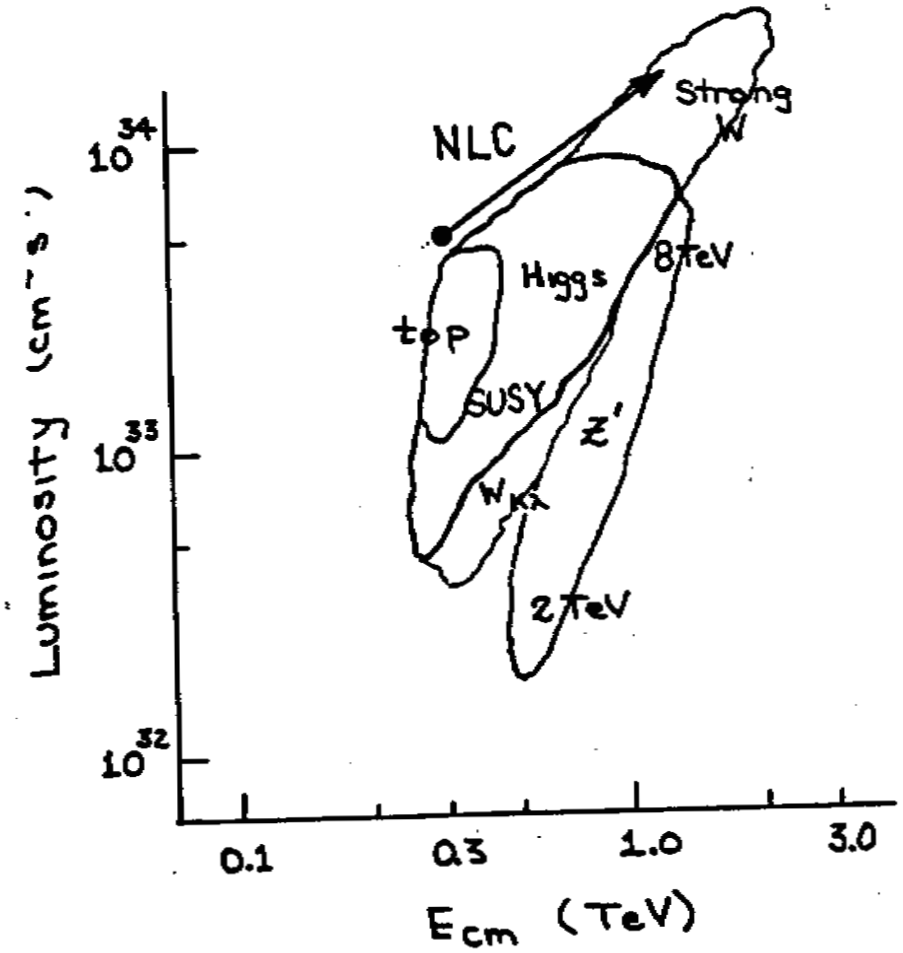

Schematic Layout of an NLC

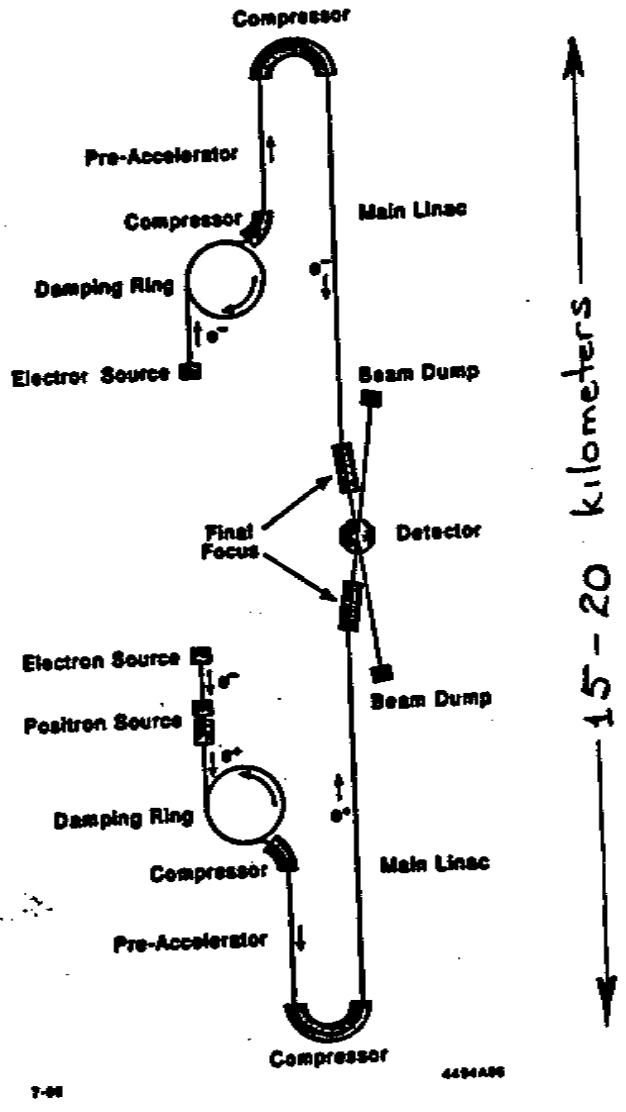

Accelerator Designs and Luminosities

	Design $\mathcal{L}$ ($cm^{-2} s^{-1}$) 500 GeV	1 TeV
SuperC (TESLA) :	5×10^{33}	1×10^{34}
S-Band (SLAC) :	4×10^{33}	0.3×10^{34}
X-Band (NLC/JLC) :	6×10^{33}	2×10^{34}

Will discuss physics capabilities at 10% and 100% of design luminosity.

Data point: SLC presently operates at ≈ 15% of its parametric design luminosity.

Cross Sections

(no radiation)

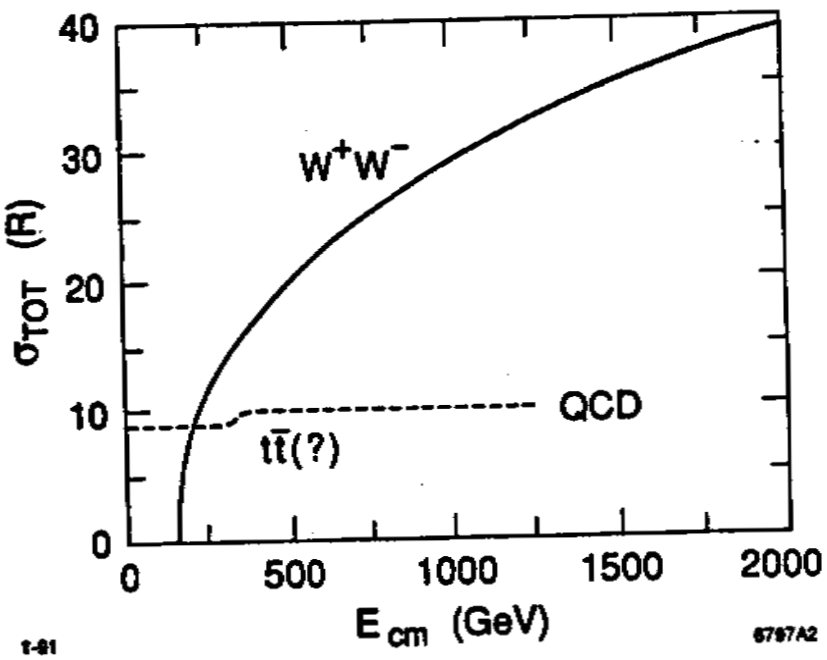

$10\ fb^{-1} \rightarrow 4000$ events / unit R

at $E_{cm} = 500$ GeV

$e^+e^- \rightarrow b\bar{b}g$

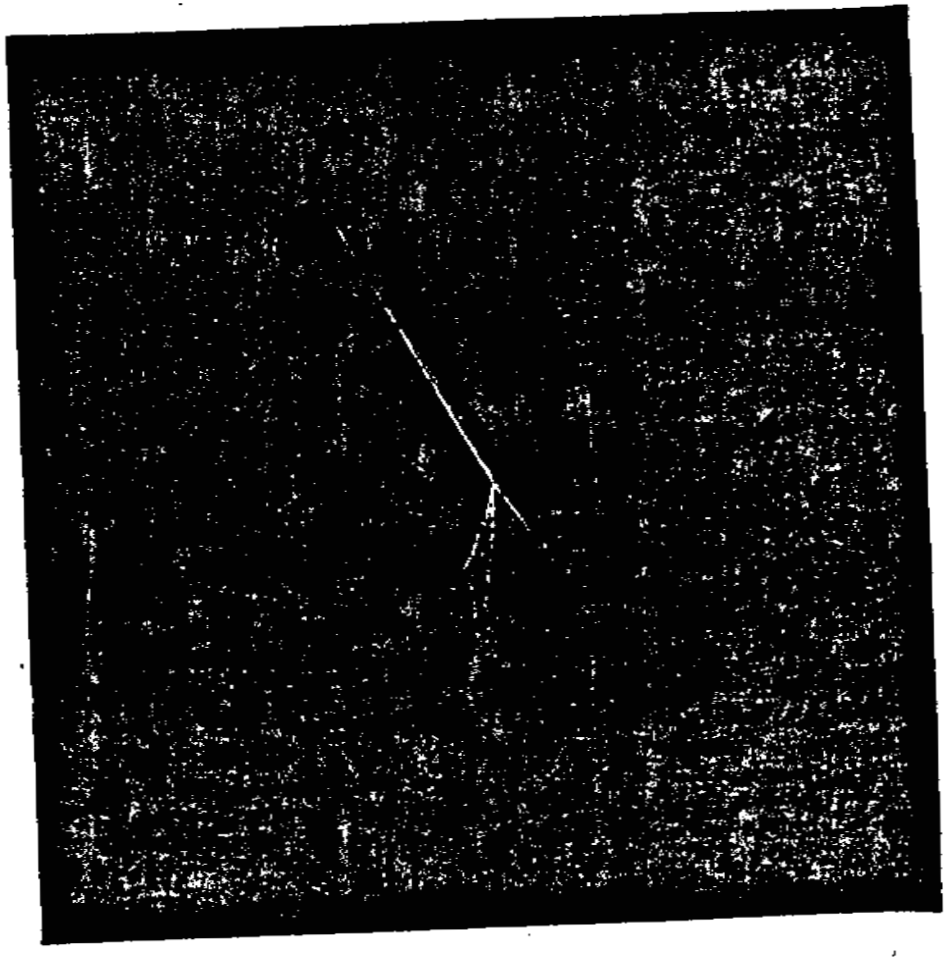

544-3

Detector Parameters

	Standard	Optimistic
Calorimetery		
σ(EM)	8% ⊕ 2%	1% ⊕ 1%
σ(HAD)	60% ⊕ 2%	30% ⊕ 2%
Δ (EM)	2°	1°
Δ (HAD)	4°	2°
Tracking		
$\delta(p_T)$	$10^{-3}\, p_\perp^2$	$2\times10^{-4}\, p_\perp^2$
vertex	$(20\mu m)^2 + \left(\frac{100\mu m}{p}\right)^2$	$(5\mu m)^2 + \left(\frac{50\mu m}{p}\right)^2$
Hermiticity		
coverage	.985	.995

"LEP/SLD"

Observed Hemisphere Mass Spectrum

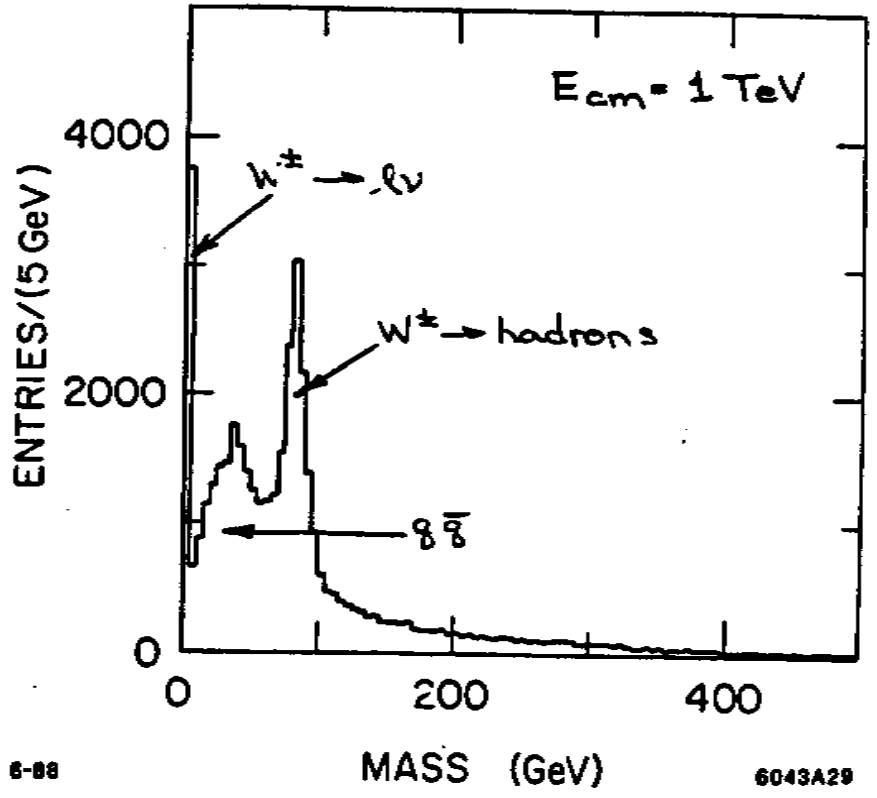

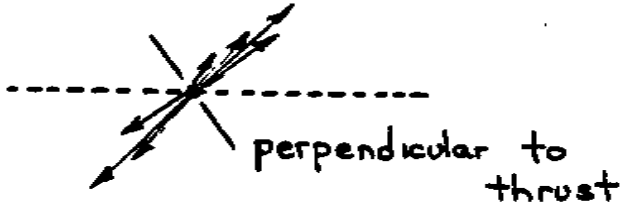

e^+e^- E_{cm} Spectra

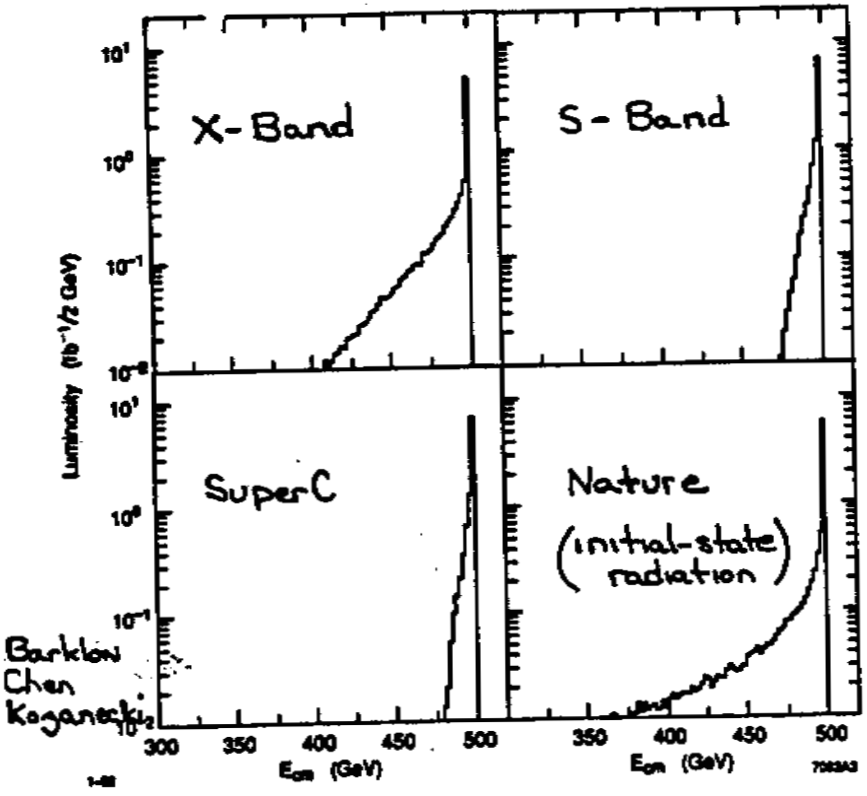

Palmer G

Beamstrahlung

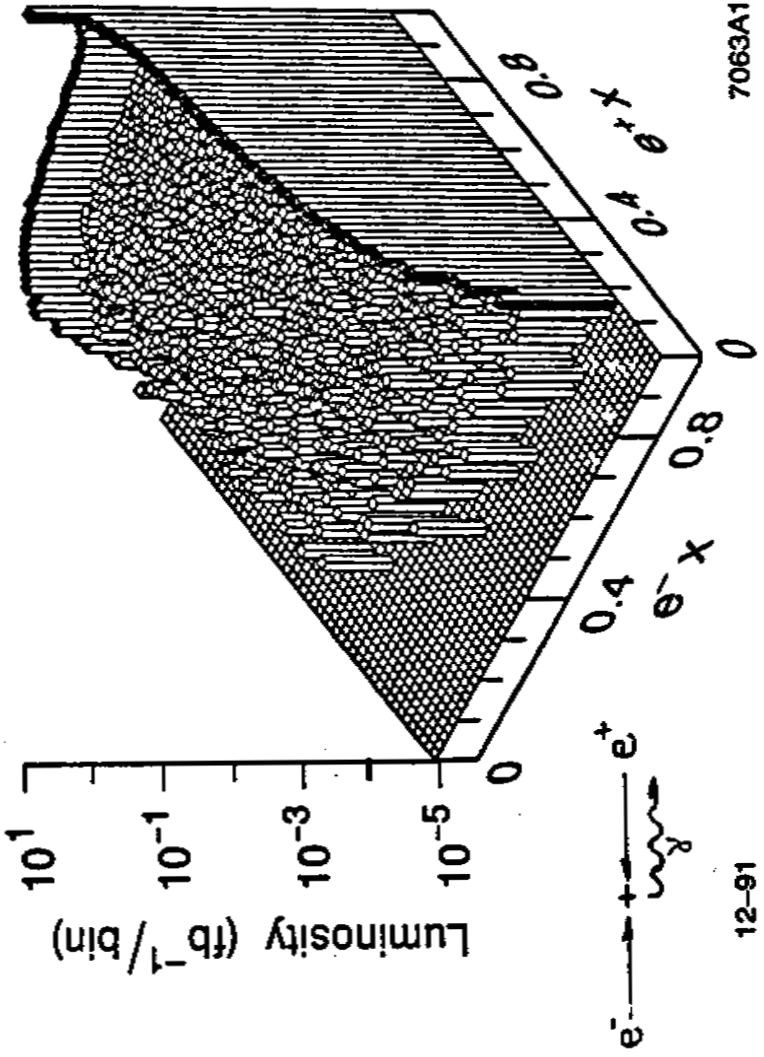

Top Quark

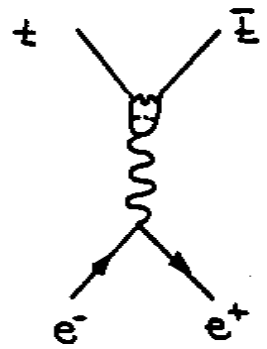

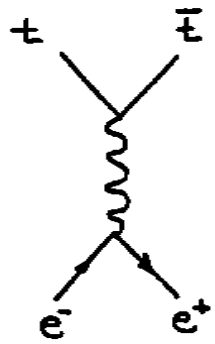

Toponium

m_t Γ_t

α_s

Continuum

m_t

non-S.M. decays

electric dipole moments

$(g-2)_{top}$

weak charged current

Yukawa coupling

Polarized initial state is an extremely powerful tool.

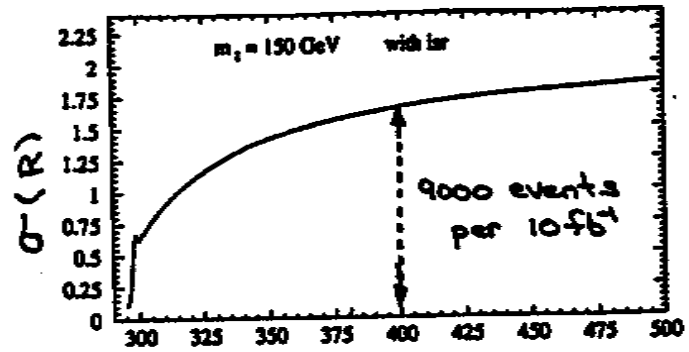

Samples of $10^4 - 10^5$ can be accumulated

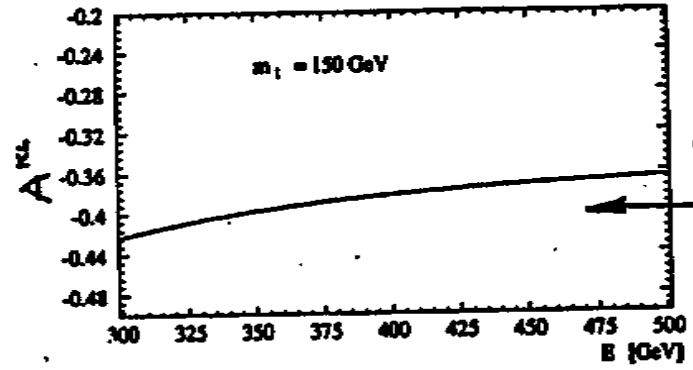

t_L polarization (e^- unpolarized) $\approx 70\%$

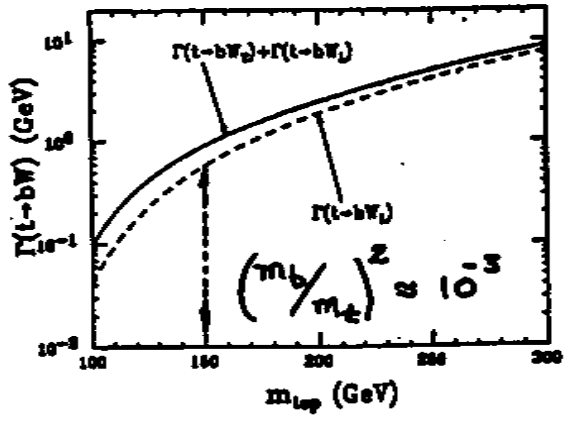

Decay can be precisely analysed

$$\frac{\Gamma(t \to bW_L)}{\Gamma_{TOT}} \gtrsim 0.6$$

TYPICAL 6-JET EVENT

FUJIX
KEK

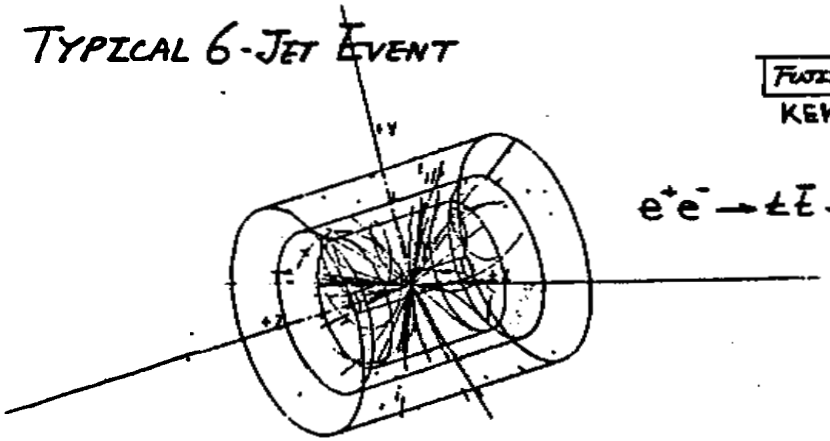

$e^+e^- \to t\bar{t} \to WbW$

DATE=910829 E_beam= 150 EVENT= 17

Signature

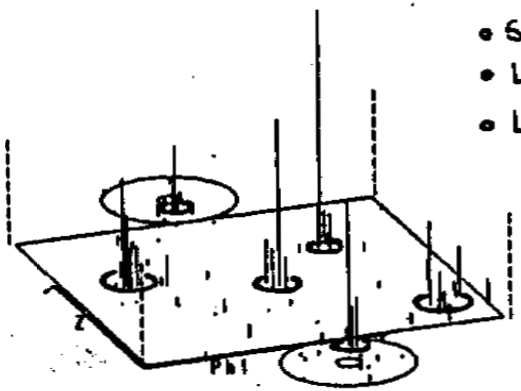

- Six (6) jets
- Low thrust
- Large hemisphere masses

DATE=910829 E_beam= 150 EVENT= 17

Top Quark Signatures

$t\bar{t} \to WbWb\ (\gamma)$

"Preselection Cuts": (Bagliesi, et al. EE500 Workshop)

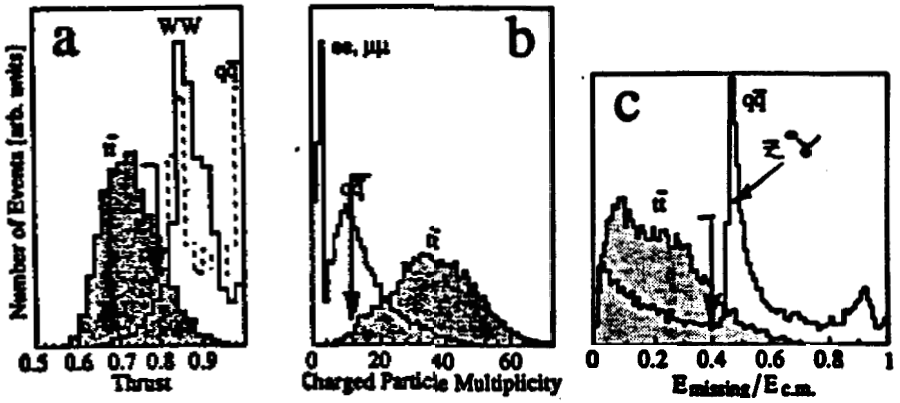

→ 80% efficiency for $t\bar{t}$

$S/B \approx 1$

$E_{cm} = 400$ GeV

$m_t \approx 150$ GeV

Final selection:

	ε	S/B
(i) $N_{jet} \geq 5$, $m_{\text{"top"}} \geq 120$ GeV	30%	7
(ii) Isolated lepton	12%	32

Measurement of Top Production Cross Section

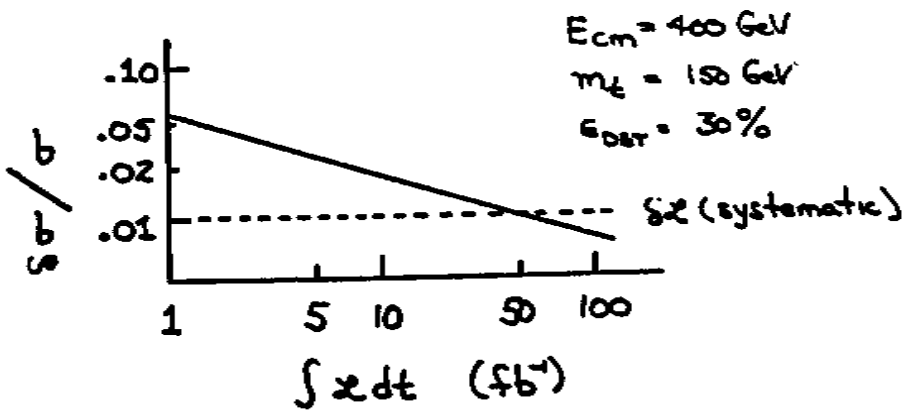

→ Measure of $g_{tt\gamma}$ (+ QCD + EW rad cor)

Luminosity Measurement

D. Miller
UC London

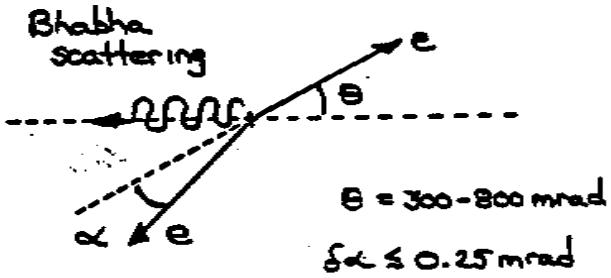

Acolinearity reflects $d\mathcal{L}/dE_{cm}$

Top Sem-leptonic Decay

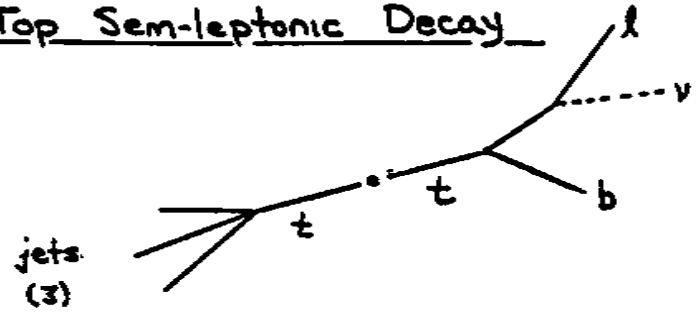

Measure: $\vec{p}_\ell$

$\vec{\beta}_b$, $\vec{\beta}_{jets} \equiv \vec{P}/E$ (calorimeter)

Constraints: E_{cm}, $\vec{P}_{tot}$

(7) $m_{\ell\nu} = m_W$ $\quad m_{\ell\nu b} = m_t$

$m_{jets} = m_t$

Unknowns: $\vec{p}_\nu$, $|p_b|$

(6) $|p_{jets}|$, p_ν^z

Fit:
- Help sort topology.
- Reconstruct $t \to \ell\nu b$ 4-vectors.

Hetrodga, Darklow, D.B.

Reconstructed (fit) Top Mass

(SLD Monte Carlo with radiation.)

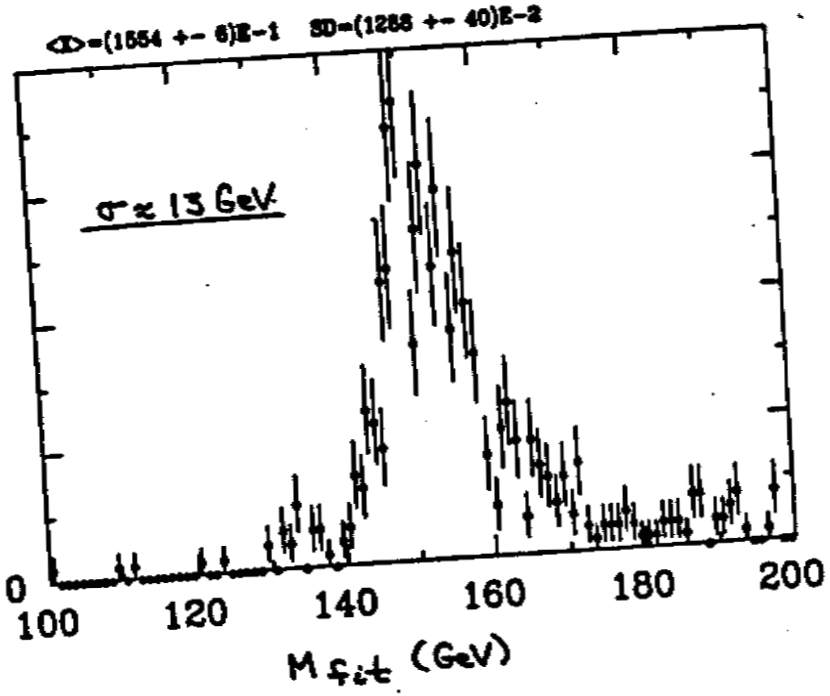

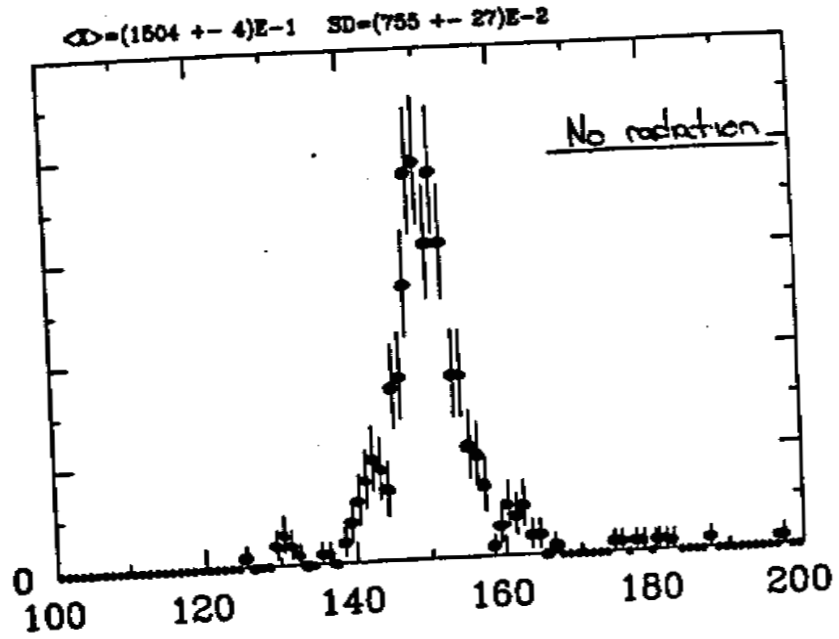

$10 fb^{-1} \rightarrow \delta m_t (\text{stat}) = 0.3 \text{ GeV}$

(Also useful for further event selection.)

Top Production and Decay

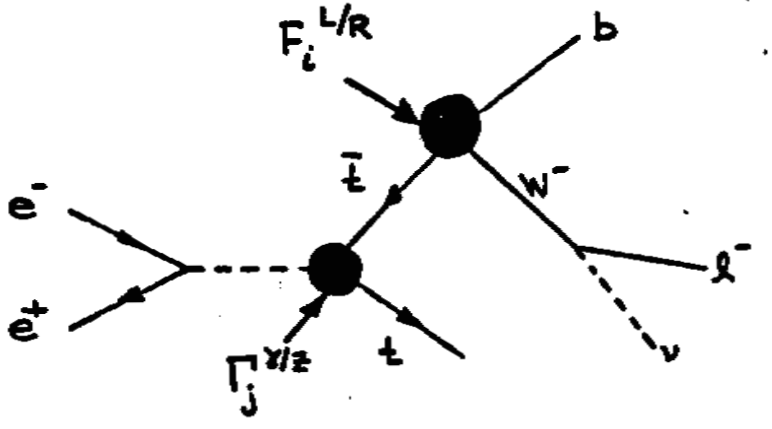

S.M.

$$V^{\mu}(\gamma,Z) = -i\,\gamma^{\mu}\left(g_V^{\gamma Z} + g_A^{\gamma Z}\,\gamma^5\right)$$

$$V^{\mu}_{cc} = -i\,g_L\,\gamma^{\mu}\,(1-\gamma^5)$$

Search for:

Non-S.M. charged currents

Quark structure

$\not{CP}$ (?)

Polarization

$e^-_L e^+ \to t\bar{t}$

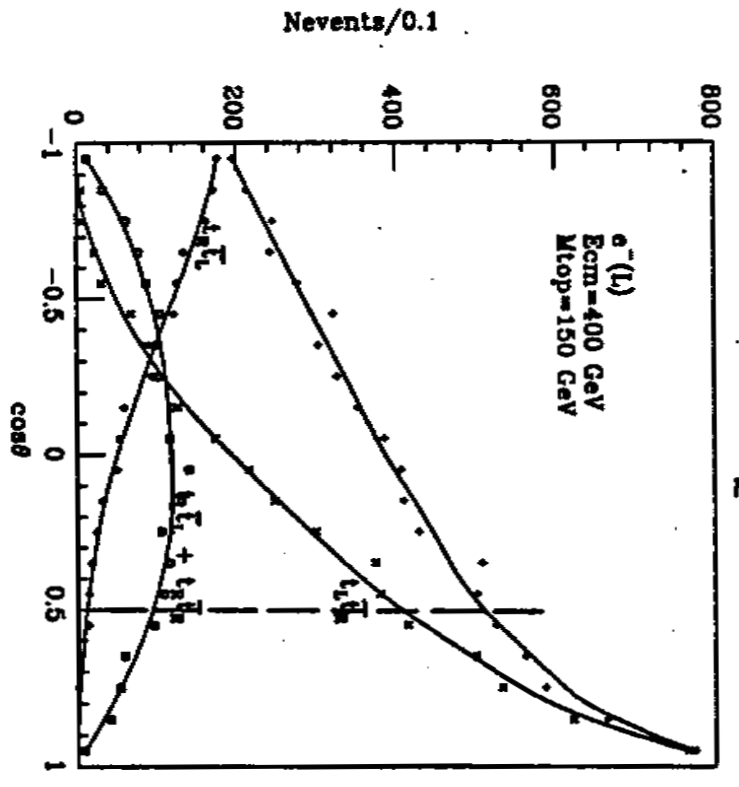

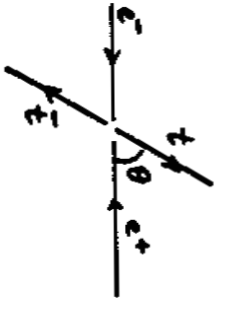

Schmidt and Peskin

Top Helicity Analysis

W Decay

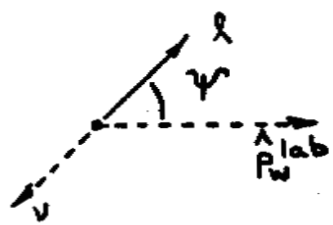

W_L	$(1-\cos\psi)^2$
W_0	$(\sin\psi)^2$
W_R	$(1+\cos\psi)^2$

Top Decay

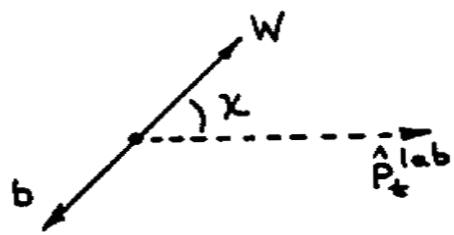

For left-handed t_L ...

$b_L W_R$	0
$b_L W_0$	$.32\ (1-\cos\chi)$
$b_L W_L$	$.18\ (1+\cos\chi)$
$b_R W_R$	$.18\ (m_b/m_t)^2\ (1-\cos\chi)$
$b_R W_0$	$.32\ (m_b/m_t)^2\ (1+\cos\chi)$
$b_R W_L$	0

$b_R \sim 10^{-3}$!!

$\approx 10^{-3}$

Top Decay – Search for New Currents

Gordon Decomposition of charged currents

$$\mathcal{M}^\mu = \frac{-ig}{\sqrt{2}}\left[\gamma^\mu\left(F_{1L}P_L + F_{1R}P_R\right) - \frac{-i\,\sigma^{\mu\nu}k_\nu}{m_W}\left(F_{2L}P_L + F_{2R}P_R\right)\right]$$

where k_ν is the W 4-vector.

S.M. $\quad F_{1L} = 1 \qquad F_{1R} = F_{2L} = F_{2R} = 0$

"Right-Handed Current" $\quad F_{1R} \neq 0$

D.B.

cos(Wl) vs cos(tW) cosθ>0.5 $t_L \bar{t}_R$

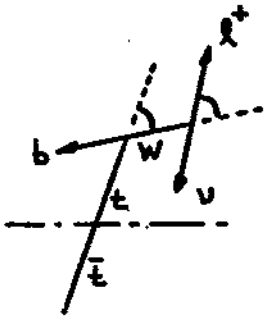

$m_t = 140$ GeV

$\sqrt{s} = 400$ GeV

$P_{e^-} = 80\%$

$L = 10\,fb^{-1}$

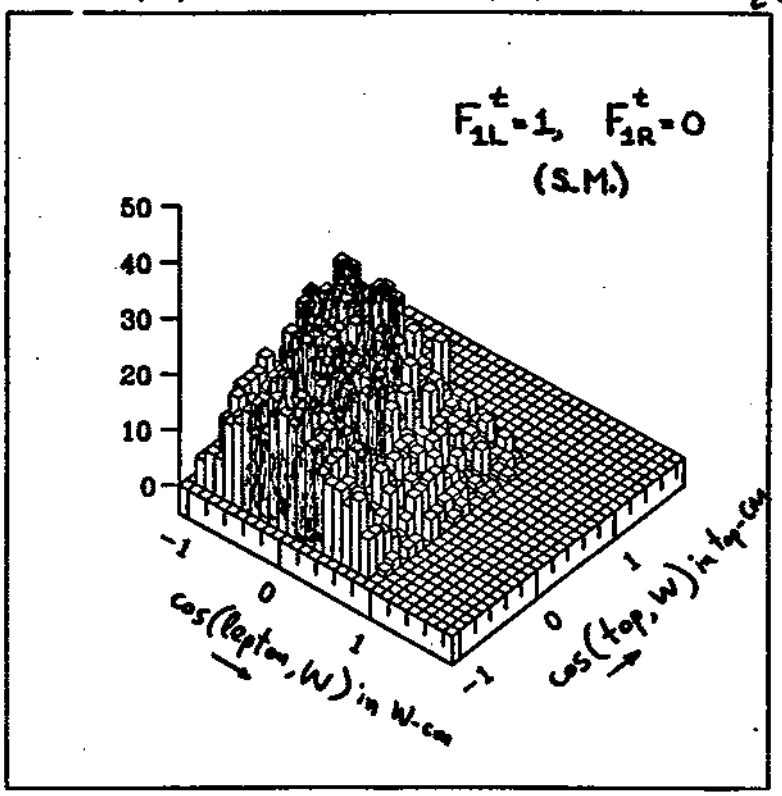

cos(Wl) vs cos(tW) cosθ>0.5 $t_L \bar{t}_R$

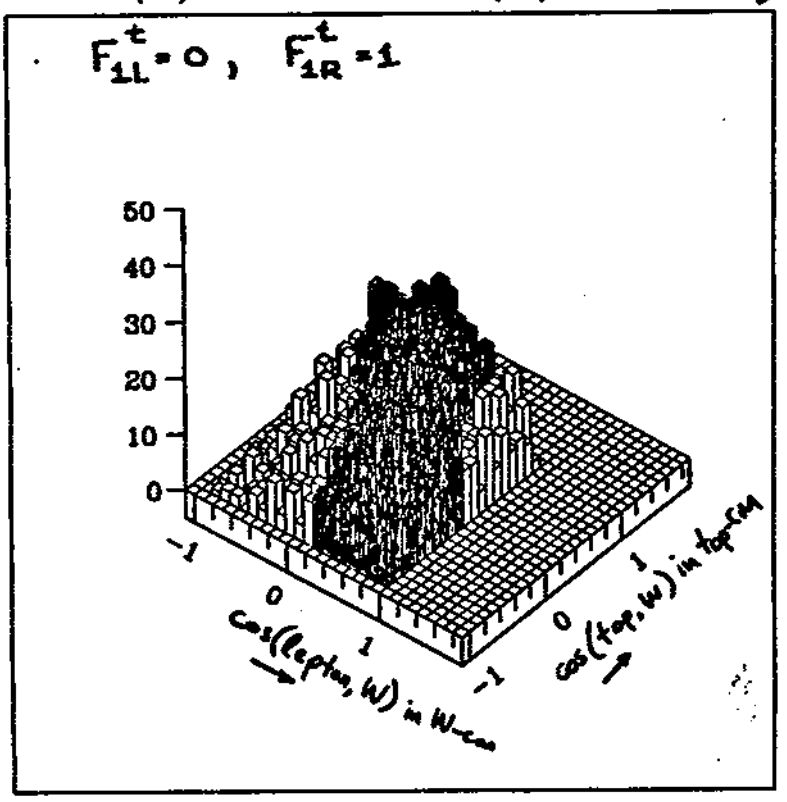

W_R in Top Decay

Crisp separation of signal and background →

Eventual ($50\ pb^{-1}$) sensitivety to

$$\left(\frac{m_t}{m_R}\right)^4 \approx \left(\frac{m_b}{m_t}\right)^2 \approx 10^{-3}$$

or $m_R \gtrsim$ TeV.

Top Dipole Moments

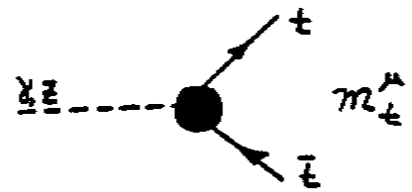

Magnetic and electric dipole moments are created by:

$$m_t^\mu \sim i\frac{\sigma^{\mu\nu}q_\nu}{2m}\left(\underset{\text{MDM}}{c_t^{\gamma,Z}} + \underset{\text{EDM}}{d_t^{\gamma,Z}}\gamma^5\right)$$

MDM occurs in S.M. at one loop.

EDM violates CP and does not occur even at two loops

Top Magnetic Moment

Schmidt
Peskin

$(g-2)_t$

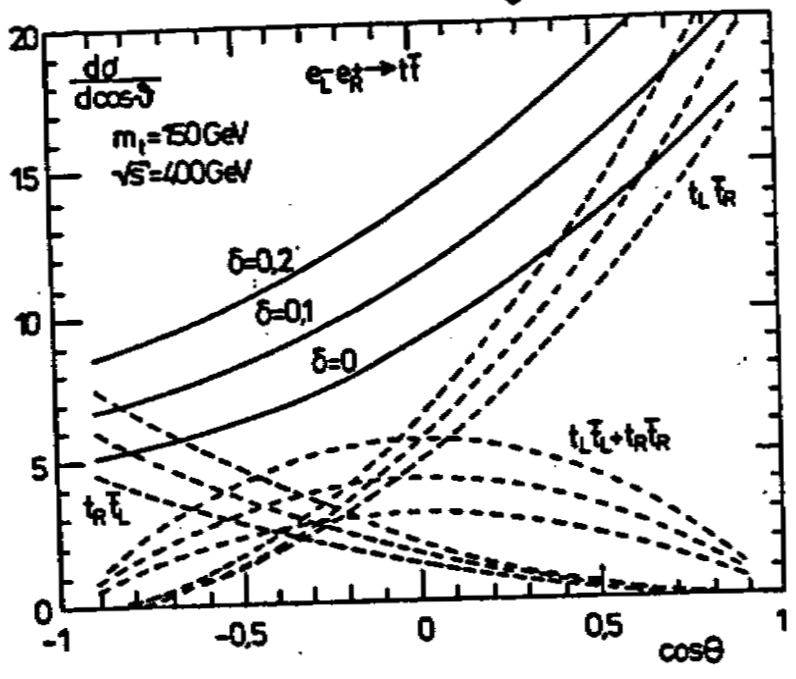

Weak dependence on helicity, but alters total cross section

→ determine $g-2$ to $\lesssim 10^{-2}$ with $10\,fb^{-1}$.

N.B. QCD loops generate $g-2 \sim \alpha_s/\pi$.

Top Electric Dipole Moments

$$\mathcal{M} \sim i\, d_t^{\gamma,Z} \frac{\sigma^{\mu\nu} q_\nu}{m_t} \gamma^5$$

complex form factor

$(\mathrm{Im}\, d_t^{\gamma,Z} \leftrightarrow \not{CP})$

- CP-odd corelations in decay products

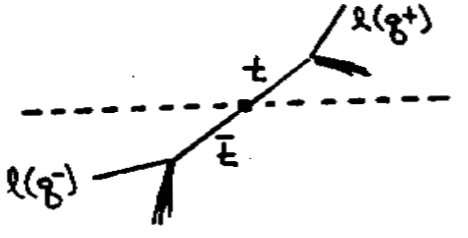

Bernreuther
Nachtman
Overmann
Schröder

e.g.

$$T_{ij} = (q^+ - q^-)_i \cdot \frac{(q^+ \times q^-)_j}{|q^+ \times q^-|_j}$$

→ semileptonic decays most useful

Top Quark Dipole Moments

$t\bar{t} \to \ell^+\nu b \; \ell^-\bar{\nu}\bar{b}$ (BR ≈ 10%)

- Complex moments d_t^γ and d_t^Z.

Atwood & Soni (1992)

Statistical errors:

$\delta(d_t^\gamma) \approx .5\text{-}1 \times 10^{-18}$ ecm

$\delta(d_t^Z) \approx 1\text{-}2 \times 10^{-18}$ ecm

with $50\,fb^{-1}$ at $E_{cm} = 500$ GeV.

- Example: Two-doublet Higgs sector

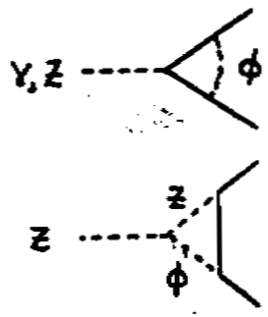

$$d_t^{\gamma/Z} \sim \frac{e G_F m_t^3}{4\pi^2 m_\phi^2} \approx 10^{-18} \text{ ecm}$$

for $m_t = 130$ GeV, $m_\phi = 100$ GeV

Top Yukawa Coupling

Tsuchi, Fujii, Miyamoto (KEK)

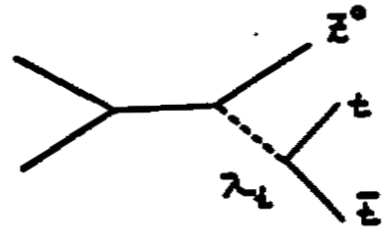

$m_{H^0} > 2 m_t$

Signature: $WbWb\,f\bar{f}$ 8 jets

(Fit m_W, m_t, m_{H^0}, m_{Z^0})

Backgrounds: Negligible, except S.M. non-resonant $Z^0 t\bar{t}$.

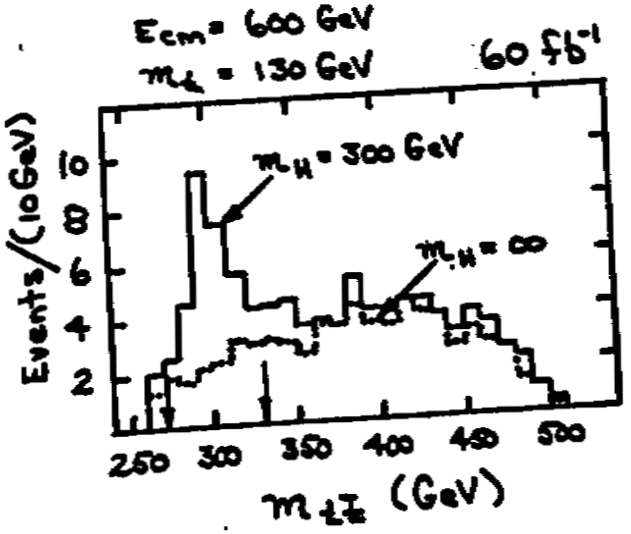

Signal of 25 events over 10 non-re

$\to \frac{\sigma(\lambda_t)}{\lambda_t} \approx 0.25$

Top Yukawa Coupling

Djouadi
Kalinowski
Zerwas

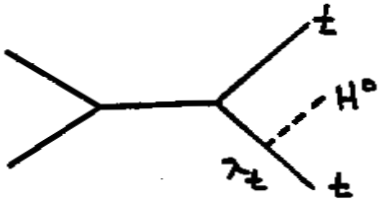

$m_{H^0} < m_t$

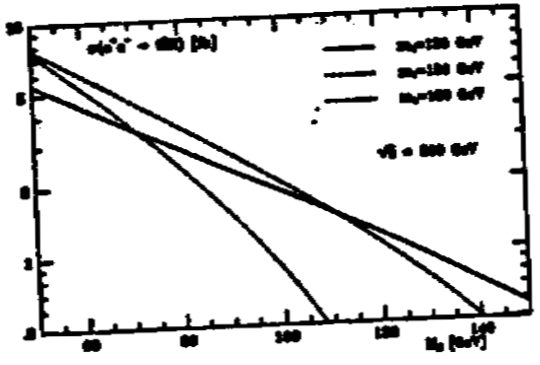

Signature WbWb bt
(No MC study yet.)

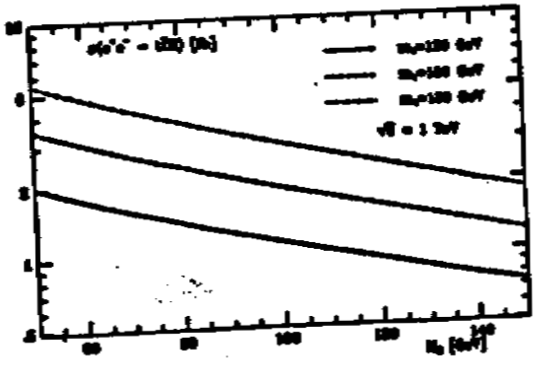

$E_{cm} = 1$ TeV
50 fb^{-1}

Detect 100-200 events
→ 10% measurement

$t \to bH^+$

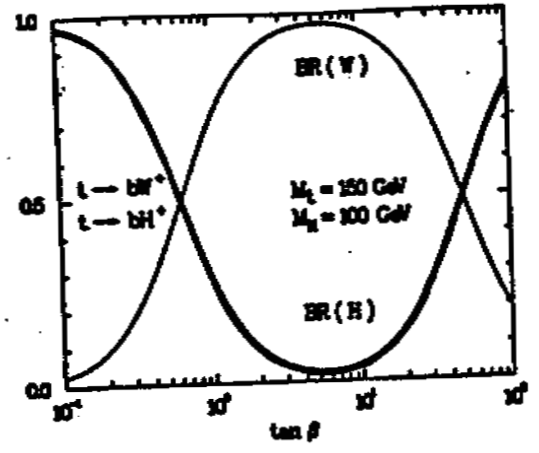

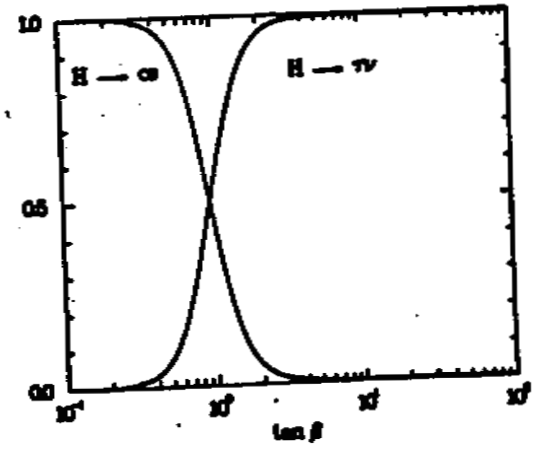

$t \to bH^+$ fraction

- $t \to bW^+$ is the only significant background
- $1 \le \tan\beta \le 50$ prefered in SUSY GUTs

H^+ decays

- $H^+ \to \tau^+\bar{\nu} \to \ell^+\nu\bar{\nu}$
  Signature: "ν" mass
- $H^+ \to c\bar{s}$
  Signature: "jj" mass

$t \to bH^+$

Dagnesi, etal.
EE500 Working Group

$\tan\beta \gtrsim 1$

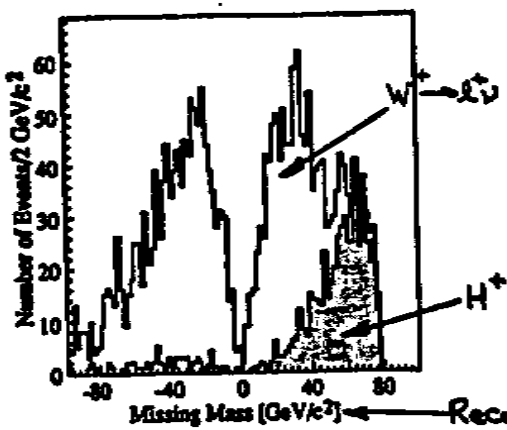

Reconstructed "ν" mass

Isolate τ decays

Leptonic decay

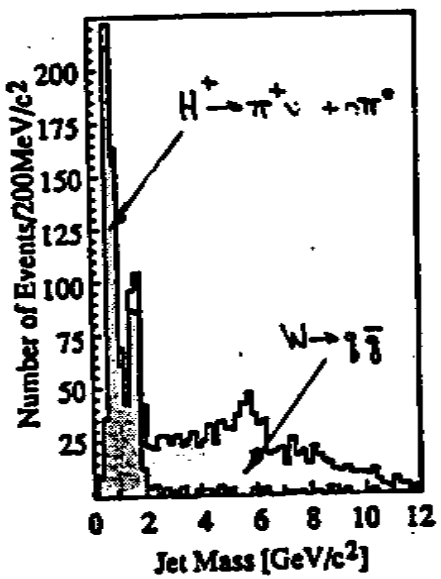

Hadronic decays

Combined detection efficiency is ≈ 30% with negligible backgr.

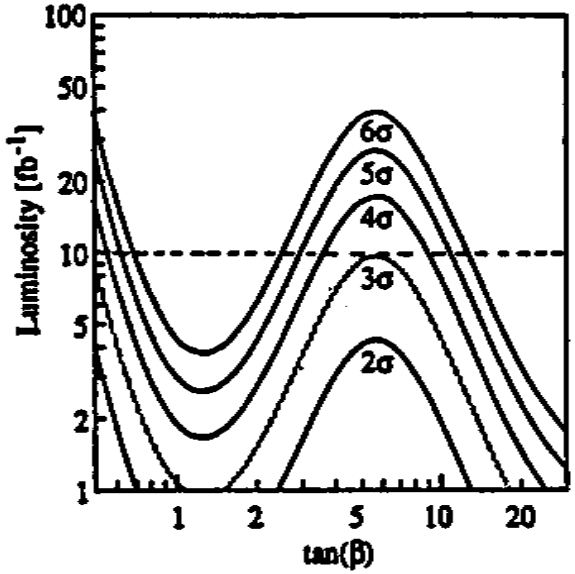

Search for $t \to Hb$
$(H \to \tau\nu)$

$10\,fb^{-1}$ ok for most values of $\tan\beta$.

Measurement of $BR(t \to Hb)$

$\tan\beta$	Events ($10\,fb^{-1}$)	Stat. error $BR(t \to Hb)$
0.1*	100	10%
1.0	70	12%
10.0	5	—
100.0	120	9%

(*) $H \to c\bar{s}$ See next slide.

$t \to bH^+$ $\tan\beta < 1$

$H^+ \to c\bar{s}$ dominates

Signature: Invariant mass of jet pairs

Background: $W \to q\bar{q}$

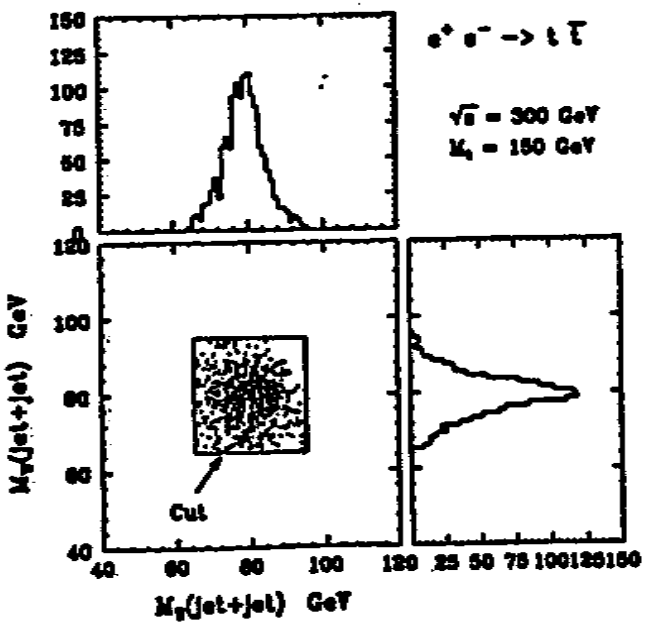

$t \to Wb$

Reconstructed W-mass

$\sigma \approx 5$–7 GeV

Unless $m_{H^+} \approx m_{W^+}$ can expect BR($t \to bH$) to measured with approximately 10% accuracy. [$10 fb^{-1}$]

Electron-positron collisions at center-of-mass energies above $t\bar{t}$ threshold (400 GeV – 1 TeV) will provide unique and important probes of the top quark and its interactions.

These well-controlled studies will yield information that is complimentary to expected results from hadron colliders.

Top decays to charged Higgs bosons

R J N Phillips
Rutherford Appleton Laboratory,
Chilton, Didcot, Oxon, OX11 OQX, England.

Abstract

The present understanding of charged Higgs bosons and their possible appearance in $t \to bH^+$ decay is reviewed. Two-Higgs-doublet models I and II are described and motivated. Various experimental and theoretical constraints are described. The bounds from the one-loop MSSM mass formula (including LEP limits on m_A) and from $b \to s\gamma$ decay are especially stringent and almost forbid $t \to bH^+$ kinematics in Model II. Future possible searches for $H^\pm$ at LEP II, SSC/LHC, Tevatron and NLC are briefly discussed.

1

Top decays to charged Higgs bosons

R. J. N. Phillips

Rutherford Appleton Laboratory – England.

Agenda : 2-Higgs doublet scenario

Models I and II

Constraints. Remaining parameter space?

Future $t \to bH^+$ search possibilities

LEP II, SSC/LHC, Tevatron, NLC

Thanks to Vernon Barger, Mike Berger, JoAnne Hewett, Alan Stange for help in preparing this review

2

Electroweak symmetry breaking mechanism ?

Standard Model : one complex scalar doublet gets vev

$$v^2 = \frac{1}{\sqrt{2}\, G_F}$$

$$\Rightarrow (W_L^+, W_L^-, Z_L^0) + H^0_{SM}$$

Extend ?? Two complex scalar doublets get vevs

$$v_1^2 + v_2^2 = v^2$$

$$\Rightarrow (W_L^+, W_L^-, Z_L^0) + \underbrace{h^0, H^0}_{\text{CP even}}, \underset{\text{odd}}{A^0}, H^+, H^-$$

Many parameters $\begin{cases} \text{masses} \\ \alpha = h, H \text{ mixing angle} \\ \tan\beta = v_2/v_1 \end{cases}$

Yukawa couplings $\leftrightarrow$ fermion masses

Avoid FCNC : same-type fermions get masses from same v_i

4 classes $\begin{cases} \text{I} & \text{all fermion masses from } v_1 \\ \text{II} & \begin{cases} \text{d-type quarks, lepton masses from } v_1 \\ \text{u-type quarks} \quad \text{from } v_2 \end{cases} \end{cases}$

MOST INTERESTING

III, IV } (permutations of the above)

3

Model I Interesting because of L3 events at LEP

excess of $Z \to \ell^+\ell^- \gamma\gamma$ events with $m(\gamma\gamma) \simeq 60$ GeV

Could interpret these as $Z \to Z^* h$, $h \to \gamma\gamma$ with $m(h) \simeq 60$.

Require $h \not\to q\bar{q}$ (no signal here) $\Rightarrow \frac{\cos\alpha}{\sin\beta} \ll 1$

$Z \to Z^* h$ unsuppressed $\Rightarrow \sin(\beta-\alpha) \sim 1$

$\tan\beta \gtrsim \frac{m_t}{500}$ to keep Yukawas perturbative

Satisfied with $\alpha \simeq -\frac{\pi}{2}$, $\tan\beta \sim 0.2 - 1$

Constraints on $H^\pm$?

$B(b \to s\gamma) < 0.8\ 10^{-3}$

$m_{H^\pm} < m_t$ allowed if $\tan\beta \gtrsim 0.2$ (depending on exact masses)

(Berger, Deshpande, Hewett, Rizzo MAD/PH/728 1992)

Relevance to $t \to bH$ decay

All $t \to bW^+, bH^+$, $H^+ \to c\bar{s}, \nu\bar{\tau}$ phenomenology is same as Model I with $\tan\beta = 1$

[see below]

4

$B(b \to s\gamma) < 0.84\ 10^{-3}$ constraint (CLEO 1992)

Excludes small $\tan\beta$

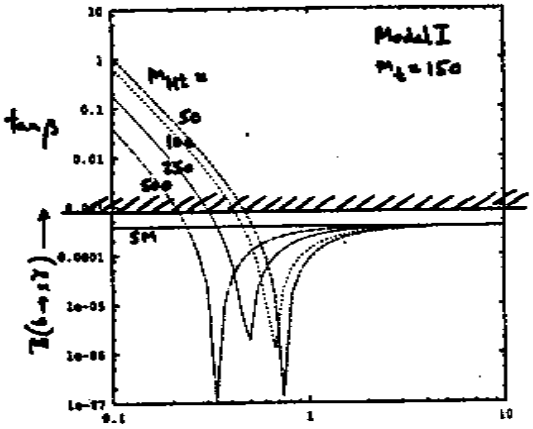

Excludes { small $\tan\beta$, some m_H

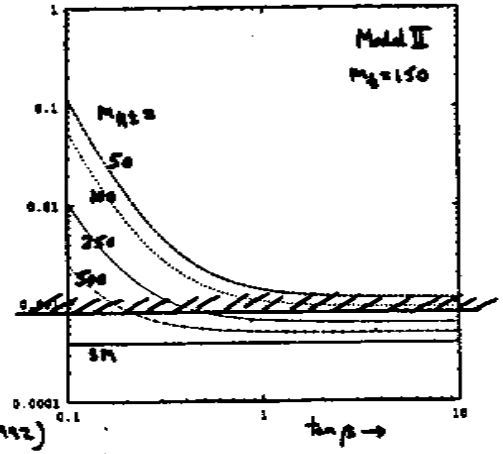

(Berger, Berger, Phillips 1992)

Model II Interesting because SUSY selects this scheme

At tree level, SUSY reduces parameters to 2 : (m_H, $\tan\beta$)

At one-loop : MSSM introduces m_t, $m_{\tilde{t}}$, ... (most important)

e.g. $\Delta m_h^2 \sim G_F m_t^4 \ln(m_{\tilde{t}}^2/m_t)$

$H^\pm$ coupling to fermions

$t \to bH^+$

$$\mathcal{L} = \left(\frac{G_F}{\sqrt{2}}\right)^{1/2} H^+ \Big\{ m_t \cot\beta\, V_{tb}\, \bar{t}(1-\gamma_5)b + m_b \tan\beta\, V_{tb}\, \bar{t}(1+\gamma_5)b$$

$$+ m_c \cot\beta\, V_{cs}\, \bar{c}(1-\gamma_5)s$$

$H^+ \to c\bar{s},\ \nu\bar{\tau}$

$$+ m_\tau \tan\beta\, \bar{\nu}_\tau(1+\gamma_5)\tau$$

$$+ [\text{terms suppressed by KM matrix or masses}] \Big\} + h.$$

All specified by masses and $\tan\beta$

Branching fractions $m_t = 150$, $m_{H^+} = 100$

Model II

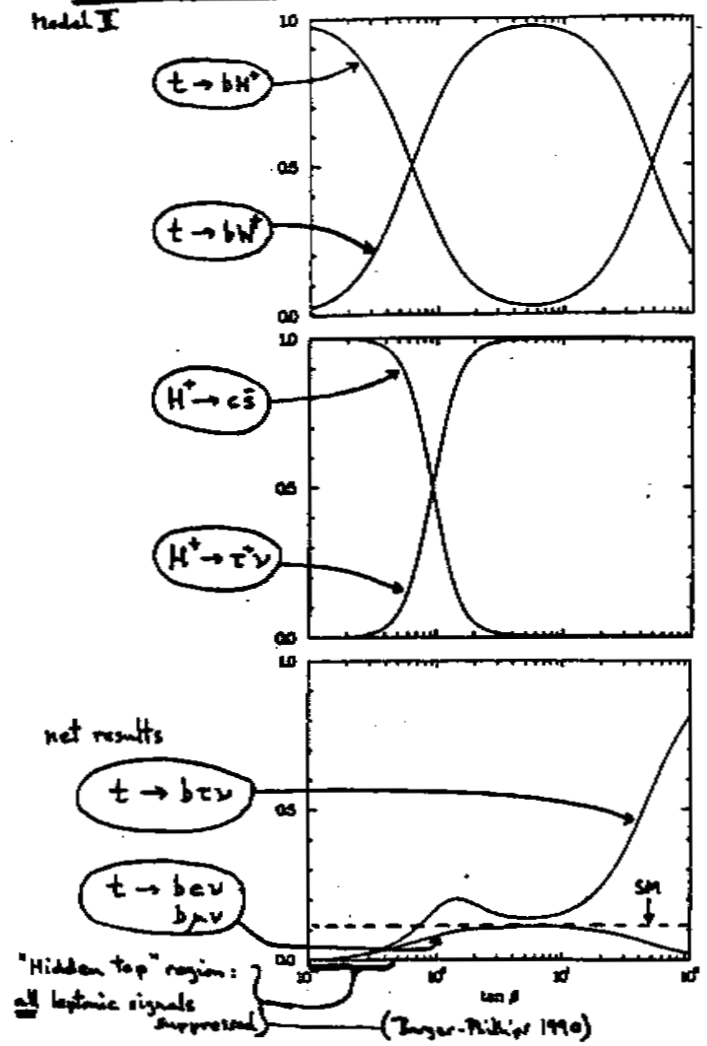

"Hidden top" region: all leptonic signals suppressed

(Barger-Phillips 1990)

7

Constraints on parameters : $m_{H^\pm}$, $\tan\beta$, m_t ....

CDF top search $\Rightarrow$ $m_t > 91$ GeV assuming $t \not\to bH^+$

[If $t \to bH^+$, absence of $\not{p}_T$ signal constrains $\tan\beta \lesssim 1$
Berger-Hewett-Rizzo 1990]

SM electroweak rad. corrections $\Rightarrow$ $m_t \simeq 145 \pm 30$ GeV (Blokhartsev talk : this meeting)

LEP $e^+e^- \not\to H^+H^-$ $\Rightarrow$ $m_{H^\pm} > 36$-43 GeV , depending on $\tan\beta$

LEP $e^+e^- \not\to Zh$, Ah $\Rightarrow$ excludes regions of $(m_A, \tan\beta)$ for MSSM

$\Rightarrow$ $m_{H^\pm} \gtrsim 90$ GeV

[at tree level, MSSM gives $m_{H^\pm} = \sqrt{m_W^2 + m_A^2}$
> 90 if $m_A > 40$]

MSSM electroweak rad. corrections $\Rightarrow$ preferred region in $(m_A, \tan\beta)$ (Ellis et al 1991)

$\Downarrow$

combine with $m_t \sim 150$ and LEP

$\Downarrow$

$m_{H^\pm} \sim 90$ GeV preferred FIGS see p. 8 a,b,c

but bigger values not excluded

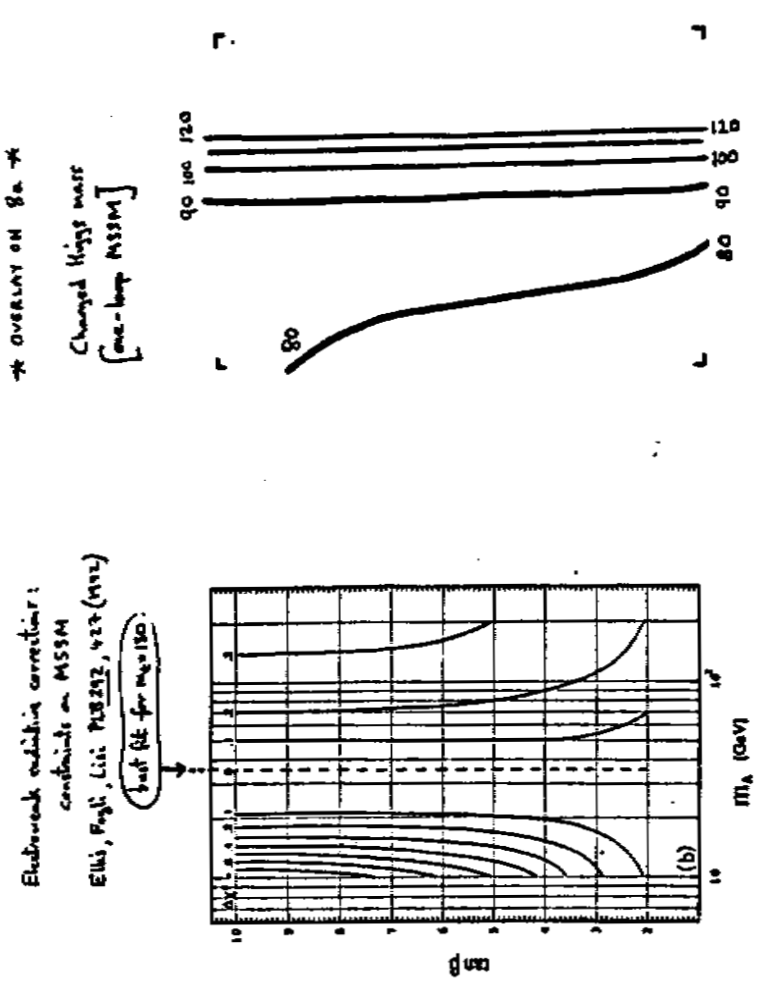

8d

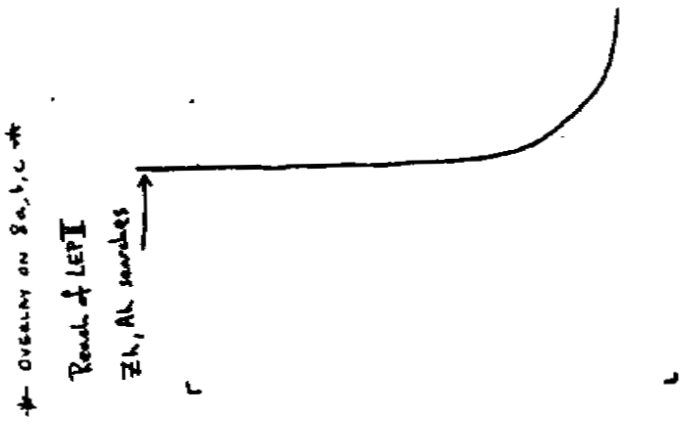

8c

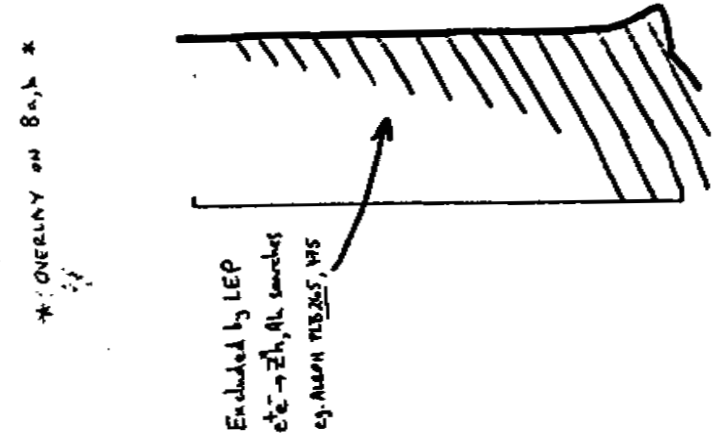

9a

<u>More constraints</u> on $m_{H^\pm}$, $\tan\beta$

Perturbative bounds : $g^2_{t\bar{b}H} \lesssim g^2_{QCD}(m_W^2)$

$\Rightarrow \quad m_t/600 \;(0.2) \lesssim \tan\beta \lesssim 600/m_b \;(120)$

Proton decay $\Rightarrow \quad \tan\beta \lesssim 85$ (Hisano, Murayama, Yanagida 1992)

Mass hierarchy $m_t \gg m_b$, $m_c \gg m_s$ suggests $v_2 \gg v_1$

$\Rightarrow \quad 1 \ll \tan\beta$

GUT-SUGRA models $\Rightarrow \quad 1 \lesssim \tan\beta \lesssim m_t/m_b \;(30)$

SUSY-GUT unification $\Rightarrow \quad 2 \lesssim \tan\beta$ Roberts, Ross 1991

$\Rightarrow$ either $\sin\beta \sim 0.78\,(m_t/150)$ } 2 branches
or $\tan\beta \gtrsim m_t/m_b$ } Barger, Berger, Ohmann 1992

FIG

B-$\bar{B}$, D-$\bar{D}$, K-$\bar{K}$ mixing Barger, Hewett, Phillips 1990
$\Rightarrow \quad 0.2-0.3 \lesssim \tan\beta$ Barnes et al 1990
(depending on $m_{H^\pm}$)

$B(b \to s\gamma) < 0.8\ 10^{-3}$

$\Rightarrow$ excludes regions of $(m_{H^\pm}, \tan\beta)$ ← see FIGS

COMBINED EFFECT small regions with $m_{H^\pm} < m_t - m_b$ remain
$t \to bH$ not excluded yet

9b

SUSY-GUT unification constraint (Berger-Berger-Ohmann) MAD/TH/74

⇒ 2 alternative $\tan\beta$ solutions for each m_t

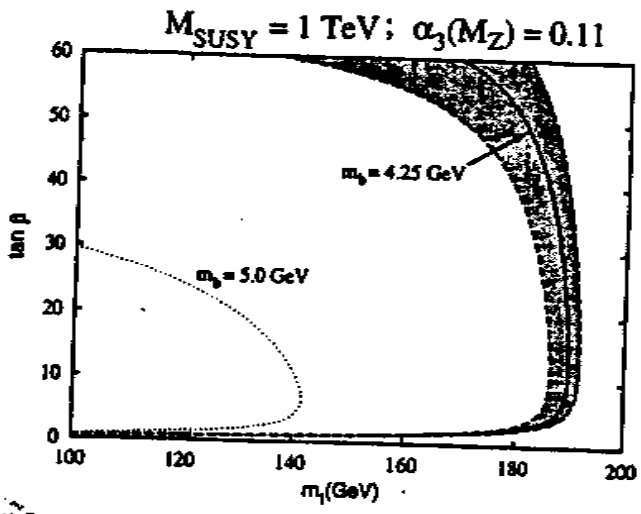

10a

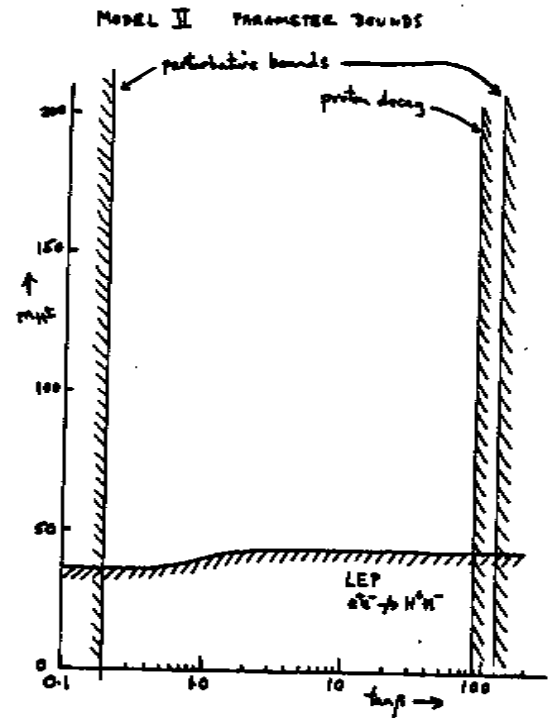

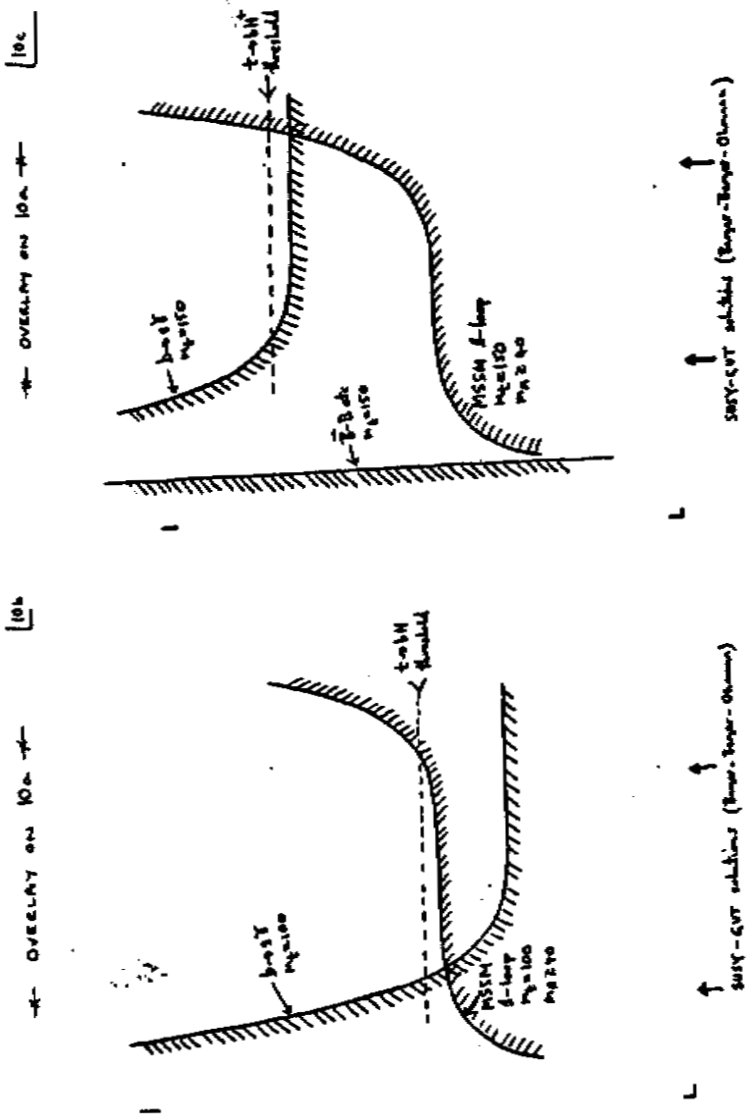

FUTURE EXPERIMENTS

11a

MSSM parameter regions accessible to $h, H, A, H^{\pm}$ searches at LEP I, LEP II, SSC/LHC

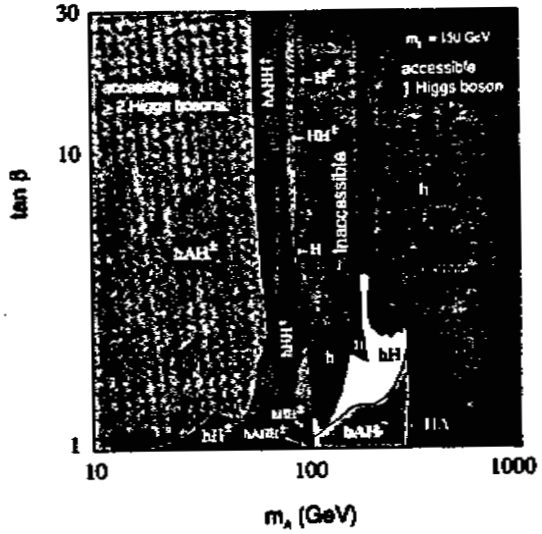

Berger - Phillips - Stange 1992
MAD/PH/696

Future searches for $H^\pm$ and $t \to bH^+$

Comment: if discover neutral scalar $\Rightarrow$ possible confusion with H^0_{SM}

" " charged " $\Rightarrow$ immediately beyond SM.

LEP II $e^+e^- \to H^+H^- \to (c\bar{s}, \nu\bar{\tau}) + (\bar{c}s, \bar{\nu}\tau)$

$\searrow W^+W^-$, ZZ } backgrounds

But $B(H^+H^- \to \tau\bar{\tau}\nu\bar{\nu})$ could be $\simeq 1$ (for $\tan\beta > 1$)

$B(W^+W^- \to \text{"}) = 0.012$

$B(ZZ \to \text{"}) = 0.013$

) relatively suppressed

Also $\tau\tau$ angular correlations differ from signal.

e.g. $\sqrt{s} = 190$, $\mathcal{L} = 500\ pb^{-1}$

$\sigma(e^+e^- \to W^+W^-) = 20\ pb \Rightarrow 120\ \tau\bar{\tau}\nu\bar{\nu}$ events

$\sigma(e^+e^- \to H^+H^-) = 0.36\ pb \Rightarrow 180$ " " $m_H = 80$

$0.074\ pb \Rightarrow 37$ " " $m_H = 90$

could detect $H^\pm$ up to $m_{H^\pm} \simeq 90$ GeV

(at least for $\tan\beta > 1$)

But this mass range is already excluded by MSSM constraints and $b \to s\gamma$. (see p.10b,c)

$\therefore$ LEP II will not discover $H^\pm$ of MSSM.

SSC / LHC copious $pp \to t\bar{t}X$ production

Idea: tag t ($\bar{t}$) by $t \to bW \to b\ell\nu$ ($\ell = e, \mu$)

study $\bar{t} \to \bar{b}W \to \bar{b}\ell\nu$

$\searrow \bar{b}H \to \bar{b}\tau\nu$ $\Leftarrow$ excess τ's break lepton universality

or $\bar{b}H \to bcs$ $\Leftarrow$ cs dijet mass peak

Detailed simulations by GEM collaboration – Letter of Intent

and by SDC " – Tech. Design Report SDC-92-201; Barnett et al SDC-92-213

① $\ell\tau$ signal

measure $t\bar{t} \to b\bar{b}WW \to ee, e\mu, \mu\mu$

predict " " $\to e\tau, \mu\tau$ background B

measure excess from $bbWH \to e\tau, \mu\tau$ signal S

statistical significance of signal $= \dfrac{S}{\sqrt{S+B}} = N_{SD}$

Numbers from SDC simulations : $\mathcal{L} = 10\,fb^{-1}$ = one year running

$\tau \to \pi\nu$ mode detected

$m_t = 150$
$m_{H^+} = 135$
$\tan\beta = 5.5$

An example of the number of events found with and without b tagging in $WWb\bar{b}$ and $WHb\bar{b}$ events where we have chosen $m_t = 150$ GeV and $m_{H^+} = 135$ GeV and $\tan\beta \approx 6$. We have only calculated the background from the $WWb\tau$ events in finding N_{SD}.

		with b tagging	no b tagging
N_{tr}^{WH}	($p_T(\pi) > 50$ GeV)	409	2061
N_{tr}^{WW}	($p_T(\pi) > 50$ GeV)	3949	14852
N_{tr}^{WH}	($p_T(\pi) > 100$ GeV)	135	456 = S
N_{tr}^{WW}	($p_T(\pi) > 100$ GeV)	668	2700 = B
N_{SD}	($p_T(\pi) > 50$ GeV)	6.2	15.8
N_{SD}	($p_T(\pi) > 100$ GeV)	4.76	11.3

Significance of $t\tau$ signals (from SDC) – $\tan\beta = 5.5$

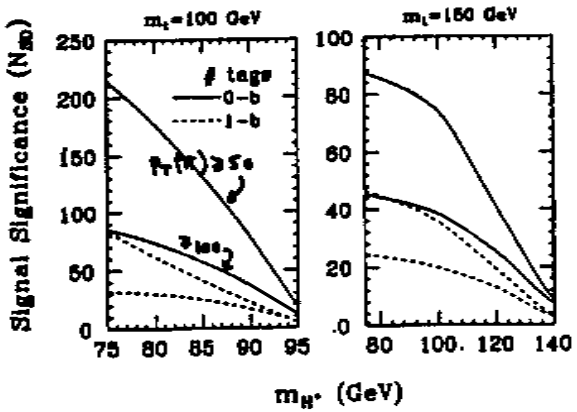

Translate SDC results ($\tan\beta = 5.5$) into ($\tan\beta$, m_{H^+}) plane.

← Can overlay this on $\beta \cdot 10$ c →

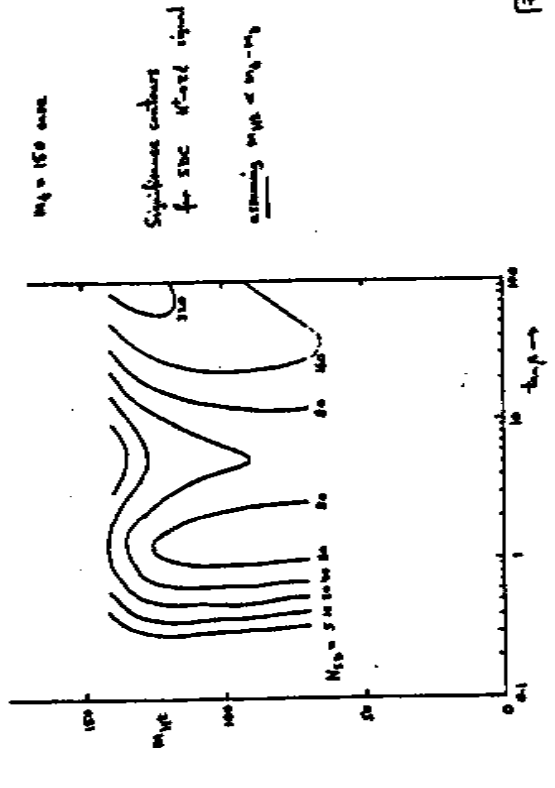

15

$H^+ \to \tau\nu$ signal does not measure $m_{H^\pm}$

but $\left.\begin{array}{l} B(t\to e\nu) \\ B(t\to\tau\nu) \end{array}\right\}$ are separately measurable

(if single-lepton $t\bar{t}$ signal is detected)

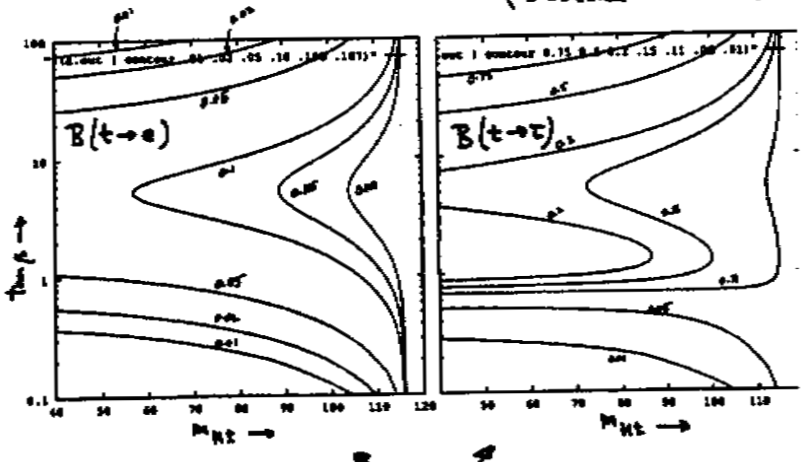

In principle they provide 2 independent data,

but their contours are not orthogonal

so they do not localize $m_{H^\pm}$, $\tan\beta$ in practice.

[Examples shown for $m_t = 120$]

16

Other observables that reflect $m_{H^\pm}$?

$$t\bar{t} \to bH^+ + \bar{b}W^- \to b\tau\nu + \bar{b}\ell\nu$$

$$m_H^2 = (p_t - p_b)^2 = m_t^2 + m_b^2 - 2p_t\cdot p_b$$

SDC suggests ways of (a) identifying b

(b) estimating p_t from final state kinematics

$\Rightarrow$ 2 alternative "masses", sensitive to $m_{H^\pm}$

e.g. compare $m_{H^\pm} = 75, 105, 125$ GeV (all $m_t = 150$)

"mass" distributions could determine $m_{H^\pm}$

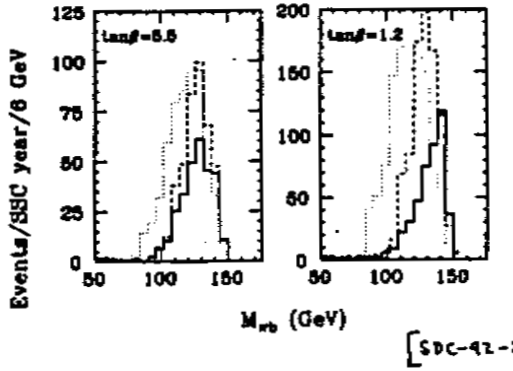

[SDC-92-213]

17

② $H^\pm \to cs$ signal $\quad t\bar{t} \to b\ell\nu$

$\hookrightarrow bW \to bq\bar{q}$

$b\bar{W} \to b\bar{c}\bar{s}$

potentially big W+multijet background

Strategy: select events with large $p_T(t)$ $p_T(\bar{t})$ back-to-back

trigger on high-p_T isolated lepton one side

require ≥ 3 high-p_T jets (one b-tagged) in opp. hemisphere

central

$|\Sigma \vec{p}_T(j)| > 200$ GeV

look at $m(jj)$ excluding b-jet: see $W \to qq$ peak

$H \to cs$ peak

Detailed simulation by SDC — see Figures.

Method fails for $\tan\beta > 1$: $B(H^+ \to c\bar{s})$ gets small

18

$H^\pm \to cs$ dijet signal [SDC simulations]

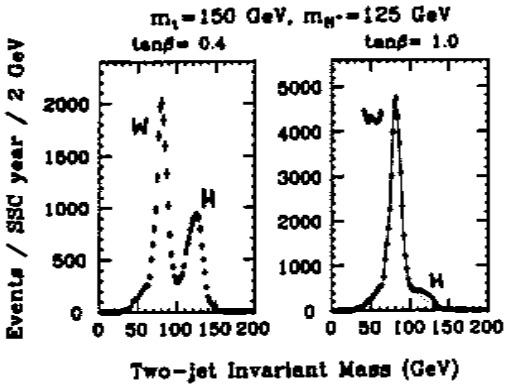

Comparison of signals

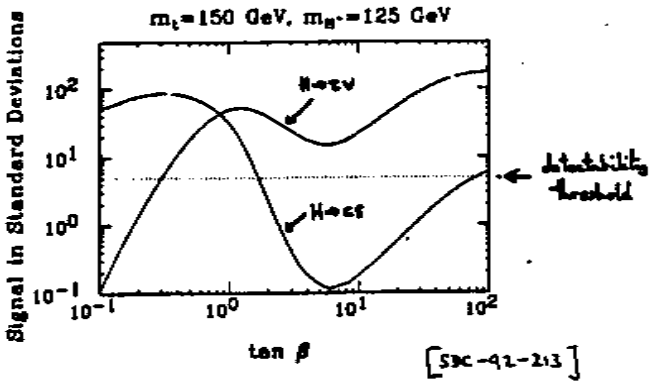

M4a

What about Tevatron ?

present $\mathcal{L} \sim 10^{-3}$ lower than SSC
$\sigma(t\bar{t}) \sim 10^{-3}$ " " " } much lower rates

but environment much cleaner ; much less stringent cuts needed

e.g. take numbers from Barr et al PRD39, 3510(89)
$t\bar{t} \to$ SM dilepton study : reasonable cuts $\begin{cases} p_T(\ell) > 15 \quad p_T(\tau \to h) > 15 \\ |\eta_e| < 3, |\eta_\mu| < 0.8, |\eta_\tau| < 1 \\ \not{p}_T > 20 \ , \ \not{\phi} \ldots \end{cases}$

add b-tag to kill remaining backgrounds ($\varepsilon = 50\%$)

assume $\int \mathcal{L}\, dt = 1000\ pb^{-1}$ (with upgrade)

SM $\Rightarrow$	$N(ee, e\mu, \mu\mu)$	$N(e\tau_{1+h}, \mu\tau_{1+h})$	m_t
	630	450	100
	270	190	120
	130	90	140

It should be possible to detect any big deviation from these $\ell\ell : \ell\tau$ ratios.

[$H^\pm$ signal $\Rightarrow$ reduction in $ee, e\mu, \mu\mu$
enhancement in $e\tau, \mu\tau$]

M4b

Contours of signal event numbers ($WH \to \ell\tau$)

$\sqrt{s} = 1.8$ TeV
$m_t = 140$
$\mathcal{L} = 1000\ pb^{-1}$

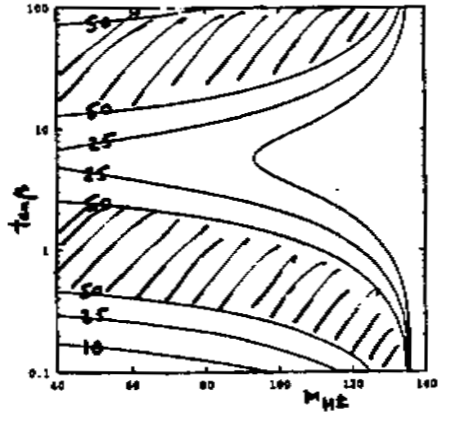

Contours of significance $\frac{S}{\sqrt{S+B}}$

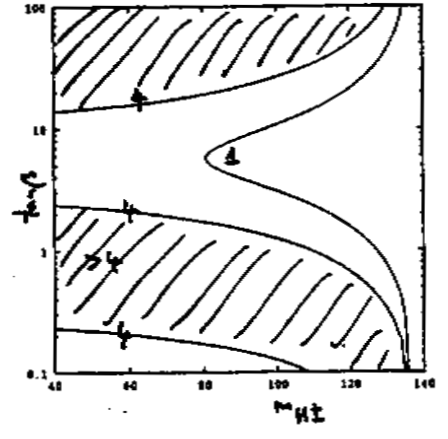

[Illustrative, assuming same acceptance for $t \to H \to \tau$, $t \to W \to \tau$]

What about the Next Linear Collider ?

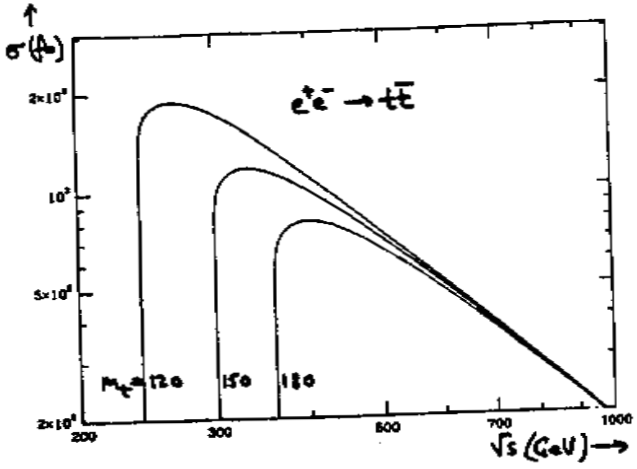

Biggest cross section close above threshold

$\mathcal{L} \sim 10\ fb^{-1}$/year

$m_t = 120$, $\sqrt{s} = 240$ } ⇒ 20000 $t\bar{t}$/year ⇔ $\mathcal{L} = 500\ pb^{-1}$ at Tevatron

$m_t = 180$, $\sqrt{s} = 400$ } ⇒ 8000 " ⇔ $\mathcal{L} = 2000\ pb^{-1}$ " "

Cleaner events than Tevatron
More " " "
Lower backgrounds " " } easier to study.

$t\bar{t} \to bW \to b\ell\nu$
$\downarrow$
$bH^+ \to bcs$
$\to b\tau\nu$

Can also search for $e^+e^- \to H^+H^-$ directly { $m_{H^\pm} = 200$, $\sqrt{s} = 500$ ⇒ 500 ev/yr; 400, $\sqrt{s} = 1000$ ⇒ 130 ev/yr

Conclusions

$H^\pm$ interesting probe of EWSB

MSSM suggests $m_{H^\pm} > 90$: inaccessible at LEP2

If $t \to bH^+$ occurs, will be able to detect at SSC/LHC

+ possibly at Tevatron

+ at NLC

But $m_{H^\pm} < m_t - m_b$ is unlikely (in Model II anyway)

$b \to s\gamma$ constraint + MSSM constraint

i.e. very possibly $t \not\to bH^+$

Supersymmetry and the Top Quark

HOWIE BAER
Dep't of Physics
Florida State University

ABSTRACT

In this talk, I will address the following topics:

- Radiative SU(2)xU(1) Breaking and m_t
- MSSM Radiative Corrections and m_t
- $\tilde{t}_1$ production and decays (Tevatron)
- $t \to \tilde{t}_1 \tilde{Z}_i$ prospects and consequences (Tevatron)
- $\tilde{g} \to t\bar{t}\tilde{Z}_i$ Yukawa enhanced decays (SSC/LHC)
- $t \to bH^+; H^+ \to \tilde{W}_1\tilde{Z}_2 \to 3l$ decays (SSC/LHC)

Thanks to my collaborators:
M. Bisset, D. Dicus, M. Drees, R. Godbole,
J. Gunion, C. Kao, X. Tata and J. Woodside

MSSM- Basics

1.) Supersymmetry · Bosons $\Leftrightarrow$ Fermions

2.) Protective symmetry needed to stabilize divergent scalar masses

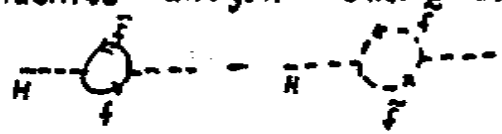

3.) Broken symmetry : spartick masses $\lesssim O(1\ \text{TeV})$ (produce at colliders?)

Minimal Supersymmetric Standard Model:

- Supersymmetric version of SM with fewest additional particles/interact
- Globally supersymmetric Lagrangian with soft- SUSY breaking terms
- No B and L violating terms $\Rightarrow$ R-parity conservation

Basic parameters of the MSSM:

m_0 - scalar mass term at GUT scale

$m_{1/2}$ - gaugino " " " "

μ - super potential Higgs mass $(-2m_1)$

m_{H_p} - pseudo-scalar Higgs mass (m_{H^0})

$\tan\beta = \frac{v}{v'}$ - ratio of Higgs field vevs

These are usually re-cast in terms of

$$(m_{\tilde{\ell}}, m_{\tilde{g}}, \mu, m_{H_p}, \tan\beta)$$

$\uparrow$ gaugino mass relation

Along with $(m_\ell, m_{\tilde{\ell}})$, these parameters fix most of the sparticle masses and couplings.

Approximate limits of MSSM parameter space:

1.) $0 < m_{\tilde{t}} < \sim 1\text{-}2$ TeV

2.) $0 < m_{\tilde{g}} < \sim 1\text{-}2$ TeV

3.) ~ -1 TeV $< \mu < \sim 1$ TeV

4.) $1 \lesssim \tan\beta \lesssim 50$ $\left(\sim \frac{m_t}{m_b}\right)$

5.) $0 < m_{H_p} < \sim 1$ TeV

Plus

91 GeV $< m_t < \sim 200$ GeV

↑

unless $t \to \tilde{t}\, \tilde{\chi}_i$

Radiative Correction Constraints on SUSY

- Zwirner:

Erice review

Peskin-Takeuchi estimate for 1 generation $SU(4)_{TC}$

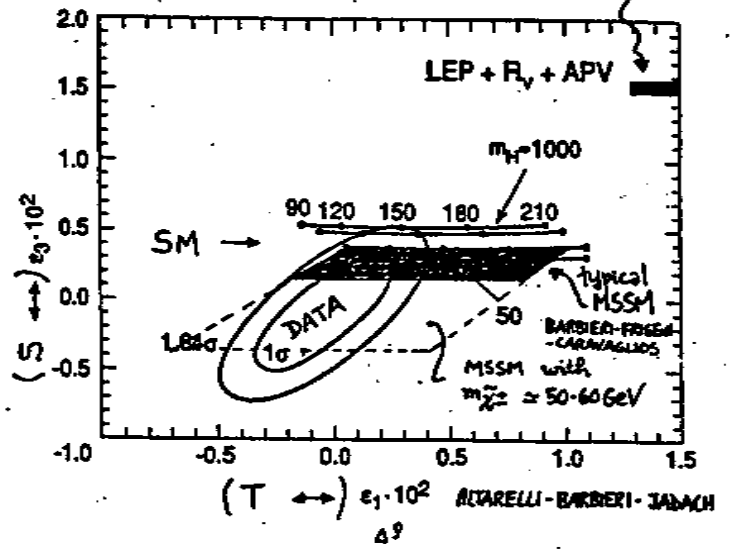

Theoretical calculations of ϵ_1, ϵ_2 in models of dynamical symmetry breaking are affected by some <u>model dependence</u> & <u>theoretical uncertainties</u>

but

the general trend gives deviations from SM predictions measurable with the present accuracy

present data disfavour the composite scenario

Radiative Breaking of EW Symmetry in SUSY GUT's:

Ibanez-Ross
Inoue et al.
(1982)

In SUSY GUT's, EW symmetry breaking can be natural consequence of massive top quark:

$$\frac{\partial m_H^2}{\partial \ln \mu} = \frac{1}{8\pi^2}\Big(\underbrace{3 f_t^2 m_{\tilde{t}}^2}_{>0} + \cdots\Big)$$

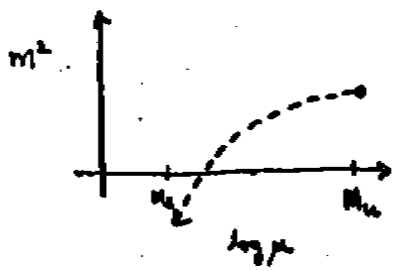

$\Rightarrow \langle H_1 \rangle \neq 0$

$\langle H_2 \rangle \neq 0$

$\langle \tilde{q} \rangle = 0$

$\langle \tilde{\ell} \rangle = 0$

$100 \lesssim M_{\tilde{t}} \lesssim 180$ GeV

Usual CDF mass bounds on squarks not applicable to $\tilde{t}_1$ squark

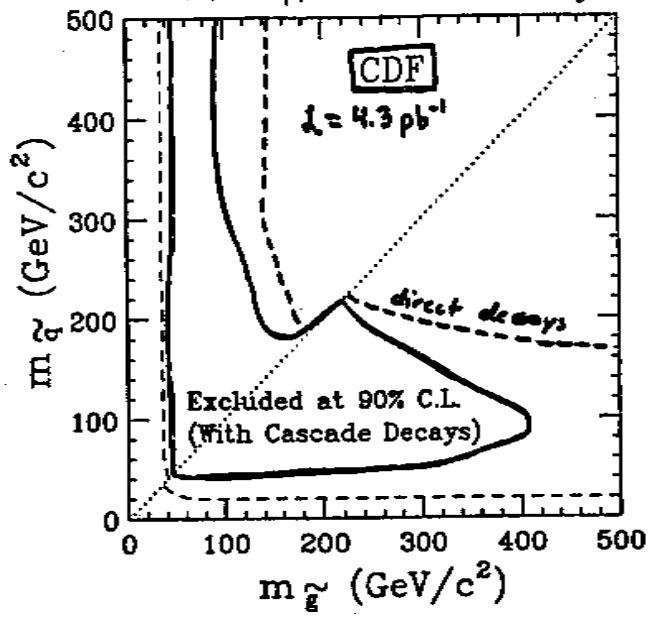

Figure 4: The shaded region of squark and gluino masses is excluded at 90% C.L for a version of SUSY with cascade decays, $\mu = -250$, $\tan\beta = 2$, and $m_{\tilde{g}} = 500$ GeV/c^2. For comparison, the dashed line shows the limits corresponding to no cascade decays.

Stop Squark Mass Matrix:

$$m_{\tilde{t}}^2 = \begin{bmatrix} m_{\tilde{t}_L}^2 + m_t^2 & m_t(a m_0 + \mu \cot\beta) \\ m_t(a m_0 + \mu \cot\beta) & m_{\tilde{t}_R}^2 + m_t^2 \end{bmatrix}$$

where
$$m_{\tilde{t}_L}^2 = m_{\tilde{Q}_L}^2 - 2 \underline{f_t^2} m_0^2 \Delta$$
$$m_{\tilde{t}_R}^2 = m_{\tilde{U}_R}^2 - 4 \underline{f_t^2} m_0^2 \Delta$$

f_t = top Yukawa coupling $= \frac{g m_t}{\sqrt{2} M_W} \frac{(v^2+v'^2)^{1/2}}{v}$

$a, \Delta \sim O(1)$

Large $m_t \Rightarrow$ * $m_{\tilde{t}_R}, m_{\tilde{t}_L}$ can be much lighter than other squarks

* mixing between $\tilde{t}_L, \tilde{t}_R$ states

$$\tilde{t}_1 = \cos\theta_t \, \tilde{t}_R - \sin\theta_t \, \tilde{t}_L$$

$$m_{\tilde{t}_1} < m_{\tilde{t}_2}$$

LEP $\underset{?}{\Rightarrow} m_{\tilde{t}_1} \gtrsim \frac{M_Z}{2}$ but what about Tevatron?

Possible $\tilde{t}_1$ decay modes:

$\tilde{t}_1 \to b \tilde{W}_1$!

$\to b \ell \tilde{\nu}$
$\to b \tilde{\ell} \nu$ } assume $\tilde{\ell}, \tilde{\nu}$ heavy

$\to b f \bar{f} \tilde{Z}_i$ (4-body)

$\to b W \tilde{Z}_i$ (competes with $b\tilde{W}_1$)

Flavor violating couplings induced in MSSM (different quark/squark mixing matrices)

$\tilde{t}_1 \to c \tilde{Z}_i$
$\to c \tilde{g}$ } suppressed by $\varepsilon \sim 1\text{-}4 \times 10^{-4}$ in amplitude

Hikasa Kobayashi

Even so, flavor-violating 2-body mode dominates 4-body mode when allowed.

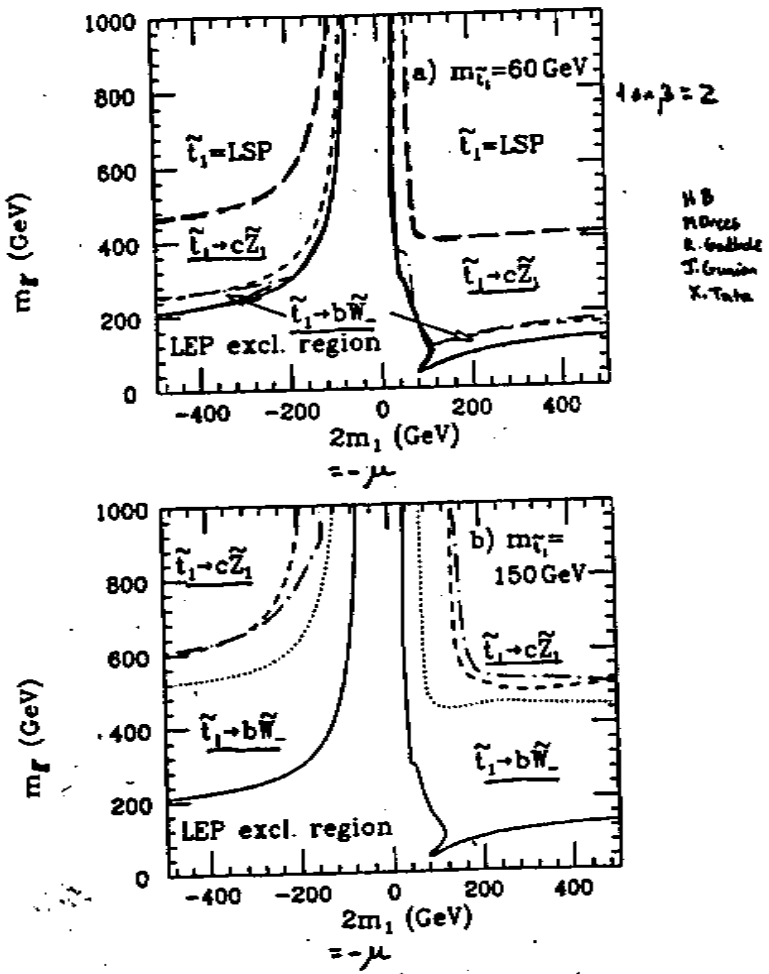

Fig. 1
Regions of parameter space where $\tilde{t}_1$ decays occur

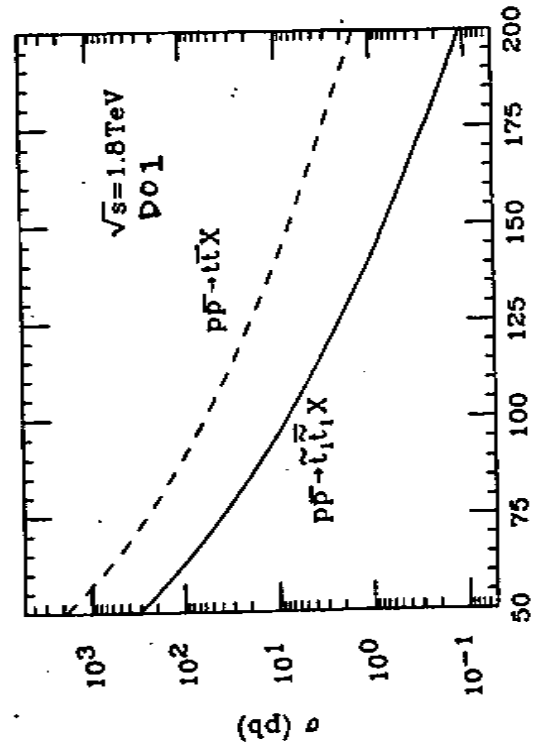

Fig. 2
Production Cross-section for stop squarks

Search for $\tilde{t}_1$ at Tevatron:

For $45\,\mathrm{GeV} < m_{\tilde{t}_1} \lesssim ?$

$\tilde{t}_1 \to c\,\tilde{\chi}_1\,,\ c\,\tilde{\chi}_2$

$\to b\,\tilde{W}_1$ if allowed

$$p\bar{p} \to \tilde{t}_1\bar{\tilde{t}}_1 \to c\bar{c}\,\tilde{\chi}_1\tilde{\chi}_1\,X$$

$\to$ 2-charm-jets + $\not{E}_T$

Look for:

1.) $\not{E}_T > 40$ GeV

2.) $p_{T_j} > 15$ GeV ; $|\eta_{j_1}| < 1$; $|\eta_{j_2}| < 3$ } Detailed simulation needed

σ (CDF) ~ 10.5 pb

We use parton level Monte Carlo with

$$E_{parton} = 1.15\,E_{jet} + 5\ \mathrm{GeV}$$

$\Rightarrow$ No bound on $m(\tilde{t}_1)$ from 4.1 pb^{-1} data if $m(\tilde{\chi}_1) \gtrsim 10$ GeV

No mass bound on $\tilde{t}_1$ if $\tilde{\chi}_1$ has mass $\gtrsim 10$ GeV

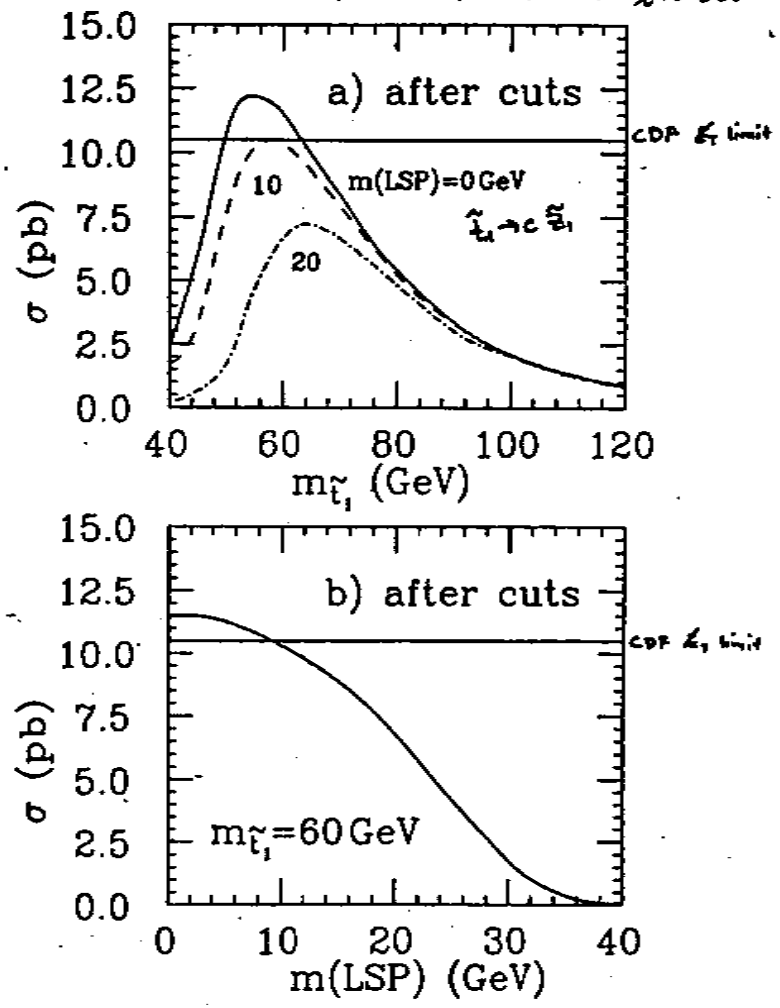

Fig. 3

Stop-squark signal cross section after cuts

Top decay to stop:

If $m_t > m_{\tilde{t}_1}$, then

- $t \to \tilde{t}_1 \tilde{Z}_1$
- $t \to bW$

} competing 2-body modes

Possible $t \to \tilde{t}_1 \tilde{Z}_1 \to c\, \tilde{Z}_1 \tilde{Z}_1$

If c-quark is soft, may be difficult to see t at Tevatron

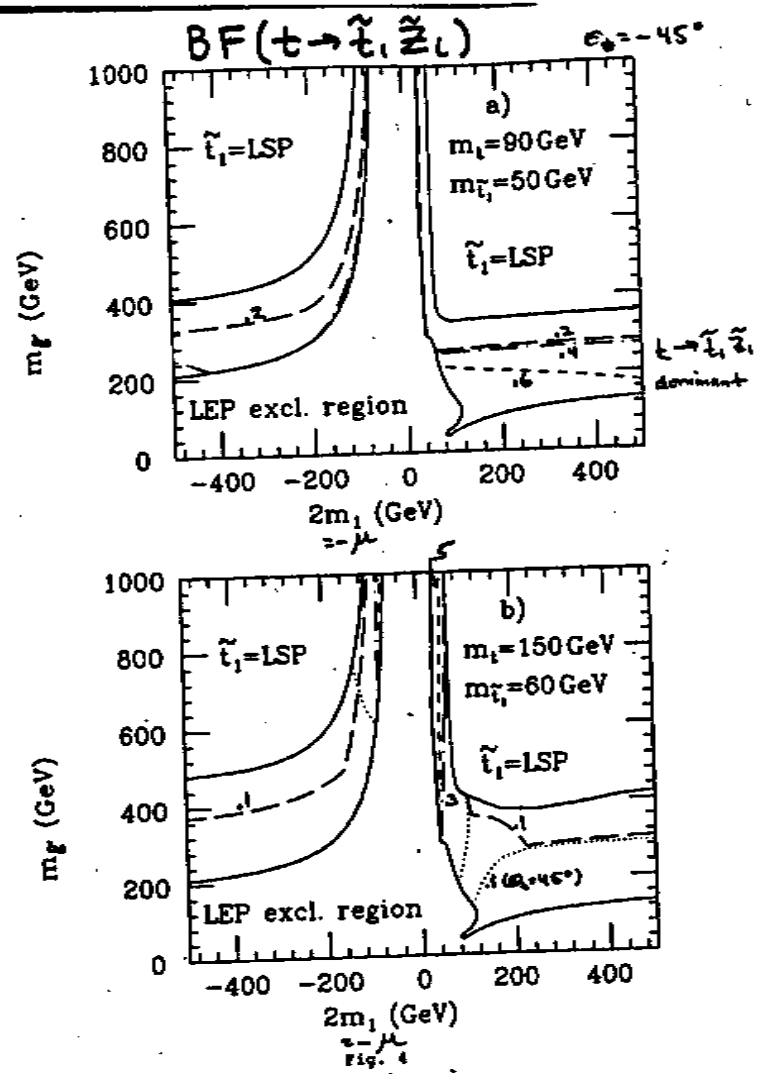

Top → stop branching fraction

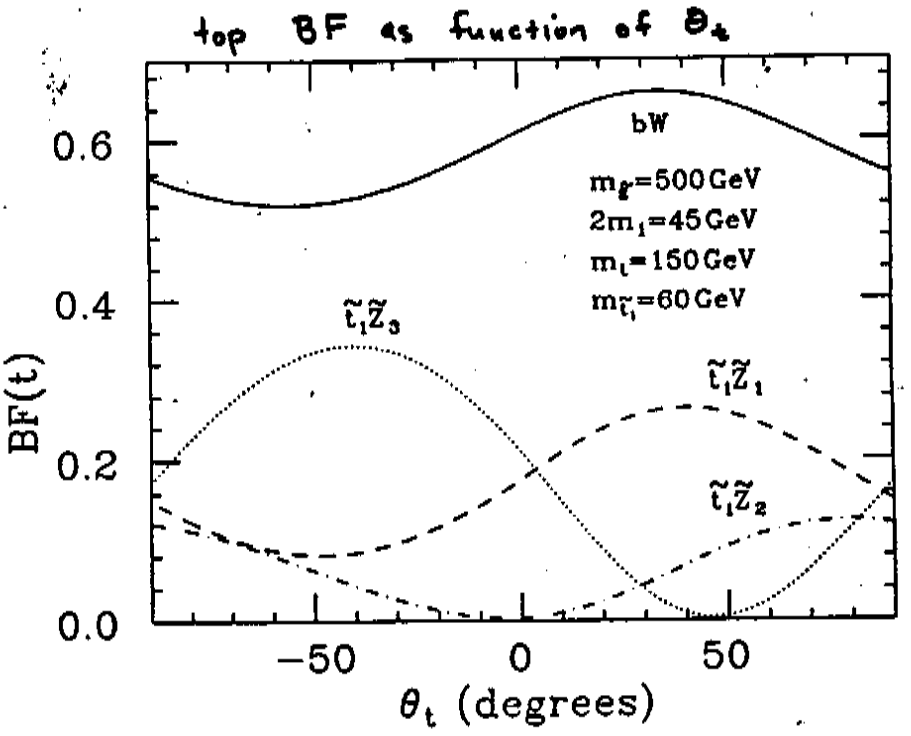

Fig. 6

Fig. 6

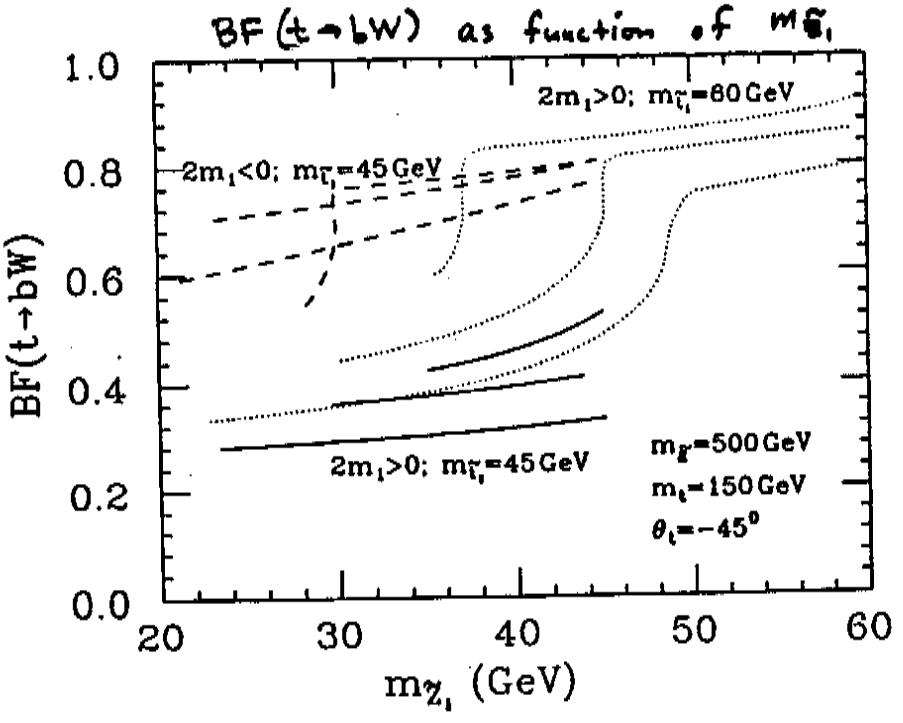

Fig. 7

BF(t→bW) can be as low as ~30% of SM value

Fig. 8

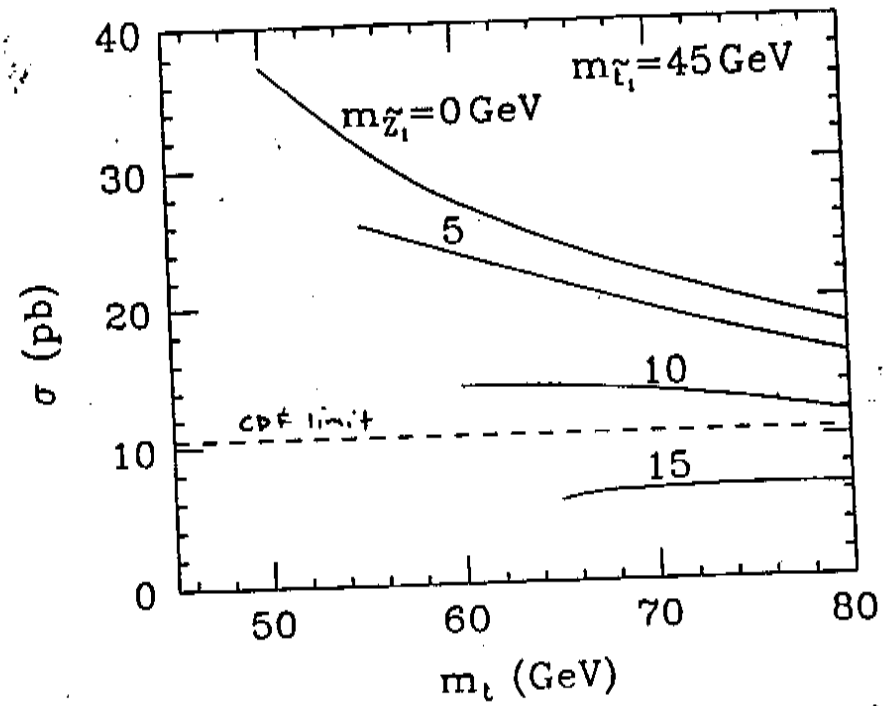

If $M_{\tilde{Z}_1} \gtrsim 12$ GeV, a 65 GeV $\tilde{t}$ could have escaped detection!

Fig. 9

$\not{E}_T$ cross section from $t\bar{t}$ and $\tilde{t}_1\bar{\tilde{t}}_1$ versus $M_{\tilde{t}_1}$

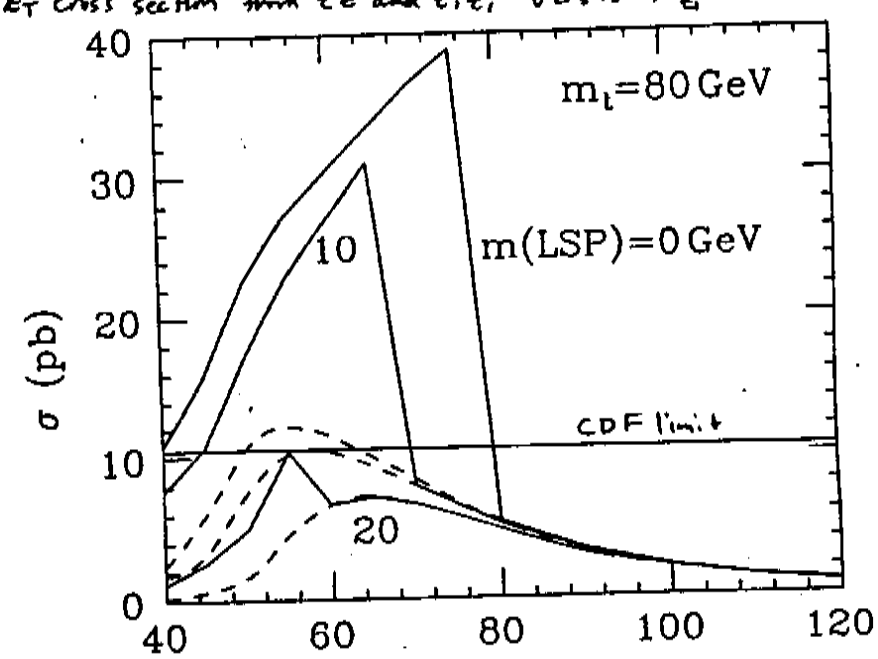

Add in $t \to \tilde{t}_1 \tilde{Z}_i$

Fig. 8

Future search for higher mass $\tilde{t}_1$:

Search for dileptons from

$$\tilde{t}_1\bar{\tilde{t}}_1 \to b\tilde{W}_1\bar{b}\bar{\tilde{W}}_1 \to b\bar{b}\,\ell\bar{\ell}\,\tilde{Z}_1\tilde{Z}_1\,\nu\bar{\nu}$$

1) $p_{T_\ell} > 15$ GeV
2) $\not{E}_T > 20$ GeV
3) $30^\circ < \Delta\phi(\ell\bar{\ell}) < 150^\circ$
4) $|\eta_e| < 3$; $|\eta_\mu| < .8$

$m_{\tilde{W}_1} = 70$ GeV ; $m_{\tilde{Z}_1} = 20$ GeV

Process	σ
$\tilde{t}_1\bar{\tilde{t}}_1$ (80)	.13 pb
$\tilde{t}_1\bar{\tilde{t}}_1$ (100)	.04
$\tilde{t}_1\bar{\tilde{t}}_1$ (120)	.01
$\tilde{t}_1\bar{\tilde{t}}_1$ (140)	.007
WW	.12
$t\bar{t}$ (90)	3.5
$t\bar{t}$ (150)	.3

Interesting effect : SSC/LHC

$\tilde{g} \to t\bar{t}\,\tilde{Z}_i$ Yukawa enhanced decay

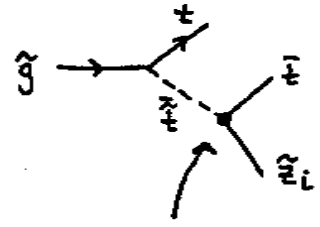

Assume $m_{\tilde{g}} < m_{\tilde{t}}, m_{\tilde{q}}$

Yukawa coupling to higgsino component of neutralino

For $m_{\tilde{g}} \gtrsim 1$ TeV , $\tilde{g} \to t\bar{t}\,\tilde{Z}_i$ dominant

Then, $\tilde{g}\tilde{g}$ event has

$$p\bar{p} \to \tilde{g}\tilde{g} \to t\bar{t}\,t\bar{t}\,\tilde{Z}_i\tilde{Z}_i \to 4W\ 4b\ \not{E}$$

2, 3, 4 lepton events ?

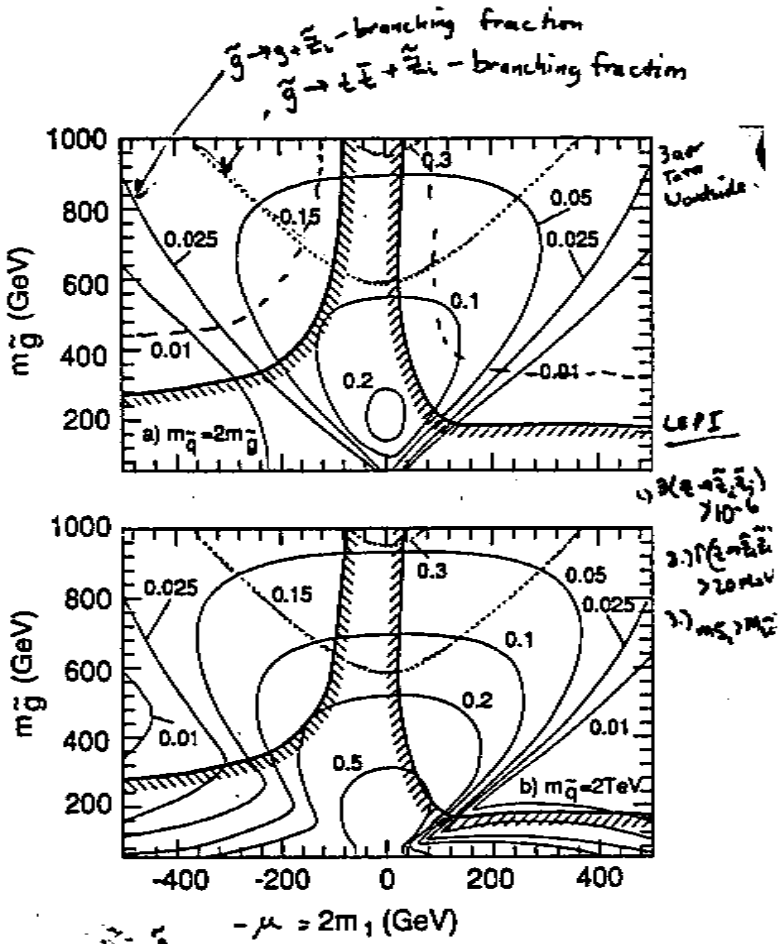
$\tilde{g} \to g + \tilde{Z}_i$ - branching fraction
$\tilde{g} \to t\bar{t} + \tilde{Z}_i$ - branching fraction
$m_{\tilde{g}}$ (GeV)
a) $m_{\tilde{q}} = 2m_{\tilde{g}}$
b) $m_{\tilde{q}} = 2$TeV
$-\mu = 2m_1$ (GeV)
LEP I
BAER 001 HDA

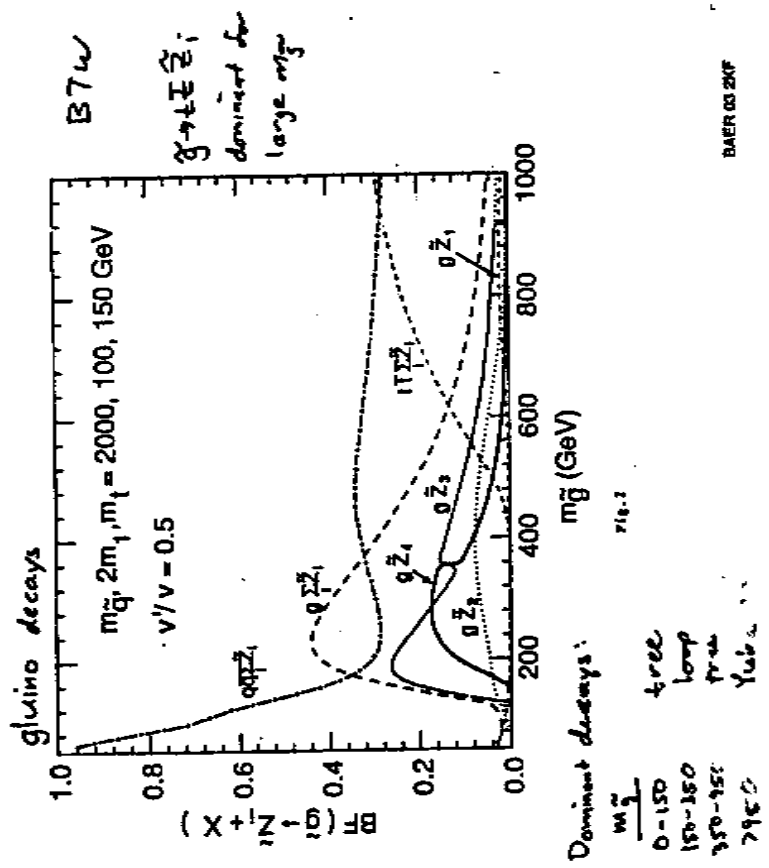
gluino decays
$m_{\tilde{q}}, 2m_1, m_t = 2000, 100, 150$ GeV
$v'/v = 0.5$
$BF(\tilde{g} \to \tilde{Z}_i + X)$
$m_{\tilde{g}}$ (GeV)
BAER 03 2KF

Interesting effect #2: $t \to bH^+$

- Supersymmetric decay modes of H^+ are possible

$$H^+ \to \tilde{W}_1 \tilde{Z}_i$$
$$\to \tilde{W}_2 \tilde{Z}_i$$
$$\to \tilde{t}\tilde{b} \text{ (not likely if } t \to bH^+)$$

H.B.
M. Gisiet
D. Dicus
C. Kao
X. Tata

- Then $t \to bH^+ \to b\tilde{W}_1\tilde{Z}_1 \to b\ell\nu\tilde{Z}_1\tilde{Z}_1$

  visible products softer;
  harder to detect

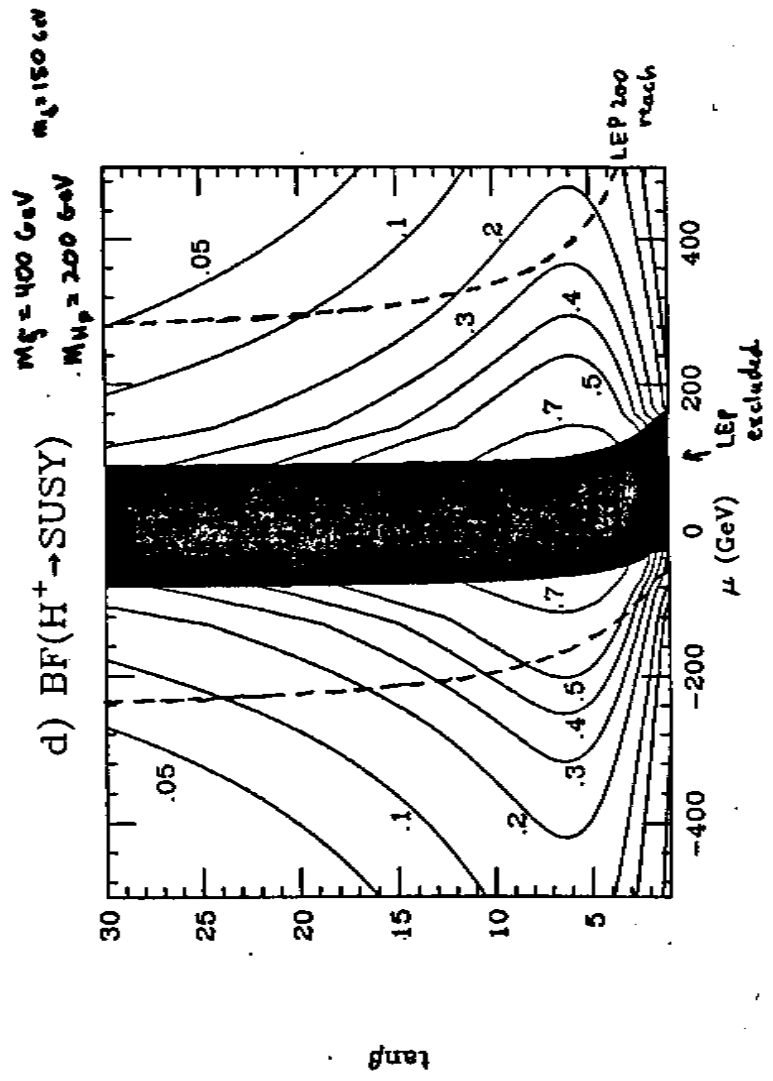

Felcini criteria for $t \to bH^+$ $\hookrightarrow \tau\nu$

(LHC, Atlas)

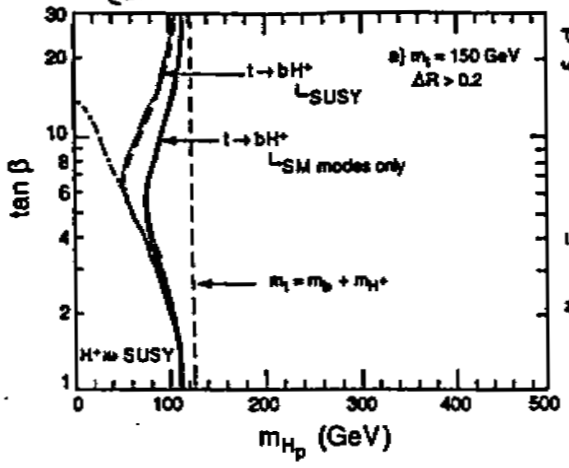

τ-lepton universality violation

BBDKT

1.) $\tilde{g}$ = inc ... = μ = ...

2.) $m_{\tilde{g}}$ = ... μ = -70 ...

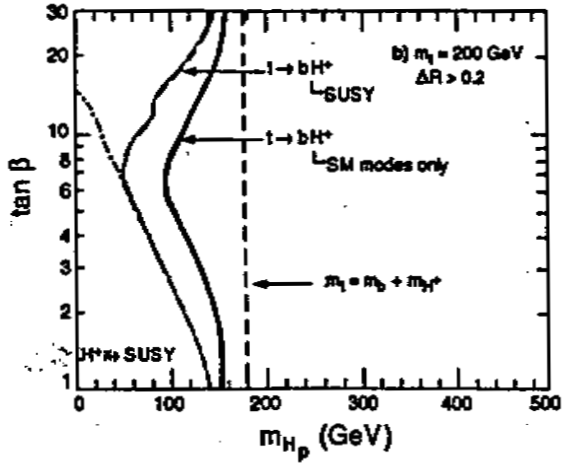

Fig. 5

Possible rare t decay: $t \to b\, 3\ell\, 2\tilde{Z}_1$

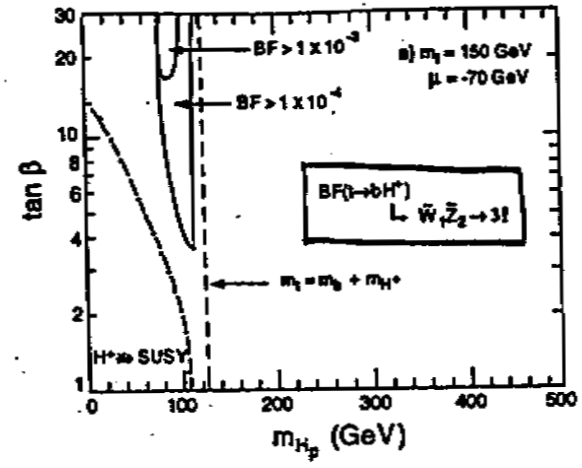

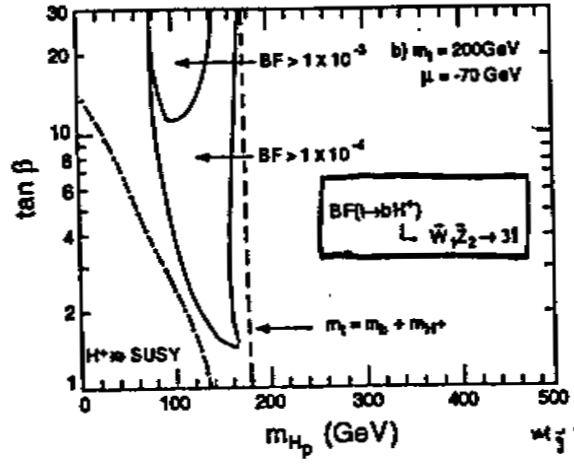

$m_{\tilde{g}}$ = 400 GeV

Fig. 18

Summary:

Lots of interesting effects: SUSY + top

- $m_t \sim 100$-200 GeV naturally leads to electroweak symmetry breaking in SUSY GUTs
- Radiative corrections o.k.
- Search for $\tilde{t}_1$ at Tevatron
- $t \to \tilde{t}_1 \tilde{z}_i \Rightarrow m_t \simeq 65$ GeV not yet ruled out by CDF
- $\tilde{g} \to t\bar{t}\,\tilde{z}_i$ dominant if $m_{\tilde{g}} \gtrsim 1000$ GeV (μ small)
- $t \to bH^+ \to b\,\tilde{W}\,\tilde{z}_i$ can change charged Higgs phenomenology
  harder to detect; but $t \to 3l$ rare decay?

TOP AND RARE DECAYS

JoAnne L. Hewett
High Energy Physics Division
Argonne National Laboratory
Argonne, IL 60439

Abstract

We examine the flavor changing neutral current decays of the top-quark $t \to cV$ where $V = g, \gamma, Z$, or H. These decays proceed through one-loop penguin-type diagrams which arise in the Standard Model (SM) and in scenarios which contain physics beyond the SM. We find that the branching fractions for these processes are hopelessly small in the SM. Enhancements are found once new physics contributions are considered, however the resulting branching fractions are still small. One should keep in mind that future TeV linear e^+e^- colliders and hadron supercolliders are expected to produce of order 10^{4-5} and 10^{7-8} $t\bar{t}$ pairs per year, respectively, at design luminosity. The effects of a heavy internal top-quark on one-loop K and B decays are also briefly discussed. In the case of $b \to s\gamma$, the 90% C.L. upper bound on the inclusive branching fraction obtained by CLEO is approaching the SM prediction and allows little room for contributions from new physics. In particular, large regions of parameter space in two-Higgs-Doublet Models are already excluded.

Top

+

Rare Decays

- Top Production Rates

Tevatron	NLC	SSC / LHC
???	10^{2-3}/yr	10^{3-4}/yr

- FCNC decays of top
- FCNC decays of K / B

[SM + beyond]

* Theoretical issues only
  - Experimental issues – see Working Group summary (L. Kane)

* CP – see talk by D. Chang

Typical Flavor Changing Neutral Current Vertex Diagram

Very weak GIM suppression!

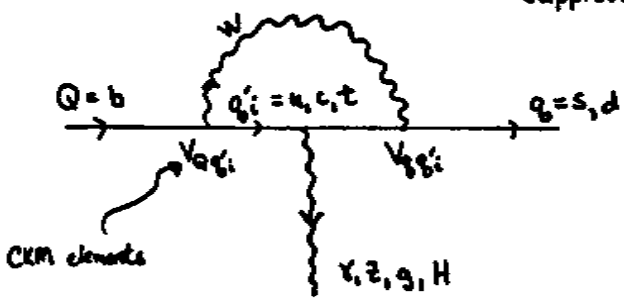

⇒ 'Large' Rates!

Typical Flavor Changing Neutral Current Vertex Diagram

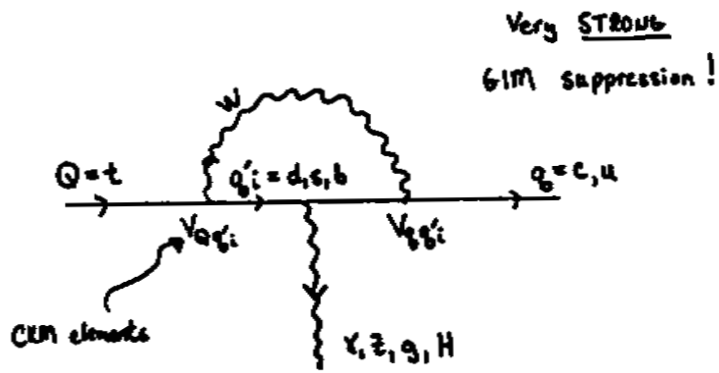

Typical Values of Branching Fractions

Meson / Quark	B
K	$10^{-10} - 10^{-9}$
D	$10^{-14} - 10^{-13}$
B	$10^{-6} - 10^{-4}$
t	???
(b'	up to a few % !)

In General - Loop processes are sensitive to SM parameters + to effects from new physics

For top-quarks:

Advantages • top is heavy!

- CLEAN - No long-distance effects
- No large 2-loop QCD corrections
  ⇒ Small Uncertainties from QCD corrections
- Top decays before hadronization
- Top is largest fermion mass scale in Standard Model
  ⇒ may provide unique window for new physics!

Disadvantages • top is heavy!

- No large 2-loop QCD corrections
  ⇒ no large log enhancements
- Strong GIM suppression = small rates (in SM)
- Large tree-level decay $\Gamma(t \to bW) \propto G_F$

$t \to cV$, $V = \gamma, Z, g, H$

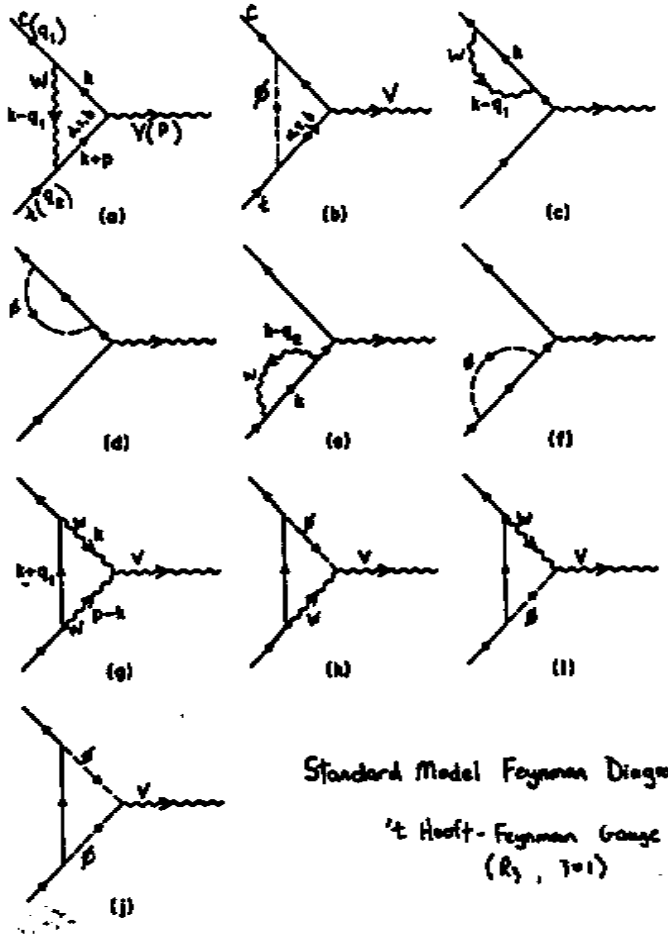

Standard Model Feynman Diagrams

't Hooft - Feynman Gauge
(R_ξ , $\xi = 1$)

Feynman diagrams responsible for the decay $t \to cV$, with $V = \gamma, Z, g, H$ in the Standard Model.

Expression for Diagram B

$$
\mathcal{B}^\mu = \frac{g^2}{2M_W}\left\{
\begin{aligned}
&\begin{bmatrix} 2s_t\sqrt{z_t}A_d[C_{12}+C_{23}-C_{11}-C_{22}] \\ +2s_M\sqrt{z_t}B_d[C_0+2C_{12}+C_{23}] \end{bmatrix}\underline{\gamma^\mu L} \\
&+\begin{bmatrix} 2\sqrt{z_t}A_d[s_d(C_{23}-C_{22})+s_M(C_{11}-C_{12})] \\ -2s_M\sqrt{z_t}B_d(C_0+C_{11}+C_{12}+C_{23}) \end{bmatrix}\underline{q^\mu L} \\
&+\begin{bmatrix} s_M A_d[s_d(C_0+C_{12}-C_{22})-s_tC_{11}-s_MC_0] \\ +s_M B_d[s_d(C_0+C_{12})+s_t(-C_{11}+C_{22})]+A_d m_b m_t C_{12} \\ +s_M B_d[\bar{C}_0+\beta C_{12}+(s_t-\beta)C_{23}-2C_{24}] \end{bmatrix}\underline{\gamma^\mu L} \\
&+\begin{bmatrix} 2\sqrt{z_t}A_d[s_M(C_0+C_{12})+s_d(C_{11}+C_{22})] \\ +2s_M\sqrt{z_t}B_d(C_{22}-C_{11}-C_{23}+C_{24}) \end{bmatrix}\underline{\gamma^\mu R} \\
&+\begin{bmatrix} -2\sqrt{z_t}A_d[s_M(C_0+C_{12})+s_d(C_{12}+C_{23})] \\ +2s_M\sqrt{z_t}B_d(C_{12}-C_{22}-C_{23}+C_{24}) \end{bmatrix}\underline{q^\mu R} \\
&+\left[\sqrt{z_t z_c}A_d\begin{bmatrix} s_M(C_0+C_{12})+\beta C_{12}+(s_t-\beta)C_{22} \\ +\bar{C}_0-2C_{24} \end{bmatrix}\right]\underline{\gamma^\mu R}
\end{aligned}
\right\}. \qquad (A.2)
$$

with $C_i(\beta, -k, \sqrt{z_M}, \sqrt{z_M}, \hat{m}_W)$,

↳ scalar integrals

(Passarino, t'Hooft, Veltman)

$x_i = m_i^2/m_W^2$

Must Keep <u>ALL</u> external + internal masses + momenta !

Eilam, Hewett, Soni

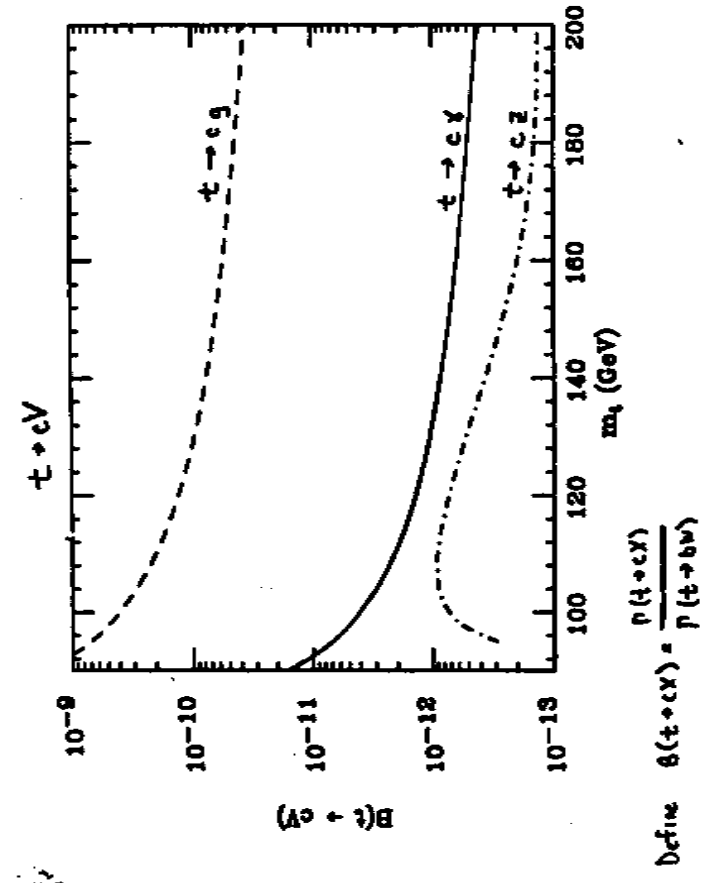

Define $B(t \to cV) = \frac{\Gamma(t \to cV)}{\Gamma(t \to bW)}$

Branching fraction for $t \to cg, c\gamma, cg$ in the Standard Model as a function of the top-quark mass.

Deshpande, Margolis, Trottier

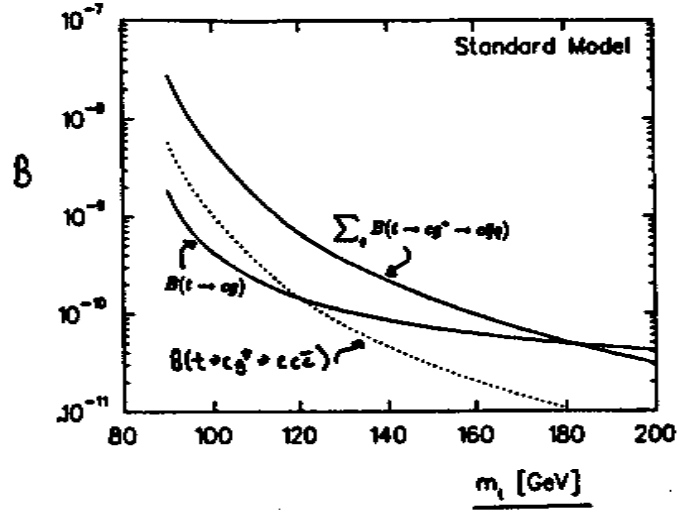

FIGURE 2

Virtual gluon mode is enhanced over on-shell gluon due to large logs in the loop quark masses
- further enhancements in anomalous threshold region

Branching fraction for the three body decay, $t \to cq\bar{q}$ in the Standard Model as a function of the top-quark mass, from Deshpande *et al.*, Phys. Rev. D45, 178 (1992).

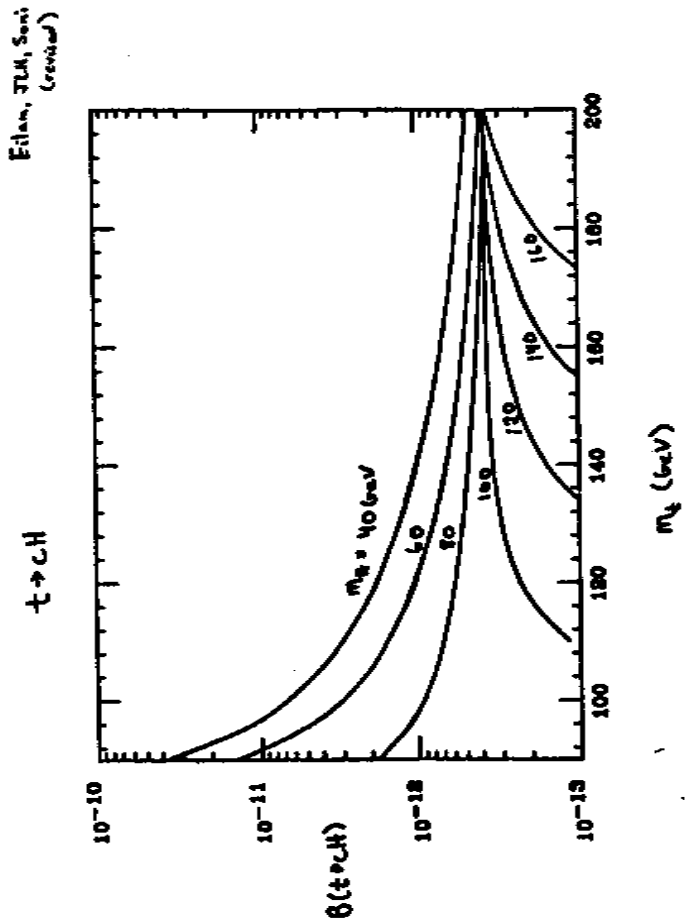

Branching fraction for $t \to cH$ in the Standard Model as a function of the top-quark mass for various values of the Higgs boson mass, as indicated.

Add New Physics

How does it affect FCNC top-quark decays?

- Fourth Generation (with heavy ν_τ)
- Two-Higgs-Doublet Models
- Minimal Supersymmetry
- Minimally non-Minimal SUSY with $\not{R}$
- Addition of Exotic Fermions

increasing "exotic-ness" = increasing rates!

$t \to c\gamma$ with 4th Generation (Diaz-Cruz et al)

need to rescale by CKM factors!

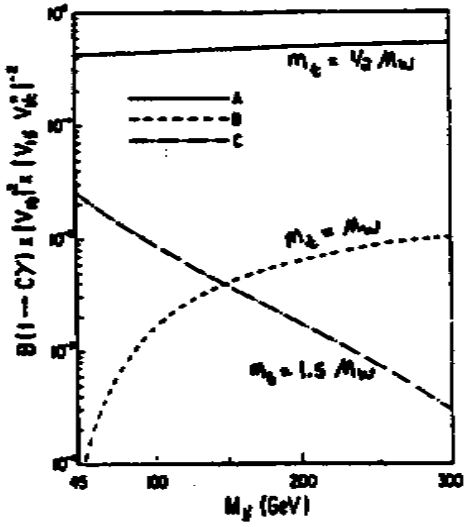

GIM Suppression weakened

$\Rightarrow$ Big Enhancements!

Branching fraction for $t \to c\gamma$, scaled to the relevant 4×4 Kobayashi-Maskawa matrix elements, in a model with 4 generations of fermions as a function of the 4th generation charged $-1/3$ quark mass. This is taken from Diaz-Cruz *et al.*, Phys. Rev. D41, 891 (1990).

Two-Higgs-Doublet Models

Contained Naturally in Many Models

- Supersymmetry (Haber + Kane, Phys. Reps.)
- Superstring-Inspired E_6 Theories [JLR, Rizzo; Phys. Rep. 183, 193 (1989)]

$\phi_1 = \begin{pmatrix} \phi_1^+ \\ \phi_1^0 \end{pmatrix}$ $\phi_2 = \begin{pmatrix} \phi_2^+ \\ \phi_2^0 \end{pmatrix}$ After Spontaneous Symmetry Breaking $h^0, H_1^0, H_2^0, H^\pm$

$\langle \phi \rangle = v_1 \quad v_2 \quad , \quad v_1^2 + v_2^2 = v_{SM}^2$ $\boxed{\tan\beta = v_2/v_1}$

Tree-level FCNC unless

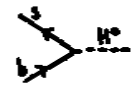

(Glashow + Weinberg)

each fermion type receives mass from only one doublet

Examine 2 models of this type

	Model I		II ← SUSY, E_6 models	
	vev	R_f	vev	R_f
$\begin{pmatrix} u \\ d \end{pmatrix}$	2	$\cot\beta$	2	$\cot\beta$
	2	$-\cot\beta$	1	$\tan\beta$
ℓ	2	$-\cot\beta$	1	$\tan\beta$

LEP Bounds: $m_{H^\pm} > 42$-45 GeV

$$\mathcal{L} = \frac{g}{2\sqrt{2}\, m_W} H^\pm \left\{ V_{ij}\, m_{u_i} R_u\, \bar{u}_i (1-\gamma_5) d_j + V_{ij}\, m_{d_j} R_d\, \bar{u}_i (1+\gamma_5) d_j + m_\ell R_\ell\, \bar{\nu} (1+\gamma_5) \ell \right\} + h.c.$$

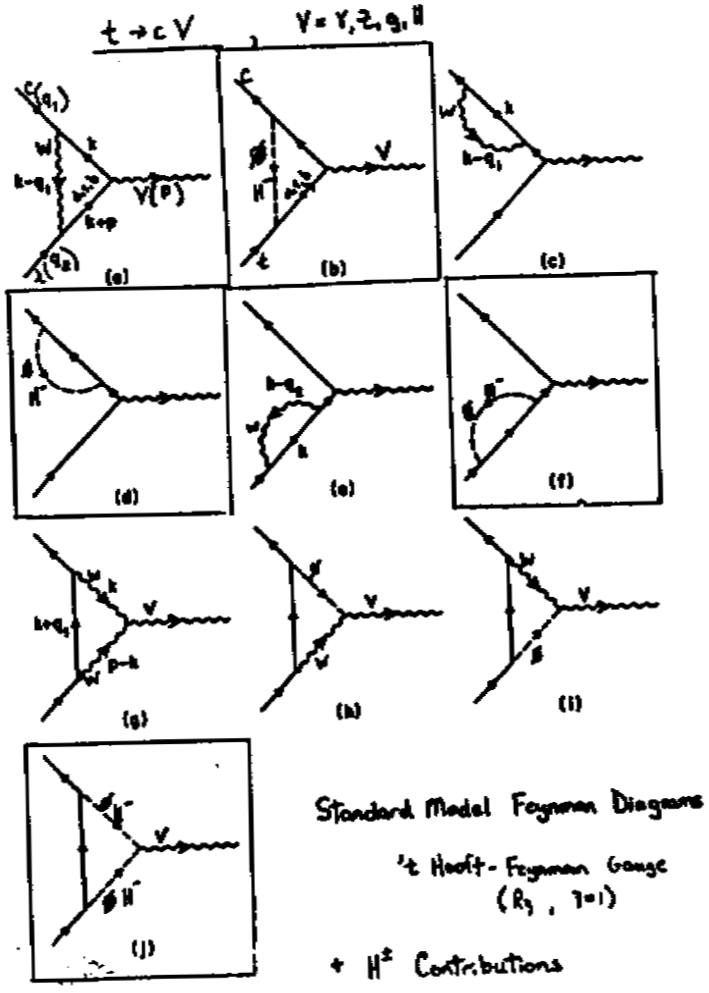

The ten Standard Model Feynman diagrams responsible for $t \to cV$, and the four diagrams which contribute in two-Higgs-Doublet Models.

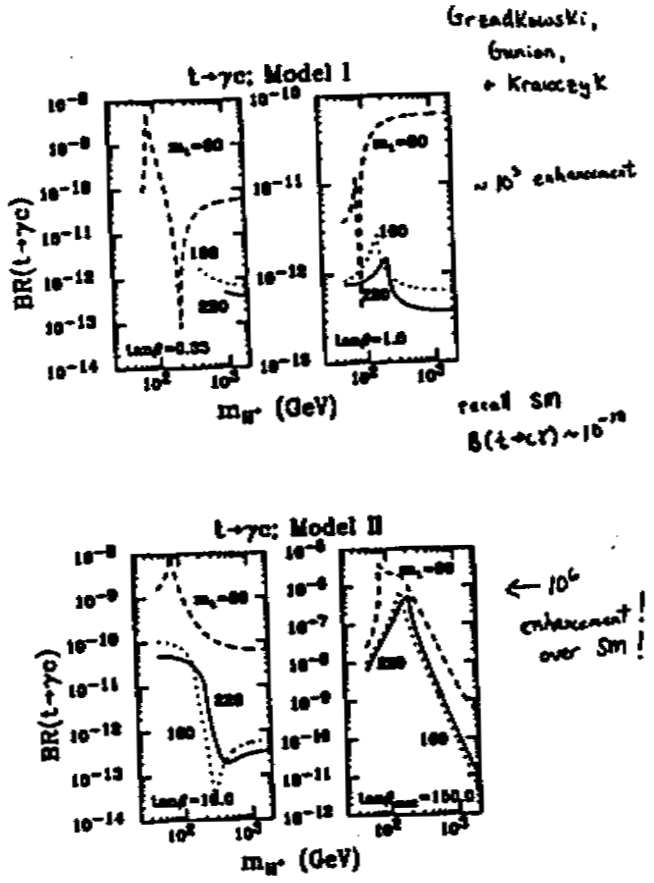

Branching fractions for $t \to c\gamma$ in two-Higgs-Doublet Models as a function of the charged Higgs mass, for various values of the parameters as indicated, from Gunion and Grzadkowski, Phys. Lett. B268, 106 (1991).

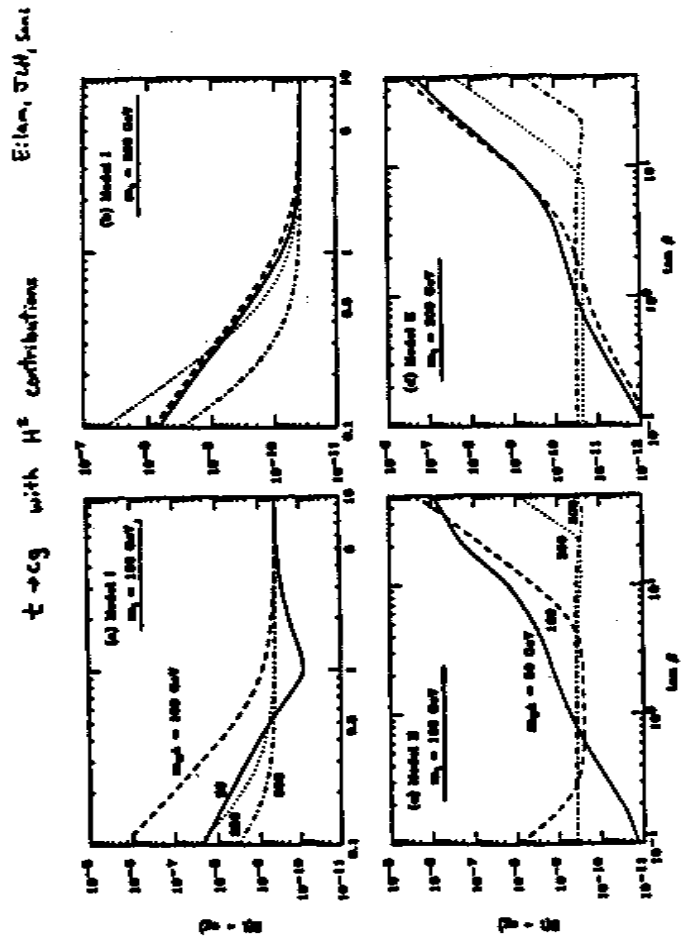

Figure 6

Branching fractions for $t \to cg$ in two-Higgs-Doublet Models as a function of $\tan\beta \equiv v_2/v_1$.

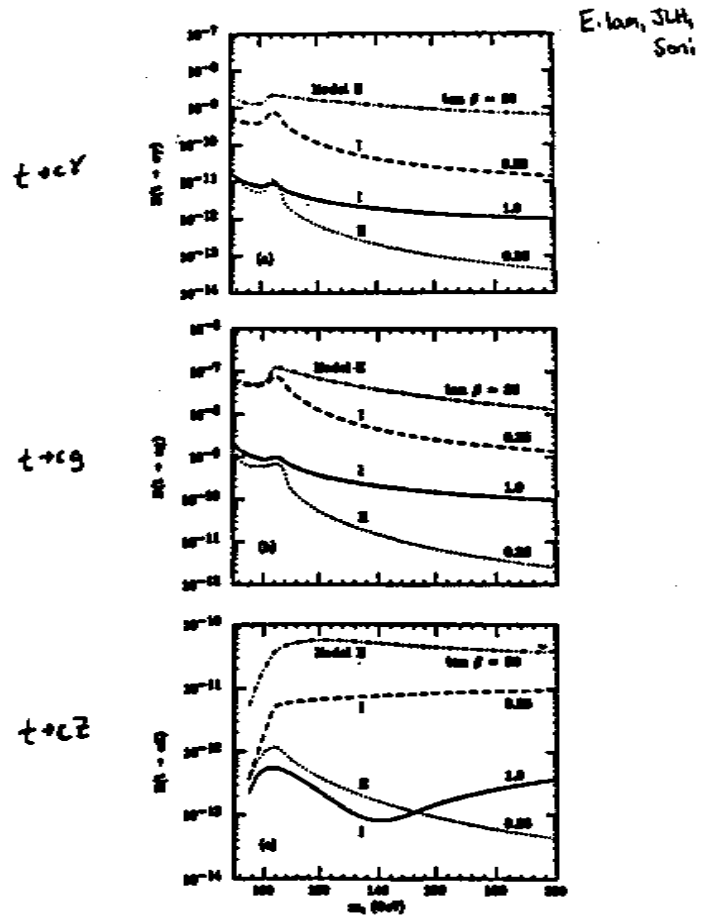

Figure 8

Branching fractions for the various flavor changing t-quark decays in two-Higgs-Doublet Models as a function of the t-quark mass.

Deshpande, Margolis, Trottier

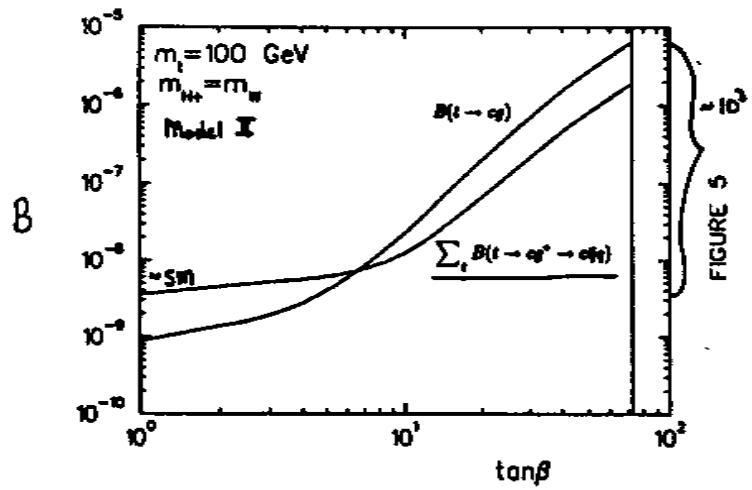

~ 10^3 Enhancement!

Branching fraction for the decay $t \to cq\bar{q}$ in two-Higgs-Doublet Models as a function of $\tan\beta$, from Deshpande *et al.*, Phys. Rev. D45, 178 (1992).

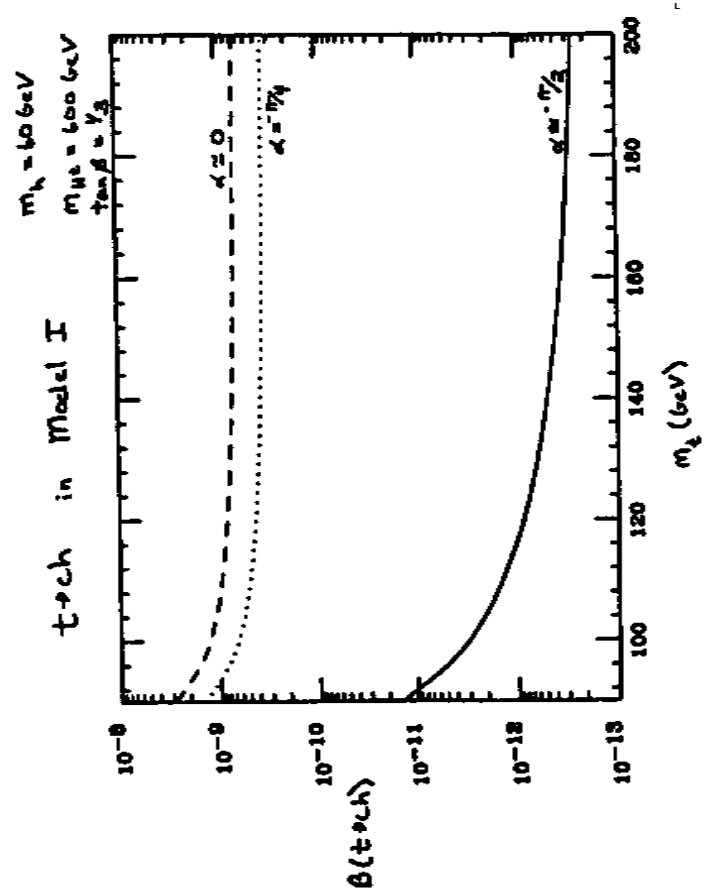

Branching fraction for $t \to ch$ in Model I, for $m_h = 60\,\text{GeV}$, $m_{H^\pm} = 600\,\text{GeV}$, $\tan\beta = 1/3$, and with various values of α as indicated. Here, α represents the mixing angle between the two Higgs Doublets.

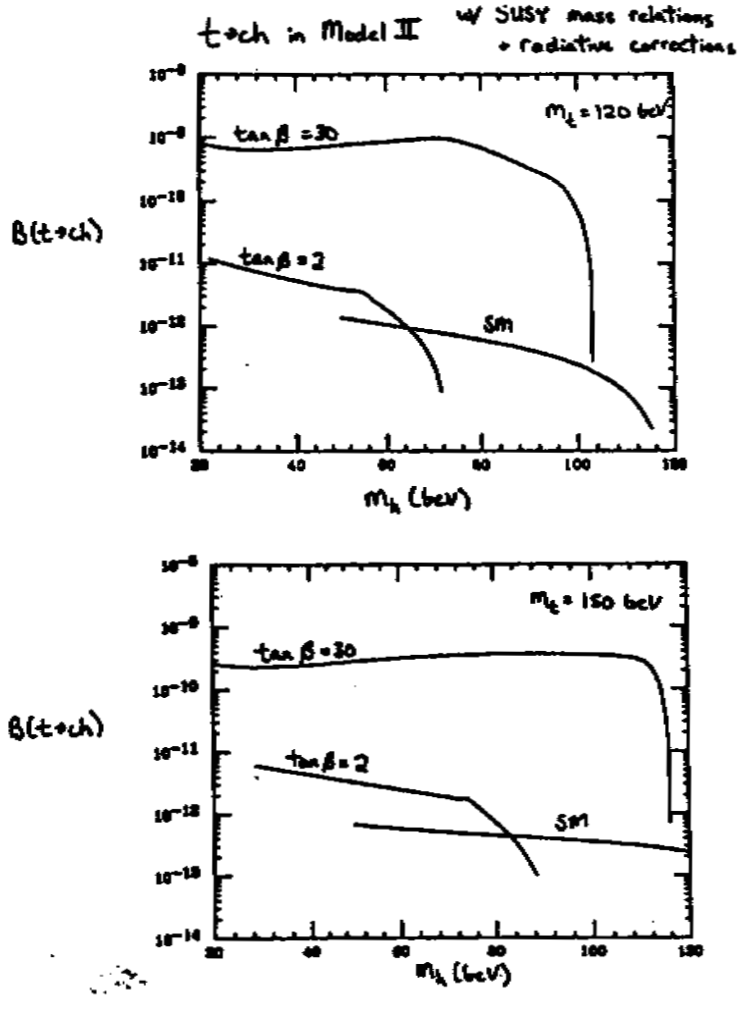

Branching fractions for $t \to ch$ in Supersymmetric models as a function of the lightest neutral Higgs mass, including the supersymmetric mass relations with full radiative corrections. The Standard Model curve is also shown for comparison.

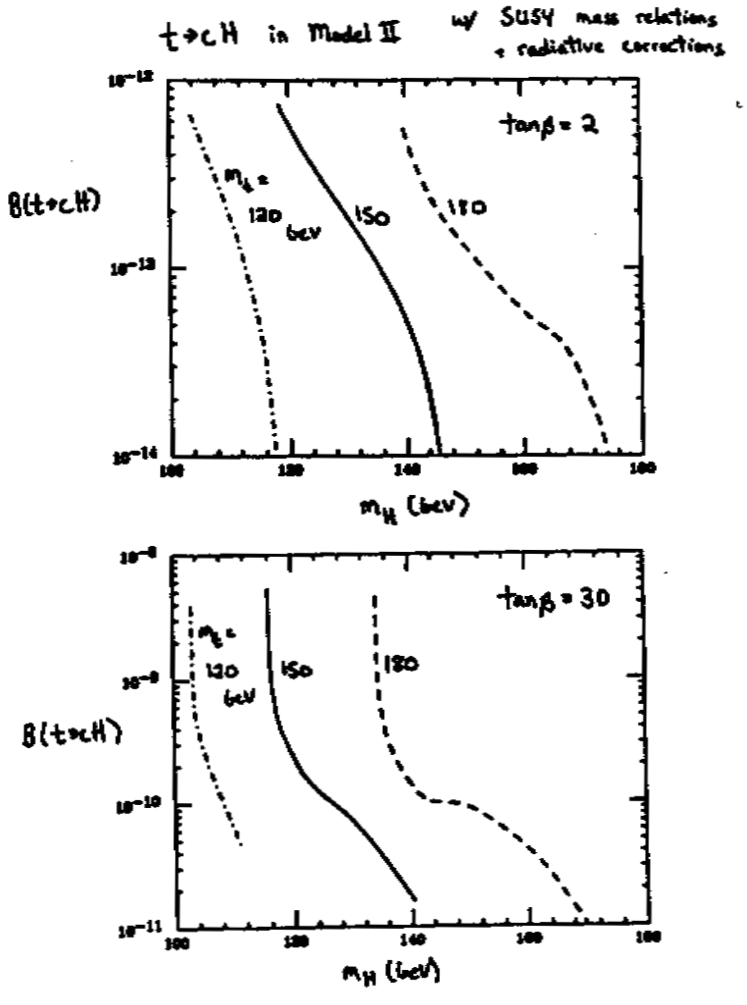

Branching fractions for $t \to cH$ in Supersymmetric models as a function of the *heaviest* neutral Higgs mass, including the supersymmetric mass relations with full radiative corrections, for the case when $m_W + m_c < m_t$.

Supersymmetry with Explicit $\not{R}$

Superpotential $W \sim \underbrace{QL\bar{D} + LL\bar{E}}_{\Delta L \neq 0} + \underbrace{\bar{U}\bar{U}\bar{D}}_{\Delta B \neq 0}$

$\Rightarrow$ can't exist simultaneously

"Baryon-Parity" - forbids $\Delta B \neq 0$ Operator

(Ibañez - Ross)

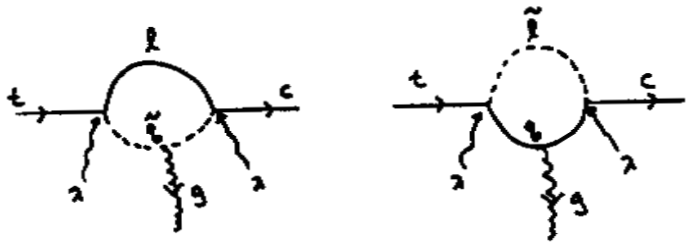

λ = "unknown" Yukawa coupling in W

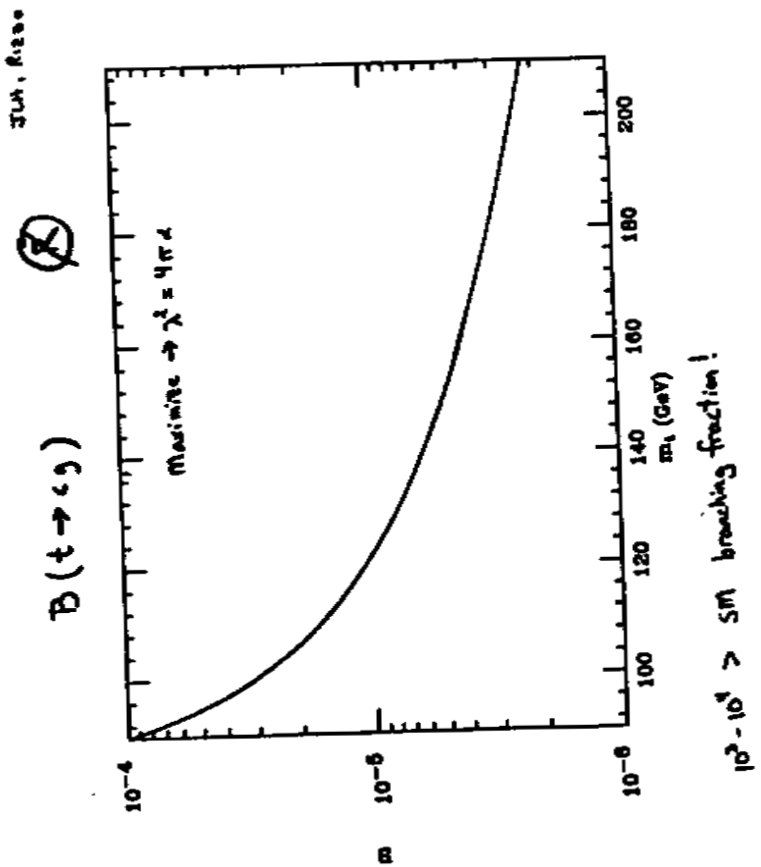

Branching fractions for the decay $t \to cg$ in supersymmetric models which contain explicit R-parity violation.

KAON PHYSICS

$K^+ \to \pi^+ \nu \bar{\nu}$

BNL E-787 $B(K^+ \to \pi^+ \nu\bar{\nu}) < 3.4 \times 10^{-7}$ (PV)
$< 5.4 \times 10^{-9}$ (PT)
$\sim 10^{-10}$ (???)

Contributing Diagrams

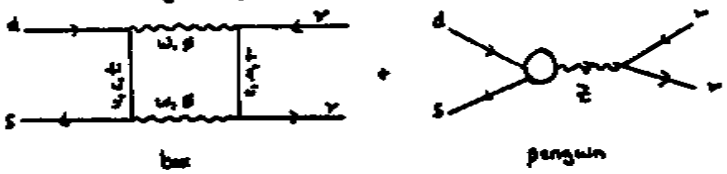

$$B(K^+ \to \pi^+ \nu\bar{\nu}) = \frac{G_F m_K^2 B(K^+ \to \pi^0 e^+ \nu)}{2\pi^2 |V_{us}|^2} \sum_{\ell i} \left| \sum_{q_j} V_{js}^* V_{jd} F\left(\frac{m_{q_j}^2}{m_W^2}, \frac{m_{\ell_i}^2}{m_W^2}\right) \right|^2$$

(Inami + Lim)

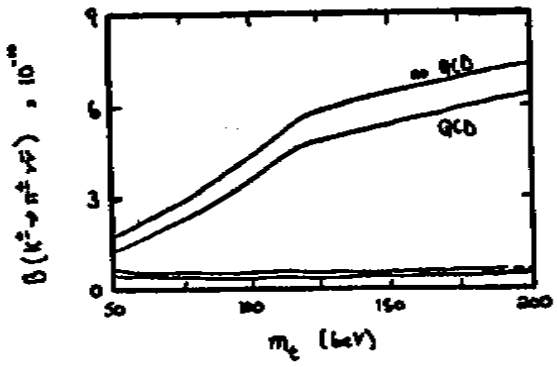

[C. Bib PhD thesis]

Caution: Watch for input parameters + approximations !!!

Rare B Decays

$b \to s e^+ e^-$

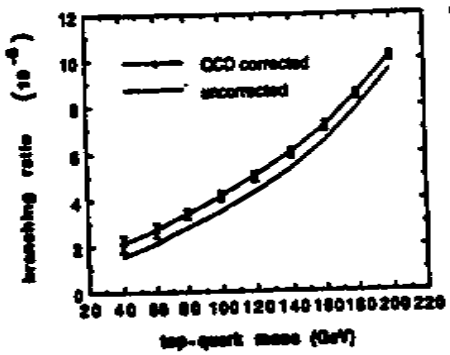

Grigjanis, O'Donnell, Sutherland, + Nawalkt

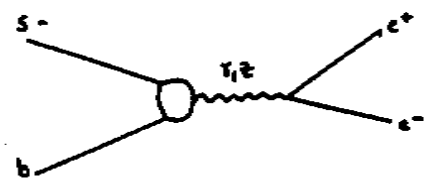

$B(b \to s e^+ e^-) \lesssim 10^{-4}$ (CLEO)

$b \to s\gamma$: Magnetic Dipole Transition

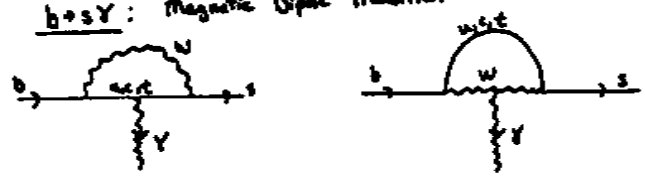

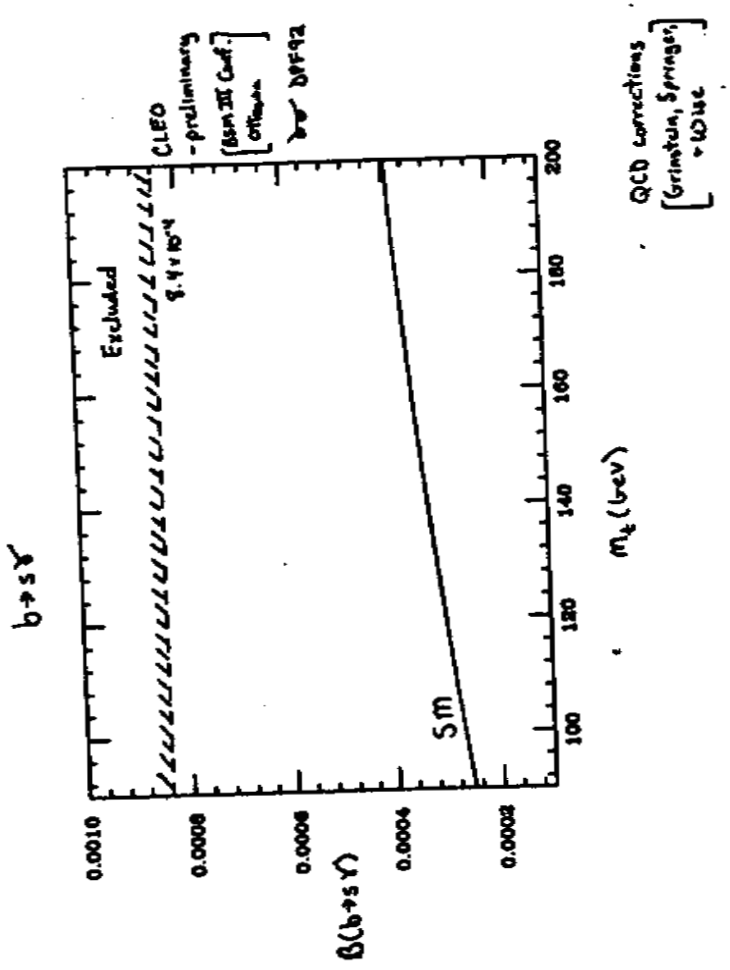

Branching fraction for the quark level process $b \to s\gamma$ in the Standard Model, employing the prescription of Grinstein *et al.*for the QCD corrections. The present 90% C.L. bound from CLEO on the inclusive process, $B(b \to s\gamma) < 8.4 \times 10^{-4}$ is also shown.

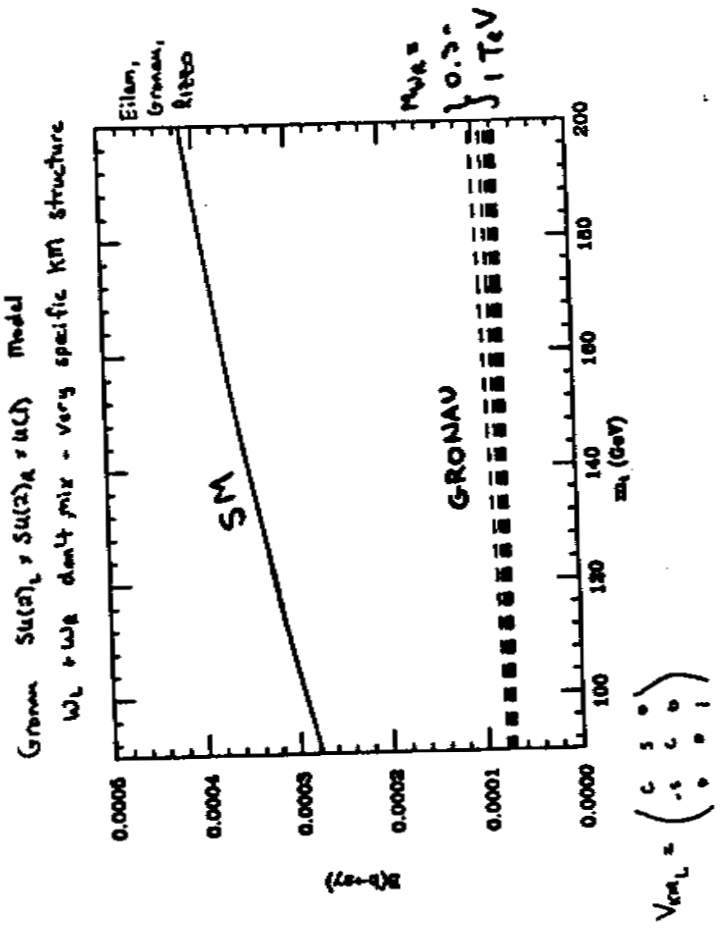

Values of $B(b \to s\gamma)$ in a $SU(2)_L \times SU(2)_R \times U(1)$ gauge model with $W_R = 0.3 - 1$ TeV as compared to the Standard Model branching fraction.

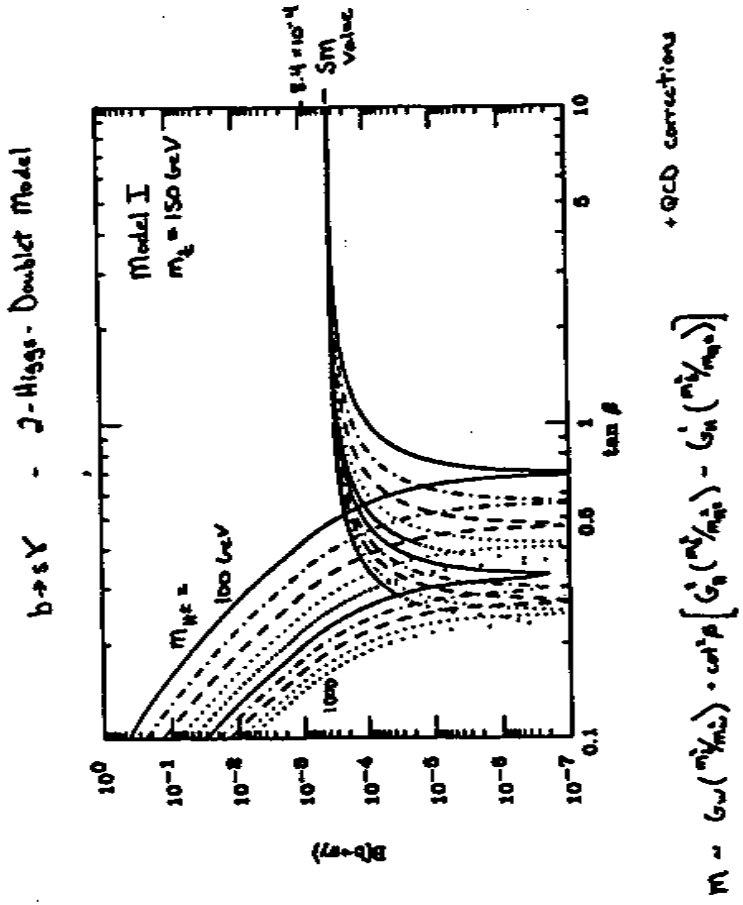

Branching fraction for $b \to s\gamma$ in the Model I version of two-Higgs-Doublet Models as a function of $\tan\beta$, for values of $m_{H^\pm} = 100 - 1000$ GeV in steps of 100 GeV and with $m_t = 150$ GeV.

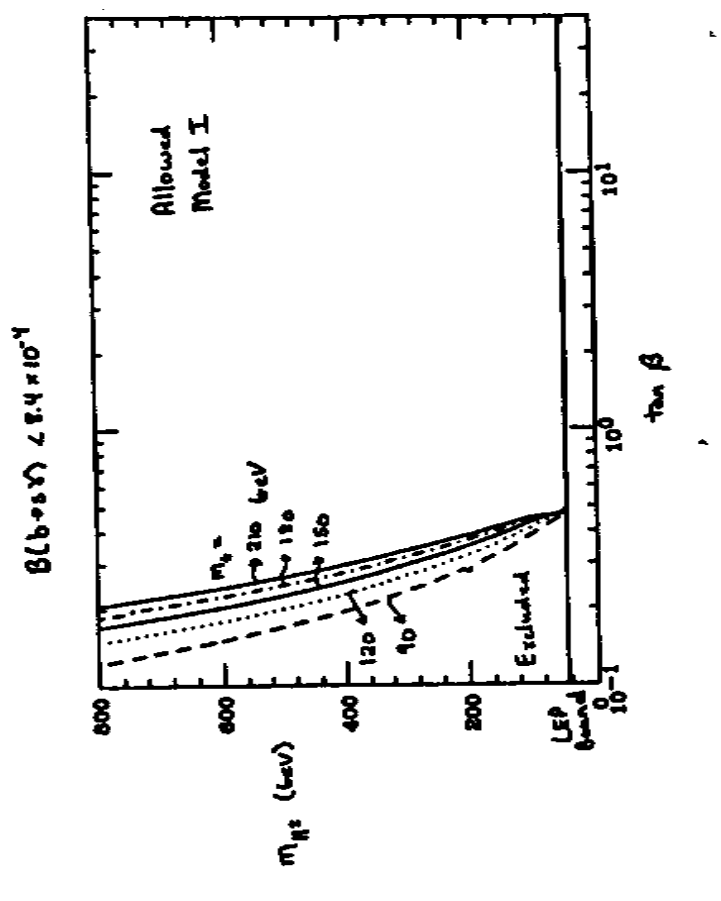

The bounds in the $m_{H^\pm} - \tan\beta$ plane in Model I for various values of m_t as indicated from imposing the CLEO limit $B(b \to s\gamma) < 8.4 \times 10^{-4}$. The excluded region lies to the left and bottom of the curves.

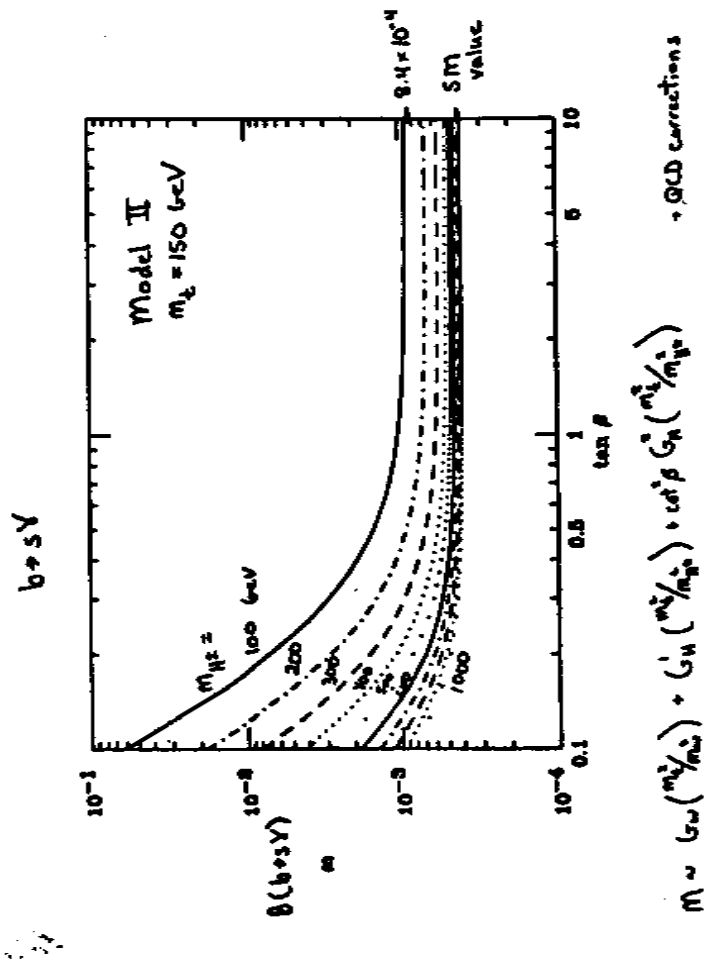

Branching fraction for $b \to s\gamma$ in the Model II version of two-Higgs-Doublet Models as a function of $\tan\beta$, for values of $m_{H^\pm} = 100 - 1000$ GeV in steps of 100 GeV and with $m_t = 150$ GeV.

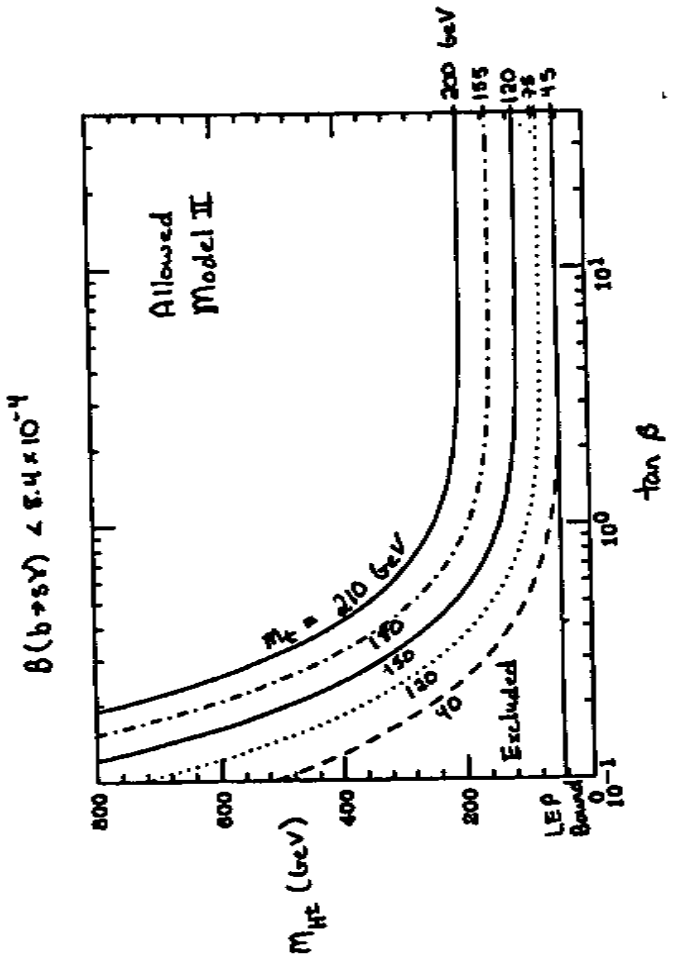

The bounds in the $m_{H^\pm} - \tan\beta$ plane in Model II for various values of m_t as indicated from imposing the CLEO limit $B(b \to s\gamma) < 8.4 \times 10^{-4}$. The excluded region lies to the left and bottom of the curves.

Summary

- Rare Decays of the top
  - rates are small in SM
  - Big enhancements for beyond SM physics
  - Should + WILL be looked for!

- $K \to \pi\nu\bar{\nu}$
  - Experiment is close to SM level

- $b \to s\gamma$
  - Experiment may be at SM level!
  - Update next week!
  - If observed @ SM rates
    $\Rightarrow$ STRONG constraints for non-SM physics

Top Quark and CP Violation

Darwin Chang

Department of Physics and Astronomy,

Northwestern University, Evanston, IL 60208, USA.

Abstract

We summarized the recent works on CP violation in high energy colliders related to top quark. After a short review of the fundementals of various kinds of CP violating observables, we use the examples worked out in the literature as examples to illustrate them in top decays and productions in the Standard Model and beyonds. Observables are all very small in the Standard Model, however, some of them may be quite promising if one is willing to goes beyond Standard Model. More detailed simulation of background and various potential event cuts are needed to investigate their feasibility.

Top and CP violation

D Chang

1. Role of top in CPX phenomenology and models
2. CPX related to top
   - (a) Decay
   - (b) Production
3. Conclusion

Top quark play 2 potential roles in CPX

(I) serves as the source of CPX (internal t)

(II) Serves as the stage of CPX (external t)

→ CPX in high energy scattering

Role (I) is more model-dependent

* In Standard K-M Model, top, as the 3rd generation plays a crucial role in the very existence of CPX

⇒ ϵ, ϵ'/ϵ are sensitive to the mass of the top quark and its mixing angles

CPX contains in 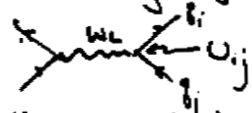

⇒ CPX quantities typically suppressed by multiple factors of mixing angles and lighter quark masses (m_c or m_s) and loop factors

→ Do not expect large effect at high energy – general (CPX at high energy "test" Standard Model)

In others models, t quark can induce CPX operators for lighter particles, such as EDM or CEDM of b quark or gluon

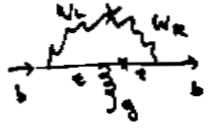

→ L-R models of CPX

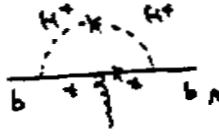

→ Charged Higgs models (Weinberg-Branco 3 doublets model)

t quark plays special role in Higgs models of CPX because the Higgs-Yukawa vertex ∝ m_q. Therefore larger m_q, larger CPX coupling

→ neutral Higgs models

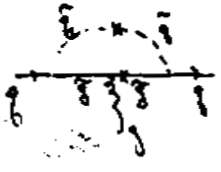

→ SUSY models (not so relevant to top)

(II) top as the stage for CPX

- Decay:
  - T-odd correlation
  - CP odd asymmetry (between t & $\bar{t}$)
- Production:
  - T odd correlation
  - CP odd correlation
  - CP odd asymmetry

Issues

(1) Where shall one looks for CPX?

(2) How well can one looks for CPX? $\delta \gtrsim 10^{-2}$?? (Im, Kane)

(3) Is there any model of CPX that gives large enough CP observables? (i.e. incentive for experiments?)

(1), (3) → overviews here

(2) → up for discussion (especially with experimentalists)

① $\hat{T}$-odd correlation (CPT in t-decay)

$t \to W^+ b$, $b \to \bar{b}c$, $t \to \bar{d}cd$, $u\gamma$

Transition matrix $\mathcal{M} = \frac{\mathcal{M}+\mathcal{M}^\dagger}{2} + \frac{\mathcal{M}-\mathcal{M}^\dagger}{2}$

<u>If $\mathcal{M}$ is invariant under T</u> then

$$\langle f|\mathcal{M}|i\rangle \overset{T}{=} \eta\left[\langle \hat{T}i|\frac{\mathcal{M}+\mathcal{M}^\dagger}{2}|\hat{T}f\rangle + \langle \hat{T}i|\frac{\mathcal{M}-\mathcal{M}^\dagger}{2}|\hat{T}f\rangle\right]$$

please

$$= \eta\left[\langle \hat{T}f|\frac{\mathcal{M}+\mathcal{M}^\dagger}{2}|\hat{T}i\rangle^* - \langle \hat{T}f|\frac{\mathcal{M}-\mathcal{M}^\dagger}{2}|\hat{T}i\rangle^*\right]$$

In Born approximation (No absorptive part)

$S \equiv \mathbb{1} + i\mathcal{M}$ — S matrix

Unitarity $SS^\dagger = \mathbb{1} \Rightarrow \mathcal{M} - \mathcal{M}^\dagger = 0 \Rightarrow \mathcal{M}$ hermitian

$\Rightarrow \langle f|\mathcal{M}|i\rangle = \eta\langle \hat{T}f|\mathcal{M}|\hat{T}i\rangle^*$

$\Rightarrow$ If O is an operator, odd under $\hat{T}$, then

$\mathrm{Prob.}(\langle O\rangle > 0) = \mathrm{Prob.}(\langle O\rangle < 0)$

e.g. $O = \vec{v}_1 \times \vec{v}_2 \cdot \vec{v}_3$ $\quad \vec{v}_i$ = momenta, spins

Therefore, in Born approx. (no absorptive part)

$\langle O_{T\text{-odd}}\rangle \neq 0 \Rightarrow T$ violation $\overset{CPT}{\underset{\text{Thm}}{\Longrightarrow}}$ CPX

<u>However</u>, at higher order approx. absorptive part of the amplitude can also give rise to $\langle O_{T\text{-odd}}\rangle \neq 0$.

At higher order, an antihermitian part of $\mathcal{M}$ will be induced (unitary correction)

$SS^\dagger = 1 \Rightarrow \mathcal{M} - \mathcal{M}^\dagger = i\mathcal{M}\mathcal{M}^\dagger$

or $\langle f|\mathcal{M} - \mathcal{M}^\dagger|i\rangle = i\sum_n (2\pi)^4\delta^4(P-P_n)\langle f|\mathcal{M}|n\rangle\langle n|\mathcal{M}^\dagger|i\rangle$

Typically $\mathcal{L}_{eff} = f_0\mathcal{L}_0 + f_1\mathcal{L}_1$

f_0: lowest order → real

f_1: complex form factor: complex due to ① CPX ② absorptive part

$\langle O\rangle$ = T-odd asymmetry $\propto \int_{\langle O\rangle>0} d\Gamma - \int_{\langle O\rangle<0} d\Gamma$

$\propto \mathrm{Im} f_1 f_0^* \propto \mathrm{Im} f_1 \propto i(\delta_{CP} + \delta_{abs})$

Make comparison with $\bar{t}$ decay (CP conjugated process)

① Distinguish between δ_{CP} and δ_{abs}

② Direct test of CP symmetry.

(1) For CP conjugated process, since all the vertices are complex conjugated

$\Rightarrow$ CPX phase, δ_{CP}, will change sign

However, the sign of the absorptive part phase, δ_{abs}, remains the same. (ignoring CPX)

$$\Rightarrow \bar{A}_{\bar{\sigma}} \propto \int_{\langle\sigma\rangle>0} d\bar{\Gamma} - \int_{\langle\sigma\rangle<0} d\bar{\Gamma} \underset{\pm}{\sim} i\left(-\delta_{CP} + \delta_{abs}\right)$$

$\Rightarrow$ $A_0 - \bar{A}_{\bar{\sigma}}$ $\rightarrow$ genuine signal of CP δ_{CP}

$A_0 + \bar{A}_{\bar{\sigma}}$ $\rightarrow$ signal of absorptive part δ_{abs}

δ_{abs} can be $\gg \delta_{CP}$, how well can one treat t and $\bar{t}$ equally in exp.

(2) CP asymmetry of partial rate

$$\propto \left|\langle f|m|i\rangle\right|^2 - \left|\langle \bar{f}|m|\bar{i}\rangle\right|^2 \qquad |\bar{i}\rangle = CP|i\rangle$$

Watch out for CPT constraint

$$CPT \Rightarrow \langle f|m|i\rangle = \langle \hat{i}|m|\hat{f}\rangle \qquad |\hat{i}\rangle = CP\hat{T}|i\rangle = \hat{T}|\bar{i}\rangle$$

$$\Rightarrow \langle f|m|i\rangle - \langle \hat{f}|m|\hat{i}\rangle^* = \langle f|m|i\rangle - \left(\langle \hat{i}|m|\hat{f}\rangle\right)^\dagger$$

$$\underset{CPT}{=} \langle f|m|i\rangle - \left(\langle f|m|i\rangle\right)^\dagger$$

In Born approx. (No absorptive part) $\Rightarrow$ m hermitian

$$\Rightarrow \langle f|m|i\rangle = \langle \hat{f}|m|\hat{i}\rangle^*$$

If $|i\rangle$ & $|f\rangle$ are $\hat{T}$ inv. then

CPT + Born approx. $\Rightarrow$ $\langle f|m|i\rangle = \langle \bar{f}|m|\bar{i}\rangle^*$

$\Rightarrow$ rate $(i \to f)$ = rate $(\bar{i} \to \bar{f})$

$\Rightarrow$ One need to go beyond Born approx. (need absorptive part) to bring out the CPX in rate asymmetry

then

$$\text{Rate}(\bar{i}\to\bar{f}) = \left|\langle \bar{f}|m|\bar{i}\rangle + \sum_{\bar{f}'} \langle \bar{f}|m|\bar{f}'\rangle\langle \bar{f}'|m|\bar{i}\rangle\right|^2 \qquad \sum_{\bar{f}} = \sum (2\pi)^4 \delta^4(p_f - p)$$

$$= \left|\langle f|m|i\rangle\right|^2 + i\sum_{f'} \langle \bar{f}|m|\bar{f}'\rangle \, \mathrm{Im}\left(\langle \bar{i}|m|\bar{f}\rangle\langle \bar{f}'|m|\bar{i}\rangle\right)$$

$$\Rightarrow \Delta_f = \text{Rate}(i\to f) - \text{Rate}(\bar{i}\to\bar{f})$$

$$= 2i\sum_{f'} \underbrace{\langle f|m|f'\rangle}_{\text{final state int}} \underbrace{\mathrm{Im}\left(\langle i|m|f\rangle\langle f'|m|i\rangle\right)}_{CPX}$$

$\Rightarrow$ (a) $f' \neq f$ (the final state interaction should be off-diagonal

(b) $\sum_{f \in \text{block}} \Delta_f = 0$

(a) (b) Typically $\rightarrow$ lead to suppression factor

- $\hat{T}$ odd correlation
- CP conjugate of $\hat{T}$ odd correlation
- CP asymmetry of partial rate

Example of $\hat{T}$ odd asymmetry — Grządkowski / Gunion / Liu / Kamefuchi / Yuan / Ito / Kane (91) / PRD 1992

$t \to W^+ b$, $\hookrightarrow \ell^+ \nu$

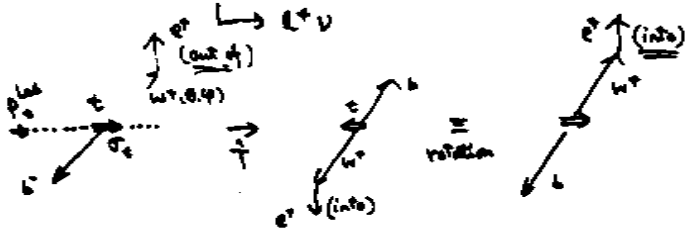

One can either use $\sigma_{top} \times P_b$ or $P_t^{lab} \times P_b$ to define decay plane

e^+ out of the plane $\xrightarrow{\hat{T}}$ e^+ into the plane

$$A \equiv \frac{\Gamma(e^+ \text{ out of } \phi) - \Gamma(e^+ \text{ into})}{\text{"} \quad + \quad \text{"}}$$

* It is easier, in the lab, to use P_t^{lab}, than σ_t, to define the plane. Then, if one integrates over $d\varphi$ of W^+, the transverse polarization $P_\perp$ of t average out $\Rightarrow$ only $P_\parallel$ contributes
* Need a production mechanism that produces large $P_\parallel$
  $W^+ g \to t\bar{b}$ from PRD 1992
* Need to reconstruct t and W momenta
* Need to cut down $gg \to t\bar{t}$ mechanism through cuts on extra jet, extra lepton veto to enhance signal and $P_\parallel$

* $G \equiv G$ estimates $A \sim 2\times10^{-3}$ is measurable
* Theory

$$\Gamma = \frac{-ig}{\sqrt{2}} \bar{u}(P_b)\left[\gamma^\mu\left(f_1^L P_L + f_1^R P_R\right) - i\frac{\sigma^{\mu\nu}k_\nu}{M_W}\left(f_2^L P_L + f_2^R P_R\right)\right]u(P_t)$$

$m_b = 0 \Rightarrow b$ is mostly left-handed in SM. $\Rightarrow f_1^L \sim 1$

$\Rightarrow$ $J \equiv (\#\, e^+ \text{ out of plane}) - (\#\, e^+ \text{ into}) \propto \mathrm{Im}\, f_1^L f_2^{R*}$
$\propto \mathrm{Im}\, f_2^R$

$\mathrm{Im}\, f_2^R = (\text{CPX contribution}) + (\text{absorptive part contribution})$

* Models: ① Standard Model $\to$ too small
  ② Neutral Higgs model (2 doublet model)

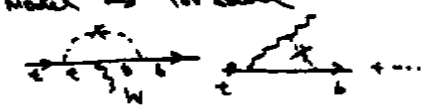

For $\langle\phi_1\rangle \hat{=} \langle\phi_2\rangle$
$M_{H^+} \approx M_h \approx 50$ GeV

$A \lesssim 5\times10^{-4}$ (m_t = 200 GeV)
1.5×10^{-3} (300 GeV)

UPR-0525T

Jiang Liu; calculate the $\hat{T}$ odd correlation due to absorptive part in Standard Model

Leading contribution

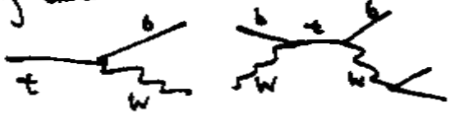

$A \cong 10^{-3} - 10^{-4}$

$m_t = 200$ GeV 100 GeV

~ One order of magnitude larger than neutral Higgs CPX (G & G)

$A = \delta_{CP} + \delta_{abs}$

$\bar{A} = -\delta_{CP} + \delta_{abs}$

CP asymmetry

I Standard Model

① $t \to q\gamma$

$q = u, c$

Jeshpande/Dattatreya/Mangelis/Trotter/Hamzeh PRD35 (1)

$A_q \equiv \dfrac{\Gamma(t \to q\gamma) - \Gamma(\bar{t} \to q\gamma)}{\text{"} \quad + \quad \text{"}}$

$A_q B(t \to q\gamma) \cong 2\times10^{-15}$ " $A^2 B < 10^{-17}$

② $t \to q W$, $W \to \bar{q} q'$ $t \to b c \bar{b}$, $d c \bar{d}$, $s c \bar{s}$

PRL62 (1)1177 Eilam/Hewett/Soni // Soares PRL62 (1)1492

A_1:

A_2: $t \to q' g$, $g \to q\bar{q}$ } use the interference of A_1 & A_2

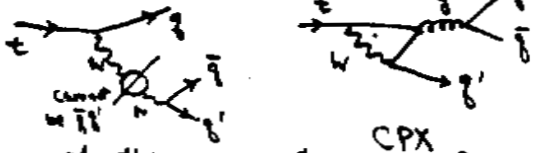

cannot w $\bar{q}q'$

absorptive part

CPX

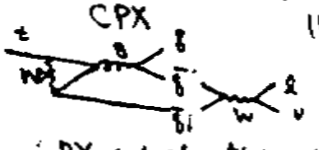

Need (for $m_t = 130$ GeV) 10^{16} tops or more

CPX and absorptive part

③ Ma/Brandenberg HB-THEP-92-11

$A \equiv \dfrac{\Gamma(t \to W^+ b) - \Gamma(\bar{t} \to W^- \bar{b})}{\Gamma(\text{"} \quad) + \Gamma(\text{"} \quad)}$

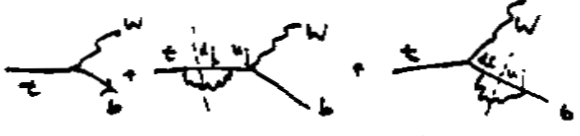

$A = -0.3\times10^{-11} J \cong 2\cdot10^{-16}$ $m_t = 130$ GeV

II Beyond S.M.

Eilam et. al. Technion-PH-92-1
Grz/Grzadkowski/Gunion UCD-92-5
Jiang Liu UPR-0526T

Charged Higgs model

$t \to W \tau \nu b$

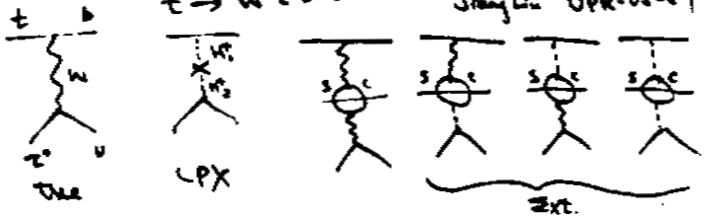

the CPX

* Ignore "Ext" and use the usual Breit-Wigner form

$$\frac{-i}{k^2-M_W^2+i\Gamma_W M_W}\left[g_{\mu\nu}-\frac{k_\mu k_\nu}{M_W^2-i\Gamma_W M_W}\right]$$

to calculate the absorptive part effect, one get ($M_{H^+}=85$ GeV, $m_t=150$ GeV)

$(\alpha^2 B)^{-1} = 3\times10^8$ (tops needed) , no m_t^2 dependence

* Liu: the width effect has to be included in the $k_\mu k_\nu$ part
– the propagator $\Leftrightarrow$ CPT
$\Rightarrow$ leading effect cancel a smaller by $10^{-4} \Rightarrow 10^{16}$ tops needed

* Just use the usual Cutkosky cut rule to calculate the absorptive part $\Rightarrow m_t^2$ not negligible $\Rightarrow$ "Ext" not negligible.

LPX in top production

I CP asymmetry

* How to see the top quark polarization ?

$t \longrightarrow W^+ b$, $W^+ \to \ell^+ \nu$ — Kang/Ladinsky/Yuan

$\uparrow$ longitudinal

In t rest frame

assuming the $m_b=0$, and b is left handed as in $SU(2)_L\times U(1)$

To get t_R (right handed helicity) in the lab., one boost to the right.
(L) (left) (left)

$\Rightarrow$ W^+ produced by t_R has higher energy than t_L

$\Rightarrow$ ℓ^+ from t_R decay has higher energy than from t_L

Similarly $W^- \longleftarrow \bar{t} \longrightarrow \bar{b}$

$\Rightarrow$ ℓ^- from $(\bar{t})_L$ decay has higher energy than from $(\bar{t})_R$

$\Rightarrow$ lepton energy can be used as top helicity analyzer (for $t\bar{t}$ above threshold)

* lepton energy is also the polarization analyzer of W

* What is polarization analyzer of Z ?

In $t\bar{t}$ production

Schmidt Peskin PRL 69 (1992)

$$t_L(\bar{t})_L \circlearrowleft CP$$
$$t_R(\bar{t})_R$$

$t_L\bar{t}_R$, $t_R\bar{t}_L$ are CP self conjugate

$$\Delta \equiv \frac{\text{Production}(t_L(\bar{t})_L) - \text{Prod}(t_R(\bar{t})_R)}{\text{all four } t\bar{t}} \quad \text{test CP}$$

measurement : use lepton energies as helicity analyzer

$$\Rightarrow \Delta_{E_\ell} = \frac{\frac{d\sigma}{dE(\ell^+)_\tau} - \frac{d\sigma}{dE(\ell^-)_\tau}}{\text{" + "}}$$

Where does it come from ?

in PP collider

$q\bar{q} \to t\bar{t}$, $gg \to t\bar{t}$ $\quad (W^+g \to t\bar{b})$

In neutral Higgs model

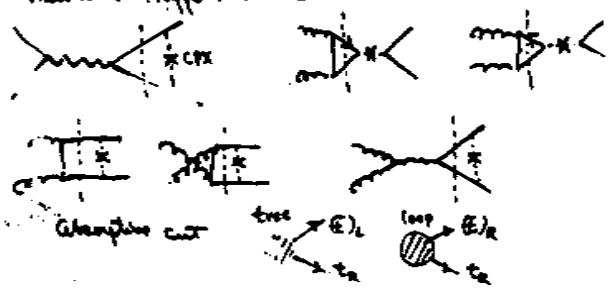

CPX
absorptive cut
tree
loop

$\Delta \to 0$ as $\beta \to 0$ due to lack of boost

$\to 0$ as $E_{CM} \to \infty$ due to helicity flip

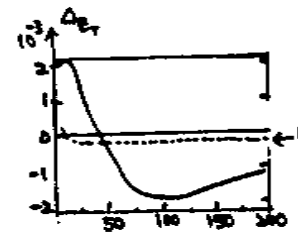
Δ_{E_τ}
background

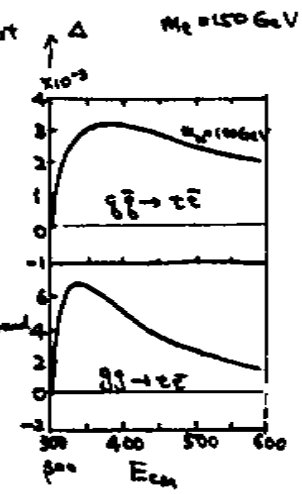
Δ
$M_H = 150$ GeV
$q\bar{q} \to t\bar{t}$
$gg \to t\bar{t}$
β_{top}
E_{CM}

Background

- Calorimeter charge symmetric ?
- q in p has more energy than $\bar{q}$ in p
  since $q\bar{q} \to t\bar{t}$ has a small loop induced F-B asymmetry
  $\Rightarrow$ more energy in $q \to$ more energy in t and $\bar{t}$
  $\to$ estimated to be small
- Other background ? (Kane)
  Wg production background. Cut ?!

Other applications of helicity analyzer

① If Higgs were identified, one can check the CP property of the Higgs using this analyzer — Chang/Keung NUHEP-TH-92-19

	C.P odd
$H \to t\bar{t}$	$(t_L\bar{t}_L)-(t_R\bar{t}_R)$
W^+W^-	$(W^+_L W^-_L)-(W^+_R W^-_R)$ ← not leading mode
ZZ	$Z_L Z_L - Z_R Z_R$ → no analyzer

$$\mathcal{A}_t = \frac{N(t_L\bar{t}_L)-N(t_R\bar{t}_R)}{\text{all}(t\bar{t})}$$

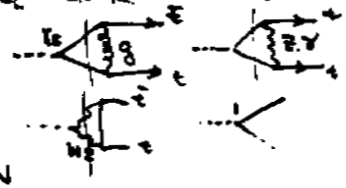

Can be as large as 10% for $M_H \cong 450$ GeV, $M_t = 200$ GeV

- $t\bar{t}$ is NOT the leading decay mode of H (5 ~ 20 %)
- Background, depending on the machine that H is produced.

$$\Delta_W = \frac{N(W^+_L W^-_L)-N(W^+_R W^-_R)}{N(W^+_L W^-_L)+N(W^+_R W^-_R)} \cong 3\% \quad \text{for } M_H = 400\text{ GeV},\ M_t = 150\text{ GeV}$$

$$\Rightarrow 2\Delta_W \times \left(\frac{\text{Transverse } W}{\text{all } W}\right) \sim 0.1\%$$

② Schmidt/Peskin observable in lepton collider

$e^+e^- \to t\bar{t}$

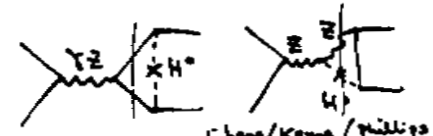

Chang/Keung/Phillips NUHEP-TH-92-19

$$\frac{N(t_L\bar{t}_L)-N(t_R\bar{t}_R)}{\text{all } t\bar{t}} \text{ can be as large as } 3\times10^{-3}$$

using $M_H = 50$ GeV, $M_t = 100$ GeV at $E_{cm} \sim 220$ GeV

* In leptonic environment, one can determine the polarization of individual top — Ladinsky/Yuan

Since $N(t_L\bar{t}_R)+N(t_R\bar{t}_L) \gg N(t_L\bar{t}_L)+N(t_R\bar{t}_R)$

Observability improved if one can select only the polarization combination we want.

$\Rightarrow$ Can probe $\dfrac{N(t_L\bar{t}_L)-N(t_R\bar{t}_R)}{N(\ )+N(\ )}$ at 10^{-2}–10^{-3} level in e^+e^- collider

↓ may not be [illegible] top [illegible]

③ Schmidt/Peskin observable in SUSY model.

Schmidt
SLAC preprint

$\Delta_{E_T} \sim 10^{-3}$ also

④ Phenomenological analysis of T-odd correlations in $e^+e^- \to \tau^+\tau^-$

Bernreuther Ma/
Schröder, Phem
HD-THEP-92-30
P.L.B 271 (92) 189

$\hat{k}_y \cdot \hat{d}_y$ $\hat{d}_y \simeq 0.013$ (MSSM $\simeq 0.010$) T-odd part of $\hat{d}_y \simeq 0.2$

T odd contribution due to CP even absorptive part

Bernreuther et. al.
HD-THEP-92-16

⑤ Phenomenological analysis of CP odd observables in e^+e^- collider (especially $e^+e^- \to t\bar{t}$)

C. Nelson
PR D41 (90) 2805

Atwood/Soni
PRD 45 (92) 2405

Conclusion

- Need more understanding of detectability and background (from experimentalists?)
- Most observables look hopeless
  But some has potential !!
- Need $\gtrsim \frac{1}{2}\%$ (as Kane said)?
- Need to look at "smarter" observables in collaboration with exp'l colleagues.
- Every beyond S.M. is just a guess out of infinite number of possibility
  Experimentalist should proceed to try to measure whatever is plausible.

Fermion Masses and Mixings

M. S. Berger

Physics Department, University of Wisconsin, Madison, WI 53706, USA

ABSTRACT

We describe the evolution of the Yukawa couplings and the CKM matrix. The constraints obtained from Yukawa coupling unification at the GUT scale is discussed. Some models for GUT scale textures and their experimental consequences are described.

Fermion Masses and Mixings

M. Berger - Wisconsin

What is the top quark mass?

- Direct Searches
- Electroweak Radiative Corrections
- Make Additional Assumptions About New Physics, e.g. GUTs
  - Heavy top quark has a substantial effect on renormalization group (RG) evolution

$$\lambda_t \simeq 1 \rightarrow y_t = \frac{\lambda_t^2}{4\pi} \simeq 0.1$$

comparable to gauge couplings

Requiring GUT Scale Constraint

$$\lambda_b(M_G) = \lambda_\tau(M_G)$$

$$|V_{cb}(M_G)|^2 = \frac{\lambda_c}{\lambda_t}(M_G)$$

puts constraint on m_t (and possibly $\tan\beta$)

OR

Knowing m_t lets us test what GUT scale constraints are viable.

Berger, MB, Hou, Zralek
Berger, MB, Ohmann

Gauge Coupling Evolution

RGE:

$$\frac{dg_i}{dt} = \frac{g_i}{16\pi^2}\Big[\underbrace{b_i g_i^2}_{\text{one-loop}} + \underbrace{\frac{1}{16\pi^2}\Big(\sum_{j=1}^{3} b_{ij} g_i^2 g_j^2 - \sum_{j=t,b,\tau} a_{ij} g_i^2 \lambda_j^2\Big)}_{\text{two-loop}}\Big]$$

- Yukawas enter at two-loop level and therefore have a small effect (often neglected)

$$\frac{d\lambda_t}{dt} = \frac{\lambda_t}{16\pi^2}\Big[-\sum c_i g_i^2 + \underline{6\lambda_t^2 + \lambda_b^2}\Big] + \text{two-loop}$$

- Much bigger effect on running of Yukawa couplings themselves

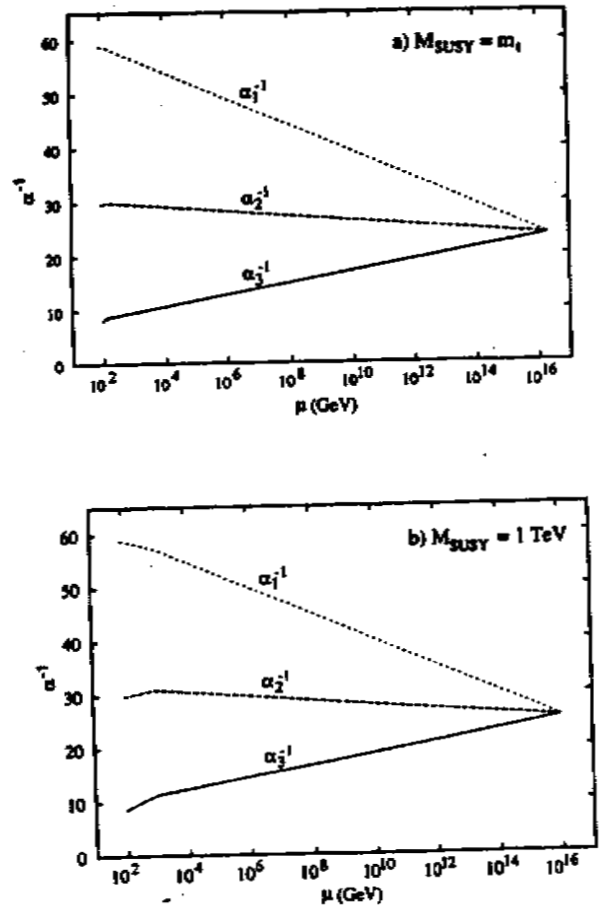

Gauge coupling evolution for two values of the supersymmetric scale.

1) Universal Scaling of CKM Matrix

2) Yukawa Evolution – Fermion Masses

3) Yukawa Evolution – Fermion Masses and Mixings (CKM elements)

Universal Evolution of Yukawa Couplings and CKM Matrix

1979 Ma, Pakvasa – evolution equation for the Cabibbo angle

1986-7 Sasaki, Babu
- evolution equations for three generation case that preserves unitarity of V

Yukawa Matrices

$\mathbb{U}$ – up-type quarks
$\mathbb{D}$ – down-type quarks
$\mathbb{E}$ – charged leptons

$$\left.\begin{aligned} \mathbb{U}^{diag} &= V_u^L\, \mathbb{U}\, V_u^{R\dagger} \\ \mathbb{D}^{diag} &= V_d^L\, \mathbb{D}\, V_d^{R\dagger} \end{aligned}\right\} \quad V_{evo} = V = V_u^L V_d^{L\dagger}$$

ONE-LOOP RENORMALIZATION GROUP EQUATIONS

$$\frac{d\mathbb{U}}{dt} = \frac{1}{16\pi^2}\left[x_u I + x_3 \mathbb{U}\mathbb{U}^\dagger + a_u \mathbb{D}\mathbb{D}^\dagger\right]\mathbb{U}$$

$$\frac{d\mathbb{D}}{dt} = \frac{1}{16\pi^2}\left[x_d I + x_3 \mathbb{D}\mathbb{D}^\dagger + a_d \mathbb{U}\mathbb{U}^\dagger\right]\mathbb{D}$$

$$\frac{d\mathbb{E}}{dt} = \frac{1}{16\pi^2}\left[x_e I + x_3 \mathbb{E}\mathbb{E}^\dagger\right]\mathbb{E}$$

$$x = x(g_i^2, \mathrm{Tr}[\mathbb{U}\mathbb{U}^\dagger], \mathrm{Tr}[\mathbb{D}\mathbb{D}^\dagger], \ldots, \lambda_j)$$

$$\frac{dV_{id}}{dt} = \frac{1}{16\pi^2}\left[a_u \sum_{i\neq j,p} \frac{\lambda_i^2+\lambda_j^2}{\lambda_i^2-\lambda_j^2}\lambda_p^2 V_{ip}V_{jp}^* V_{jd} + a_d \sum_{p\neq d,j} \frac{\lambda_d^2+\lambda_p^2}{\lambda_d^2-\lambda_p^2}\lambda_j^2 V_{jp}^* V_{jd} V_{ip}\right]$$

– gauge couplings cancel

The one-loop renormalisation group equations for the Yukawa matrices U, D and E. Only the terms involving a_u and a_d can contribute to the evolution of the CKM matrix V. The one-loop evolution equation is given for V.

UNIVERSAL SCALING IS VALID TO LEADING ORDER IN THE

1) MASS HIERARCHY $m_u, m_c \ll m_t$, $m_d, m_s \ll m_b$, $m_e, m_\mu \ll m_\tau$

2) CKM HIERARCHY $|V_{cb}|^2, |V_{ub}|^2, J \ll 1$

$$\boxed{J = \mathrm{Im}(V_{ud}V_{cb}V_{ub}^* V_{cd}^*) \quad \text{rephase-invariant}}$$

$$\mathbb{U}^{\mathrm{diag}}(\mu') = \begin{pmatrix} S_u(\frac{\mu'}{\mu})\lambda_u & & \\ & S_u(\frac{\mu'}{\mu})\lambda_c & \\ & & S_t(\frac{\mu'}{\mu})\lambda_t \end{pmatrix}$$

Babu, Shafi

$$|V|^2(\mu') = \begin{pmatrix} |V_{ud}|^2(\mu) & |V_{us}|^2(\mu) & S(\frac{\mu'}{\mu})|V_{ub}|^2(\mu) \\ |V_{cd}|^2(\mu) & |V_{cs}|^2(\mu) & S(\frac{\mu'}{\mu})|V_{cb}|^2(\mu) \\ S(\frac{\mu'}{\mu})|V_{td}|^2(\mu) & S(\frac{\mu'}{\mu})|V_{ts}|^2(\mu) & |V_{tb}|^2(\mu) \end{pmatrix}$$

$$J(\mu') = S(\frac{\mu'}{\mu})\, J(\mu)$$

The mixing between the first and third generations and the second and third generations and the rephase-invariant CP violating parameter J scale by the same factor $S(\mu'/\mu)$ to leading order in the mass hierarchy $m_u, m_c \ll m_t$, $m_d, m_s \ll m_b$, $m_e, m_\mu \ll m_\tau$ and the CKM hierarchy $|V_{cb}|, |V_{ub}|, J \ll 1$. See also K. S. Babu and Q. Shafi, Bartol Research preprint BA-92-70 (1992).

TO LEADING ORDER

$$\frac{dW_1}{dt} = -\frac{W_1}{8\pi^2}\left(a_d\lambda_s^2 + a_u\lambda_b^2\right)$$

$$\frac{dW_2}{dt} = \frac{W_2}{8\pi^2}(0)$$

$W_1 = |V_{cb}|^2, |V_{ub}|^2, |V_{us}|^2, |V_{cd}|^2, J$

$W_2 = |V_{us}|^2, |V_{cd}|^2, |V_{cb}|^2, |V_{cs}|^2, |V_{ud}|^2$

CONSEQUENCES

- $|V_{cb}|(M_Z) \neq 0 \Rightarrow |V_{ub}|(M_Z) \neq 0.$
- $\left|\frac{V_{ub}}{V_{cb}}\right|$ does not scale.
- $|V_{us}|$ does not scale.
- All orders in perturbation theory.

The evolution equations to leading order in the mass and CKM hierarchies.

- UNIVERSALITY OF SCALING IS MODEL-INDEPENDENT (Standard Model, Two-Higgs Doublet Minimal Supersymmetric)

- Scaling FACTORS DEPEND ON MODEL

$S\left(\frac{\mu'}{\mu}\right) > 1$ SM

$S\left(\frac{\mu'}{\mu}\right) < 1$ Two-Higgs, MSSM

$\mu' > \mu$

The pattern (i.e. universality) of scaling is model-independent but the amount of scaling depends on the model. For example, in the standard model V_{ub}, V_{us} and J grow with increasing scale, while in the MSSM these quantities decrease. This behaviour is dictated by the sign of a_u and a_d.

$$\frac{dW_1}{dt} = -\frac{W_1}{8\pi^2}\left[a_u\lambda_b^2 + a_d\lambda_t^2\right]$$

In MSSM: $a_u = a_d = 1$

$$\boxed{S(m_t) = \exp - \frac{1}{8\pi^2}\int_{m_t}^{M_G}\left(a_u\lambda_b^2 + a_d\lambda_t^2\right)}$$

approximation good to $\leq 0.1\%$

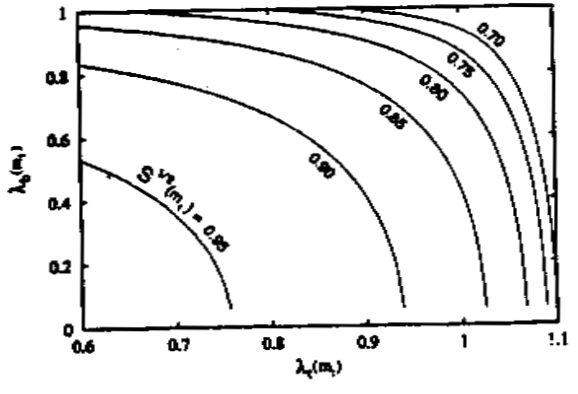

A concrete example of the scaling in the MSSM. The universality is violated by $\lesssim 0.1\%$. For example the ratio $|V_{td}/V_{ts}|$ changes by less than 0.1% between the GUT scale and the electroweak scale.

---- $\lambda_b(M_G) = \lambda_\tau(M_G)$

$S^{1/2} \simeq 0.75$

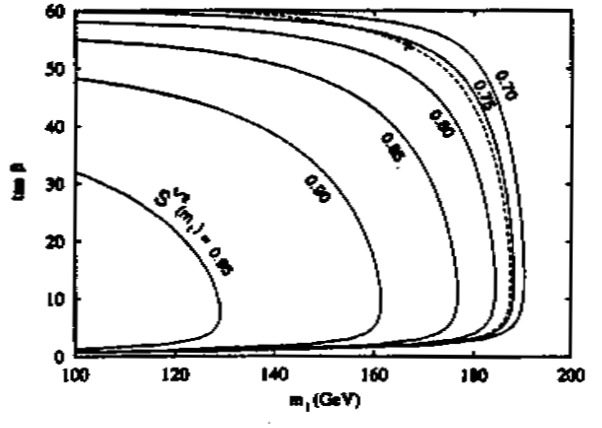

Requiring that $\lambda_b(M_G) = \lambda_\tau(M_G)$ fixes $S^{1/2} \simeq 0.75$.

YUKAWA EVOLUTION

CHANOWITZ, ELLIS, GAILLARD:

$$\lambda_b(M_G) = \lambda_\tau(M_G) \xrightarrow{\text{RGE}} \lambda_b(m_b) = S'\lambda_\tau(m_b)$$

QCD + QED scaling

$$\boxed{m_b(m_b) = S'\frac{\eta_b}{\eta_\tau}\, m_\tau(m_\tau)}$$

S', η_b, η_τ are calculable scaling factors that depend on gauge couplings and Yukawa couplings.

$\alpha_s^{(M_Z)} \sim 0.11$ $\quad \eta_b = 1.47$, $\eta_c = 1.90$, $\eta_s = \eta_d = 2.04$, $\eta_u = 2.05$ $\quad \frac{\eta_b}{\eta_\tau} = 1.45$

$\alpha_s(M_Z) = 0.12$ $\quad \eta_b = 1.55$, $\eta_c = 1.90$, $\eta_s = \eta_d = 2.04$, $\eta_u = 2.05$ $\quad \frac{\eta_b}{\eta_\tau} = 1.53$

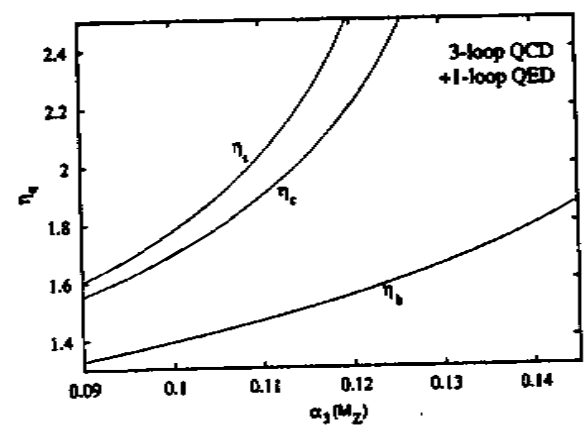

Scaling factors as a function of $\alpha_s(M_Z)$.

One-Loop Renormalization Group Equations (RGEs)

$$\frac{d\lambda_b}{dt} = \frac{\lambda_b}{16\pi^2}\left(-\sum c_i' g_i^2 + \lambda_t^2 + 6\lambda_b^2 + \lambda_\tau^2\right)$$

$$\frac{d\lambda_\tau}{dt} = \frac{\lambda_\tau}{16\pi^2}\left(-\sum c_i'' g_i^2 + 3\lambda_b^2 + 4\lambda_\tau^2\right)$$

$$c_i' = \left(\tfrac{7}{15}, 3, \tfrac{16}{3}\right) \qquad c_i'' = \left(\tfrac{9}{5}, 3, 0\right)$$

$$\boxed{R_{b/\tau}(\mu) = \frac{\lambda_b}{\lambda_\tau}(\mu)}$$

$$\boxed{\frac{dR_{b/\tau}}{dt} = \frac{R_{b/\tau}}{16\pi^2}\left(-\sum d_i g_i^2 + \lambda_t^2 + 3\lambda_b^2 - 3\lambda_\tau^2\right)}$$

$$d_i \equiv c_i' - c_i'' = \left(-\tfrac{4}{3}, 0, \tfrac{16}{3}\right)$$

One-loop renormalization group equations for the Yukawa couplings and the λ_b/λ_τ ratio.

For $\tan\beta \leq 10$ the bottom and tau Yukawas can be neglected in the RGE evolution

$$\lambda_b \ll 1 \;, \quad \lambda_\tau \ll 1$$

$$\frac{dg_i}{dt} = \frac{g_i}{16\pi^2}\left[b_i g_i^2\right] \qquad b_i = \left(\tfrac{33}{5}, 1, -3\right)$$

$$\frac{dR_{b/\tau}}{dt} = \frac{R_{b/\tau}}{16\pi^2}\left(-\sum d_i g_i^2 + \lambda_t^2\right)$$

Solution is

$$R_{b/\tau}(\mu) = \frac{x^{1/2}}{x}\, y\, \overbrace{R_{b/\tau}(M_G)}^{\equiv 1}$$

$$\frac{x^{\frac{1}{2}}}{x} = \left(\frac{g_G}{g_i}\right)^{d_i/b_i} = \left(\frac{g_G}{g_i}\right)^{\frac{c_i' - c_i''}{b_i}} \sim 2.$$

$$y = \exp\left\{-\frac{1}{16\pi^2}\int_{\mu}^{M_G} \lambda_t^2(\mu')\, d\ln\mu'\right\}$$

A useful approximation for small to moderate $\tan\beta$ is to neglect the bottom and tau Yukawa couplings relative to the top Yukawa coupling and the gauge couplings. Then the RGEs admit an semi-analytic solution at the one-loop level.

LINEAR RELATIONSHIP BETWEEN m_t and $\sin\beta$ for $\tan\beta \lesssim 10$

$$\frac{dR_{b/\tau}}{dt} = \frac{R_{b/\tau}}{16\pi^2}\left(\frac{4}{3}g_1^2 - \frac{16}{3}g_3^2 + \lambda_t^2\right)$$

Given fixed values for $g_1(m_t)$, $g_3(m_t)$, m_b, m_τ determines a unique value for $\lambda_t(m_t)$.

$$\lambda_t(m_t) = \frac{\sqrt{2}\, m_t}{v_2} = \frac{\sqrt{2}\, m_t}{v \sin\beta} = \underline{\text{constant}}$$

The top Yukawa coupling λ_t must be large enough to suppress the m_b/m_τ ratio. This leads to $\lambda_t(m_t)$ near its infrared fixed point for small enough $\tan\beta$.

One-loop semi-analytic solution

$$\frac{m_b}{\sin\beta} = m_\tau \sqrt{\frac{27}{32}}\left[1 - \eta^n\right]^{1/2}$$

$$I \equiv \int_{m_t}^{M_G} \eta(\mu')\, d\ln\mu' \sim 115$$

INCLUDING FULL TWO-LOOP EVOLUTION

$$\sin\beta = \left(0.78 \underbrace{\pm 0.05}_{\alpha_s,\ M_{SUSY},\ \text{thresholds}}\right)\left(\frac{m_t}{150\,\text{GeV}}\right)$$

This result is valid for

$m_t \lesssim 175$ GeV or $\tan\beta \lesssim 10$

A fixed point exists at $\lambda_b \approx 1$, so that $\lambda_b(\mu)$ grows as one approaches the GUT scale, $\mu \to M_G$.

From the $\frac{m_b}{m_\tau}$ constraint, smaller m_b requires larger $\lambda_b(\mu)$.

$$\boxed{\frac{m_b}{m_\tau} = \frac{\eta^{1/2}}{x}\, y\, \frac{\eta_b}{\eta_\tau} \qquad y = \exp\left\{-\frac{1}{16\pi^2}\int_{m_b}^{M_G} \lambda_b^2(\mu')\, d\ln\mu'\right\}}$$

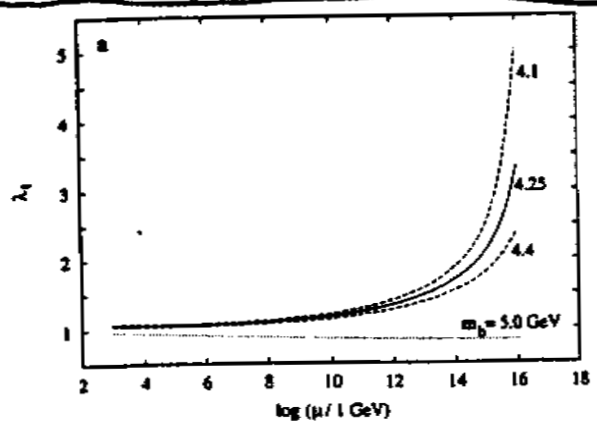

The amount of scaling is given by the integral $y(\mu) = \exp\left\{-\frac{1}{16\pi^2}\int_{\mu}^{M_G} \alpha_4 \lambda_b^2(\mu')\, d\ln\mu'\right\}$. From the curve one sees that the fixed point in $\lambda_b(m_t)$ is obtained for a wide range of values for y.

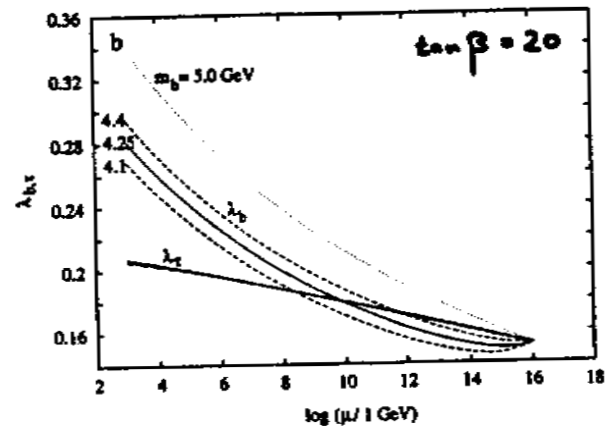

Evolution of the bottom and tau Yukawa couplings. We have taken $\lambda_b(M_G) = \lambda_\tau(M_G)$ exactly. Larger values of $\lambda_b(M_G)$ are required for the smaller target values of m_b.

Perturbative CONSTRAINT :

Require that $\lambda_t(\mu)$ be perturbative over the entire range $m_t < \mu < M_G$

$$\frac{d\lambda_t}{dt} = \frac{\lambda_t}{16\pi^2}\Big[\Big(-\sum c_i g_i^2 + 6\lambda_t^2 + \lambda_b^2\Big) + \frac{1}{16\pi^2}\Big(\mathcal{O}(g_i^2 g_j^2) + \mathcal{O}(\lambda_t^2 g_i^2) - 22\lambda_t^4 + 5\lambda_t^2\lambda_b^2 + 5\lambda_b^4 + \lambda_b^2\lambda_\tau^2\Big)\Big]$$

Increasing $\alpha_3(M_Z)$ $\Rightarrow$ increasing $\lambda_t(\mu)$

$$\frac{dR_{b/\tau}}{dt} = \frac{R_{b/\tau}}{16\pi^2}\Big(\frac{4}{3}g_1^2 - \frac{16}{3}g_3^2 + \lambda_t^2\Big)$$

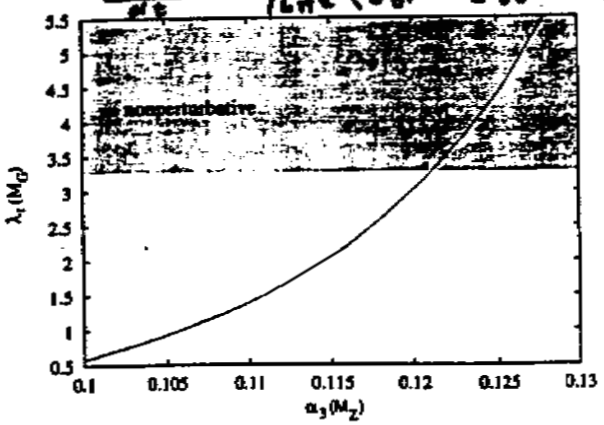

By considering the two-loop contributions a quantitative estimate of the viability of perturbation theory can be obtained. Here we require that the two-contribution to the evolution of $d\lambda_t/dt$ always be less than a quarter of the one-loop contribution. This gives the constraint $\lambda_t(M_G) \leq 3.3$.

• INCREASING $\alpha_3(M_Z)$ $\Rightarrow$ increasing λ_t i.e. larger values of m_t

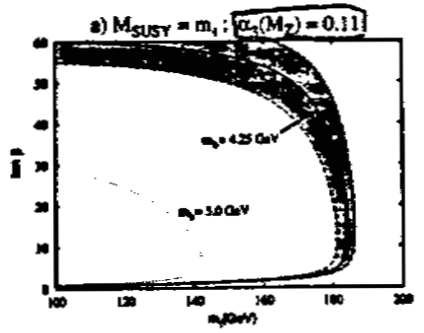

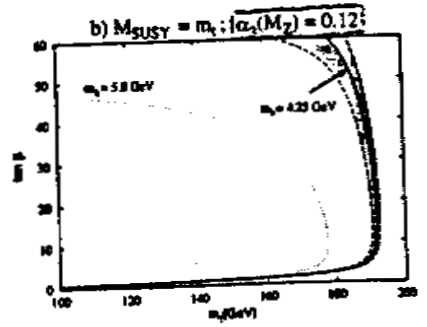

FOR LARGE $\tan\beta$ ($\gtrsim 10$), analytic solutions are not available

- approximations
- numerical

CAN UNDERSTAND BEHAVIOR QUALITATIVELY

$$\frac{dR_{b/\tau}}{dt} = \frac{R_{b/\tau}}{16\pi^2}\left(-\sum d_i g_i^2 + \lambda_b^2 + \underbrace{3\lambda_b^2 - 3\lambda_\tau^2}\right)$$

predominantly positive over the range $m_t < \mu < M_q$

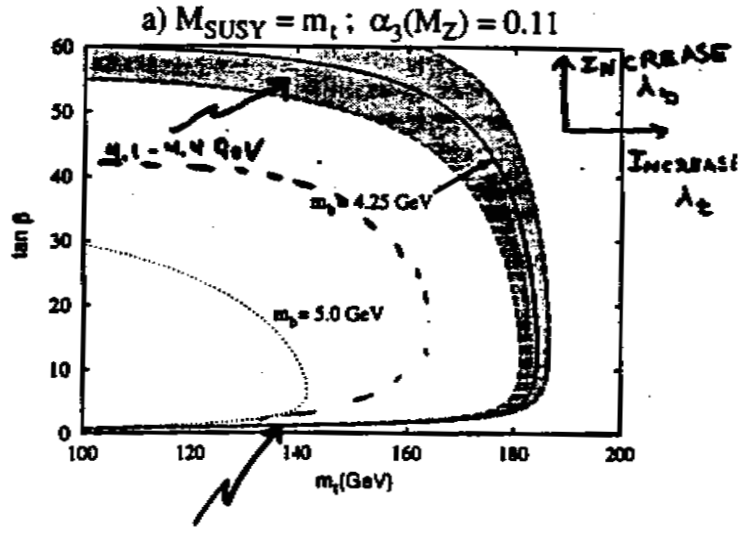

Linear region $\sin\beta \approx 0.78\left(\frac{m_t}{150\,\text{GeV}}\right)$

1) Upper limit on m_t

2) Two solutions for $\tan\beta$ for most values of m_t

The constraint from $\lambda_b(M_G) = \lambda_\tau(M_G)$. The lower "linear" region is the fixed point region for λ_τ. By making λ_b (and hence $\tan\beta$) sufficiently large, this region can be avoided by suppressing the required top quark Yukawa coupling. Another possibility is to take sufficiently large GUT scale threshold corrections to unification constraint $\lambda_b(M_G) = \lambda_\tau(M_G)$.

• Increasing M_{SUSY} ⇒ increasing λ_t
Top squark scaling in the SUSY regime must be increased to counteract inverse scaling in the non-SUSY regime

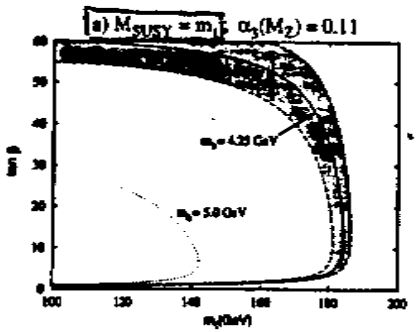

• Effect is rather mild.

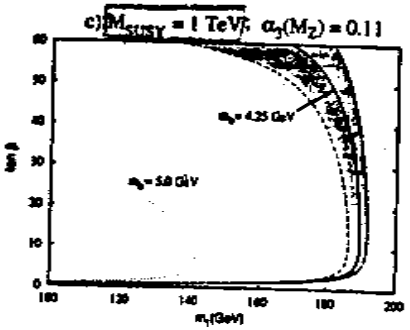

• For $\alpha_3(M_Z) = 0.11$, all solutions are perturbative.

• $\lambda_t = \lambda_b = \lambda_\tau(M_G)$ for large $\tan\beta$

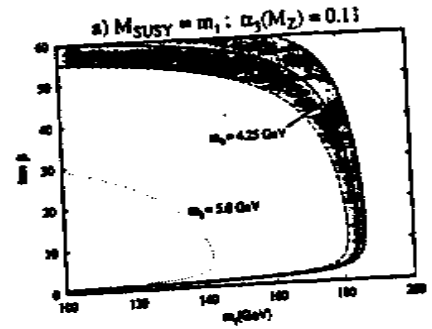

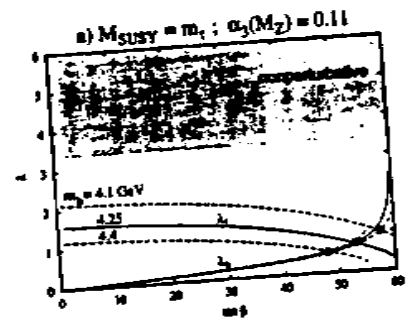

- For $\alpha_3(M_Z) = 0.12$, $m_b = 4.1$ GeV contour has a nonperturbative $\lambda_t(\mu)$ near the GUT scale.

- Raising M_{SUSY} is similar to raising $\alpha_3(M_Z)$ but generally the effect is smaller.

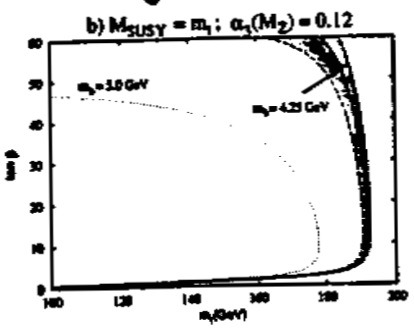

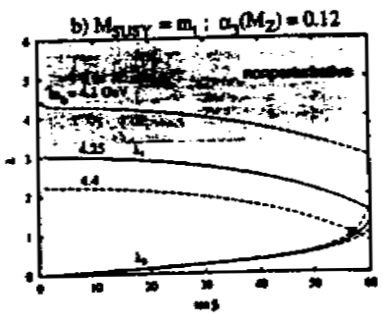

Also

$$R_{s/\mu} = \frac{\lambda_s}{\lambda_\mu} \qquad R_{d/e} = \frac{\lambda_d}{\lambda_e}$$

$$R_{s/\mu}(M_G) = \frac{1}{3} \qquad R_{d/e}(M_G) = 3$$

$$\frac{dR_{s/\mu}}{dt} = \frac{R_{s/\mu}}{16\pi^2}\left(-\Sigma d_i g_i^2\right)$$

$$\boxed{\frac{\lambda_s}{\lambda_\mu} = \frac{\eta^{1/2}}{x}\,\frac{1}{3}}$$

$$\boxed{\frac{\lambda_d}{\lambda_e} = \frac{\eta^{1/2}}{x}\,3}$$

Other Yukawa unification conditions.

FERMION MIXINGS

GATTO, SARTORI, TONIN
CABIBBO, MAIANI (1968) $\tan\theta_c = \sqrt{\frac{m_d}{m_s}}$
OAKES

WEINBERG (1977) $\tan\theta_c \approx \sqrt{\frac{m_d}{m_s}} - \sqrt{\frac{m_u}{m_c}}$
WILCZEK, ZEE

FRITZSCH: $\mathbb{U} = \begin{pmatrix} 0 & C & 0 \\ C & 0 & B \\ 0 & B & A \end{pmatrix}$

$$\mathbb{D} = \begin{pmatrix} 0 & F & 0 \\ F & 0 & E \\ 0 & E & D \end{pmatrix}$$

$$V_{cb} = \sqrt{\frac{m_s}{m_b}\frac{q_b}{q_s}} - \sqrt{\frac{m_c}{m_t}\frac{1}{q_t}}$$

GEORGI-JARLSKOG SU(5)

$$\mathbb{U} = \begin{pmatrix} 0 & C & 0 \\ C & 0 & B \\ 0 & B & A \end{pmatrix} \qquad \mathbb{D} = \begin{pmatrix} 0 & F & 0 \\ F' & E & 0 \\ 0 & 0 & D \end{pmatrix}$$

$$\mathbb{E} = \begin{pmatrix} 0 & F & 0 \\ F' & -3E & 0 \\ 0 & 0 & D \end{pmatrix}$$

- $m_b \sim m_\tau$ $\quad m_s \sim \frac{m_\mu}{3}$ $\quad m_d \sim 3m_e$
- $|V_{cb}|$ originates in $\mathbb{U}$ matrix $S\sqrt{\frac{m_c}{m_t}\frac{1}{q_t}}$

GEORGI-NANOPOULOS (SO(10))

$\mathbb{D}, \mathbb{E} \longrightarrow$ symmetric form

HARVEY, RAMOND, REISS

- realized the GJN texture with specific Higgs representation
- obtained single phase form

DIMOPOULOS, HALL, RABY

- obtained predictions at the electroweak scale using supersymmetric evolution

$$\mathbb{U} = \begin{pmatrix} 0 & C & 0 \\ C & 0 & B \\ 0 & B & A \end{pmatrix} \qquad \mathbb{D} = \begin{pmatrix} 0 & Fe^{i\phi} & 0 \\ Fe^{-i\phi} & E & 0 \\ 0 & 0 & D \end{pmatrix}$$

$$\mathbb{E} = \begin{pmatrix} 0 & F & 0 \\ F & E & 0 \\ 0 & 0 & D \end{pmatrix}$$

7 parameters $\longrightarrow$ 13 parameters + $\tan\beta$

9 masses + 4 CKM elements

$\mathbb{U}$ = up-quark Yukawa matrix

$\mathbb{D}$ = down-quark

$\mathbb{E}$ = charged-lepton

At one-loop (Inoue, Kakuto, Komatsu, Takeshita)

$$\frac{d\mathbb{U}}{dt} = \frac{1}{16\pi^2}\left[\left(-\sum c_i g_i^2 + 3\mathbb{U}\mathbb{U}^\dagger + \mathbb{D}\mathbb{D}^\dagger + \mathrm{Tr}[3\mathbb{U}\mathbb{U}^\dagger]\right)\mathbb{U}\right.$$

$$\frac{d\mathbb{D}}{dt} = \frac{1}{16\pi^2}\left[-\sum c_i' g_i^2 + 3\mathbb{D}\mathbb{D}^\dagger + \mathbb{U}\mathbb{U}^\dagger + \mathrm{Tr}[3\mathbb{D}\mathbb{D}^\dagger + \mathbb{E}\mathbb{E}^\dagger]\right]\mathbb{D}$$

$$\frac{d\mathbb{E}}{dt} = \frac{1}{16\pi^2}\left[-\sum c_i'' g_i^2 + 3\mathbb{E}\mathbb{E}^\dagger + \mathrm{Tr}[3\mathbb{D}\mathbb{D}^\dagger + \mathbb{E}\mathbb{E}^\dagger]\right]\mathbb{E}$$

These can be extended to two-loops.

$\alpha_s(M_Z) = 0.11 \quad \tan\beta = 5$

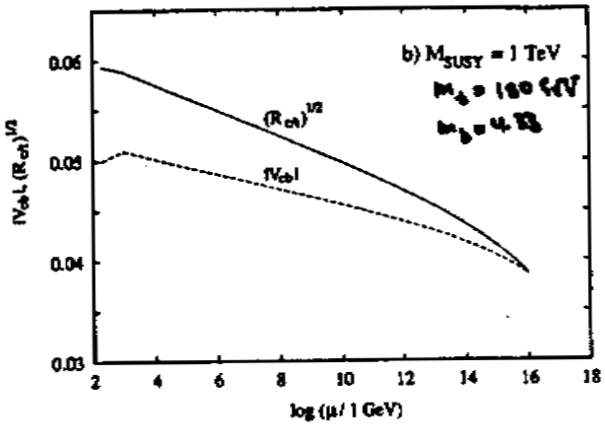

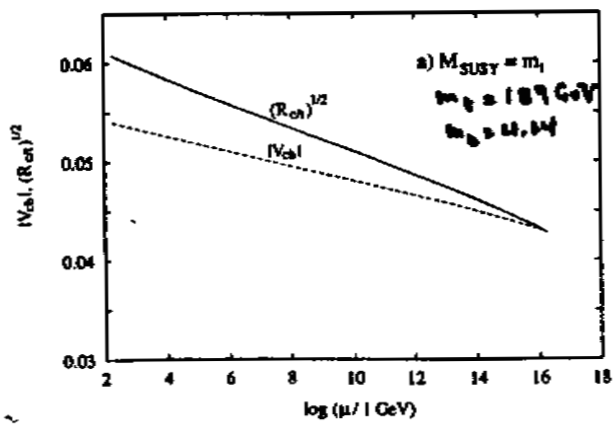

The evolution of the constraint $|V_{cb}|(M_G) = \sqrt{\lambda_c/\lambda_t}(M_G)$ to electroweak energies for two different supersymmetric scales.

One-loop results neglecting λ_b and λ_τ in the RGE evolution.

Bagger, MB, Hon, Zralek

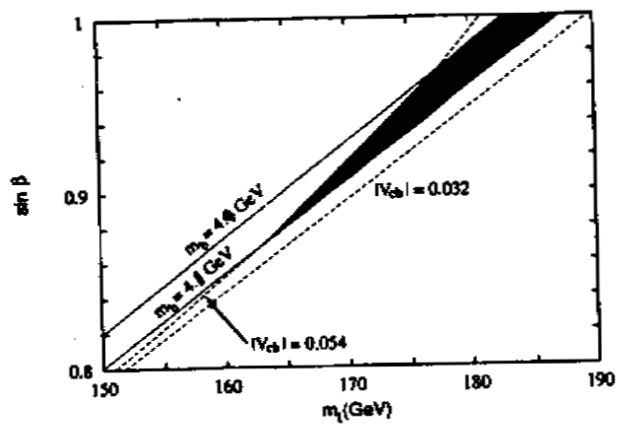

Allowed region obtained at the one-loop level neglecting λ_b and λ_τ.

REQUIRE ALL QUANTITIES TO BE WITHIN 90% C.L.

$m_b = 4.1 - 4.4$ GeV

$m_t = 1.19 - 1.35$ GeV

$|V_{cb}| = 0.032 - 0.054$

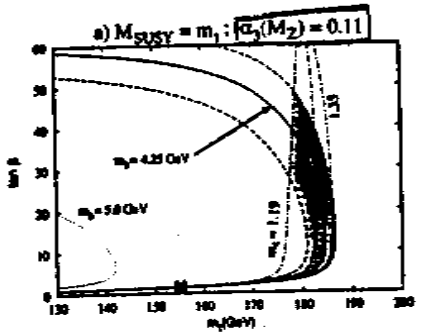

$|V_{cb}| = 0.054$ contours

upper limit on $\tan\beta \simeq 50$

lower limit on $m_t \simeq 155$

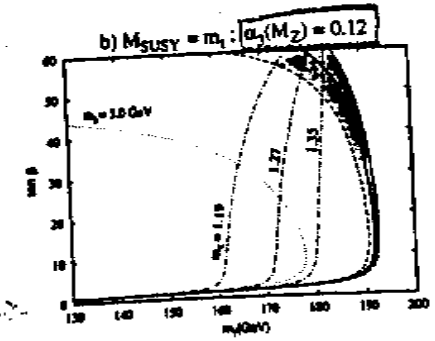

Allowed region obtained at the two-loop level. The dash-dotted contours are $|V_{cb}| = 0.054$ and $m_t = 1.19$, 1.27, 1.35 GeV. Increasing contours shifts the $|V_{cb}| - m_t$ contours to the left.

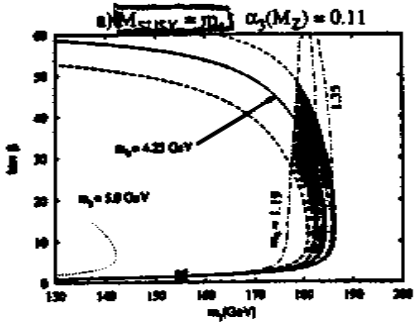

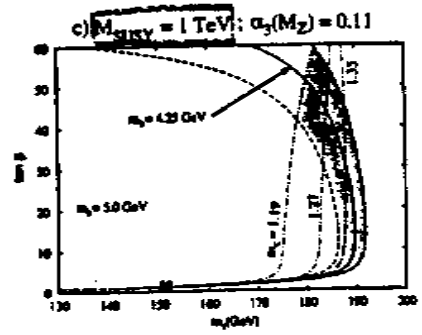

Effect of changing the supersymmetric scale on the allowed regions.

$\alpha_3(M_Z) = 0.11$

$m_c = 1.27$ GeV contours
(central value)

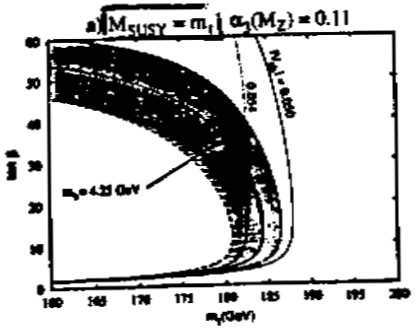

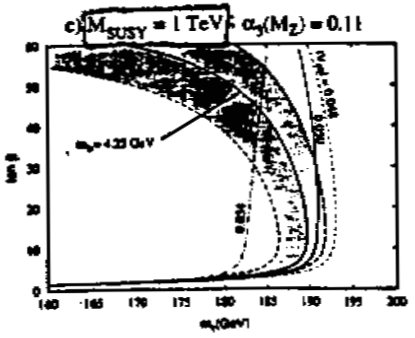

$\alpha_3(M_Z) = 0.12$
closer to that expected from the two-loop gauge coupling evolution

$m_c = 1.27$ GeV contours

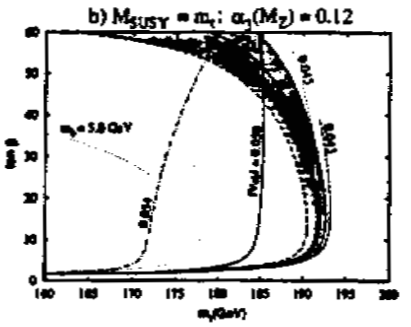

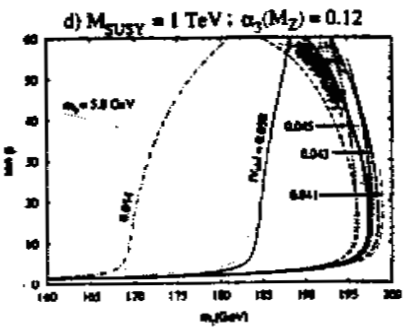

Allowed region obtained at the two-loop level. The dash-dotted contours are $m_c = 1.27$ GeV and $|V_{cd}| = 0.054, 0.050, 0.045, 0.043, 0.041$.

The CP violating phase is well-constrained in the U model.

In the first two generations

$$\begin{pmatrix} 0 & c \\ c & m_s \end{pmatrix} \qquad \begin{pmatrix} 0 & Fe^{i\phi} \\ Fe^{-i\phi} & m_d \end{pmatrix}$$

$$\theta_1 \sim \sqrt{\frac{m_d}{m_s}} \qquad \theta_2 = \sqrt{\frac{m_d}{m_s}}\, e^{i\phi}$$

$$|V_{us}| = |\theta_1 + \theta_2|$$

$$= \left[\frac{\eta_s}{\eta_d}\frac{m_d}{m_s} + \frac{\eta_c}{\eta_u}\frac{m_u}{m_c} + 2\sqrt{\frac{\eta_s \eta_c}{\eta_d \eta_u}\frac{m_u m_d}{m_c m_s}}\, c_\phi\right]^{1/2}$$

Well-measured

$|V_{us}| \longrightarrow$ constraint on $\phi = 70 - 90^\circ$

CP asymmetries in B decays

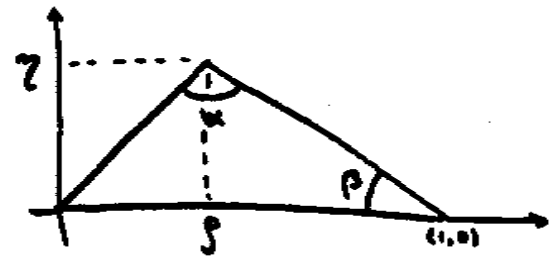

Also Dimopoulos, Hall, Raby
Nir, Sarid

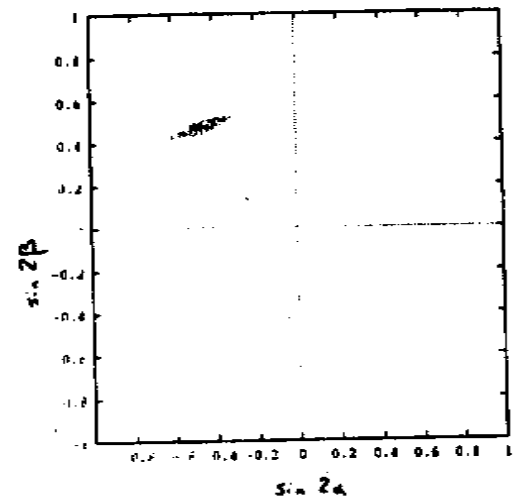

Only a small region is allowed by the U Model.

The D Model (Giudice)

$$U = \begin{pmatrix} 0 & 0 & b \\ 0 & b & 0 \\ b & 0 & a \end{pmatrix} \qquad D = \begin{pmatrix} 0 & fe^{i\phi} & 0 \\ fe^{-i\phi} & d & nd \\ 0 & nd & e \end{pmatrix}$$

$$E = \begin{pmatrix} 0 & f & 0 \\ f & -3d & nd \\ 0 & nd & e \end{pmatrix}$$

Giudice: $n=2$

- Geometric Mean Relation: $m_c^2 \approx m_u m_t$
- Retains Relations: $m_b \approx m_\tau$

  $m_s \approx \frac{m_\mu}{3}$

  $m_d \approx 3 m_e$
- CP violating phase is not so well determined

$$|V_{us}| = 3\sqrt{\frac{m_e}{m_\mu}}\left(1 - \frac{25}{2}\frac{m_e}{m_\mu} + \frac{4n^2}{9}\frac{m_\mu}{m_\tau}\frac{\eta_\tau}{\eta_\mu}\right)$$

$$|V_{cb}| = \frac{n}{3y}\frac{m_\mu}{m_\tau}\frac{\eta_\tau}{\eta_\mu}\left(1 - \frac{m_e}{m_\mu} + \frac{(n^2-3)}{9}\frac{m_\mu}{m_\tau}\frac{\eta_\tau}{\eta_\mu}\right)$$

$$|V_{ub}| = \frac{\chi^2}{\eta_c}\frac{m_c}{m_t}$$

$$m_u = y^3\frac{\eta_u}{\eta_c^2}\frac{m_c^2}{m_t}$$

$$m_d = \frac{\eta^{1/2}}{\chi}\frac{\eta_d}{\eta_e}3m_e\left(1 - 8\frac{m_e}{m_\mu} + \frac{4n^2}{9}\frac{m_\mu}{m_\tau}\frac{\eta_\tau}{\eta_\mu}\right)$$

$$m_s = \frac{\eta^{1/2}}{\chi}\frac{\eta_s}{\eta_\mu}\frac{m_\mu}{3}\left(1 + 8\frac{m_e}{m_\mu} - \frac{4n^2}{9}\frac{m_\mu}{m_\tau}\frac{\eta_\tau}{\eta_\mu}\right)$$

$$m_b = y\frac{\eta^{1/2}}{\chi}\frac{\eta_b}{\eta_\tau}m_\tau$$

The solutions of the RGEs in the D Model.

SUMMARY

- UNIVERSAL SCALING PATTERN OF CKM MATRIX

$$|V|^2 \sim \begin{pmatrix} 1 & 1 & S \\ 1 & 1 & S \\ S & S & 1 \end{pmatrix} \qquad J(\varphi') = S\left(\frac{\varphi'}{\varphi}\right) J$$

- The GUT scale constraint $\lambda_b(M_G) = \lambda_\tau(M_G)$ yield $\sin\beta \simeq 0.79 \left(\frac{m_t}{150\,\mathrm{GeV}}\right)$ for $\tan\beta \leq 10$ in the MSSM.

- Predictions of U and D models are consistent with all experiments. For $\alpha_3(M_Z) = 0.12$ the central value of $|V_{cb}| = 0.043$ is closer to the predicted value in the U Model.

Top quarks at Hadron Colliders Summary Talk

R. Hollebeek

Wisconsin top quark workshop

November, 1992

My favorite questions about the top:

Does it exist? - Yes, see Kane's talk

Could we have missed it? Yes! see Baer's talk

How do you find it? Protopopescue (FNAL)

How do you measure its properties? Sinervo (SSC)

Why is it so heavy? Still unanswered !

If the top quark is the only very heavy quark, and its mass is close to the weak scale, perhaps the top is a VERY special particle. Why does a plot of quark mass vs quark type look like this ?

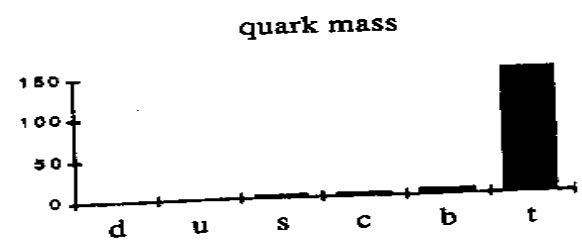

Does it Exist?

Three major items give us rather good confidence that the top quark does indeed exist. They all come from measurements of the properties of b mesons.

$$b \rightarrow l^+ l^- X$$

$$A^b_{FB}$$

$$Z \rightarrow b^+ b^-$$

$b \rightarrow l^+ l^- X$

G.L. Kane M.E. Peskin, Nucl.Phys.**B195**(1989)29.

If the b quark is a singlet, expect > 1.3 10**-2

Standard Model value 10**-4 smaller.

CLEO measurement 90%CL < 1.2 10**-3

A.Bean et al.,Phys.Rev.**D35**(1987)3533.

UA1, C.Albajar et al.,Phys.Lett.**B262**(1991)163.

A^b_{FB}

The forward-backward asymmetry is proportional to

$$T^b_{3L} - T^b_{3R}$$

evidence(cont.)

A^b_{FB}

Note that the asymmetry is zero if the b quark is an isosinglet.

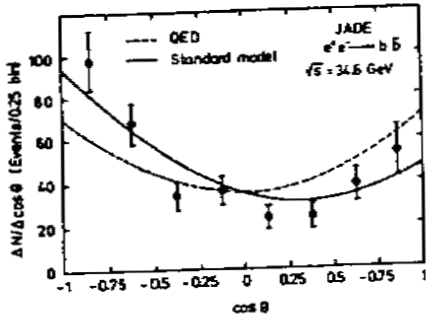

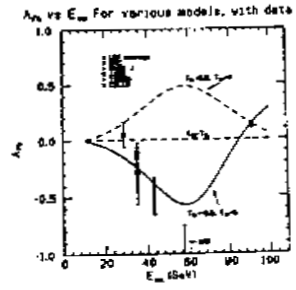

Measurements prior to LEP gave

$$T^b_{3L} = -0.54 \pm 0.13$$

(Standard Model value = -1/2)

LEP

J. Carter, Lepton Photon Conference, Geneva,July 1991.

$$A^b_{FB} = 0.126 \pm 0.022$$

See also Kane's talk:

$$T^b_{3L} = -0.504 + 0.018 -0.011$$

OK, I'm convinced!

Radiative Corrections

The mass of the top quark often affects the cross section for other processes through radiative corrections. This provides indirect means to measure the top quark mass or place limits on it.

Ratio of W and Z cross sections

The Z and W production cross sections depend on m(top). By taking a ratio, some of the dependence on theory as well as structure function uncertainties cancels. Using the dilepton detection mode for the Z and the single lepton plus missing Et for the W, the ratio is

$$R = \frac{\sigma_W}{\sigma_Z} \frac{\Gamma(W \to l\nu)}{\Gamma(Z \to l\,l)} \frac{\Gamma_Z}{\Gamma_W}$$

Solve for W total width.

This is a good example of a process which can be used to set a lower bound on the top mass in a way which is general enough to have few if any caveats.

W Z Cross Section Ratio

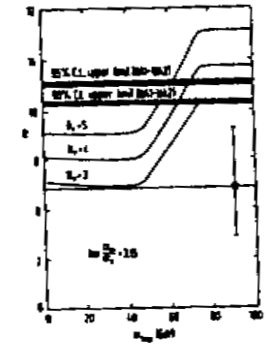

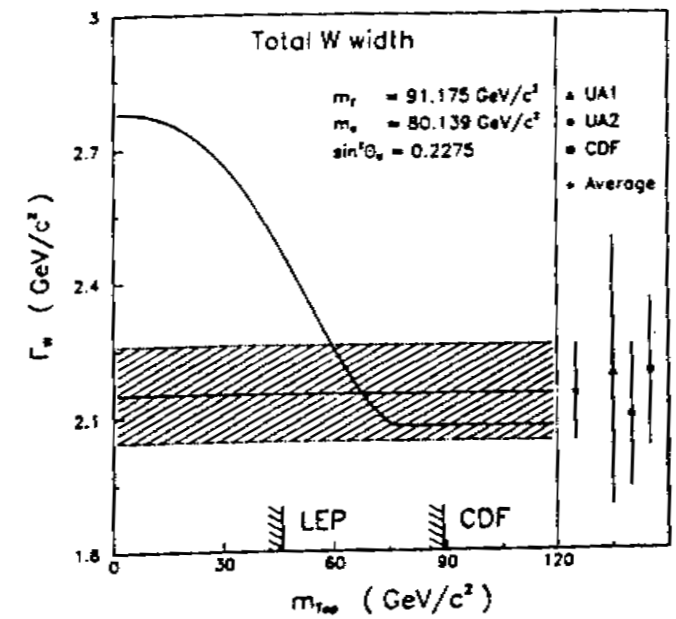

Figure 21: Total width of the W boson as a function of the top mass[56].

Relation between Mt and Mw

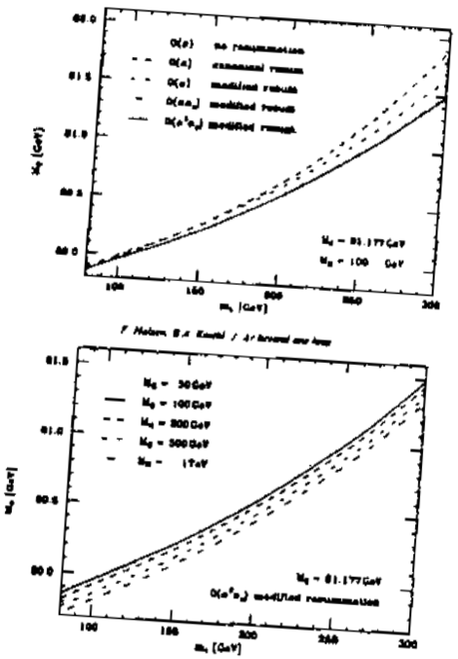

Figure 22: $m_t - m_W$ interdependence[44c] for different calculations (bottom) and for different values of m_H (top).

We have a complicated three parameter space involving Mw, Mh, and Mt. We badly need Mt to help us reduce the size of this parameter space for testing the Standard Model.

Combined Fits

D.Schaile,CERN-PPE/91-187(November 1991).

$$m_t = 144^{+23}_{-26}\,{}^{+19}_{-21}\ \text{GeV}$$

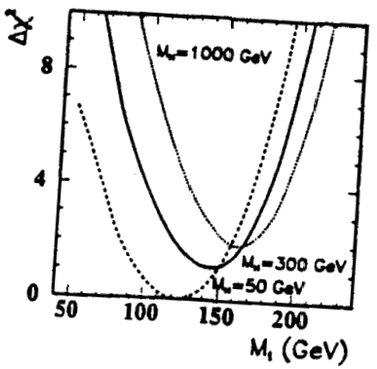

Figure 26: χ^2 curves[84] as function of m_t for the combined fit to LEP data, M_W/M_Z from UA2, M_Z/UA2, M_W from CDF and $\sin^2\theta_W$ from the νN-scattering experiments CHARM and CDHS.

J.Carter,Int.Lepton-Photon Symposium,Geneva,1991. 91.

J.Ellis,Int.Lepton-Photon Symposium, Geneva,1991. 1.

$$m_t = 125 \text{ to } 144 \pm 30 \text{ GeV}$$

$$m_t < 181 \text{ GeV} \quad [95\% \text{ CL}]$$

combined analysis of mz, mw/mz, **and** sinsq theta w gw give upper limit of 200 GeV

fit for mt gives 130 GeV

P. Langacker, Phys. Rev. **Lett. 63** (1989)p.1920.

J. Ellis and G.L. Fogli, Phys. Lett. **B232**(1989)p.139.39.

J. Ellis and G.L. **Fogli**,CERN TH/5862 (1990).

J. Pilcher's Talk
This conference

ZFitter Results

$M_Z = 91.187 \pm 0.007$

$\Gamma_Z = 2.492 \pm 0.007$

$\sigma_{Z\ pole} = 41.16 \pm 0.18$ [nb]

$M_t = 145 \begin{matrix} +23 \\ -28 \end{matrix} \begin{matrix} +17 \\ -20 \end{matrix}$ α_s unconstrained

$M_t = 153 \begin{matrix} +21 \\ -25 \end{matrix} \begin{matrix} +18 \\ -20 \end{matrix}$ $\alpha_s = 0.120 \pm 0.006$

Including data from the W mass and neutrino scattering

$M_t = 145 \begin{matrix} +19 \\ -21 \end{matrix} \begin{matrix} +17 \\ -19 \end{matrix}$ α_s unconstrained

$M_t = 150 \begin{matrix} +18 \\ -20 \end{matrix} \begin{matrix} +17 \\ -19 \end{matrix}$ α_s constrained

See D. Schaile, Z.Phys.C54,387.

Comment: The variation of the chi-squared is being determined from the data, and this is not the same as the sensitivity of the measurement to a given parameter (M-Higgs for example).

Direct input on Mt would be extremely useful

Top quark fragmentation

The top quark width scales like

$$\Gamma \sim 0.17\ \text{GeV}\ (m_t/m_W)^3$$

and the lifetime is $\tau = 1/\Gamma$

If the top quark is heavy enough,

the width is large

the lifetime is short

there is insufficient time for fragmentation before the top quark decays.

If the top quark is light

the lifetime is longer

there is time for the usual fragmentation process

This situation may lead to changes in the t quark z fraction as well as the colinearity of radiated gluons.

A.Blinov,V.Khoze,N.Uraltsev,DESY 88-102.

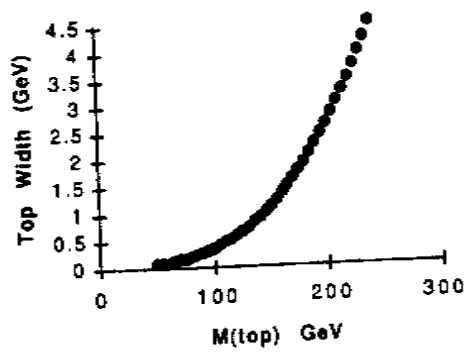

Given current experimental and theoretical bounds, the likely values of the top width are between about 0.5 and 2.5 GeV.

Difficult to measure directly.

See discussion of W gluon fusion.

How to Find it ?

FNAL

The task

σ_{TOT}	~ 70 mb	
$b\bar{b}$	30 μb	10^{-3}
W	20 mb	10^{-6}
Z	2 mb	
$m_t = 150$	10 pb	10^{-9}

≈ 2x in $\mathcal{L}$ ⇒ 20 GeV in reach

MAIN INJECTOR ⇒ 1.000 p

present goal $25\,pb^{-1}$

$\mathcal{L}_{peak}$ 5×10^{30} goal now @ 3.5 10^{30}

92-93	$25\,pb^{-1}$		
93-94	$\mathcal{L} = 10^{31}$	⇒	$100\,pb^{-1}$
95-96	6 bunch → 36 bunch		
	1.8TeV → 2.0 TeV		
	$\mathcal{L}$ → 1.1	⇒	$100\,pb^{-1}$
97	MAIN INJECTOR	$5\cdot10^{31}$ ⇒	$1000\,pb^{-1}$

Decay Modes

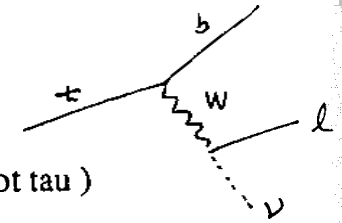

leptonic

great for detection (e and mu but not tau)

e

em calorimeter techniques

chief backgrounds - π0 overlap, Z, conversions, B semil-leptonic decays

mu

m n chambers

good for high rate env.

tau

1 prong modes

3 prong modes

exclusive modes???

hadronic

high rate

difficult detection

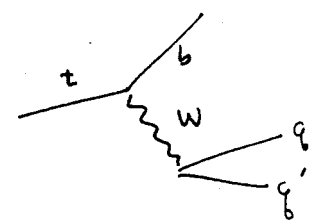

electron properties

The electromagnetic and hadronic calorimeters are used to select electron candidates. The hadronic fraction of the total energy should be small.

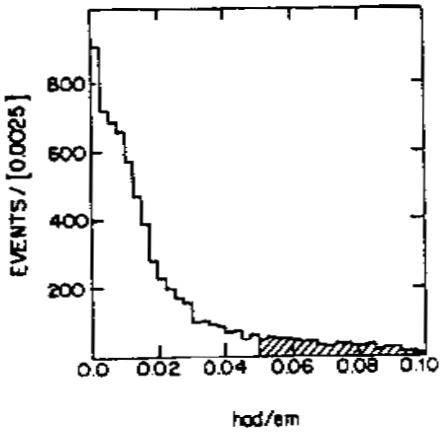

Conversion pair and Z backgrounds are eliminated with invariant mass cuts and using the VTPC

electrons from B mesons are reduced by isolation cuts.

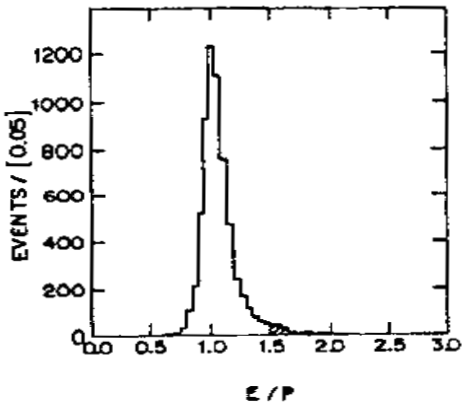

A charged track must be present with a momentum which matches the calorimeter energy except for the radiative tail.

Strip chambers within the electromagnetic calorimeter provide a profile for the shower which must have a good "electron" chisquare and have a position which matches the track.

CDF Searches

The principal production mechanisms for top at hadron machines are the decay to the W for light top, and pair production. UA1 and UA2 searches relied primarily on the former.

CDF searches extend the mass range by being sensitive to the direct pair production.

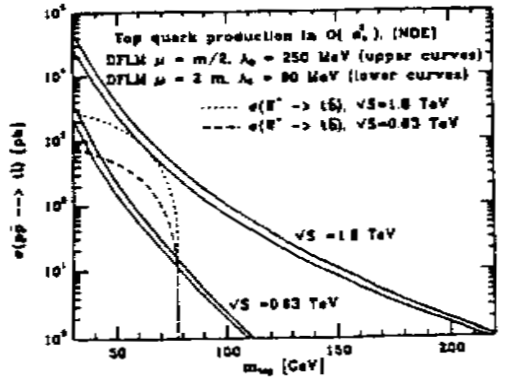

Three search modes

electrons + jets

electron muon events

dileptons (ee μμ)

electron + jets

start with the observed distribution of electron energy and missing energy for events with two jets.

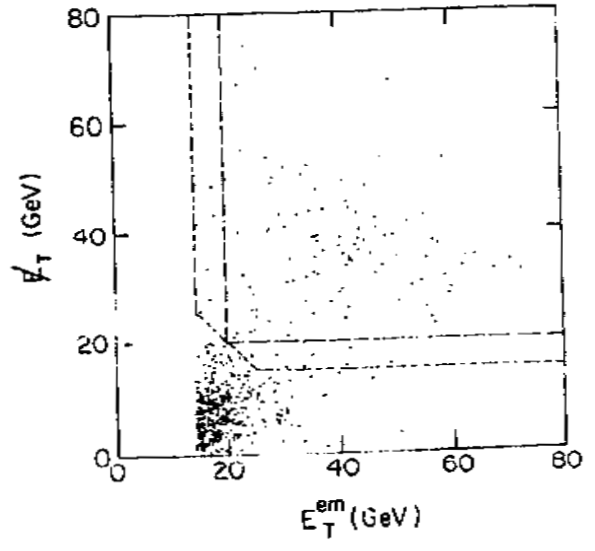

Two sources, B's and W's

limit

The transverse mass distributions of top and W's are sufficiently different to place a limit on top production.

F.Abe et al.,Phys.Rev.Lett.**64**(1990)142.

F.Abe et al.,Phys.Rev.**D43**(1991)664.

Monte Carlo transverse mass distributions from W + 1 jet events are compared to experimental data from the electron + 1 jet sample at high transverse mass which is expected to be dominated by W's.

The 95% CL limit from the electron plus jet channel is the most stringent single channel limit.

40 < mt < 77 GeV

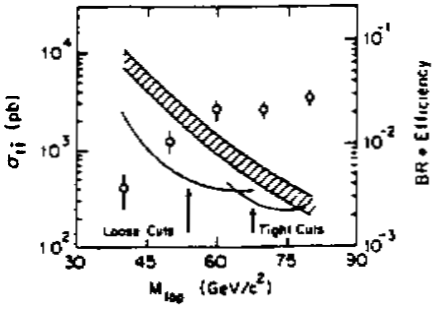

CDF (cont.)

B's contribute events with soft electrons and small missing Et. W -> e ν however gives both high energy electrons and large missing Et. For low Pt W's, the two are correlated.

In a parton-parton collision, the longitudinal momentum is unknown, so we calculate the invariant mass of the e ν system ignoring the longitudinal momentum of the electron. The invariant mass calculated in this way is called the transverse mass.

$$M_T^{e\nu} = \sqrt{2\, E_T^e\, E_T^\nu \left(1 - \cos \phi_{e\nu}\right)}$$

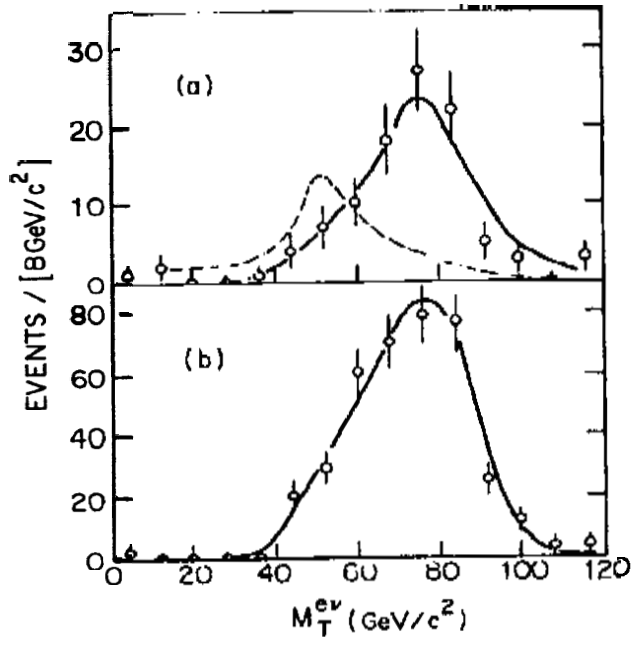

CDF e μ Search

Search for events with high pt (> 5 GeV) muon and a high pt (> 15 GeV) electron of opposite sign.

F.Abe et al.,Phys.Rev.Lett.64(1990)147.

Backgrounds from B decays will dominate at low pt.

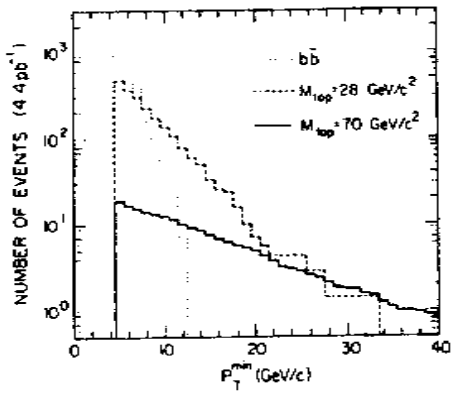

FIG. 2. The expected number of opposite-sign events for 4.4 pb^{-1} with $E_T(e) \geq P_T^{min}$ and $P_T(\mu) \geq P_T^{min}$ as a function of the threshold P_T^{min} for simulated $t\bar{t}$ events with $M_{top}=70$ GeV/c^2, $M_{top}=28$ GeV/c^2 and for simulated $b\bar{b}$ events. The analysis P_T thresholds have been lowered to 5 GeV/c for this plot in order to show the shape of $b\bar{b}$ background at low P_T.

The top search region uses a pt cut of 15 GeV for both the electron and the muon. One candidate event survives the cuts with Et(e)=31.7 and Et(μ)=42.5 GeV

Total efficiency for 70 GeV top is about 10%

e μ (cont.)

One observed event is combined with the systematic uncertainties in the efficiency, production cross section, fragmentation effects, and yields a 95% CL limit

mt > 72 GeV

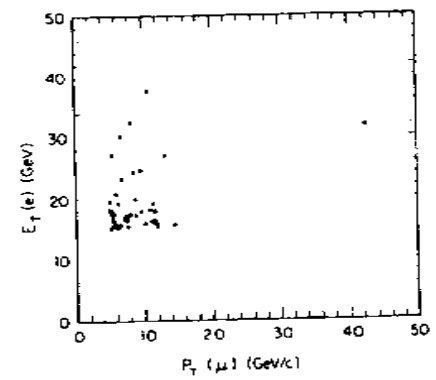

FIG. 1. Electron transverse energy vs muon transverse momentum for the CDF data with an integrated luminosity of 4.4 pb^{-1}.

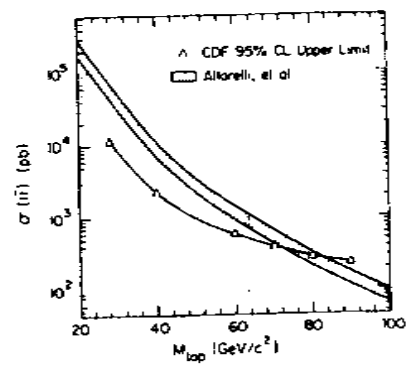

FIG. 4. The 95%-C.L. upper limit on the $t\bar{t}$ production cross section as a function of top-quark mass. The shaded band shows the result of a theoretical calculation of the $t\bar{t}$ production cross section (Refs. 3 and 10).

The event also has a second muon candidate in the forward muon detector as well as a jet with 14 GeV Et.

Further Improvements

Coupled channel analysis: more channels combined together give better limits or detection efficiency.

e and μ + 3 jets

challenges - jet energy scales and corrections

QCD corrections for W + multijet backgounds

e and μ + 4 jets -- need to reduce the combinatorial background by using vertex tagging of b jets.

Vertex tagging

30% efficiency (CDF) for single b tag in a top event (120<mt<160)

often considered the "smoking gun" for top searches, it would be nice to see b vertices in coincidence with a top signal.

ft lepton tags

challenges - soft lepton identification and background studies.

Constrained fits ala SDC and LHC stu s.

dijet constraints to Mw for example

$\sigma(mt=90) \sim 10\ \sigma(mt=140)$

$\sigma(mt=90) \sim 100\ \sigma(mt=200)$

Vertex tagging efficiency

Single b tag in a top event (CDF)

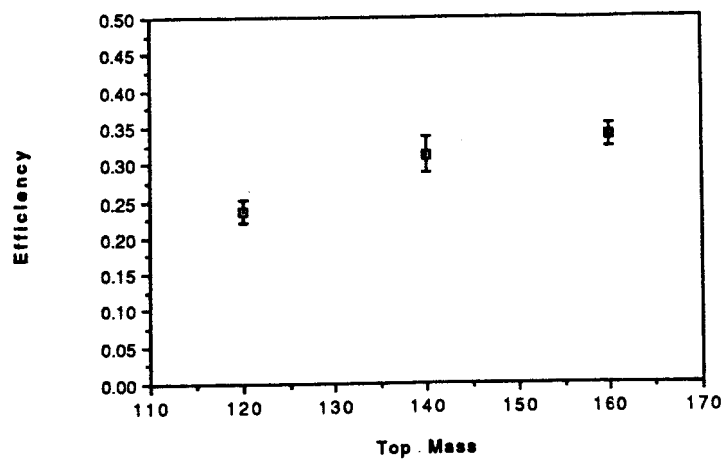

The importance of the b tag is illustrated on the next page which shows the rates for top events seen in the 3 and 4 jet samples and compares them to the chief background which is W plus 3 and 4 jet production. Without a b tag, the W plus 3 jet background is above the signal level for top quarks. The b tag reduces this background by about an order of magnitude, and makes the top signal visible out to masses of order 170 GeV

Effectiveness of b tagging in removing W plus jet backgrounds in the lepton plus 3 and 4 jet samples

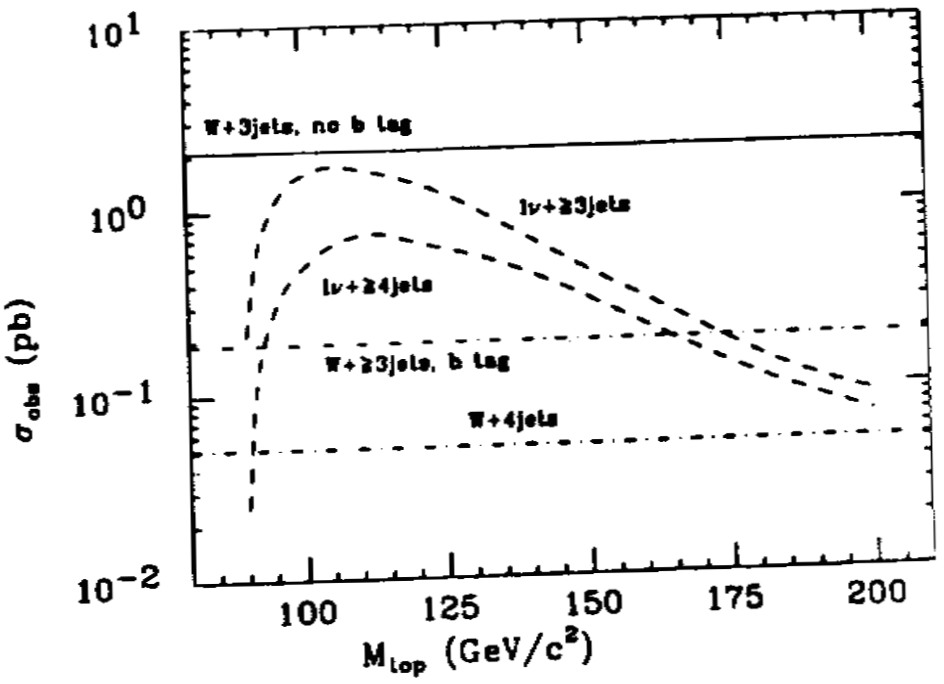

Signal and background in the electron muon final state

The chief background is Z -> ττ with subsequent leptonic decays of the tau leptons.

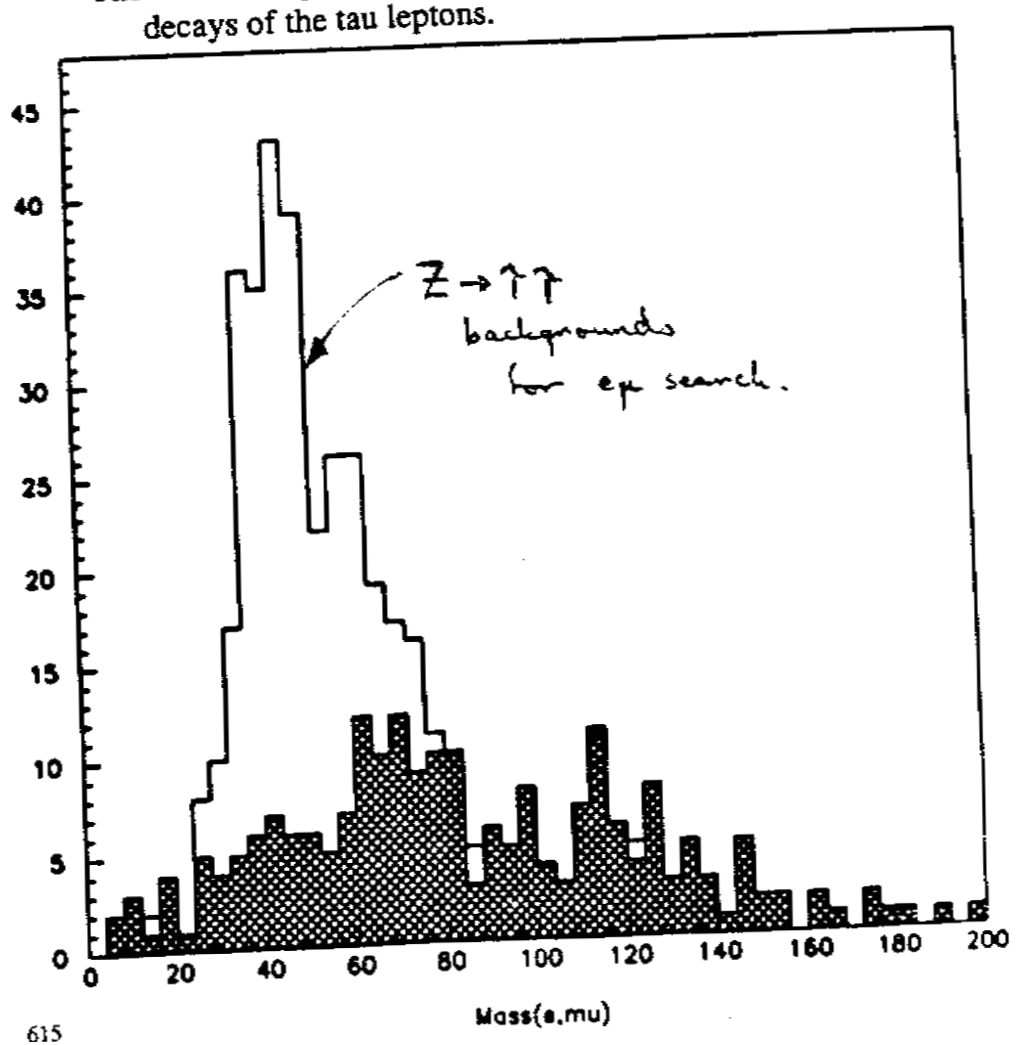

Leptons plus jets

A reconstructed W can be combined with a tagged b quark jet to give the top mass. There is a combinatorial background from the presence of more than one such b jet in the final state.

These combinatorial backgrounds are however much worse without the ability to identify b candidate jets. The advantages of this tagging have been clearly seen in SDC studies.

Additional backgrounds come from extra gluon jets. 30% of the events will contain a jet which does not come from the hard process.

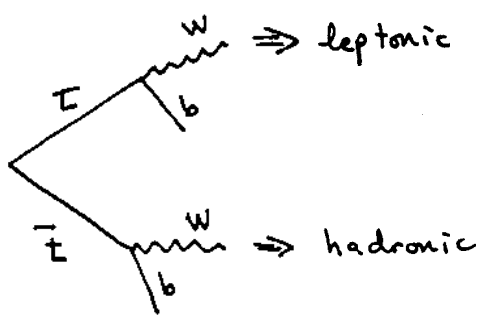

two jets

While it's a somewhat novel idea to begin to apply the same kinematic constraints to jets which we used to apply to single particles in a bubble chamber fashion, the event below (two 200 GeV jets) illustrates that it is indeed possible.

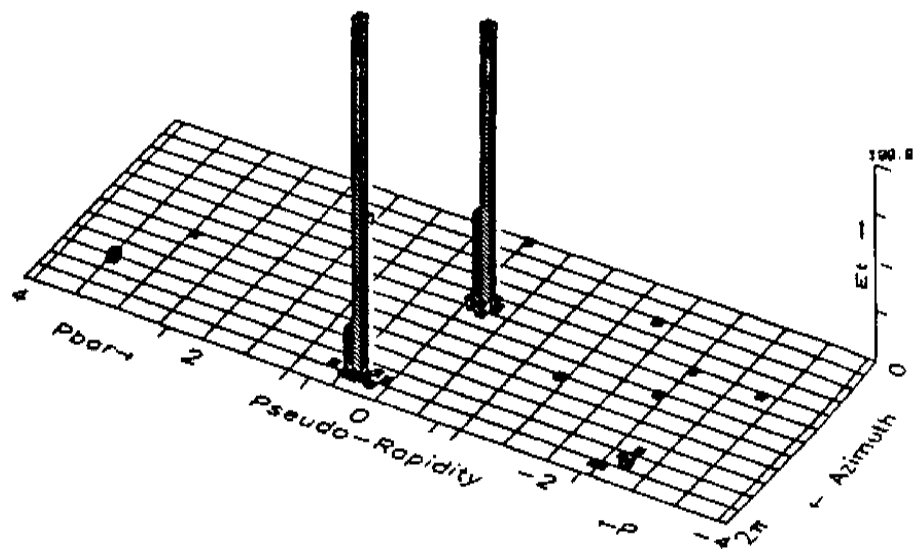

$$M^2 = (\mathbb{P}_1 + \mathbb{P}_2)^2 = \underbrace{m^2_{JET1} + m^2_{JET2}}_{\text{NEEDS WORK}} +$$

Jet reconstructed masses for the top (D0)

$$\int L\,dt = 200\ \mathrm{pb}^{-1}$$

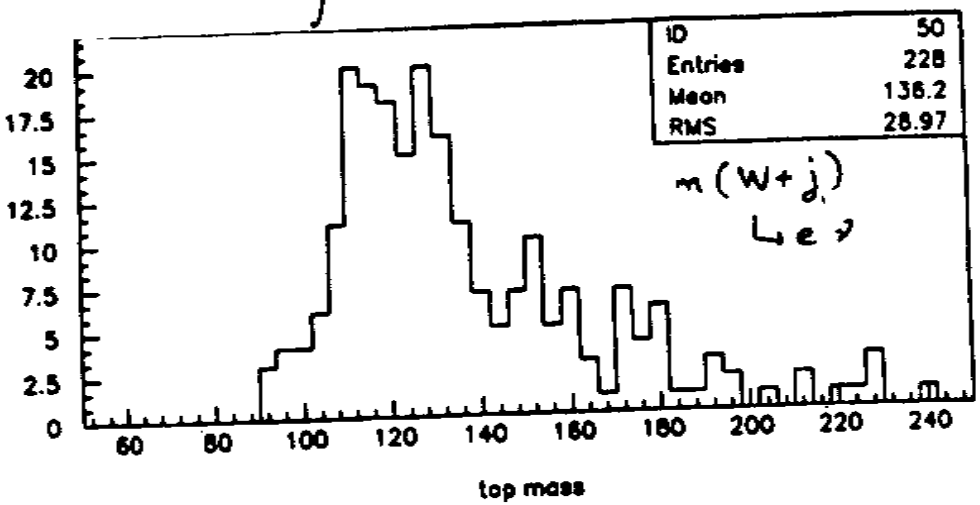

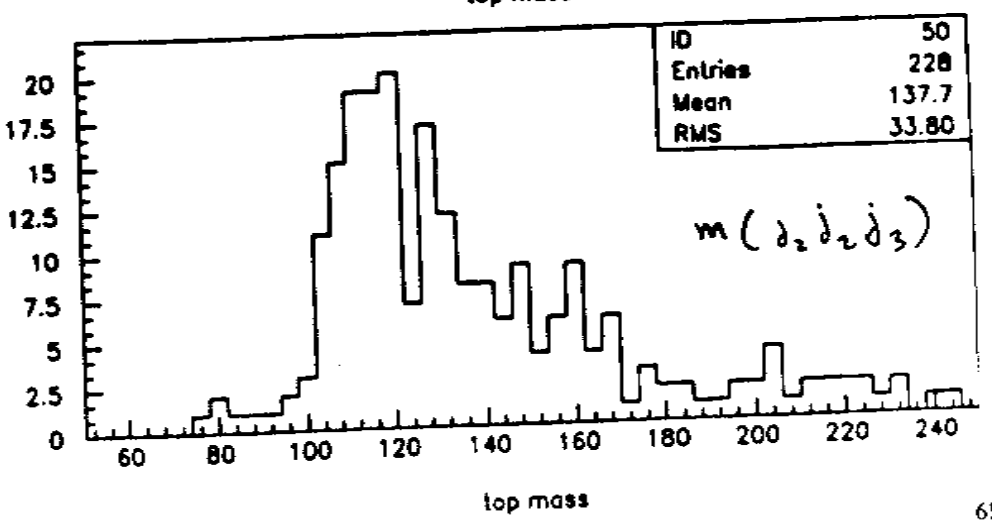

Production of top

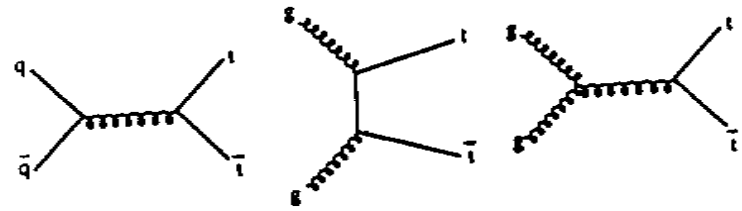

Lowest order diagrams for top production from quark anti-quark and two gluon initial states. The relative importance of the diagrams depends on the top mass. Heavier masses suppress the glue-glue contribution which has larger systematic errors.

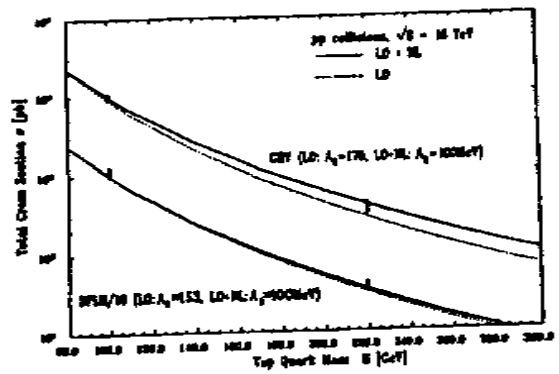

Figure 2: Predictions of top quark cross sections [17]

E. Reya et al.,CERN 90-10 (1990) 304.The cross section varies weakly with the parameterization of the parton densities and the choice of scale. The vertical bars represent the change from μ = m(top) to μ = 2 m(top)

Top Production and Decay

$\sigma_{t\bar{t}}$ h been calculated to order α_s^3 by Nason *et al.* (NP 3, 607 (1988)).

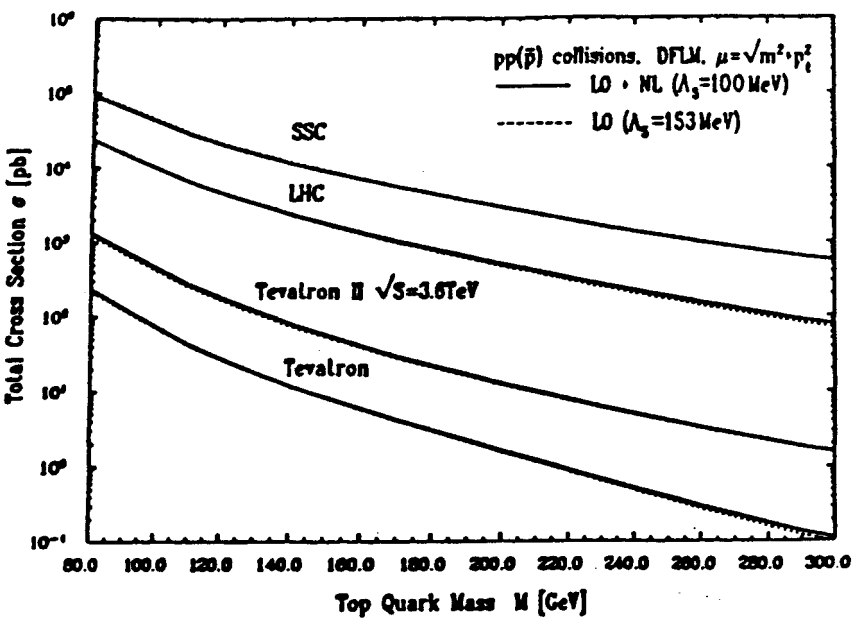

- Uncertainties are order ±30% (NP B308, 724 (1988))

Rates e enormous by Tevatron standards

SSC	12 nb	1.2×10^7 per year	for M_{top}= 150 GeV/c^2
LHC	2 nb	2.0×10^7 per year	

Top production

3rd order calculation of the top cross section has been done by Nason et al. Nucl.Phys.**B303**,607(1988).

Uncertainties are 30% , Nucl.Phys.**B308**,724(1988).

Rates a the SSC/LHC are enormous

150 GeV top quark

cross section	events per year
SSC 12nb	1.2 10^7
LHC 2nb	2.0 10^7

Tevatron goals

Run	Luminosity	top mass
1991	25 pb -1	120
1993	75	160
1995	325	200

1992 Run

6x6 bunches 3.5 μsec spacing 10**31 peak lum.

1994 Run

100 to 500 pb-1 400 nsec bunch spacing 10*32 peak

1998 ? 20 nsec 10**33

1992 D0 starts

CDF

Vertex Detector - Silicon

New VTPC

Central Muon Upgrade - chambers and scintillators

Level 0 trigger - calorimetry and muons

CEM Preradiator

total cross section is 46 mb

(10**31)(46*10**-26)(3.5*10**-6) = interactions per bunch

ssc t production

Top quarks in the 150 GeV mass range are copiously produced at SSC/LHC. 10**7 per year.

Primary production mechanism would be (low x) glue-glue.

Principal background - W + jets

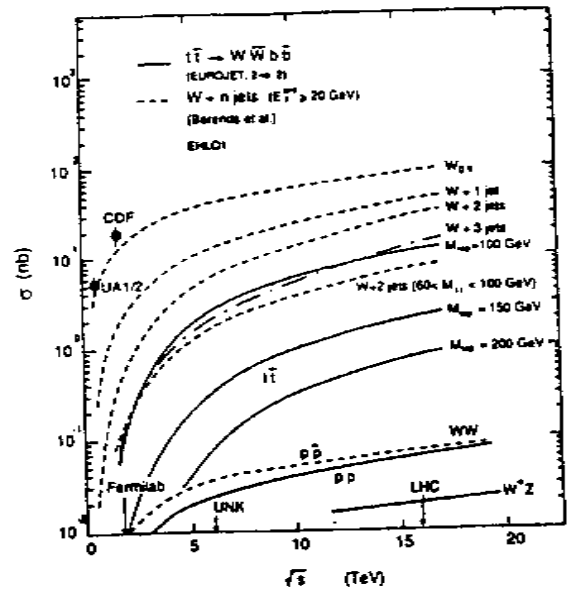

tt̄ signal for various m_t values vs W+n-jets and WW, WZ background

3rd order calculation of the top cross section has been done by Nason et al. Nucl.Phys.**B303**,607(1988).

Uncertainties are 30% , Nucl.Phys.**B308**,724(1988).

Rates at the SSC/LHC are enormous.

measuring m(t)

Would like to achieve better than 5% accuracy on the top mass (5-10 GeV). Production cross section with 30% syst. error gives a top mass error of order 10 GeV

Simplest Measurement

Inclusive electron or muon spectra.

Disadvantages are the effect of initial pt of the top and secondary leptons from t->b or t->b->c which require knowledge both branching fractions and decay spectra.

Dilepton Invariant Mass

Some ambiguity remains from secondary leptons (2-3%).

Again need fragmentation information, pt top dependence, possible polarization effects...

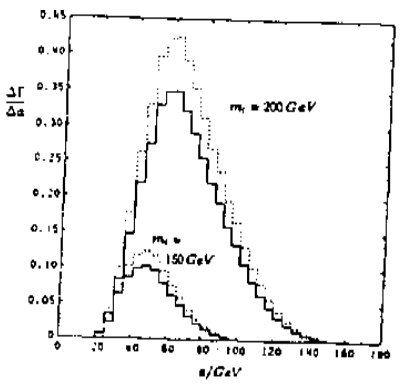

Fig. 2. Histogram for the distribution $\Delta\Gamma/\Delta a$ for $m_t = 150$ GeV and $m_t = 200$ GeV; dashed line: lowest order result; solid line: including first order QCD corrections. The width is given in the units defined in eq. (5) and $\Delta a = 5$ GeV. The following cuts have been applied. $E(\mu^+) > 30$ GeV, $E(\mu^-) > 10$ GeV, $\cos\theta < 0.8$

Need Inclusive spectrum of leptons from B decays.

Corrections for top width are small.

Figure uses 10**6 tops with E1>30,E2>10,cos<0.8

Error due to B fragmentation estimated at 1%

QCD still 5%

Δ t

Sources:

LHC Workshop, Aachen, Oct. 90

SDC Technical Design Report

GEM Letter of Intent

See also C.P. Yuan's contribution, this conference.

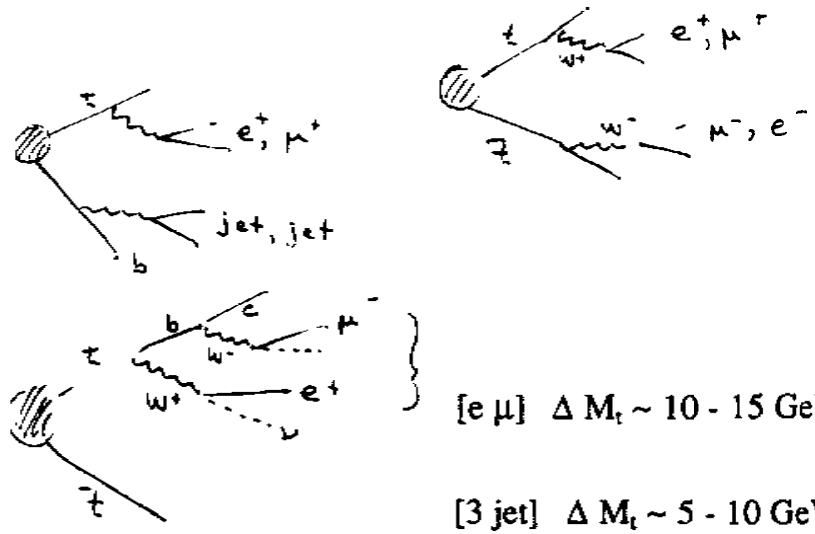

[e μ] $\Delta M_t \sim 10 - 15$ GeV

[3 jet] $\Delta M_t \sim 5 - 10$ GeV

[same t. e μ] 150 ± .5 (stat per year) ± 2.4 (syst)

250 ± .8 (stat per year) ± 3.9 (syst)

Note that the gg process dominates at the SSC/LHC machines because the top mass is smaller relative to the cm energy of the machine so small x parton densities are relatively more important. In general, the heavier the mass, the larger the relative qq contribution as can be seen from the FNAL curve. (see previous page.)

Curves from G.L.Kane, G.A.Landinsky and C-P Yuan, SSCL-486(June 1991)

Other top production mechanisms

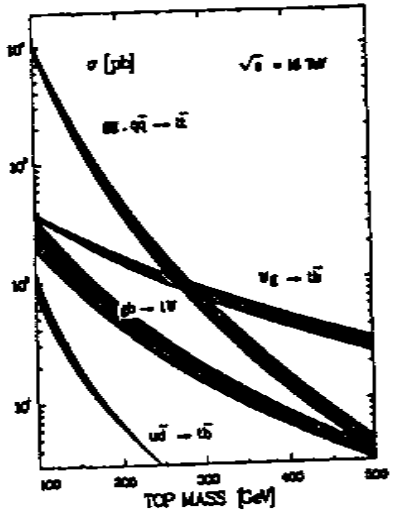

Figure 7 shows the cross sections for various mechanisms of top quark production at LHC.

Top quark production via W gluon fusion

Fermilab-PUB-92/132-T

R.K. Ellis and Stephen Parke

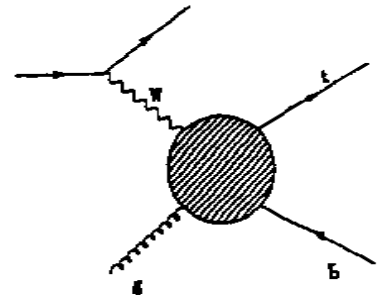

two top production mechanisms

gg

quark anti-quark

as the top mass increases, second process begins to dominate

The W gluon fusion process needs to produce only a single top quark. What is the relative contribution of these processes?

the conclusion is that while for some heavy top masses the tb production mechanism is larger than tt, after event cuts (CDF type) the signal is smaller. Reason: smaller pt of the b jet and larger rapidity of the quark jet in this mechanism.

C.P.Yuan, this conference

process allows a measurement of the top width into Wb and perhaps the form factors

100% polarized t sample !

W gluon fusion (cont.)

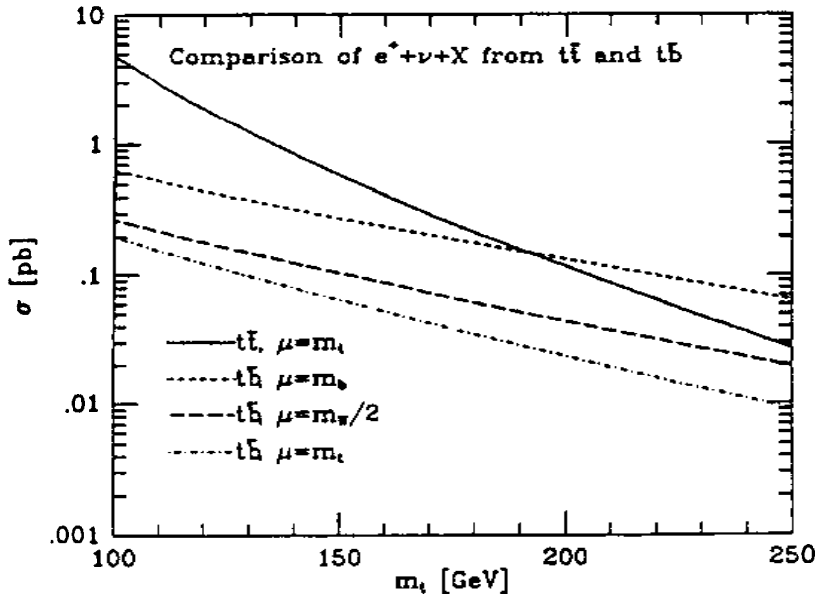

Figure 3: Comparison of total rate for $e^+ + \nu$ + jets production from $t\bar{t}$ and $t\bar{b}$ production at tree graph level.

For top masses greater than 190, the W gluon fusion process (using the largest estimate) is larger than the annihilation process.

W gluon fusion (cont.)

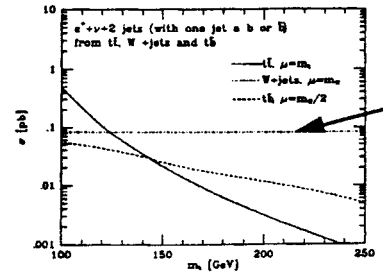

background from W's

Figure 6: Comparison of total rate for $e^+ + \nu$ + 2 jet production from $t\bar{t}$, W + jets and $t\bar{b}$ production.

Note that in these plots, one jet is required to be a b, assuming some degree of experimental b tagging.

For the two jet case with large top masses, both processes are below the W plus jet background.

For the three jet case, the background situation is better, but the W gluon process is small for most top masses.

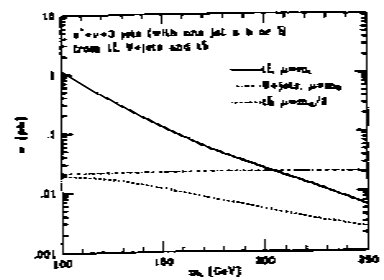

Figure 4. Comparison of total rate for $e^+ + \nu$ + 3 jet production from $t\bar{t}$, W + jets and $t\bar{b}$ production.

Can the samples be separated?

It's no good having a subsample of 100% polarized t's unless you can separate it from the unpolarized sample. The two samples are a tb sample and a t pair sample.

Principles for finding the tb's

fewer jets

harder b spectrum

larger η range for t's and b's

perhaps double tag with isolated plus non-isolated pair of leptons from tb ???

We need work on this separation before we can determine whether such a sample would be useful in CP tests.

Dilepton Channels

The $e^{\pm}\mu^{\mp}$ channel is the cleanest channel

- Rate is equal to e^+e^- and $\mu^+\mu^-$ combined
- No Drell-Yan backgrounds

At SSC, requiring lepton P_T

- $P_T > 20$ GeV/c
- $|\eta| < 2.5$

yields $\sim 10^6$ events per SSC year (10^{40}cm^{-2})

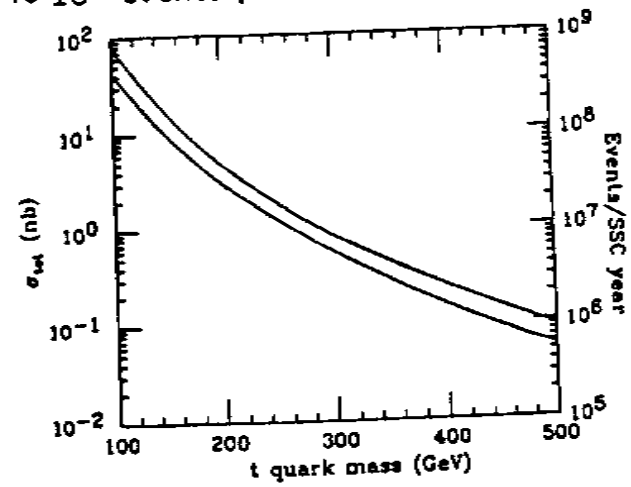

Theoretical uncertainty in $\sigma_{t\bar{t}}(M_{top})$

$\Rightarrow \sigma_{M_{top}} \sim 10 - 15$ GeV/c^2

Low Backgrounds

A similar analysis for LHC illustrates cleanliness

- Require lepton $P_T > 50$ GeV/c
- $\sum E_T < 10$ GeV in cone of $R = 0.4$ for both leptons
- $|\eta| < 1.5$

yields 3×10^5 events in $\int \mathcal{L}\, dt = 10^{41}$ cm^{-2}

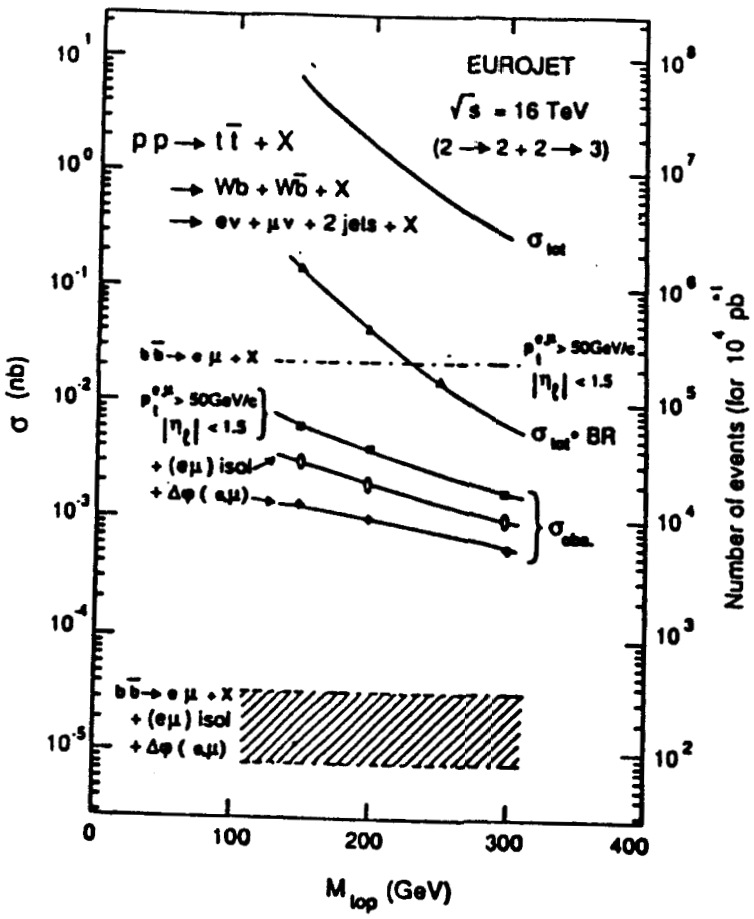

e mu mass plots

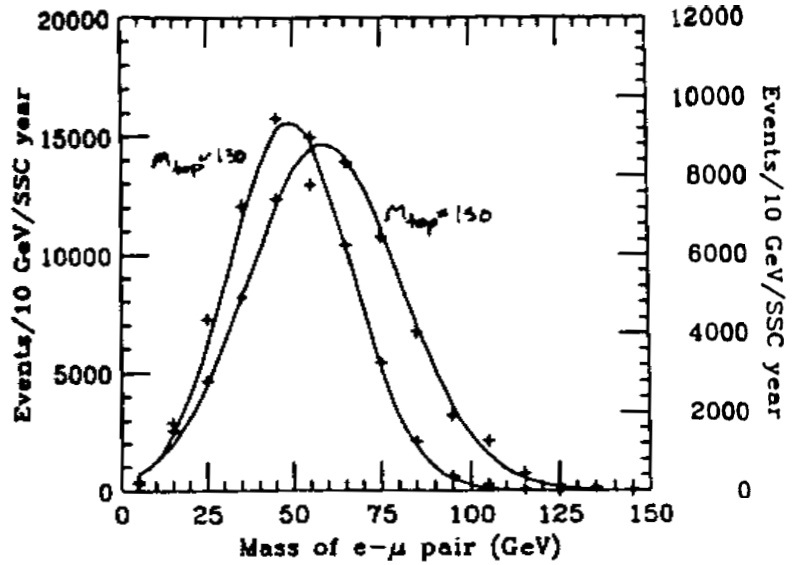

$< M(e\mu) >$ sensitive to M_{top}

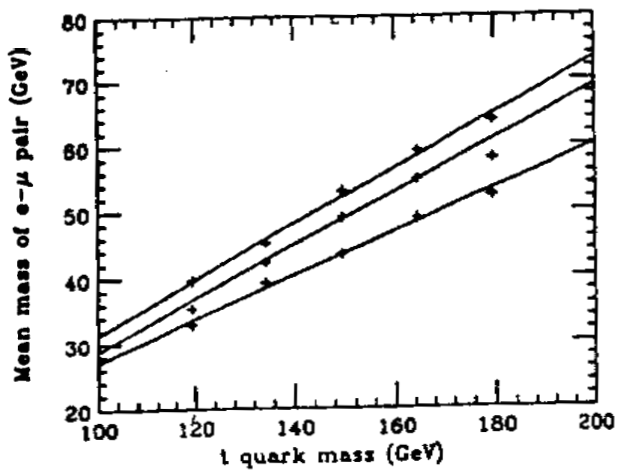

Dominated by systematics

Uncertainty in M_{top} dominated by systematic uncertainties

Effect	$\sigma_{M_{top}}$ (GeV/c^2)
b quark fragmentation	1.5
t quark P_T	1.9
Statistics (1 year)	0.5

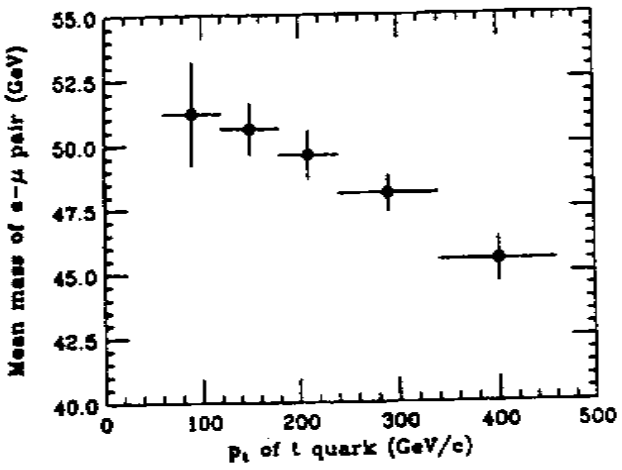

⇒ Can expect to measure M_{top} to $\sim 2-3$ GeV/c^2

What will be the effect of a sample of 10^{7-8} t's on the systematics above?

Leptons plus jets

The *lepton + jets* mode provides inherently more rate

- Can perform full reconstruction
- Can directly measure M_{top} and BR

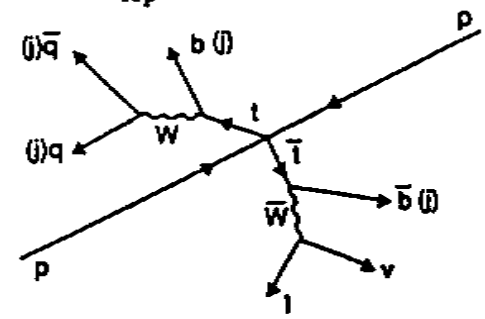

- However, jet combinatorics are a problem

SSC and LHC groups have made extensive studies

- Agree that kinematical selection can reconstruct top
  - Require isolated lepton with $P_T \gtrsim 40$ GeV/c
  - Require 3 jets with high P_T cut
- More efficiently done using b quark tag

SDC approach takes advantage of b quark tagging

- Allows measurement to be done at low luminosity
- Better control of systematics in M_{top} measurement

150,250 mass plots

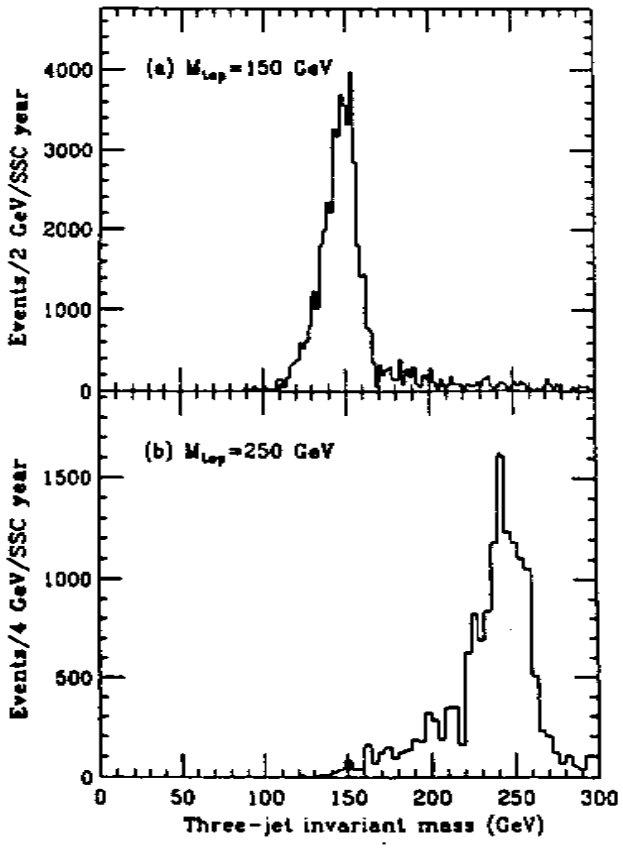

Jet energy scales

Systematics in M_{top} dominated by jet energy scales

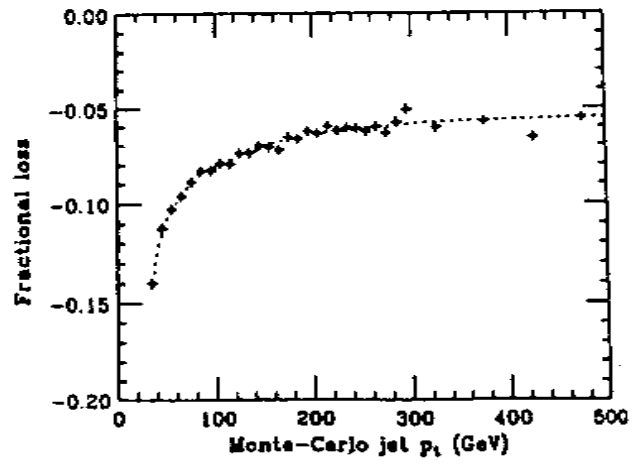

- Use MC to correct for clustering effects, etc.
- Can calibrate low-energy jet scale using W signal
- b quark fragmentation

$$\sigma_{M_{top}} \sim 2 - 3\mathrm{GeV/c^2}$$

top branching ratios

Although $e^{\pm}$ and $\mu^{\pm}$ decay modes are most accessible,

$$t \to \tau \nu_\tau b$$

is detectable using single-prong $\tau \to \pi^- X$ decays

Require

- isolated lepton with $P_T > 40$ GeV/c(from W decay)
- one jet with $P_T > 30$ tagged as b hadron
- isolated, charged track with $P_T > 50$ GeV/c

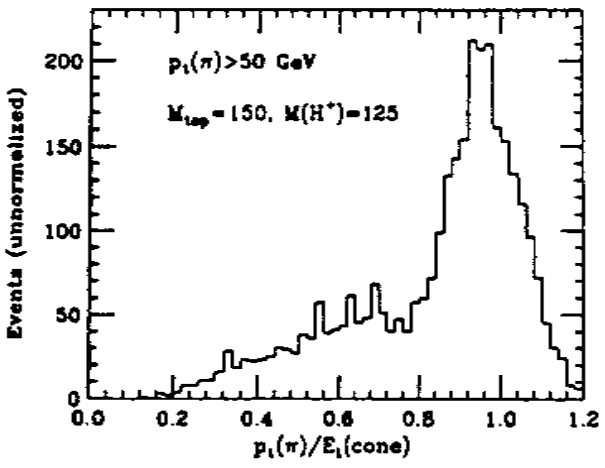

$\Rightarrow$ uncertainty in relative τ rate is $\lesssim 5\%$

UA2 Charged Higgs Search

UA2 Collab.,Phys.Lett.**B280**(1992)137.

Search for events with electrons or taus and with large missing Et. The number of such events with electrons is used to find the W contribution. An excess of τ's would signal the presence of Higgs production.

Cuts

Missing pt > 20 GeV

Leading jet Et > 17 GeV

No opposite jet with Et>10 GeV

τ cuts

hadronicity=had/tot

profile

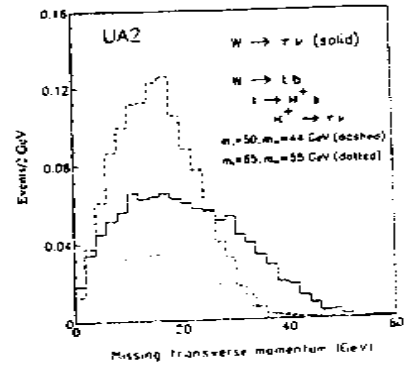

Fig. 2. Simulated p_T distributions for $W \to \tau\nu$ and $H^+ \to \tau\nu$ events.

τ cuts

hadronicity ξ = had/tot

require $0.01 < \xi < 0.90$ so there is some hadronic energy and some electromagnetic energy
Require one track in a 10 degree cone around the cluster.

profile ρ = (Em +Em')/Etot $\rho > 0.75$

where Em and Em' are the leading and neighboring cell energies (i.e. tight cluster)

UA2 (cont.)

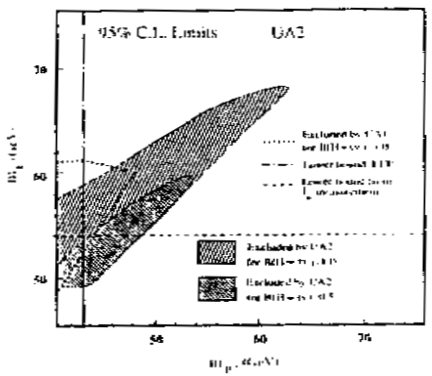

Fig. 6. Regions of the m_H–m_t plane excluded at 95% CL. the LEP bound is for $B = 1$, 95% CL

Branching Ratios

Observation of top in

$$pp \to e^{\pm}\mu^{\mp} \qquad \propto BR(t \to e\,\nu_e\,b) \times BR(t \to \mu\,\nu_\mu\,b)$$
$$pp \to l^{\pm}l^{\mp} \qquad \propto BR(t \to l\,\nu_l\,b)^2$$
$$pp \to \mu^{\pm} + jets \qquad \propto BR(t \to \mu\,\nu_\mu\,b) \times BR(t \to q\,\bar{q}\,b)$$
$$pp \to e^{\pm} + jets \qquad \propto BR(t \to e\,\nu_e\,b) \times BR(t \to q\,\bar{q}\,b)$$
$$pp \to \tau^{\pm}\tau^{\mp} \qquad \propto BR(t \to \tau\,\nu_\tau\,b) \times BR(t \to q\,\bar{q}\,b)$$

Allows measurement of relative BR's to 1 – 5%

- Limited by systematic uncertainty in efficiency
- Depends on isolation of lepton and physics models

Charged Higgs Decays

Br(t → H⁺ b)

It is possible that the top has not been seen due to charged Higgs decay modes. If the top is heavier than the mass of the charged higgs plus the mass of the b, then the situation depends on tanβ, which is the ratio of the vacuum expectation value of the Higgs doublet.

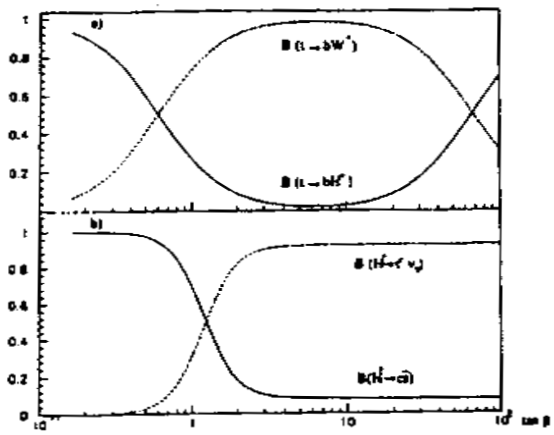

Figure 9: Branching ratios (m_t = 200 GeV, m_{H^+} = 130 GeV)

For this scenario, find a region where W decay is small, i.e. either large or small tanβ. Small tanβ would still be found because there the dominant decay mode of the Higgs is two jet. For large tanβ however, tau decays would dominate.

Breakdown of e μ τ universality would be a strong clue.

Low tan β

(disfavored)

but good signal for H^+

Resulting $M(jj)$ distribution for $M_{H^+} = 125$ GeV/c² is

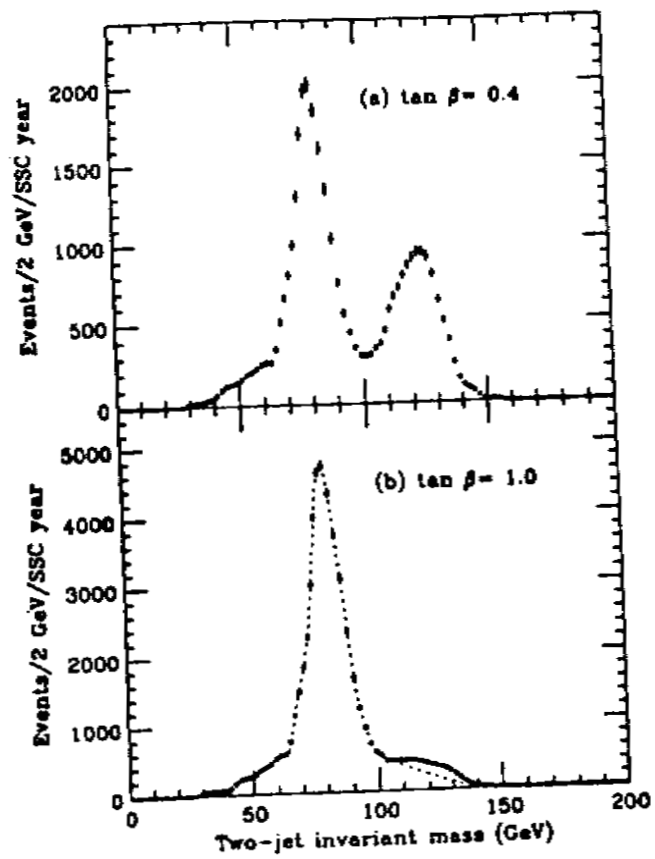

Top Tagging

Associated Top Production

$pp \to H\, t\bar{t}$ may be important for a light Higgs search

- The WW channel is closed and $Z\,Z^*$ is rate-limited
- $H \to \gamma\gamma$ is largest potential rate
  - QCD diphoton backgrounds are enormous

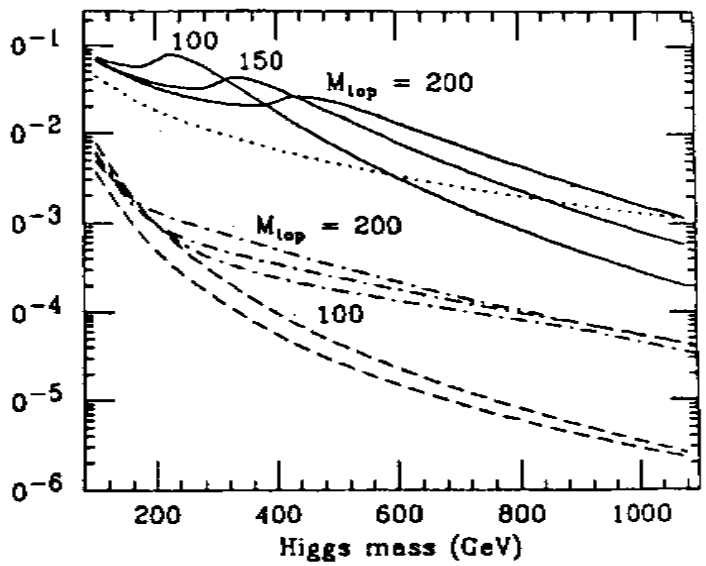

Tag $t\bar{t}$ system with isolated, high P_T lepton

- Reduces QCD fake backgrounds to manageable level
- Isolation removes $b\bar{b}\,\gamma\gamma$ background
- No longer need high-precision EM calorimetry

gamma gamma and ZZ

"Reach" in $\gamma\gamma\, l\, X$ channel complements $Z\,Z^*$

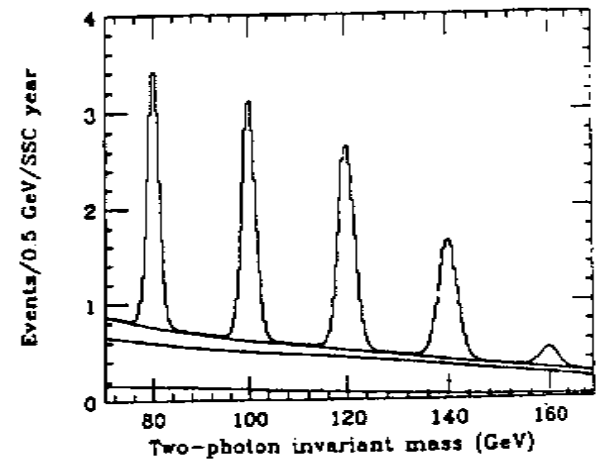

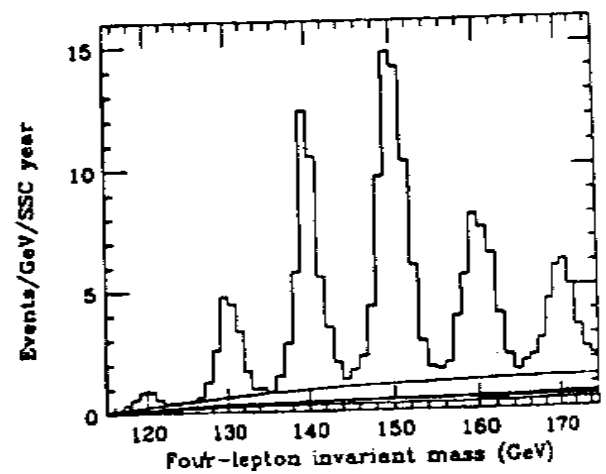

$H \to ZZ^*$

copious production

$\boxed{\text{SSC / LHC}}$ copious $pp \to t\bar{t}X$ production

Idea tag t ($\bar{t}$) by $t \to bW \to b\ell\nu$ ($\ell = e, \mu$)

study $\bar{t} \to \bar{b}W \to \bar{b}\ell\nu$

$\searrow \bar{b}H \to \bar{b}\tau\nu$ ⇐ excess taus break lepton universality

or $\bar{b}H \to bcs$ ⇐ cs dijet mass peak BUT (see next pg)

Detailed simulations by GEM collaboration – letter of intent

and by SDC " ↗ Tech. Design Report SDC-92-201 ↘ Barnett et al SDC-92-213

① $\ell\tau$ signal

measure $t\bar{t} \to b\bar{b}WW \to ee, e\mu, \mu\mu$

predict " " $\to e\tau, \mu\tau$ background B

measure excess from $b\bar{b}WH \to e\tau, \mu\tau$ signal S

statistical significance of signal $= \dfrac{S}{\sqrt{S+B}} = N_{SD}$

info from b-> s gamma

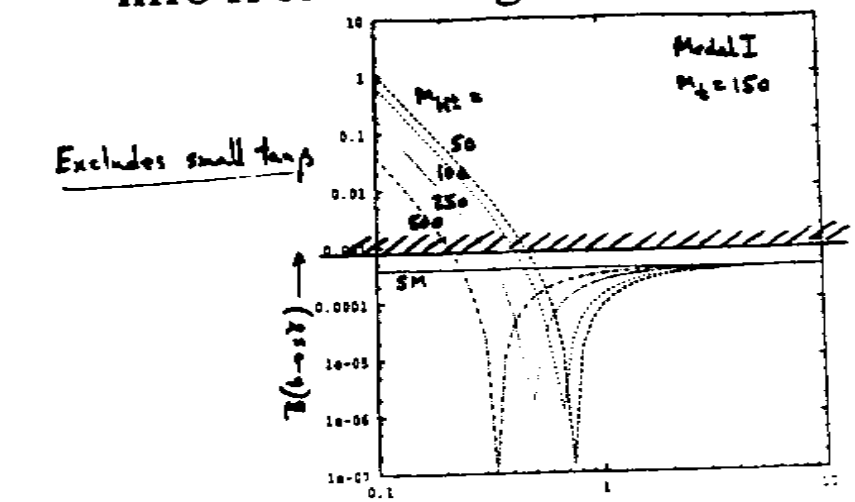

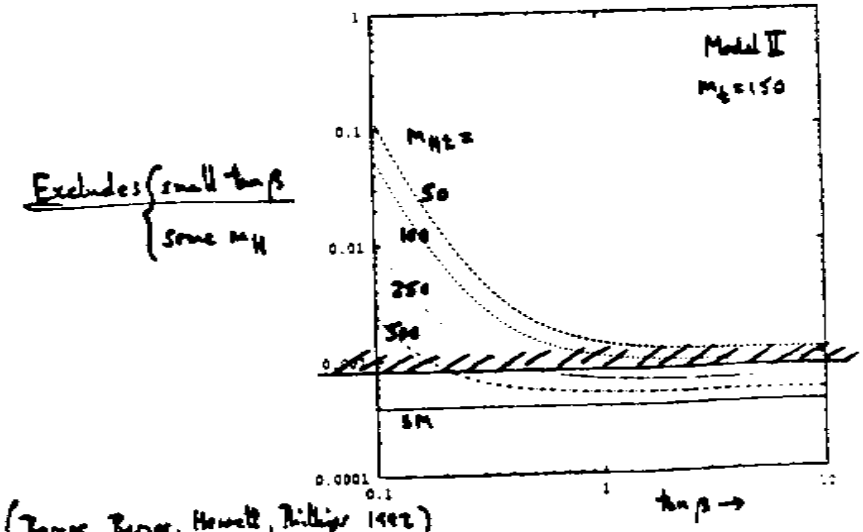

(Barger, Berger, Hewett, Phillips 1992)

SDC simulations

One year run gives integrated luminosity of 10 fb -1

Look for $\tau \to \pi \nu$

$M_t = 150$
$M_{H^\pm} = 135$
$\tan\beta = 5.5$

An example of the number of events found with and without b tagging in $WWb\bar{b}$ and $WHb\bar{b}$ events where we have chosen $m_t = 150$ GeV and $m_{H^\pm} = 135$ GeV and $\tan\beta \approx 6$. We have only calculated the background from the $WWt\text{-}\tau$ events in finding N_{SD}.

		with b tagging	no b tagging
$N_{t\tau}^{WH}$	($p_T(\pi) > 50$ GeV)	409	2061
$N_{t\tau}^{WW}$	($p_T(\pi) > 50$ GeV)	3949	14852
$N_{t\tau}^{WH}$	($p_T(\pi) > 100$ GeV)	135	656 = S
$N_{t\tau}^{WW}$	($p_T(\pi) > 100$ GeV)	668	2700 = B
N_{SD}	($p_T(\pi) > 50$ GeV)	6.2	15.8
N_{SD}	($p_T(\pi) > 100$ GeV)	4.76	11.3

Significance of $t\tau$ signals

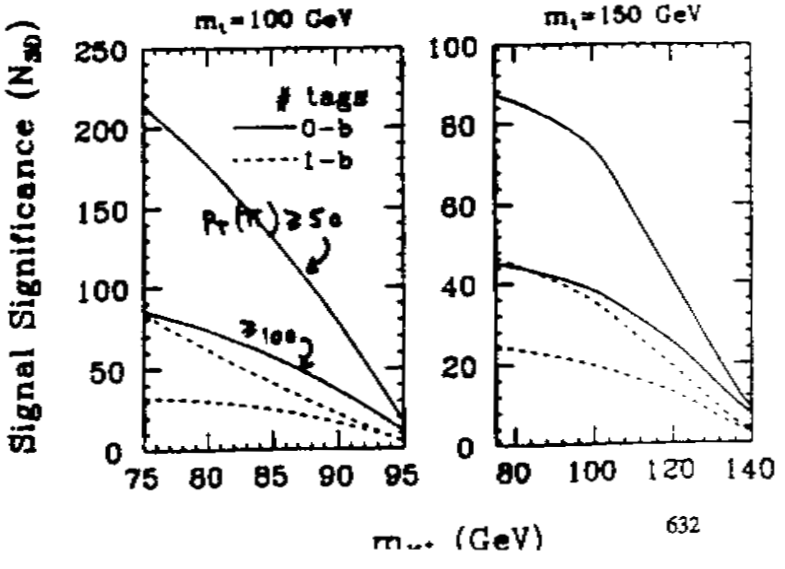

Tevatron tau searches

See contributions by Phillips and Baer, this conference:

Present Tevatron luminosity is 10**-3 times smaller than the SSC, and the cross section is also 10**-3 times smaller.

See Baer et al Phys.Rev.**D39**,3310(1989)

search for dileptons from top

add b tag and assume luminosity of 1000 pb-1

m_t	$N(ee, e\mu, \mu\mu)$	$N(e\tau \to h, \mu\tau \to h)$
100	630	450
120	270	190
140	130	90

The table above shows the standard model rates. It should be possible to detect excesses in these ratios, which would indicate charged Higgs

CDF SUSY

Could we miss it ?

Baer says yes.

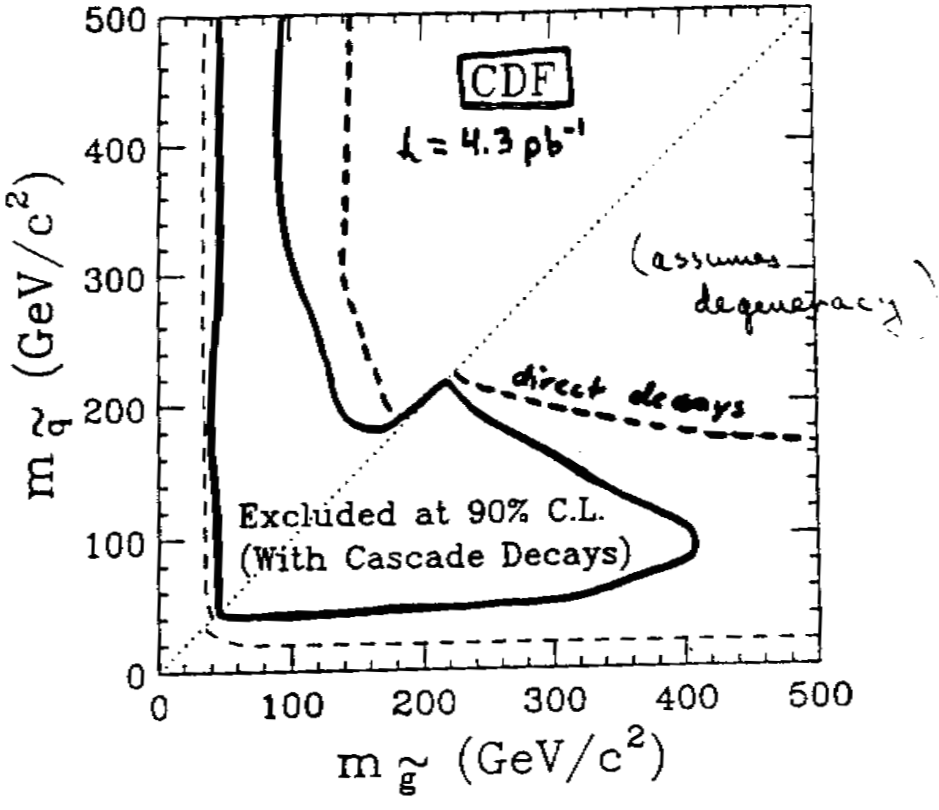

Figure 4: The shaded region of squark and gluino masses is excluded at 90% C.L for a version of SUSY with cascade decays, $\mu = -250$, $\tan\beta = 2$, and $m_H = 500$ GeV/c^2. For comparison, the dashed line shows the limits corresponding to no cascade decays.

SUSY vs the SM

N.Krasnikiv,S.Pokorski,CPTH-A164-0492(1992)Apr.

The mass of the Higgs and the top can distinguish in some cases between these two models when the top mass is greater than 150 GeV.

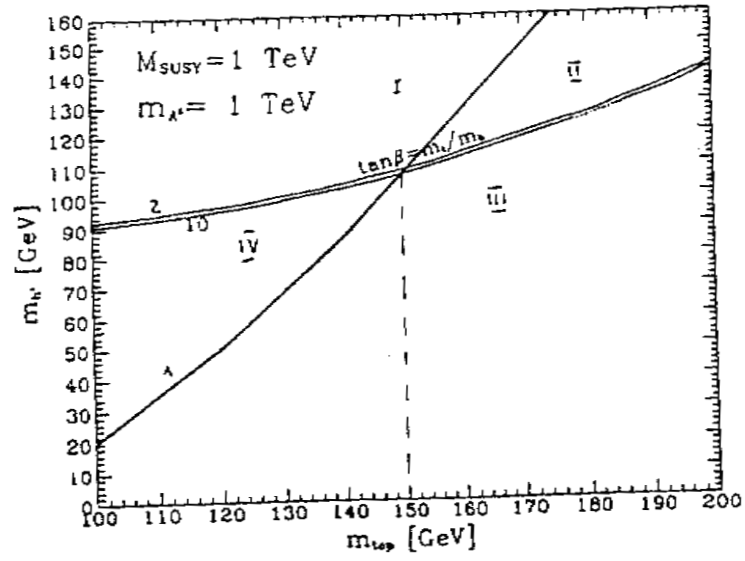

Region I	Standard Model Only
Region II	Excluded - both models
Region III	SUSY Only
Region IV	Allowed - both models

stop

H.Baer,M.Drees,R.Godbole,J.Gunion,X.Tata,
Phys.Rev.D44(1991)725.

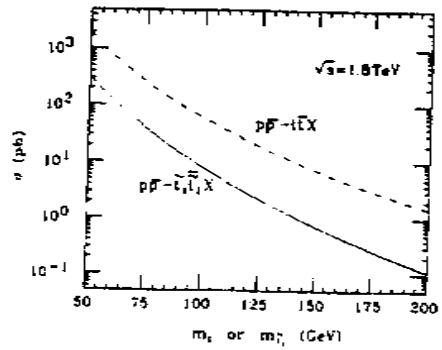

FIG. 2. We have shown the cross sections for the production of top-quark and top-squark pairs at the Tevatron. In our computation we have used the Duke-Owen structure functions (set 1) with Λ_5=0.14 GeV for five flavors, and have taken $Q^2=t$.

If the stop's decay to b+supersymmetric W's which in turn cascade decay to lsp's (lightest supersymmetric particles), then the detection mode would be b jet plus missing Et. Decays in the cascade which lead to Zinos with electrons in the decay might produce multilepton events which would probably be easier to detect.

Felcini criteria for $t \to bH^+$ $\hookrightarrow \tau\nu$

(LHC, Aachen)

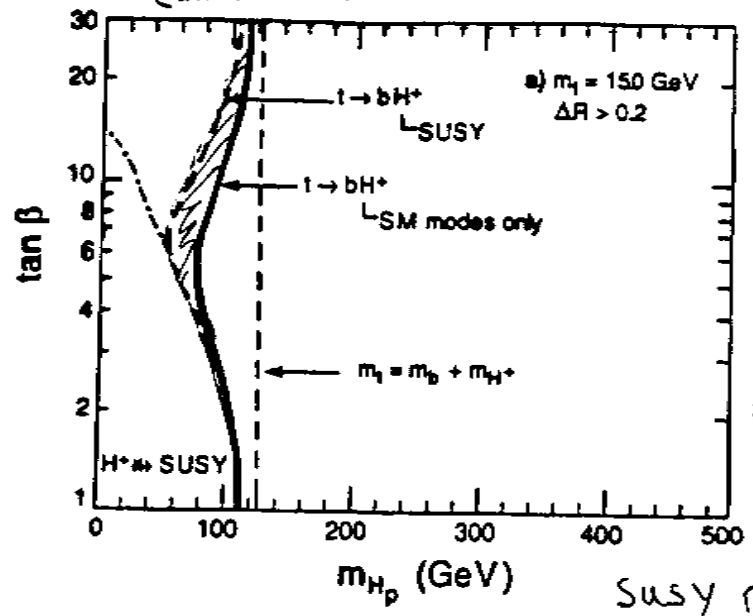

τ-lepton universality violation

BBDHT

1.) $\tilde{g}$ = 100 GeV, $\mu = m_{\tilde{g}}$

2.) $m_{\tilde{g}}$ = 400 GeV, μ = -70 GeV

SUSY RELAXES CONSTRAINTS.

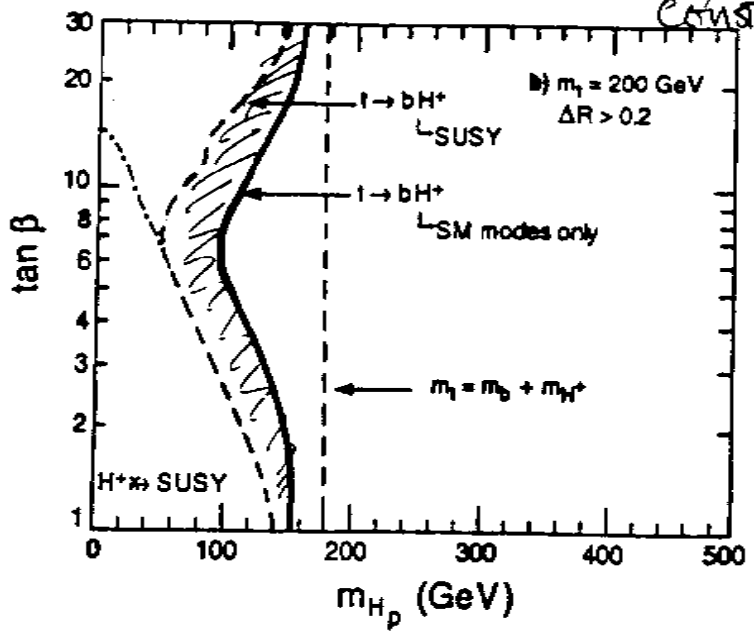

top backgrounds to the Higgs Search

For SSC/LHC, one of the more attractive Higgs search modes is the $\gamma\gamma$ decay. For Higgs up to 80 GeV, one can rely on LEP. Above 140 GeV, the best mode is the 4 lepton decay. In the intermediate mass range, the $\gamma\gamma$ mode is best.

Z.Kunzt,Z.Trocsanyi,W.Stirling,ETH-TH/91-17

A.Ballestrero,E.Maina,Phys.Lett.**B268**(1991)437.

Prompt photon pairs produced along with t pairs can represent a significant background for this search in the low mass (<100) region. Previous studies have concentrated on backgrounds to the search from light quark processes.

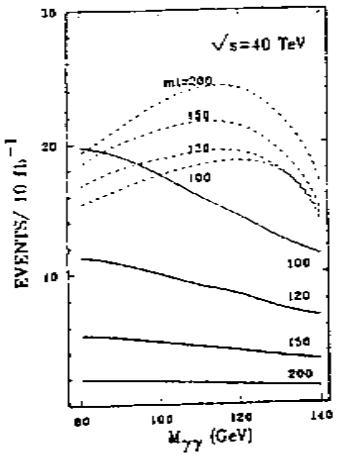

Fig. 3. Expected number of $t\bar{t}\gamma\gamma$ events at SSC, in one year at the design luminosity, with the cuts described in the text. From prompt photons (continuous curves) and from $t\bar{t}H$ (dashed) in a window $\Delta M = 6$ GeV centered around the Higgs mass. Results are presented for $m_t = 100, 120, 150, 200$ GeV.

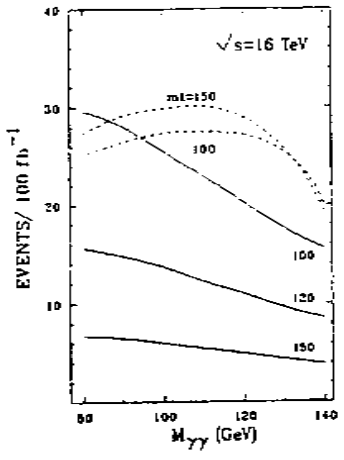

Fig. 4. Expected number of $t\bar{t}\gamma\gamma$ events at LHC, in one year at $\mathcal{L} = 100$ fb^{-1}, ten times the design luminosity, with the cuts described in the text. From prompt photons (continuous curves) and from $t\bar{t}H$ (dashed) in a window $\Delta M = 6$ GeV centered around the Higgs mass. Results are presented for $m_t = 100, 150$ GeV. For $m_t = 120$ GeV we give only the prompt photon result.

The Top Quark at Linear e^+e^- Colliders

MICHAEL E. PESKIN

Stanford Linear Accelerator Center
Stanford University, Stanford, California 94309

ABSTRACT

I review the aspects of top quark physics which can be studied at a linear e^+e^- collider operating as a top quark factory in the energy region between 300 and 500 GeV.

the top quark

at linear e^+e^- colliders

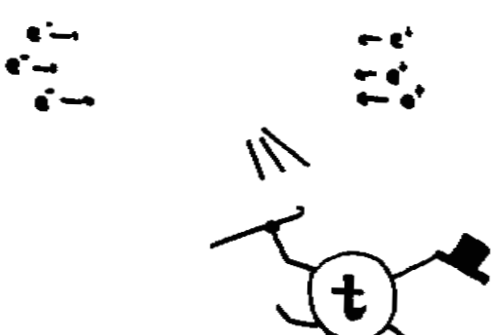

issues for the study of the top quark:

- discovery
- mass measurement
- exotic decays
- threshold structure
- form factors, (g-2)
- CP violation

Prospects for a next-generation linear e^+e^- collider:

Begin at $\sqrt{s} = 200$-500 GeV, $\mathcal{L} \sim 5\times10^{33}\,cm^{-2}sec^{-1}$

international collaboration, concept of extendable machine

advance to $\sqrt{s} \sim 1$-2 TeV $\quad \mathcal{L} \sim 5\times10^{34}\,cm^{-2}sec^{-1}$

(SSC result set the goal)

Critical technologies are at prototype stage

ready ~ 1995

Already at $\sqrt{s} \sim 400$ GeV there are interesting experiments at the edge of our understanding of the standard model.

$\rightarrow$ $e^+e^- \to W^+W^-$ $\quad \gamma\gamma \to W^+W^-$

$\rightarrow$ study of h^0 if $m(h^0) \lesssim 250$ GeV

$\rightarrow$ top quark

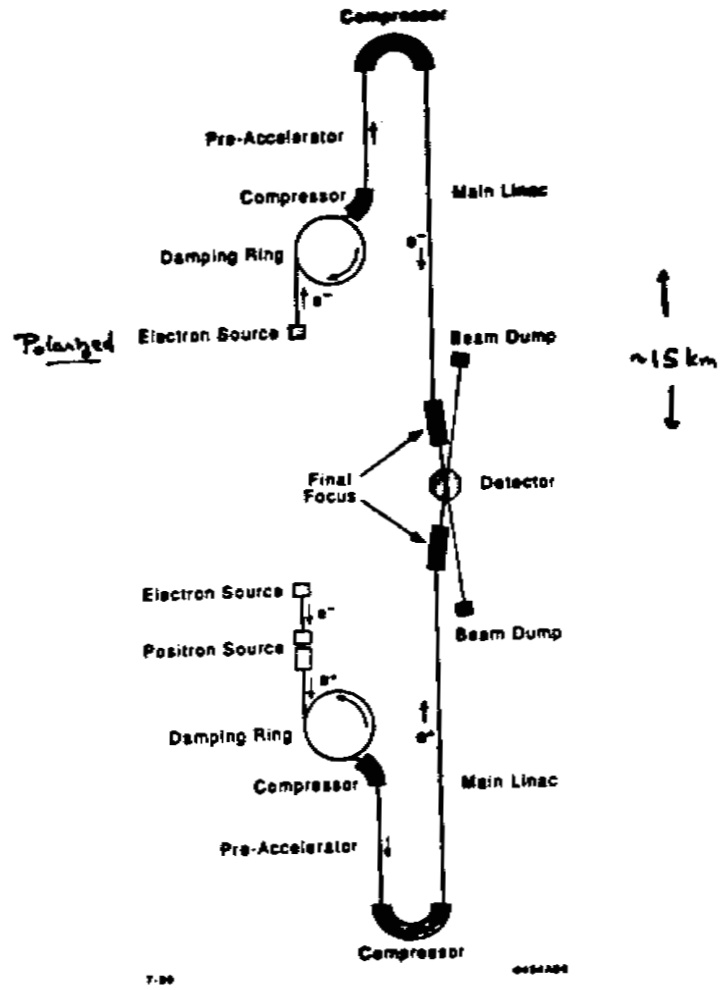

A schematic design for a 500 GeV linear e^+e^- collider.

Components of the linear e^+e^- collider:

e^+e^- sources: SLC already has high intensity
a new technology (SLAC/Nagoya) offers
Pol ~ 70% or higher; working guns by
spring '93 (?)

damping rings: A prototype w. required small
emittance is designed at KEK

accelerating structure: Currently 2 approaches

(most $ are here)

SLAC/KEK:
conventional klystrons / Copper cavities
operated at X-band (4x SLAC)
run in 1 psec pulses

Cornell/DESY:
superconducting RF cavities

both groups are designing test accelerator
segments; shakeout in 1995?

beam dynamics
accelerator structure damps higher modes

BNS damping; active feedback of
accelerator alignment
proven at SLC

final focus

(tightest tolerances are here)

steering, feedback, control of
backgrounds are issues studied
at SLC

test of demagnification:
Final Focus Test Beam summer '93

SLAC - KEK - Orsay - DESY - Munich
- Novosibirsk

Properties of top (for comparison to hadron colliders)

m_t: PP $\Delta m_t \sim \pm 2\text{-}3$ GeV Sinerva
systematics limited

e^+e^- $\Delta m_t \sim \pm 0.2$ GeV - threshold
± 0.5 GeV - accelerator

Schaile: $\Delta m \sim \pm 1$ GeV is needed to extract max. info from precision electroweak Pilcher

Σ_t: PP no direct measurement
indirect measurement from $W_g \to t\bar{b}$ Yuan
should have QCD accuracy $\sim 30\text{-}40\%$

e^+e^- direct measurement to Fujii
$< 15\%$

Branching fractions:

$t \to H^+ b$ $m_t = 150$ $m_H = 100$ 3σ effect
$BR(t \to Hb)\, BR(H \to \tau\nu)$

PP 5% (?) already at Fermilab
1½% in an SSC year
Sinerva

e^+e^- 6% 30pb' EES00

(but remember, $\sigma(e^+e^- \to H^+H^-) = 0.35\beta^3$ R
if these particles are there and have $m_H < m_t$,
NLC will study them directly in normal
decay channels.

similar story for $t \to \tilde{t}\tilde{\gamma}$

for truly rare decays, e^+e^- often limited statistics

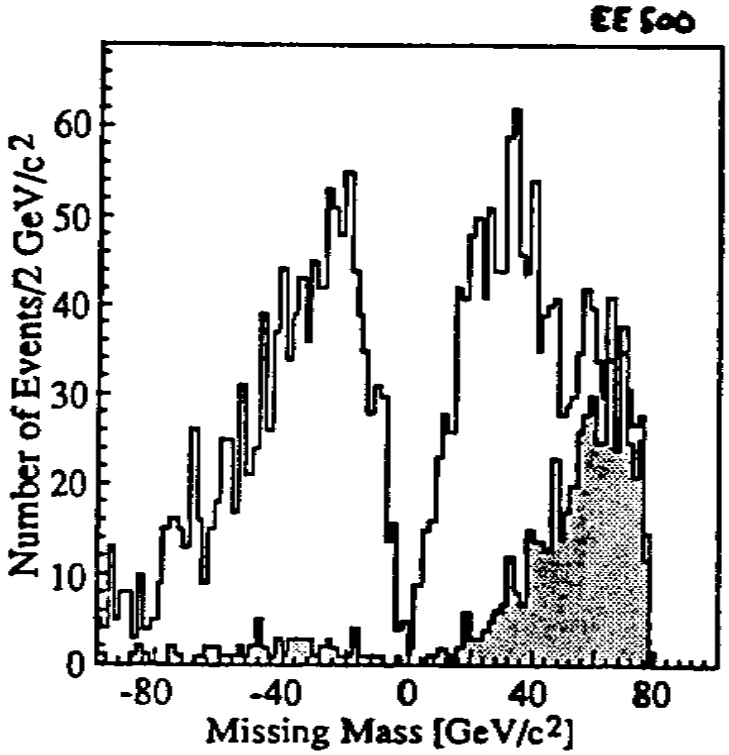

Search for $t \to H^+b$, $H^+ \to \tau^+\nu$, using $\tau^+ \to \ell^+\nu\bar{\nu}$ and reconstructing the 3-neutrino missing mass, from the EE500 Workshop Proceedings (P. Zerwas, ed., 1991). The unshaded histogram is the background from standard leptonic top decays.

but this comparison is not the real issue

consider: $\Gamma_t \to$ 300 120 $\sim m_t$
650 130
1000 150
MeV GeV

Systrand:
above $m_t \sim 120$ GeV,
the top string gives a small contribution
to hadronization, vanishing as
$e^{-\Gamma/T}$ $T \sim 100\text{-}200$ MeV

Kühn: above $m_t \sim 120$ GeV,
the confining part of the $q\bar{q}$ potential is
irrelevant to toponium
or $\sim (m_t \Gamma_t)^{-1} \sim [30\ \text{GeV}]^{-1}$ 150 GeV

Yuan: above $m_t \sim 120$ GeV
soft QCD effects which flip the top spin are
negligible

$$\frac{1}{\Gamma_t} \cdot \left(\Delta m_{B-B^*} \cdot \frac{m_c}{m_t}\right) \sim 10^{-3}$$ 150 GeV

thus, above $m_t \sim 120$ GeV

t becomes the ideal quark of perturbative QCD !

We would like to do experiments

- to visualize t dynamics
- to use the simplicity of t as a tool to probe new physics

$t\bar{t}$ threshold

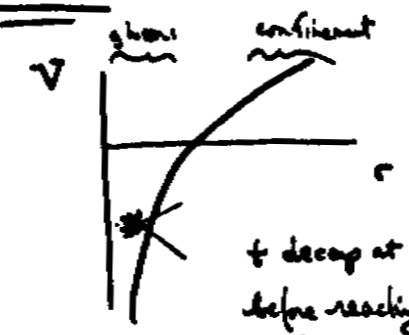

Fadin-Khoze

t decays at $r \sim (m_t \Gamma_t)^{-1}$ before reaching the confinement region

essential interplay of Γ_t with Coulombic $t\bar{t}$ spectrum

"the hydrogen atom of the strong interactions"

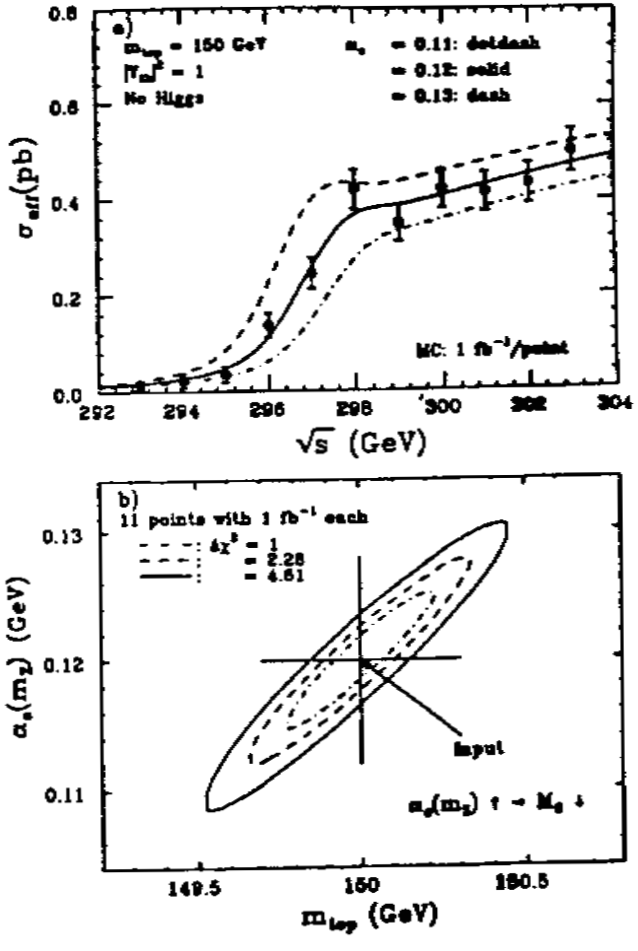

Simulation of the $t\bar{t}$ threshold measurement (by Fujii), including 0.3% beam energy spread; fit of the simulation results to extract m_t and $\alpha_s(m_Z^2)$.

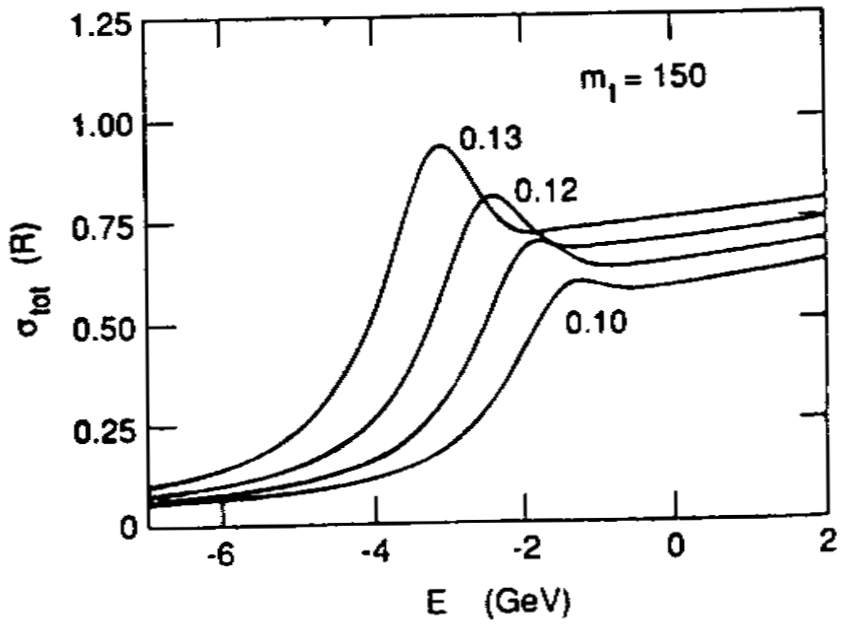

Dependence of the $t\bar{t}$ threshold shape on $\alpha_s(m_Z^2)$, for m_t = 150 GeV.

Theoretical subtleties — Kühn, Fujii

→ Green's function technique

→ t resonance effects

→ t width depends on band state environment

→ S wave – P-wave interference

But ultimately, the theoretical edifice depends only on

m_t, Γ_t, $\alpha_s(m_t^2)$

without further phenomenological input (except Higgs, other new physics)

Theorists now quarrel about 5% corrections

Energy distribution of W from t decay

Kühn

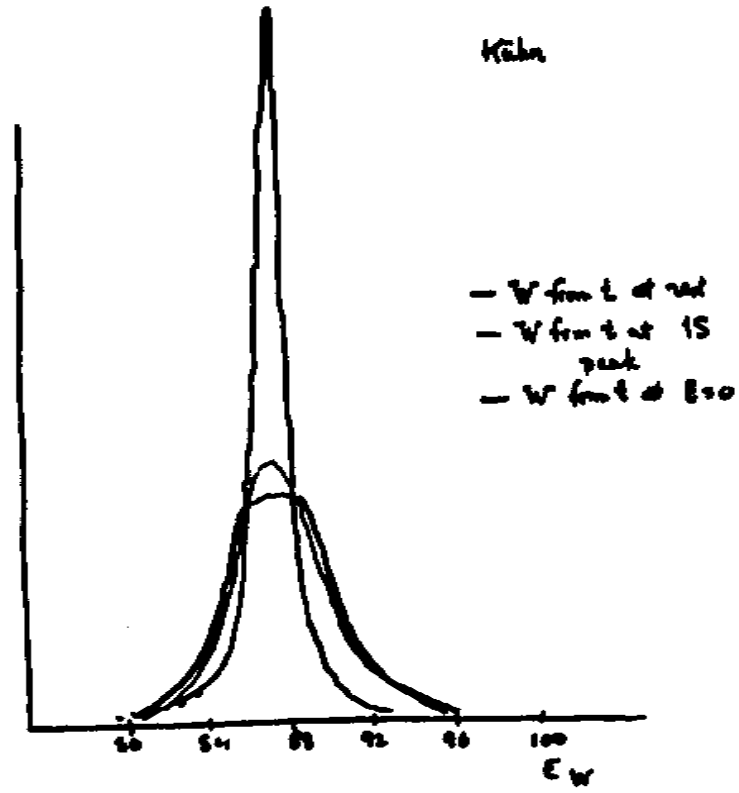

When well understood, the $t\bar{t}$ threshold can be a tool.

→ m_t !

→ method for extracting the $t\bar{t}H$ coupling!

(Kühn: dilute by 0.7 for $m_H \sim 100$ GeV)

$$\frac{\Delta\lambda_{t\bar{t}H}}{\lambda_{t\bar{t}H}} \sim 30\%$$

[Bunke: at e^+e^- colliders, this number can be independently determined to the same accuracy by $e^+e^- \to t\bar{t}Z^0$, $e^+e^- \to t\bar{t}H^0$]

→ 3 methods for extracting Γ_t !

shape of $\sigma(\sqrt{s})$

momentum spectrum of t

FB asymmetry

Fujii

each at 20% level for 90 pb^{-1}

(~1 in fit effective α_s)

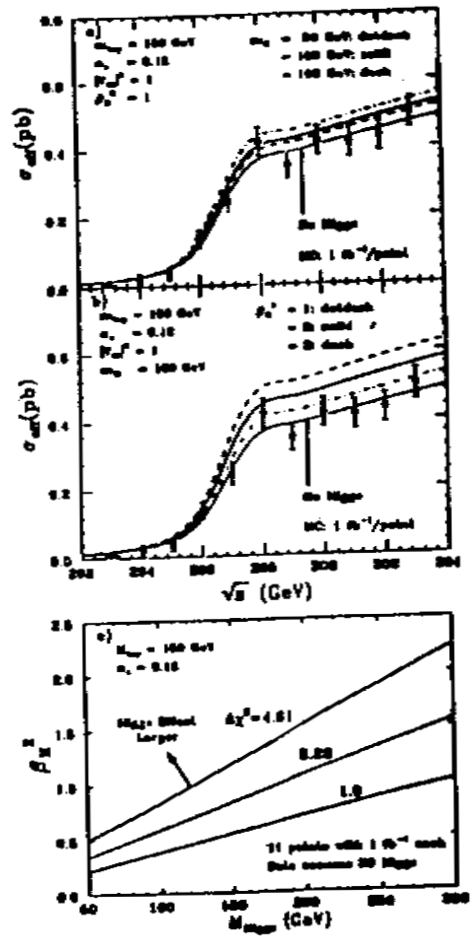

Comparison of the $t\bar{t}$ threshold simulation results to the enhancement expected from the top quark interaction with a a 100 GeV Higgs boson.

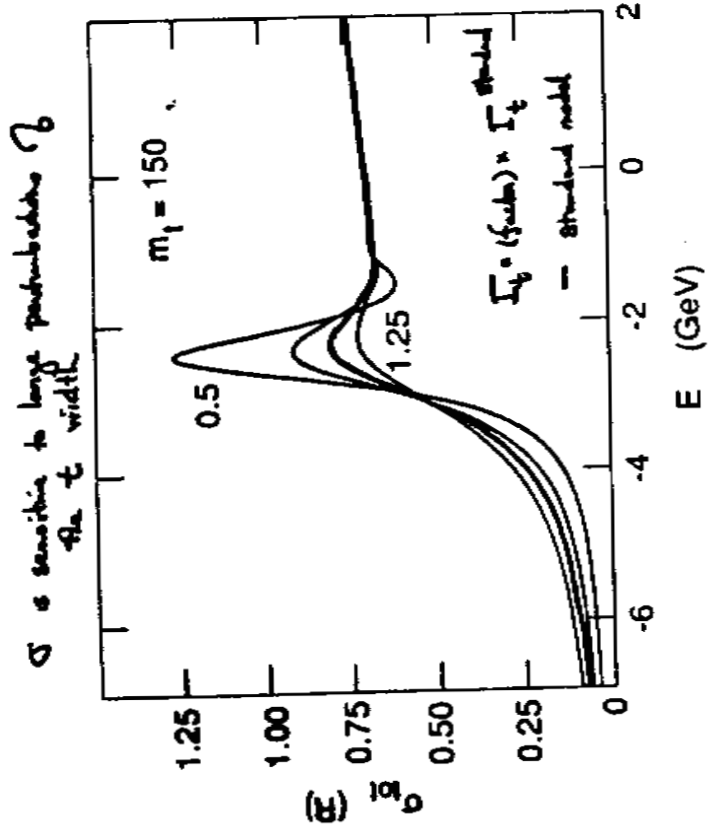

Effect of the top quark width on the shape of the threshold cross section.

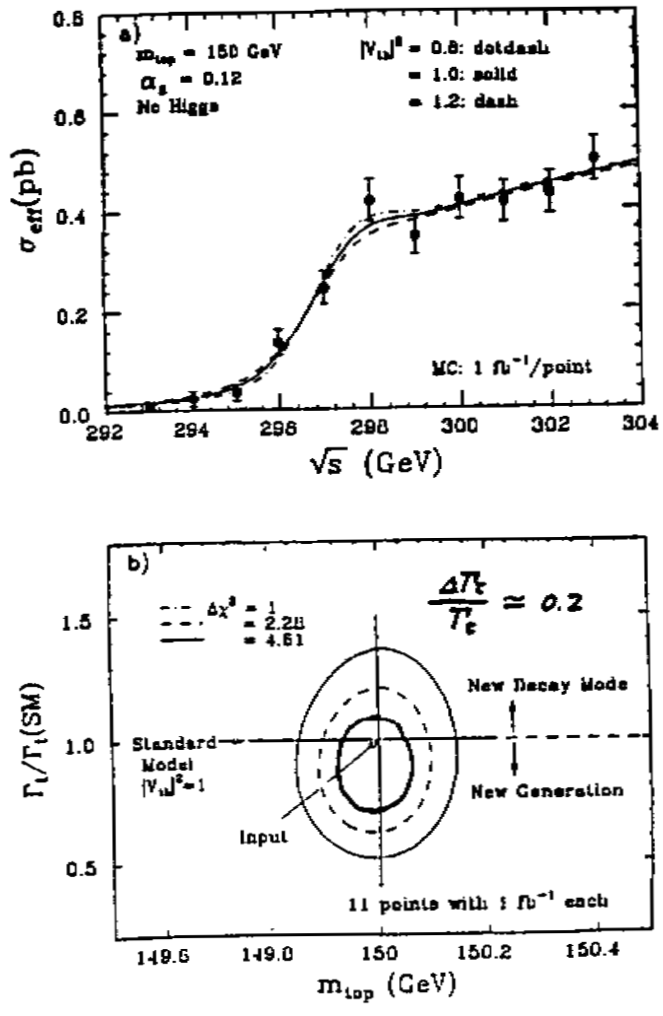

Comparison of Fujii's simulation of the $t\bar{t}$ threshold cross section to the effect of varying the top quark width.

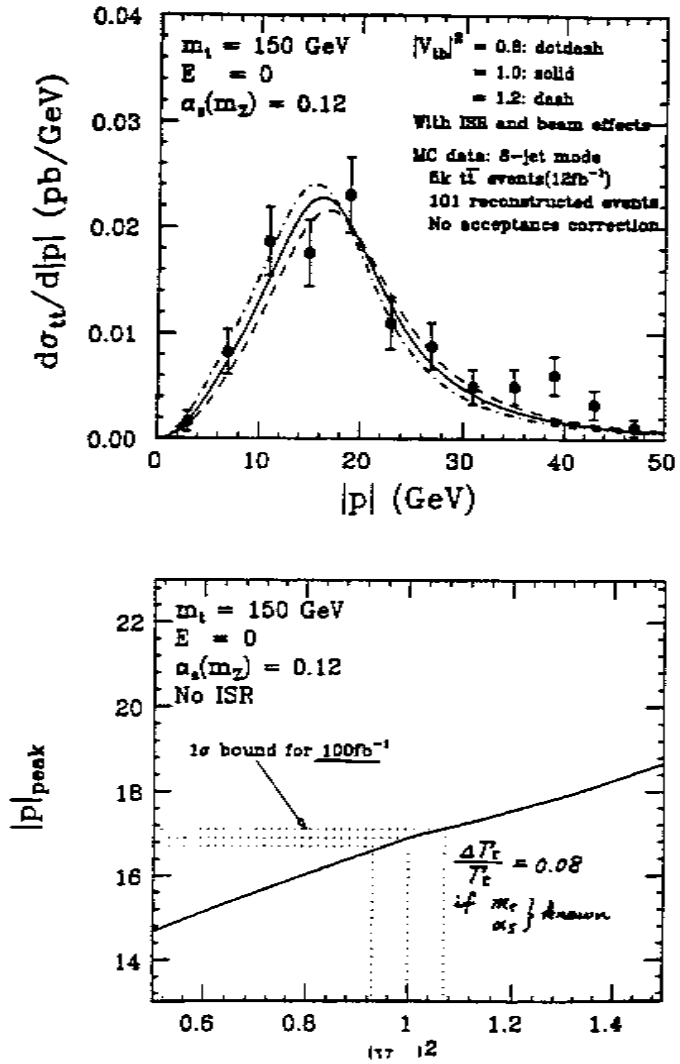

Comparison of Fujii's simulation of the top quark momentum distribution to the effect of varying the top quark width.

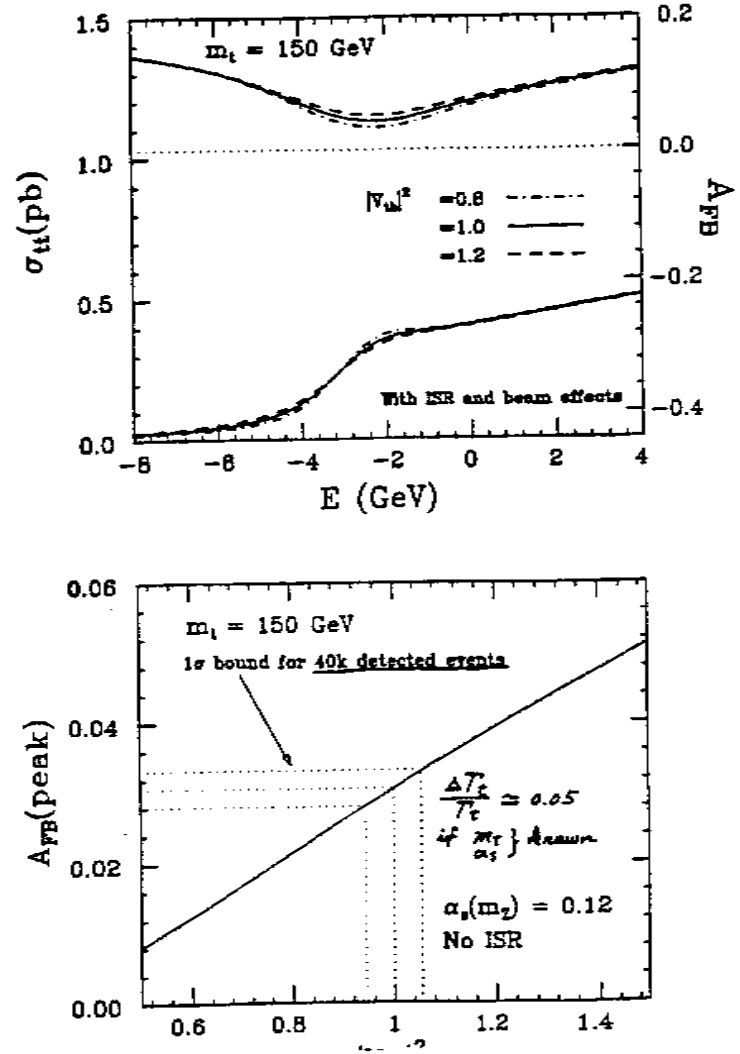

Comparison of the $t\bar{t}$ forward-backward asymmetry expected near threshold to the effect of varying the top quark width.

$t\bar{t}$ above threshold

$e^+e^- \to t\bar{t}$ gives the cleanest possible 6-jet system

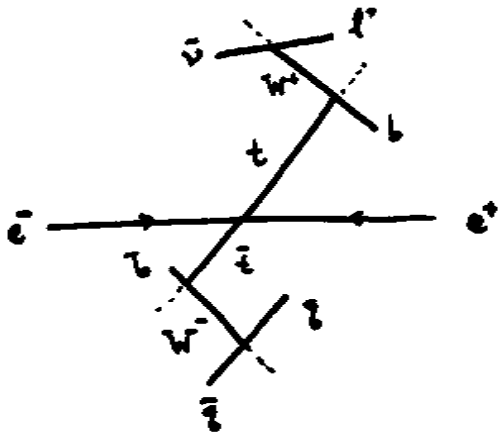

2 jet pairs sum to m_W

2 W-jet combinations sum to m_t

momentum is balanced up to initial st. rad, fragmentation

Enormous information in jet angles, correlations!

EE500

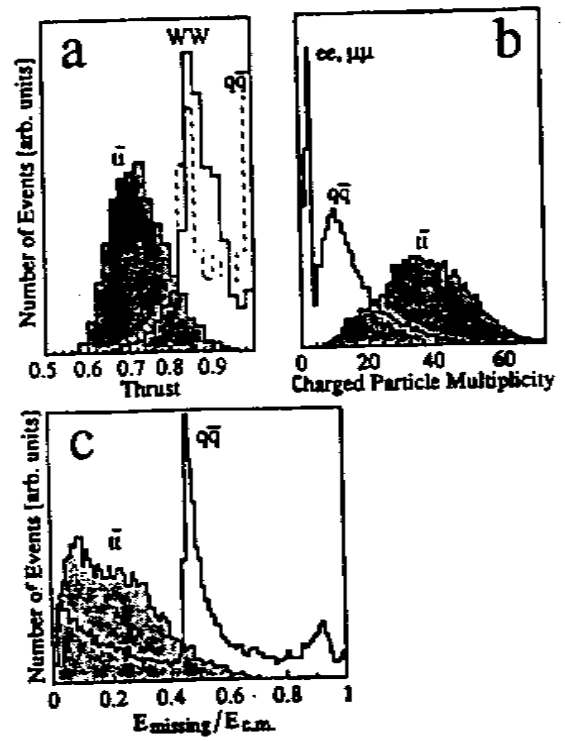

Separation of $t\bar{t}$ events from standard model backgrounds, as reported in the EE500 proceedings.

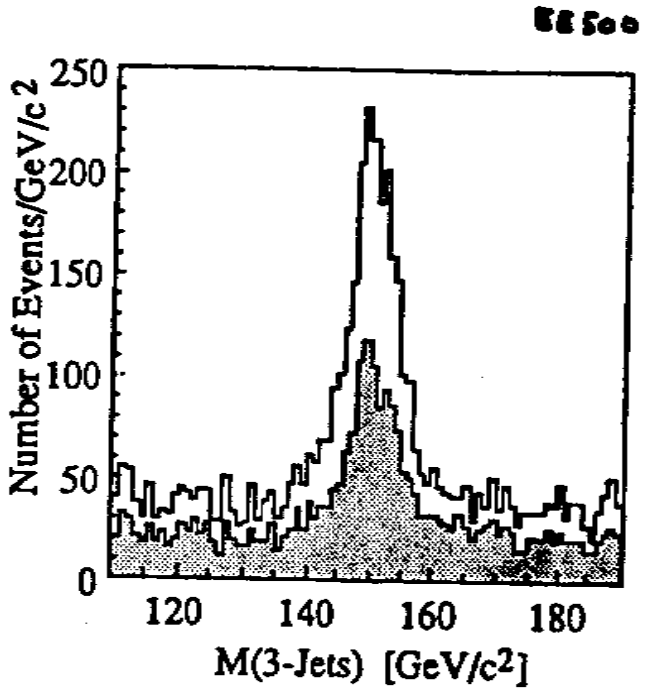

Reconstruction of the top quark mass as a 3-jet invariant mass, as reported in the EE500 proceedings.

In addition,

every step of the decay chain is parity violating

so each step analyzes the spin of the previous one

- the t spin is not affected by soft hadronic processes
- hard gluon corrections are small

as 1% in $t \to W^+_{long} b / t \to W^+_L b$

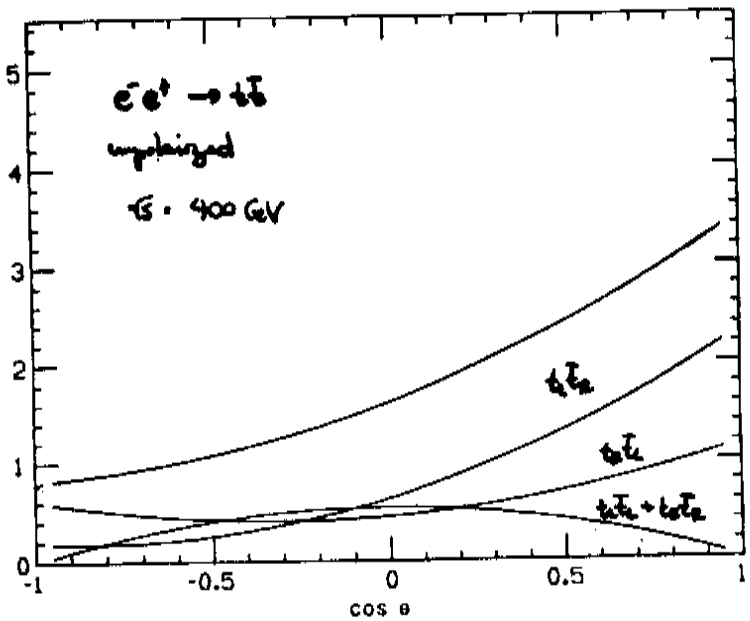

Distribution of $t\bar{t}$ production events in the production angle θ, for an unpolarized electron beam, showing the contributions from the various helicity components.

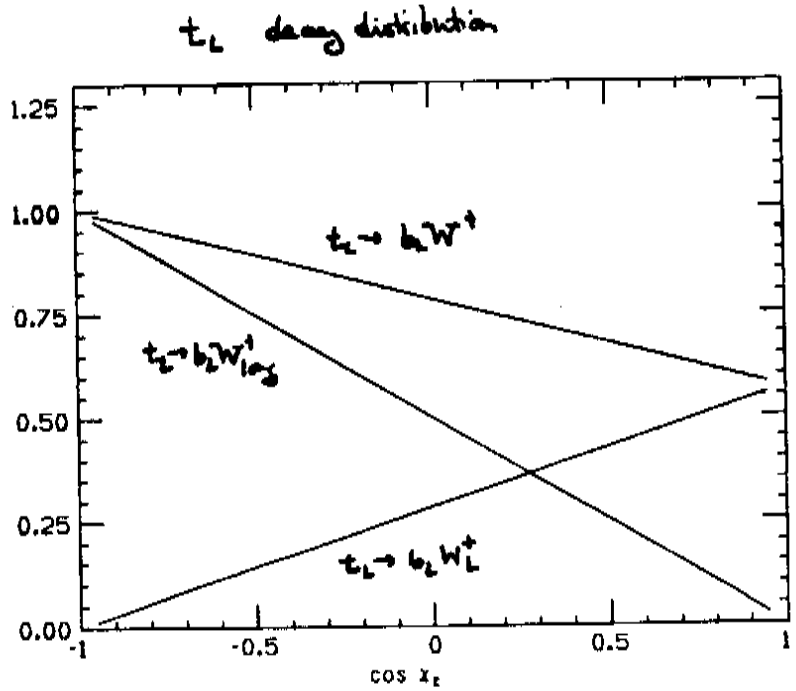

Distribution of decays of a polarized top quark in the decay angle x_t, and the contributions from the two helicity components.

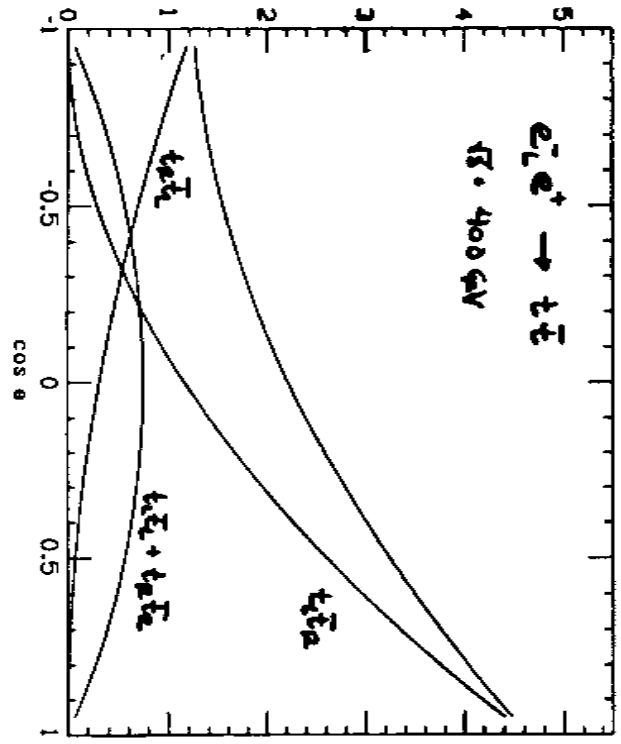

Distribution of $t\bar{t}$ production events in the production angle θ, for a left-handed polarized electron beam, showing the contributions from the various helicity components.

This is an ideal setting for detailed studies of quark dynamics

Top is heavy; does this mean form factors, (g-2) ?

Yuan

$$= \frac{ig}{\sqrt{2}}\,\bar{b}_L\left[\gamma^\mu F_{1L} + \frac{i\sigma^{\mu\nu}q_\nu}{2m_t} F_{2L}\right] t$$

$$i\mathcal{M}(t_L \to b_L W^+_L) = g(m_t^2 - m_W^2)^{1/2}\left[F_{1L} - \tfrac{1}{2}F_{2L}\right]\sin\chi_t/2$$

$$i\mathcal{M}(t_L \to b_L W^+_R) = g(m_t^2 - m_W^2)^{1/2}\underbrace{\left(\frac{m_t}{\sqrt{2}\,m_W}\right)}_{\frac{\lambda_{t\bar{t}H}}{g}}\cdot\underbrace{\left[F_{1L} - \frac{m_t^2}{2m_t^2}F_{2L}\right]}_{\text{effect of } F_2}\underbrace{\cos\chi_t/2}_{\text{char. dep on } \chi_t}$$

Sensitivities:

		Burke Dopb''
F_{2L}, $F_2^{\gamma Z}$	1%	(QCD 2%)
F_{1R}	0.1%	
$t \to b_R W^+$		

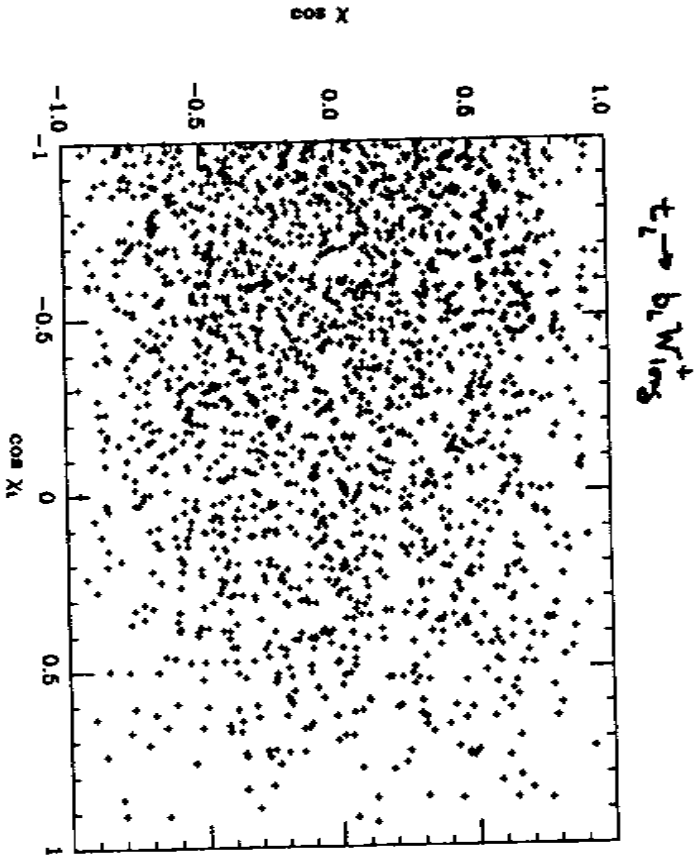

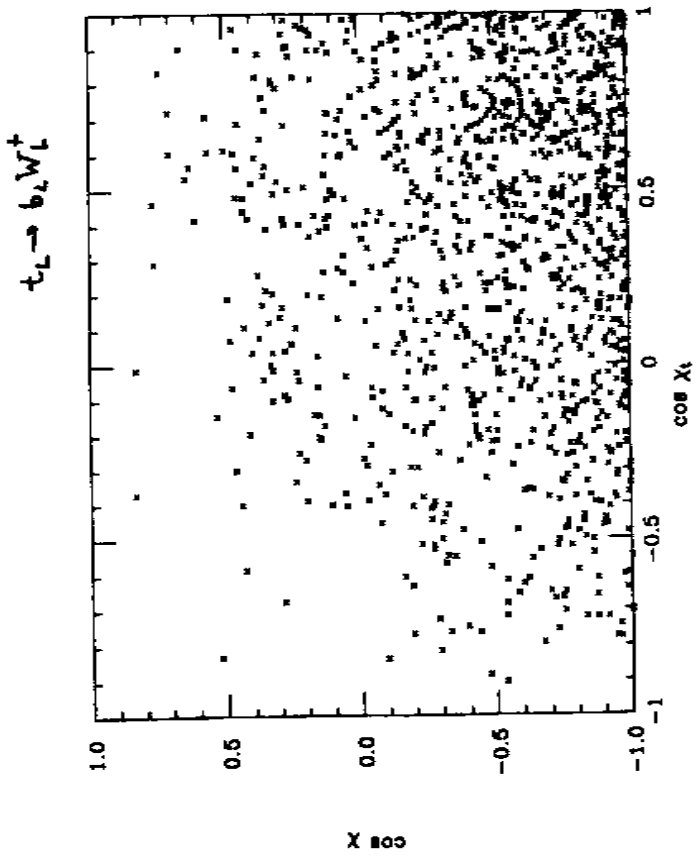

Scatter plot of decays of a polarized top quark in the plane of the top and W^+ decay angles. The three plots show the two helicity components and their sum.

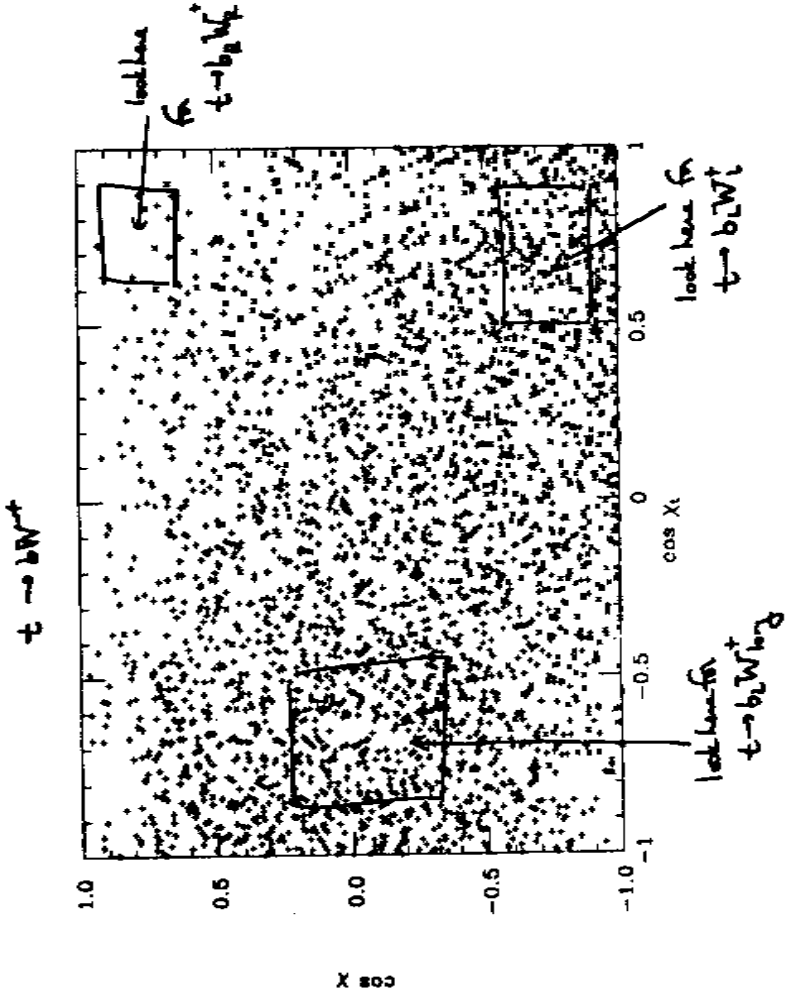

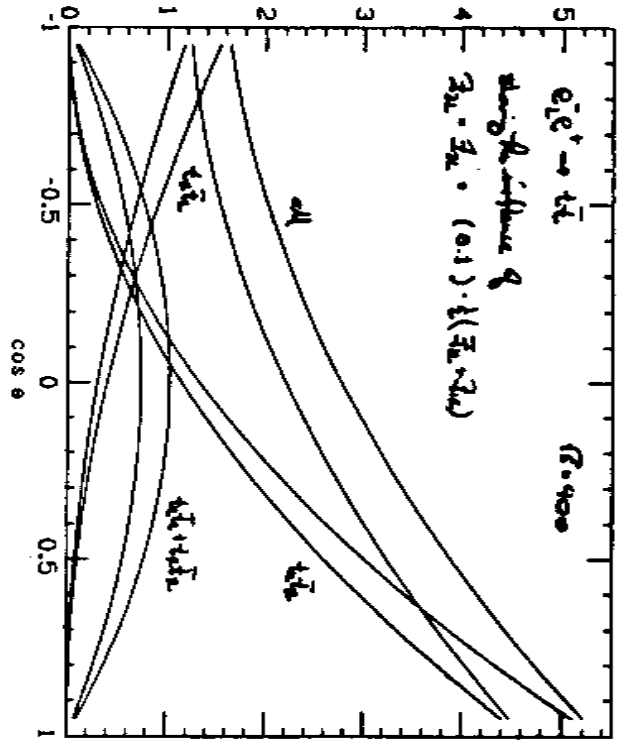

Effect of a top quark anomalous magnetic moment on the θ distribution of $t\bar{t}$ production events, for a left-handed polarized electron beam. The plot shows the separate effects on the various helicity components.

CP violation ?

$e^+e^- \to t\bar{t}$ can probe only to the 1% level;
expected asymmetries are $\sim 10^{-3}$

but

Gunion + Grządkowski :

at a $\gamma\gamma$ - collider

can have an $O(1)$
production asymmetry between

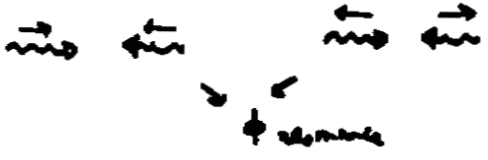

Conclusion :

We expect that the cleanliness
+ simplicity of e^+e^- experiments
will carry through to $e^+e^- \to t\bar{t}$

These features are well matched to the
property of t as a quark of
idealized perturbative QCD

Experiments at threshold and above
visualize top dynamics and
probe consistency for new effects.